THE UNIVERSITY
of EDINBURGH

USE OF MICROBIAL CONSORTIA FOR CONVERSION OF BIOMASS PYROLYSIS LIQUIDS INTO VALUE-ADDED PRODUCTS

JULIAN DARIUS PIETRZYK

DECLARATION

I declare that this thesis has been composed solely by myself and that it has not been submitted, in whole or in part, in any previous application for a degree. Except where stated otherwise by reference or acknowledgment, the work presented is entirely my own.

Signed:

Date: 7th May 2018

ACKNOWLEDGEMENTS

I would like to thank my supervisors Dr Andrew Free and Dr Ondřej Mašek for their support throughout the project and the specialist supervision from Dr Jan Mumme for his assistance with AD and Dr Logan Mackay for his assistance with the ICR. I would also like to thank the students who helped with the experiments as part of their courses at the University of Edinburgh: Raminta Kazlauskaite for her efforts on the aerobic portion of the project, the MSc Biotechnology class of 2016 for their efforts on AD3 and Sabrina Yeo for her efforts on AD4. Thanks also to the three that took a chance and enabled me to get anywhere in science: Lizzy, Anny and Rosie. And, of course, thanks go to the Free lab, particularly Helen Williamson, for their help throughout, my flatmates for the coffee and Hannah Wright for everything else.

ABSTRACT

Lignocellulosic biomasses are considered promising feedstocks for the next generation of biofuels and chemicals; however, the recalcitrance of lignocellulose remains a barrier to its utilisation over conventional sources. Pyrolysis is the heating of biomass to several hundred degrees Celsius in the absence of oxygen, which can thermally depolymerise lignocellulose. Products of pyrolysis are a solid biochar, liquid bio-oil and syngas. Biochar has roles in both carbon sequestration and soil amendment however bio-oil has no defined use, despite a high concentration of fermentable sugars. Bio-oil is a complex organic microemulsion with a host of biocatalyst inhibitors that makes its microbial degradation a challenge.

In this work, the use of aerobic cultures using microbial communities isolated from natural environments saw limited potential; however, the use of anaerobic digestion (AD) successfully generated a higher volume of biogas from reactors with bio-oil than controls. Biogas yield test reactors were set up with anaerobic digestate from a wastewater treatment plant as the substrate for degradation and conversion of bio-oils. Next-generation 16S rRNA gene sequencing was utilised to characterise the communities in the reactors while the ultrahigh resolution mass spectrometry technique of Fourier transform ion cyclotron resonance (FT-ICR) was used for characterisation of the chemical changes occurring during AD. Both sets of high-resolution data were additionally combined for multivariate analysis and modelling of the microbial genera that correlated best with the changes in digestate chemistry. This represents a novel analysis method for the microbial degradation of complex organic products.

Bio-oil from common lignocellulosic feedstock was the most easily degradable by the AD communities, with significant inhibition observed when bio-oils from anaerobic digestate and macroalgae were used. Additionally it was found that the inclusion of biochars that were pre-incubated in anaerobic digestate prior to use in AD were capable of significantly reducing the lag time observed for biogas production in bio-oil-supplemented reactors. The addition of biochars that were not

pre-incubated had no effect on biogas production. Specific inhibition of methanogenesis was also capable of causing the digestates to accumulate volatile fatty acids (VFAs) as a product of greater value than biogas. Scale-up experiments will be required to confirm the precise practicalities of the addition of bio-oil to AD as well as to establish the potential for isolation and purification of VFAs.

LAY SUMMARY

Biomass from plant-based materials is considered the next-generation source of our fuels and chemicals. However, these biomasses are extremely difficult to convert into useable commodities without significant treatment; which makes the process expensive and uncompetitive to conventional sources. One such treatment is pyrolysis, the heating of biomass to several hundred degrees Celsius without oxygen. Pyrolysis converts biomass into a solid charcoal-like material, called biochar, and the gases that are produced can be distilled into a bio-oil. This bio-oil has no practical use, however, contains a great deal of useable carbon, and so there is interest in converting this waste into products of greater value, and it is the aim of this project to investigate this conversion biologically using microbial communities.

Bio-oil contains thousands of compounds and is currently not well understood, it does however contain several chemicals that are known to cause the inhibition of microbial growth, and thus attempts growing microbial communities isolated from the natural environment with oxygen were not promising. However, the digestate from an anaerobic digester, used to produce biogas from a wastewater treatment plant, was used to set up multiple reactors with the addition of bio-oil and no oxygen. These biogas yield tests were characterised for the changes in digestate chemistry, using ultrahigh resolution mass spectrometry techniques, and biology, using next-generation sequencing methods. Both sets of data were then analysed and combined to gain an understanding of how bio-oils were being converted to biogas.

It was found that bio-oils made from woody biomass were the most easily degradable by anaerobic digestion (AD) and those bio-oils made from anaerobic digestate and seaweed caused a high level of inhibition. By including biochar into the reactors, a significant reduction in bio-oil inhibition was observed; however, the biochars had to first be pre-incubated in anaerobic digestate prior to use, presumably to allow for microbial growth on the biochar surfaces. The specific inhibition of the final step of AD, responsible for the generation of biogas, allowed for the accumulation of volatile fatty acids (VFAs) instead of biogas, which are a product of greater value

than biogas. Additional work will be required to scale-up the experiments to confirm the ability of AD to convert bio-oil to biogas in large-scale reactors and to isolate and purify accumulated VFAs.

TABLE OF CONTENTS

LIST OF FIGURES AND TABLES

ABBREVIATIONS

AD	Anaerobic Digestion	MP/BO	*Macrocystis Pyrifera* Bio-Oil
AD/BO	Anaerobic Digestate Bio-Oil	MS	Mass Spectrometry
AGE	Agarose Gel Electrophoresis	NB	Nutrient Broth
ANOVA	Analysis Of Variance	NMDS	Nonmetric Multidimensional Scaling
APPI	Atmospheric Pressure Photoionisation	OD	Optical Density
APS	Ammonium Persulphate	OTU	Operational Taxonomic Units
ATB	Leibniz-Institut Far Agrartechnik Und Biookonomie	PCoA	Principal Coordinates Analysis
BES	Sodium 2-Bromoethanesulfonate	PCR	Polymerase Chain Reaction
BHB	Benhar Bing	PERMANOVA	Permutational Multivariate Analysis Of Variance
BP	Blackford Pond	PERMDISP	Homogeneity Of Dispersions
CED	Conventional Electrodialysis	PID	Proportional Integral Derivative
COD	Chemical Oxygen Demand	PRIMER	Plymouth Routines In Multivariate Ecological Research
CR	Cramond Beach	PYNAST	Python Nearest Alignment Space Termination
CSTR	Continuous Stirred-Tank Reactor	QIIME	Quantitative Insights Into Microbial Ecology
DGGE	Denaturing Gradient Gel Electrophoresis	qPCR	Quantitative PCR
DIET	Direct Interspecies Electron Transfer	RNA	Ribonucleic Acid
DNA	Deoxyribonucleic Acid	SDS	Sodium Dodecyl Sulfate
DNTP	Deoxynucleotide Triphosphates	SWP/BO	Softwood Pellet Bio-Oil
EDTA	Ethylenediaminetetraacetic Acid	TAN	Total Ammonia Nitrogen
ESI	Electrospray Ionisation	TEMED	Tetramethylethylenediamine
FT-ICR	Fourier Transform Ion Cyclotron Resonance	THP	Thermal Hydrolysis Plant
GC	Gas Chromatography	TOC	Total Organic Carbon
HMF	5-Hydroxymethylfurfural	TS	Total Solids
HPLC	High-Performance Liquid Chromatography	UKBRC	UK Biochar Research Council
IR	Infrared	UV/VIS	Ultraviolet-Visible
ITS	Internal Transcribed Spacer	v/v	Volume/Volume
LDI	Laser Desorption Ionisation	VFA	Volatile Fatty Acid
mcrA	Methyl Coenzyme-M Reductase A	WP/BO	Wood Pellet Bio-Oil
ME	Malt Extract		

CHAPTER 1: INTRODUCTION

1.1 Foreword

The following project investigates the use of microbial consortia for the bioconversion of pyrolysis liquids into value-added products. In this chapter, I will introduce the background of the project and the two technologies that are at its core: pyrolysis and anaerobic digestion (AD), and examples from the literature of how they have been used similarly. I will also cover the background of additional techniques and supplements used during the project that steered the research towards its conclusion.

1.2 Project Background

With an ever increasing need for fuels and chemicals and a rising global concern for the environmental effects of using them, there has been a boom in the renewable energy and chemical industries to find new sources and methods of acquisition. Biomass has been highlighted as a major source of available carbon for the production of renewable fuels, with annual estimations of biomass produced by land plants reaching 200×10^9 tons (Vanholme *et al*., 2013). Considered a renewable energy source, where the release of carbon when burned for energy production is counteracted by the atmospheric carbon stored as a result of photosynthetic growth (Mohan, Pittman and Steele, 2006), biomass has the potential to be a critical component of a sustainable bio-based economy.

First-generation biofuels, made from easily extracted sugar or starch crops, have been the topic of much controversy due to competition with the food requirements of a growing population (Sims *et al*., 2010). Due to this, the second generation of biofuels produced from various woody crops, industrial residues or waste products have a distinct environmental and economic advantage. This biomass, mainly in the form of lignocellulose, is a major constituent of most natural ecosystems and a waste product of several large industries such as agriculture and forestry. The abundance

and availability of biomass therefore makes it an attractive source of future fuels (Lynd, Wyman, and Gerngross, 1999).

Lignocellulose however, is a particularly difficult compound to degrade and its processing for release of fermentable sugars has been one of extensive study (Bosch and Hazen, 2013; Chandel *et al*., 2013). Its resistance to degradation is due to its robust tertiary structure, composed mainly of hydrogen bonded crystalline cellulose microfibrils attached to hemicellulose polysaccharides, all of which are tightly bound by lignin, the composition of which varies from plant to plant (Malherbe and Cloete, 2002; Sanderson, 2011). Currently, the conversion of lignocellulosic biomass into value-added products is reliant on several stages of processing, many of which involve pre-treatment of the biomass to overcome the recalcitrant nature of lignocellulose, particularly lignin, which is then followed by enzyme production, saccharification, and finally sugar fermentation (Parisutha, Kim and Lee, 2014). Every additional stage increases the overall cost of the conversion of the biomass and therefore makes it less of an attractive source of fuel. If is to be considered as a genuine alternative to today's sources of energy, the conversion of lignocellulosic biomass will have to prove a financially viable substitute.

1.3 Pyrolysis

Thermochemical processing of biomass such as pyrolysis has been shown to overcome recalcitrance of lignocellulosic biomass. Pyrolysis of biomass, which uses temperatures of several hundred degrees Celsius in the absence of oxygen, thermally depolymerises the constituent compounds of the biomass making them easier to extract. Products of pyrolysis form as solids (biochar), liquids (bio-oil) and gases (syngas), each of which has the potential for further utilisation (Tang *et al*., 2013). Bio-oil is the product of interest for this project, with biochar used as a supplement in some of the tests.

1.3.1 Biochar

Biochar is a charcoal-like material formed from the incomplete combustion of biomass. Of increasing interest is its use as a climate change mitigation strategy by carbon sequestration and as a soil amendment to improve soil quality and crop yield. Biochar is carbon-rich and shows a high degree of chemical stability with a high affinity for heavy metal ions, phosphate and nitrate. It has been reported to confer numerous benefits to soil health including reducing soil acidity and increasing soil electrical conductivity and cation exchange capacity (Oguntunde *et al*, 2004; Laird *et al*, 2010). It also shows a high degree of microbial stability due to its porous structure granting a large surface area that has been reported to increase microbial biomass and diversity in soils (Grossman *et al*, 2010). As such there are several pilot pyrolysis plants that use agricultural waste biomass as a feedstock for biochar production (Spokas *et al*., 2012; Kong, Liu & Zhou, 2014) with more plants planned and the expected amount of pyrolysis products rising.

Biochars have further been found to be partially conductive and so suitable materials for direct interspecies electron transfer (DIET). DIET has been proposed to be an alternative mechanism to mediated electron transfer, where soluble electron carriers shuttle electrons between syntrophic partners. This is particularly important in methanogenic communities where interspecies hydrogen transfer is a key functional step. Proposed mechanisms of interspecies electron transfer are through electrically conductive pili, electron transport proteins, and soluble electron shuttles and via electrically conductive materials, although it is likely several strategies remain undiscovered (Lovley, 2017). Biochar, and other conductive carbon materials, supply a surface for microbial attachment where the cells do not require close proximity to one another to exchange electrons, relying instead on their physical connection to the conductive material. This is thought to save the microorganisms considerable energy, as they do not require the production of extensive extracellular electrical connections.

1.3.2 Bio-Oil

An alternative form of pyrolysis known as “fast pyrolysis”, which generally uses higher heating rates to maximise production of the liquid fraction (Kersten & Garcia-Perez, 2013), can be employed to specifically produce bio-oil for further upgrading into useable fuels. However, even in conventional pyrolysis, bio-oil is still produced as a waste product and is generally burned with the syngas to further heat the pyrolysis reaction. Due to the potential availability of fermentable sugars, bio-oil has been highlighted as a potential source of future fuels and there is therefore a need to develop technologies that can further degrade and utilise this pyrolysate.

Bio-oils are generally composed of a light brown aqueous phase and a dark brown organic phase (Figure 1.1), with this project focusing solely on the conversion of the aqueous phase. They are formed by the rapid fragmentation of cellulose, hemicellulose and lignin under high temperature (Bridgwater & Peacocke, 2000). After the initial heating, the products of fragmentation are rapidly quenched which locks in the intermediate compounds that could be further degraded by continuous heating. Considered a microemulsion, bio-oil is an extremely complex mix of compounds including catechol, guaiacol, syringol, isoeugenol, pyrones, vanillin, furans, acetic acid and formic acid, as well as major groups of compounds including sugars, carboxylic acids, phenolics, hydroxyketones and hydroxyaldehydes. Fragmentation of the biomass polymers also generates a substantial amount of water (~25 wt %) which is responsible for an extremely high oxygen content along with more than 300 other compounds that have been identified in bio-oil, most of which contain oxygen (Mohan, Pittman & Steele, 2006).

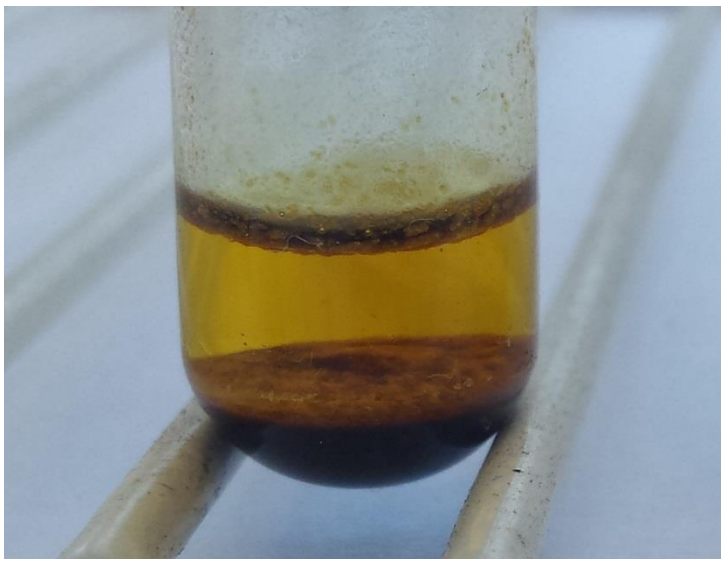

Figure 1.1 Bio-oil from softwood pellets. Of note is the substantial amount of aqueous phase oil and smaller volume of organic phase.

Bio-oil also begins to age immediately after its recovery due to chemical reactions continuing in the oil leading to the formation of larger molecules and this is usually seen as an increase in viscosity, a decrease in volatility and phase separation (Czernik & Bridgwater, 2004). However, ageing is heavily dependent on the temperature of storage; with little-to-no ageing observed below -5°C (Oasmaa *et al*., 2012). Its complexity makes it a difficult substance to degrade and this is compounded by the fact that its composition is dependent on the feedstock used to create it, so no two samples are the same. They do however generally have a low pH, high oxygen content and a compliment of biocatalyst inhibitors, for many of which, the method of inhibition is still not fully understood (Jarboe *et al*., 2011).

That is not to say degradation of bio-oil is impossible: several groups have succeeded in generating fuel, usually ethanol (Bennett, Helle & Duff, 2009; Layton *et al*., 2011; Sukhbaatar *et al*., 2014), from the pyrolysate by fermentation with microorganisms and it is the aim of this project to biochemically convert bio-oils into value-added products using communities of microorganisms.

Biochemical processing of biomass utilises microorganisms to create specific products using pure cultures of specific bacterial species or an assemblage of different microorganisms that are able to exist as a functional consortium such as those found in nature (Kumar, Singh, & Singh, 2008). When utilising

microorganisms for biotechnological purposes it is common to use cultures of a single bacterial species known to produce a desired product, such as therapeutic proteins in Escherichia coli (Baneyx, 1999). The metabolic pathways associated with the production of a single product are in these cases achievable in a single strain (Pandhal & Noirel, 2014). When more than one product or substrate for degradation is present, single strains are unable to perform every step in the multiple metabolic pathways; it is then when a consortium of microorganisms becomes a more attractive option. Such a scenario is certainly present for the degradation of lignocellulosic biomass which requires several aforementioned processing steps.

1.4 Microbial Degradation

It is rare in nature to find an environment dominated by a single strain of bacteria as no single species is able to cope with the immeasurable fluctuations in environmental parameters. Having numerous species each with an ecological function within a system enables the community as a whole to be extremely resilient to these environmental fluctuations as it evolves to adapt to the new conditions. In the case of the degradation of bio-oil, where its composition is dependent on the feedstock, it is extremely important to have a flexible consortium of species that can change depending on the differing compounds within the oil. That is not to mention the complexity and number of different compounds within bio-oil, of which it is unlikely a single species could degrade. Werner *et al*. (2011) stated that for full-scale bioenergy systems it is imperative to have a microbial community that has a stable metabolic function despite the unavoidable instability of such real-life systems. Regardless of this, understanding every pathway for every organism in a bacterial community is no easy task and as such our knowledge of microbial community dynamics is limited.

In spite of these limitations it is not essential to understand every part of a microbial community as long as it can be steered toward the required goal and shows stability in doing so. One method that follows this concept is artificial ecosystem selection (AES). Swenson, Wilson and Elias (2000) suggested that selection can operate above

an individual level and that if the best population of units, where success is measured by a phenotypic trait such as degradative ability or product formation, is artificially selected to be the parents of future generations, the successive generations will retain that phenotypic trait (Williams & Lenton, 2007). These traits are therefore postulated to be heritable and with successive generations where the parent population selection is based on these desired traits it is possible to adapt a population towards whatever that trait may be. An advantage of such a method is that it does not focus on analysis of individual species, some of which are unculturable, within the population as only the population's ability to, for example, degrade the environmental pollutant 3-chloroaniline (Swenson, Arendt & Wilson, 2000) is important. This natural environmental selection of microorganisms by successive culturing shows great potential for the biodegradation of bio-oil as individually isolating bacterial species that can metabolise the multitude of compounds in the bio-oil and exist as a stable consortium would be extremely challenging.

When degrading bio-oil there is no longer the concern of having to break down the individual components of biomass; however early research on microbial utilisation of the oils identified several biocatalyst inhibitors which must be addressed if there is to be successful degradation (Prosen *et al*., 1993). Microbial inhibitors therefore place another step that would need to be overcome for bio-oil degradation, which could require augmenting a consortium of bacteria with individual microorganisms that have the ability to degrade biocatalyst inhibitors. This bioaugmentation approach has seen limited success in the scientific literature as established communities are unlikely to accept new species if their metabolic capabilities are already present. It can be hypothesised however, that a high degree of ecological disturbance, such as from the presence of bio-oil, may disrupt some metabolic pathways due to the death or inhibition of existing members of a consortium. This could allow the introduction of a novel microorganism to be accepted into the community and therefore enhance the degradation rate of a specific compound. Alternatively, a bioaugmentation approach may require additional reinoculation of the individual species, as it becomes competitively excluded over time; such an approach has been reported to

work for the remediation of soil contaminated with environmental pollutants such as pentachlorophenol (Beaudet *et al*., 1998).

Parisuthum, Kim and Lee (2014) recently discussed the potential of consolidated bioprocessing for biofuel production and agreed that it remains a valid and cost-effective method for the production of biofuels using microbial consortia designed for the bioconversion of biomass. It is therefore feasible and the aim of this project to identify and develop microbial consortia for the conversion of biomass pyrolysate into value-added products.

1.4.1 Anaerobic Digestion

Anaerobic Digestion (AD) is the sequential degradation of organic substrates by a microbial consortium of mutually dependant microorganisms in the absence of oxygen. The technology is based on the natural phenomenon of anoxic decomposition, and simply aims to replicate and enhance the degradation of organic substrates seen in nature. Organic substrates undergo four main degradation events to the common end product of biogas, a mixture of carbon dioxide and methane. Biogas is considered a value-added product and a widely utilised renewable fuel for rising global energy needs. In 2014 there were a total of 17 240 biogas plants in Europe, 10 786 of which located in Germany, with a combined total capacity of 8 293 MW_e, and a high rate of growth in the sector in many countries including the UK and France (EBA Biomethane & Biogas Report 2015). Meanwhile in China, 26.5 million biogas plants were built by 2007 with a 2010 output of 248 billion m^3 of biogas annually (Deng *et al*., 2014). There are numerous additional environmental benefits to biogas production such as the ability to utilise organic waste streams such as agricultural, industrial, municipal and household wastes as biomass for biogas production and decreasing greenhouse gas emissions as it substitutes conventional energy sources.

The degradation of organic substrates follows the following four main steps: hydrolysis, acidogenesis, acetogenesis and methanogenesis (Figure 1.2). Hydrolysis is the process by which high molecular weight organic polymers are split into smaller more bioavailable monomers and sees the conversion of proteins, carbohydrates and

fats into amino acids, monosaccharides and fatty acids, plus hydrogen. Hydrolytic bacterial genera such as *Streptococcus* and *Enterobacterium* are regularly found in digestates (Ali Shah *et al*., 2014). This is then followed by acidogenesis, where acidogenic microorganisms, such as *Pseudomonas*, *Bacillus* and *Clostridium*, ferment the hydrolysed products into short chain volatile acids (propionic, butyric, acetic, formic, lactic), alcohols (ethanol, methanol), hydrogen, carbon dioxide, ammonia and hydrogen sulphide (Cooney *et al*., 2016). These products are further digested by acetogens, such as *Syntrophomonas* and *Syntrophobacter*, during acetogenesis into hydrogen, carbon dioxide and acetic acid. These microorganisms rely on their products being utilised and so many species of these microorganisms form syntrophic relationships with methanogenic species. Methanogenic microorganisms are only found within the archaeal domain and members of this group are generally capable of methanogenesis via one of two pathways: hydrogenotrophic or acetoclastic methanogenesis which utilises either hydrogen or acetic acid, respectively, with carbon dioxide to produce methane, carbon dioxide and water as the final end products of AD (Mao *et al*., 2015).

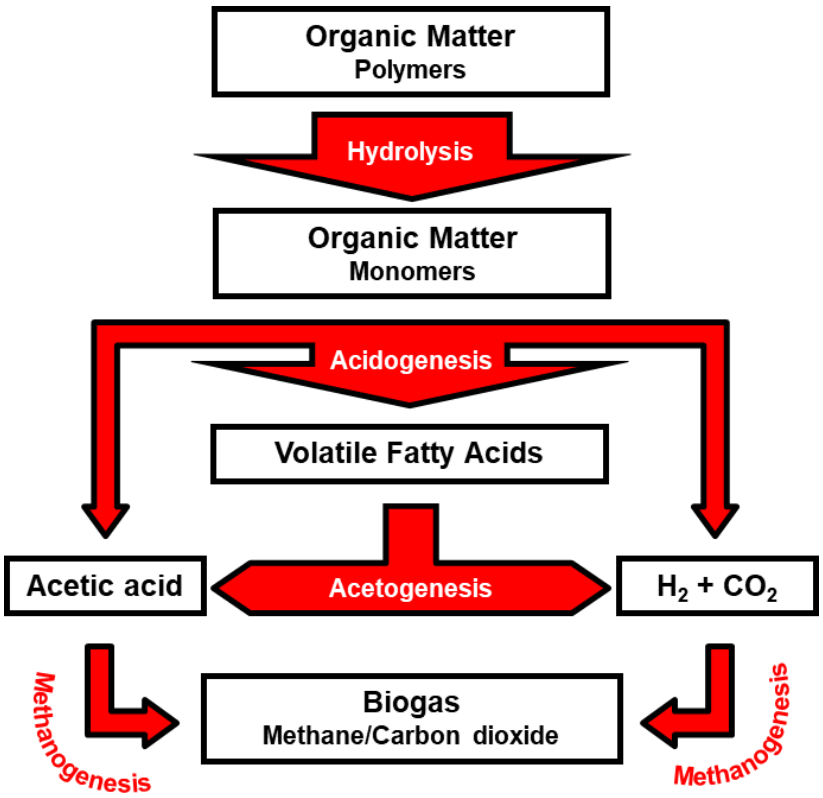

Figure 1.2. Schematic representation of the four main processes (red) in anaerobic digestion and their products (Amaya, Barragán and Tapia, 2013).

Evaluation of the organic strength of digestates is commonly performed by measuring chemical oxygen demand (COD), the methods of which are detailed in Chapter 2. Oxidation of the organic carbon to carbon dioxide is measured and expressed as oxygen equivalents with the COD of methane calculated as 64 g of oxygen per mole (Heidrich, Curtis and Dolfing, 2011). Following the ideal gas law at standard temperature and pressure, this allows a theoretical limit of 350 mL of methane generated per gram of COD. The efficiency of biomass conversion to methane varies depending on the operating conditions of the reactor, this calculation assumes all COD is converted to methane, however, the composition of biogas is generally 50 – 60% methane with the rest predominantly carbon dioxide. Additionally there are competing metabolic pathways present in AD systems that can be more thermodynamically favourable than methanogenesis and are thus alternative

terminal electron acceptors, such as sulphate. Thus the amount of methane recovered per gram of COD will likely be less than this theoretical limit.

Although a well-established technology, there is still a great deal of research regarding the microbial characterisation of AD systems and which microorganisms are important for optimal operation and which are indicative of system failures. The technology currently faces major challenges in the form of the stability of biogas output due to process inhibition. This inhibition can be a major obstacle for any AD process and occurs when either the direct source of material or metabolic intermediates inhibits their microbial degradation. Substrates with high levels of proteins, lipids, metals, pesticides, antibiotics and other organic products have been reported to cause substrate-induced inhibition (Fagbohungbe *et al*., 2017). The most important inhibitors are arguably ammonia and ammonium, which accumulate to inhibitory levels when the substrates contain a high amount of proteins and lipids which are hydrolysed to these compounds (Yenigün and Demirel, 2013).

While both the ammonium ion (NH_4^+) and free ammonia (NH_3) are inhibitory to AD, free ammonia is membrane-permeable and is thought to be the main inhibiting compound (Chen, Cheng and Creamer, 2008). Its diffusion into the cell is capable of disrupting the proton balance, increasing maintenance energy requirements and inhibiting enzymatic reactions (Wittmann, Zeng and Deckwer, 1995).

In addition to ammonia, the presence of sulphate in an AD reactor can also lead to inhibition of methanogenesis. Sulphates are reduced to hydrogen sulphide in the absence of oxygen by sulphate-reducing bacteria which can outcompete methanogens for substrates and proliferate in sulphate-rich environments (Madden *et al*, 2014). Sulphate-reducing bacteria have a higher affinity for hydrogen than methanogens leading to inhibition of methanogenesis in AD reactors with high sulphate content and limited hydrogen (Kristjansson, Schönheit and Thauer, 1982).

Process inhibition leads to decreased biogas production and can severely impact the operational costs of a large working AD plant. As such, technologies and research

that investigates the causes of inhibition and their mitigation techniques are of great need by the industry.

Due to the potential waste streams that can be utilised for biogas production by AD, it becomes a potential candidate for bio-oil degradation. The idea being that the highly recalcitrant lignocellulose is thermally degraded by pyrolysis to produce bio-oils that can then be further processed to biogas using AD. And even going a step further to utilise the solid fraction of pyrolysis in AD reactors, and to pyrolyse the digestate from AD for further production of bio-oils and biochars. This pairing of the two technologies is still a relatively novel proposal, with few reports in the scientific literature. However, this field is rapidly receiving more attention with Fabbri and Torri (2016) terming the pairing as Py-AD.

The AD of bio-oil is extremely promising as AD utilises a vast range of microorganisms capable of bioconversion across a spectrum no single species could accomplish and as such it becomes an ideal platform for the detoxification of complex organic mixtures such as bio-oil. Righi *et al*. (2016) performed a life cycle assessment of the use of lignocellulosic biomass pyrolysis coupled with anaerobic digestion and found relevant primary energy savings for lignocellulosic biomass of non-renewable sources, without worsening abiotic resource depletion, as well as seeing a strong reduction of greenhouse gas emissions.

Reports of successful biogas production from bio-oils have been reported (Andreoni *et al*., 1990; Moita Fidalgo *et al*., 2014; Torri and Fabbri, 2014; Hübner and Mumme, 2015); however, inhibition is still observed, the scale of which rises with increasing bio-oil concentrations up to a point where it completely inhibits biogas production. The presence of high concentrations of organic acids, phenols and furans in bio-oil are thought to be mainly responsible for the inhibition (Hübner and Mumme, 2015). It has therefore been proposed that the inclusion of biochar for the AD of bio-oil can assist in alleviating the inhibition.

Biochar addition to AD systems without bio-oil is a subject of increasing research due to its aforementioned abilities to both adsorb inhibitory compounds and to act as a surface for microbial adherence, conferring advantages to microbial species capable of surface attachment, biofilm formation and DIET. Increases in total biogas production and methane content of biogas have been reported due to the addition of biochars to AD (Desai and Madamwar, 1994; Cai *et al*., 2016). Additionally, Torri and Fabbri (2014) reported that the inclusion of both biochar and bio-oil, when co-produced, to an AD system results in significantly lessened inhibition than the bio-oil added to AD on its own, and proposed biochar as a low-cost catalyst for the AD of potentially inhibitory compounds.

1.5 Analysis Methods

Scientific literature on the microbial conversion of biomass into value-added products, particularly for technologies such as AD, focus predominantly on analysis of either the biomass chemistry or the microbial community. High-throughput technologies such as high resolution mass spectrometry for chemical compounds and next-generation sequencing of microbial marker gene amplicons give high resolution characterisation of the chemistry and biology of a system respectively, however, are rarely paired. This project will characterise the chemical profiles of bio-oils and growth media using Fourier transform ion cyclotron resonance mass spectrometry (FT-ICR MS) while simultaneously characterising the microbial populations using Illumina 16S rRNA sequencing. Analysis of the patterns generated from such techniques should give an in-depth understanding of the relationships between the microbial community and the bio-oil-supplemented growth medium.

1.5.1 Chemical Analysis

The characterisation of bio-oil is extremely challenging due to its complexity and constantly changing chemistry due to ongoing reactions. Early estimates of the number of compounds which constituted bio-oil were constrained by the technologies used for their analysis, mainly gas and liquid chromatography linked to mass spectrometers. These early estimates were in the range of a few hundreds

(Garcia-Perez *et al*., 2007; Lian *et al*., 2010); however, more recent ultrahigh resolution mass spectrometry techniques push those estimates further into the thousands (Miettinen *et al*, 2015).

One such technique is Fourier transform ion cyclotron resonance mass spectrometry (FT-ICR MS) which will be utilised in this project with an electrospray ionisation source (ESI) for characterisation of the chemistry of the bio-oils and anaerobic digestates. ESI FT-ICR MS is capable of providing ultrahigh resolution mass accuracy to the thousands of peaks generated from the ionised samples in a cyclotron (Marshall, Hendrickson and Jackson, 1998) and has been instrumental in the understanding of similarly complex petroleum chemistry (Marshall and Rodgers, 2004). After calibration, a mass list can be assigned to chemical formulas matching the precise mass to within 0.1 ppm. Although it gives no structural information about the compounds in the sample, details of the elemental composition can provide information on likely heteroatom groups and thus provide a detailed characterisation of the sample. Visualisation of the data will be through the use of van Krevelen diagrams (Wu, Rodgers and Marshall, 2004) which can cluster groups of samples based on their likely chemical class and have been developed for the analysis of complex organic compounds such as bio-oil.

1.5.2 Biological Analysis

Next-generation sequencing technology has revolutionised the field of microbiology with the ability to now characterise, to a far greater resolution than previous culture-based studies, the microbial community of a sample, including those species that are considered unculturable. Indeed, the advent of next-generation sequencing has seen such momentum that the new challenges in microbial ecology lie predominantly in data handling and interpretation.

Illumina 16S rRNA gene amplicon sequencing of DNA from samples provides millions of reads of potential microbial sequences, and will be utilised in this project for the characterisation of environmental sediments and anaerobic digestates. Analysis and assignment of the sequence data will be via the command pipeline:

quantitative insights into microbial ecology (QIIME), developed specifically for the high-throughput analysis of next-generation sequencing data (Caporaso *et al*., 2010; Caporaso *et al*., 2012). The biological characterisation of samples at different time points will allow for abundance profiles of the key microbial components to be observed and compared such that patterns of shifts in microbial abundance can be investigated.

1.6 Project Aims

Bio-oil is not a well-studied product, its chemical complexity renders it particularly difficult to analyse, and thus its utilisation by mixed microbial communities is thought to be the best method for its successful degradation and eventual conversion to a value-added product. It is the aim of this study to characterise both the chemical and biological species involved in the degradation of bio-oils from different feedstocks and develop techniques for their detoxification and conversion to value-added products using mixed microbial communities.

CHAPTER 2: MATERIALS AND METHODS

2.1 Pyrolysis

All pyrolysis was conducted at the UK Biochar Research Council (UKBRC), located at the King's Buildings Campus of the University of Edinburgh using the apparatus show in Figure 2.1. The lab-scale unit consists of a vertical quartz tube static bed reactor of 50 mm inner diameter and 200 mm sample bed depth, able to accommodate ~50 g of biomass sample. Samples were heated and controlled by a 12 kW infrared gold image furnace with a proportional–integral–derivative (PID) controller (ULVAC RHL-P610C, Yokohama, Japan) connected to thermocouples within the reactor, positioned 10 mm from the inner surface. The system was purged with nitrogen gas and supplied at a controlled rate through the base of the reactor vessel and heated by a bed of ceramic heating bricks before reaching the sample. The flow of nitrogen carried volatiles and syngas through a series of condensation vessels held at different temperatures to collect the condensable liquid fraction of the pyrolysed biomass.

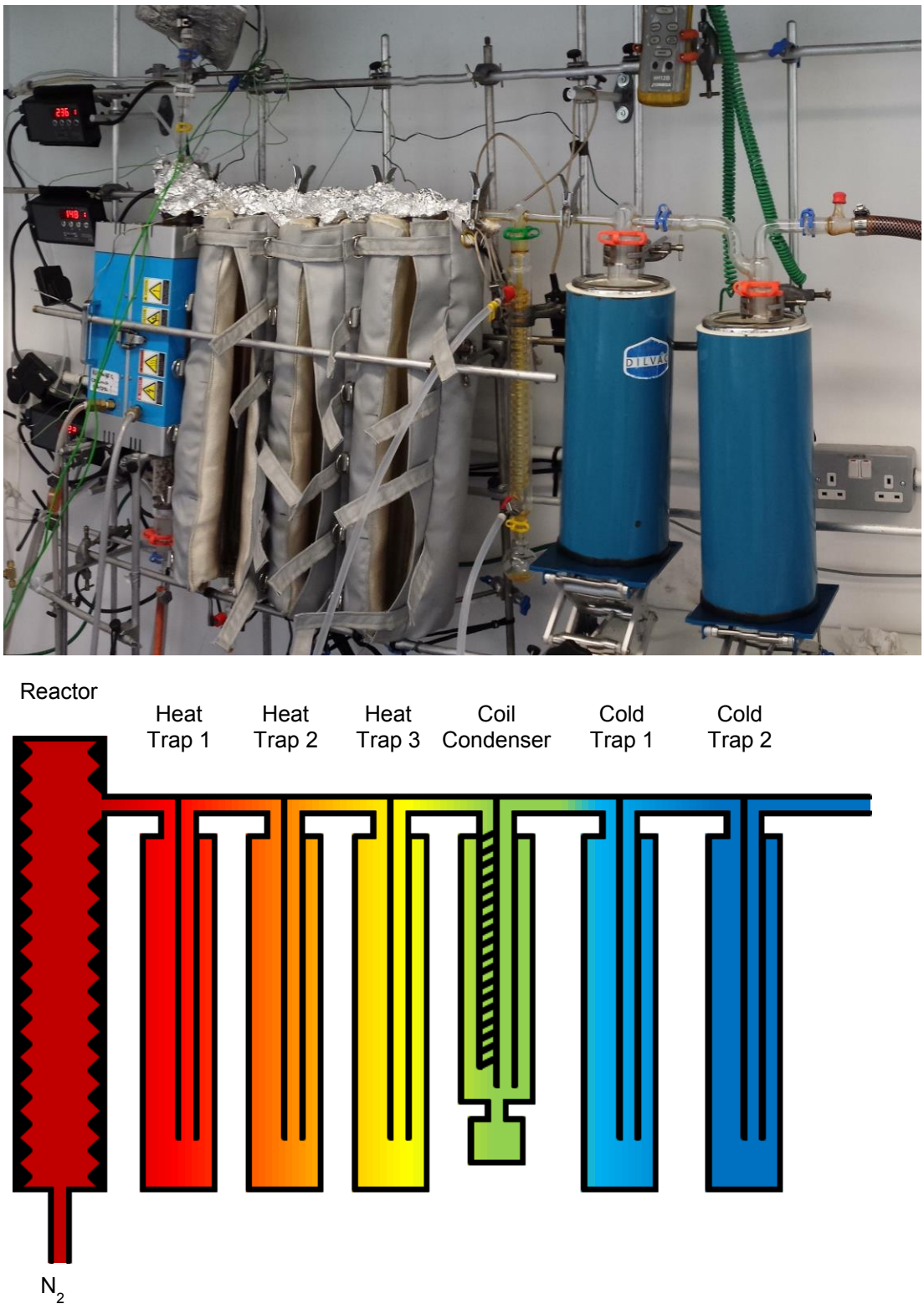

Figure 2.1. Lab-scale pyrolysis unit equipment (top) and schematic (bottom).

All pyrolysis for bio-oil production was performed at 350 °C, the first three condensation vessels or 'heat traps' were held at decreasing temperature increments at 240 °C, 180 °C and 120 °C using heating jackets fitted with thermocouples placed in the centre of the vessels. The gas was then carried through a water-cooled coil condenser (room temperature) and then through two 'cold traps' immersed in a mixture of acetone and liquid nitrogen to a temperature range of -30 to -60 °C. Fluctuations in temperature and pressure were recorded in real time by LabVIEW software. The yield of solid and liquid products was determined by weighing the vessels before and after pyrolysis and calculated proportional to the mass of the initial biomass. The majority yield of aqueous phase bio-oil (20 to 45%) was collected in the coil condenser and stored in glass vials at 4 °C until required. All bio-oils were passed through a 0.22 μm syringe filter (Millex) before use.

2.1.1 Bio-Oil

Initial bio-oil samples for early experiments were directly acquired from the UKBRC, and had been made previous to this project using the same pyrolyser as previously described. Bio-oils for use in later aerobic cultures and AD were produced fresh. Table 2.1 lists the production condition details of the bio-oils used in this project.

Code	Feed	Temp (°C)	Heating Rate (°C Min^{-1})	Residence Time (Min)
WP/BRC	Wood Pellets	650	5	40
AD/BO	Anaerobic Digestate	350	20	30
MP/BO	*Macrocystis pyrifera*	350	20	30
SWP/BO	Softwood Pellets	350	20	30

Table 2.1. Bio-oil production conditions.

2.1.2 Biochar

The two biochars used in this project were obtained directly from the UKBRC and Carbogenics Ltd. The UKBRC supplied their Standard Biochar from mixed softwood pellets pyrolysed at 550 °C (SWP550); full analytical data is available online. Carbogenics Ltd, a University of Edinburgh spin-out company, supplied their CreChar®, made from waste paper cups pyrolysed at 450 °C in a pilot-scale rotary kiln pyrolysis unit. Both chars were sieved to 125-500 μm before application.

2.2 Chemical Methods

2.2.1 Electrospray Ionisation Fourier Transform Ion Cyclotron Resonance Mass Spectrometry (ESI FT-ICR MS)

Samples for ESI FT-ICR MS were prepared by adding 1:1 (v/v) HPLC grade methanol (Sigma-Aldrich) to the sample, mixed by vortex for 15 seconds and then centrifuged with a bench-top 1-15 Microfuge (Sigma Zentrifugen) at 18,000 × g for 15 minutes. The supernatant was stored at 4 °C prior to analysis.

A 12 Tesla SolariX FT-ICR equipped with an ESI ionisation source (Bruker Daltonics) was used for the analysis with all bio-oil runs performed in both positive and negative ion mode. Positive mode used an injection rate of 200 μL/h into the ion source with a capillary voltage of 4,000 V and an end plate offset of 200 V. Ion accumulation time was set to 0.3 s per scan for 500 scans summed to give the final mass spectrum with a range of 98.3 – 2,500 m/z. The source gas was tuned with nebulizer gas (1.8 – 2.2 bar), dry gas (4-6 L/min) and heated to 180 °C. Negative mode used identical settings however the sample injection rate was increased to 500 μL/h with a 0.6 s ion accumulation time for 1,000 scans, giving a final spectrum range of 129–1,800 m/z. End plate offset was -200 V. Digestate samples were run in negative ion mode only and differed to bio-oil negative ion mode with a reduction of scans to 100, with a spectrum range of 129 – 1,000 m/z, and an injection rate of 200 μL/h. Transient length was 3 s with a mass resolution of ≈680,000 at m/z 400.
Transient length was 3 s with a mass resolution of ≈680 000 at m/z 400.

Post-acquisition the mass spectra were analysed using Data Analysis V4.4, build 102.47.2299 (Bruker Daltonics). Calibration files were created by spiking sample runs with electrospray ionisation (ESI) tuning mix G2421-60001 (Agilent) and identifying calibrant peaks on the spectra shared between samples. Sample runs were first calibrated against these reference peaks and a mass list was generated for those peaks with an intensity above the background noise ($\gtrapprox$ 40 000) and an S/N ratio greater than 4. Mass lists comprising m/z and intensity values for each peak were then imported to PetroOrg software (Florida State University) for peak assignment. Assignment of the peaks to a chemical formula was based on the ultra-high accuracy of the mass values, with a tolerated mass error of ±1 ppm, and calculated against the following elemental parameters: C1-100; H2-200; O1-30; N0-4.

Assigned peak lists were visualised and merged using Python scripts adapted from Kew *et al.* (2017) with the output aligned peak lists imported to PRIMER (Quest Research Limited) for statistical analysis.

2.2.2 Chromatography Mass Spectrometry

Bio-oil samples were additionally analysed externally by the Leibniz-Institut für Agrartechnik und Bioökonomie (ATB) according to the standard procedures of the Department of Bioprocess Engineering. Samples were diluted 1:1 (v/v) with 10% acetonitrile and filtered through a PTFE syringe and then immediately measured for phenols and furans. Determination of fatty acids was by Gas Chromatography (GC) after acidification and dilution (1:1 v/v) with phosphoric acid. Lactic acid was determined by High-Performance Liquid Chromatography (HPLC) after filtration.

2.2.3 Hach Cuvette Tests

Several chemical parameters were measured with the use of pre-dosed reagent cuvettes (Hach) and subsequent photometric analysis. Test designations LCK914 and LCI400 were used to measure Chemical Oxygen Demand (COD) in the ranges of 5-60 g/L O_2 and 0-1000 mg/L O_2 respectively. The working procedure required 200 µL or 2 mL of sample be added to the vial and mixed by inversion, followed by heating in an LT200 thermostat (Hach) to 148 °C for 2 hours before mixing again once cool.

The principle is that potassium dichromate enables the oxidation of carbon via the hexavalent dichromate ion ($Cr_2O_7^{2-}$) giving up its oxygen to create carbon dioxide (CO_2). This reaction reduces $Cr_2O_7^{2-}$ to the trivalent chromium(III) ion (Cr^{3+}), and these two ions absorb at different wavelengths (420 nm and 605 nm respectively), thus the lower range tests calculate a decrease in $Cr_2O_7^{2-}$ whereas the high range tests measure an increase in Cr^{3+}. The reaction is dependent on the high temperature and the presence of sulphuric acid and silver sulphate acting as the catalysts for complete oxidation. The presence of mercury sulphate in the tests ensures no interference from chloride as a competitor for the oxidation of organic carbon by reacting to form mercuric chloride.

Total Organic Carbon (TOC) was measured using kit LCK386 in the range of 30 – 300 mg/L C. The test requires 1 mL of sample be added to a digestion cuvette and then shaken without a cap on a TOC-X5 (Hach) vertical shaker for 5 minutes. A gas-permeable membrane and indicator cuvette are then attached to the digestion cuvette and this is heated to 100 °C for 2 hours. The test works by acids in the digestion cuvette converting the inorganic carbonates of the sample into CO_2, which is purged out with a fan and vibration by the shaker. The organic species are then oxidised with acid, peroxodisulphate and heat to generate further CO_2 which passes through the membrane into the indicator cuvette, where it causes a colour change to occur.

Kit LCK365 was used to measure organic acid concentrations in the range of 50 – 2500 mg/L of acetic acid equivalents, described as the collective reference for low-molecular fatty acids, in particular: acetic acid, propanoic acid and butanoic acid. The test requires 400 µL of sample be added to a mixture of diols and acids and heated to 100 °C for 10 minutes before the addition of iron(III) salts. The reaction with fatty acids generates fatty acid esters which further react with iron(III) salts to form a reduced red iron complex. All Hach test cuvettes are then measured spectrophotometrically on a DR5000 Spectrophotometer (Hach) which reads the cuvette barcodes, selects the necessary wavelengths and calculates the desired test parameter.

2.2.4 Total Solids (TS)

Samples of digestate (2.3.1) were weighed in aluminium dishes before being heated to 105 °C for 24 hours in a Universal Oven (Memmert). The samples were then weighed and heated repeatedly until a stable final weight had been achieved. The remaining weight of the sample after evaporation was the total solids (TS) of the digestate.

2.3 Biological Methods

2.3.1 Environmental Sampling

Sediment samples were taken from the natural environment for the purpose of isolating microbial communities that may have the ability to degrade bio-oil aerobically (Section 2.4). Three sites were sampled; two located in the Scottish council area of Edinburgh, the coastal area of Cramond beach (Cr) and an artificial freshwater pond in Blackford (BP), and the third from Benhar Bing located in North Lanarkshire (BHB), a constructed wetland for the treatment of acid drainage from an ironstone spoil heap (Heal and Salt, 1999). Figure 2.2 shows the location and co-ordinates of the sampling sites.

Figure 2.2. Sediment sampling locations. Benhar Bing (BHB) (55°50'48.6"N 3°45'58.3"W), Blackford Pond (BP) (55°55'30.1"N 3°11'47.8"W) and Cramond (Cr) (55°58'51.5"N 3°17'58.6"W).

Sediment cores were taken from each site using a corer consisting of a sterilised hollow steel tube with a plastic core tube inside, embedded directly into the sediment which, when sealed at the top, removes ~30 cm of intact sediment when withdrawn. Samples were then taken from the core using 50 mL Falcon tubes embedded directly into the sediment at the required depth and stored at 4 °C. Microbial communities were isolated as described in Section 2.3.2.

It was expected that communities from BHB would be the most likely to survive the toxicity of bio-oil due to the acidic nature of the environment so for the initial bio-oil toxicity tests three sediment sample were taken from Cr, one from BP and seven sediment samples were taken from random locations at BHB plus two water samples. However further tests on environmental isolates were all taken from BHB on a separate occasion and within this location four sub-sites were sampled (Figure 2.3), the shore of the first outflow pool (BHB1), the second outflow pool (BHB2), the run-off (BHB3) and a nearby shallow pool observed to be covered with a layer of oil

(BHB4). The first two sites' cores were sampled twice, ~30 cm apart (BHB1-1, BHB1-2 and BHB2-1, BHB2-2), giving a total of six sediment samples.

Figure 2.3. Benhar Bing sediment sampling locations.

All AD tests (Section 2.6) were performed using digestate obtained from the AD reactors at Seafield Wastewater Treatment Plant located in Edinburgh. The reactors handle sludges from three different sources, a primary sludge (solids settled out from sewage), a secondary biological sludge (bacteria/biomass used for settled wastewater treatment) and imported sludge from satellite sites (mix of primary and secondary sludges). The sludges are mixed together and thickened to an 18% – 20% total solids (TS) cake with the liquor (centrate) returned to the wastewater plant for treatment. The cake is then pumped into a Thermal Hydrolysis Plant (THP) which utilises high temperature and pressure to sterilise the sludge and improve biodegradability. The sludge exits at approximately 100 °C, is cooled to ~45 °C and watered down to approximately 10% TS before it is fed to the digesters. The digesters are mixed Continuous Stirred-Tank Reactors (CSTR) which operates with a retention time of 22 – 28 days at mesophilic temperatures. The digesters are constant volume vessels which overflow when they are filled into sludge (digestate) holding tanks which are fed to centrifuges to produce a final cake at 33% TS. The return liquors from this

(<0.2% TS) are returned to the wastewater process for treatment. The overflow digestate was obtained on two separate dates and stored at 4 C° until required.

2.3.2 Growth Media

All microbial culturing was performed under aseptic conditions over Bunsen burner flame and cultured at 30 °C in a G24 Environmental Incubator Shaker (New Brunswick Scientific). Microbial communities from environmental samples were isolated by adding 3 g of sediment to 10 mL of phosphate-buffered saline (PBS), shaken for 30 mins and then left to settle for a further 30 mins, the resultant supernatant was used as the culture of organisms.

Single species of microbial organisms that were identified for their potential ability to degrade bio-oil were isolated from pyrolysis product samples, acquired from collaborators or purchased directly from the German Collection of Microorganisms and Cell Cultures (DSMZ). A list of the species acquired is given in Table 2.2.

Organism	Source	Culture Medium
Bacillus cereus	DSMZ	Nutrient broth
Cupriavidus basilensis	DSMZ	Nutrient broth
Halomonas sp. Strain TGOS-10	Gutierrez *et al*., 2013	Nutrient broth
Trichosporon sp.	M9 Bio-Oil Medium	Malt extract

Table 2.2. Pure cultures of organisms used in the project with source and culture medium.

The bacterial species *B. cereus*, *C. basilensis* and *Halomonas* sp. were all able to grow in nutrient broth which was prepared by dissolving 5 g peptone (VWR) and 3 g meat extract (Thermo Scientific) in 1 litre of deionised water and adjusting the pH to 7.0. Malt extract medium was used as the growth medium for the fungal strain

Trichosporon sp. and was prepared by dissolving 17 g malt extract (Thermo Scientific) and 3 g soya peptone (Sigma) in 1 litre of deionised water and adjusting the pH to 5.4. For the purposes of cloning (Section 2.3.7), One Shot® INVαF′ Chemically Competent *Escherichia coli* (Thermo Fisher) were used to produce high quantities of plasmid DNA. *E. coli* culture was performed in Lysogeny broth (LB) and was prepared by dissolving 10 g bacto-tryptone (VWR), 5 g yeast extract (Thermo Scientific) and 10 g NaCl (Thermo Fisher) to 1 litre of deionised water and adjusting the pH to 7.5. All culturing media were sterilised by autoclave (121 ˚C, 15 mins) before use and could be converted to solid medium plates by adding 12 g/l agar (VWR), microwaving until molten and then pouring whilst cooling. For the purposes of selection, the antibiotic kanamyacin and X-gal (5-bromo-4-chloro-3-indolyl-β-D-galactopyranoside) (Simga) were added to LB agar plates to a final concentration of 50 and 80 µg/mL respectively.

Liquid cultures of all microbial isolates were prepared for long term storage in bacterial freezing medium. The medium consisted of a 1:1 mix of the respective culture medium and 50% deionised water and 50% glycerol (Sigma), 750 µL of the medium was mixed by inversion with 750 µL of overnight culture in cryotubes and stored at -80 °C.

Bio-oil toxicity tests (Section 2.5.1) and bio-oil culture passaging (Section 2.5.2) were performed using bio-oil as a carbon source for microbial growth in M9 minimal and wastewater media; nutrient broth was used as a positive control. M9 minimal medium was prepared using 200 mL M9 salt solution, 2 mL 1 M $MgSO_4$, 100 µL 1 M $CaCl_2$ and 20 mL carbon source solution (bio-oil) added and adjusted to 1 litre. The M9 salt solution was made using 64 g Na_2HPO_4-$7H_2O$, 15 g KH_2PO_4, 2.5 g NaCl and 5 g NH_4Cl adjusted to 1 litre and sterilised. Due to the increase in bio-oil ageing at higher temperatures and the corresponding unpredictable changes in chemistry, the medium was sterilised before the addition of bio-oil.

2.3.3 DNA Extraction

Microbial community DNA was extracted and purified from samples using the PowerSoil® DNA Isolation Kit (QIAGEN; Mo-Bio pre-January 2017) according to the manufacturer's instructions available online. Due to the unknown nature of natural microbial communities and the presence of particulate-bound organisms, a more thorough cell disruption technique is required to disrupt the membranes of potential yeasts or gram-positive bacteria and disassociate cells from particulate matter. In brief, ~0.25 g of sample was added to the extraction tube with cell lysis achieved both mechanically and chemically via a bead-beating step and the addition of SDS to disrupt cell membranes. After this, inhibitors were removed by precipitation and the DNA was adsorbed to silica membranes in the presence of high salt. Further residual contaminants were removed using ethanol and then the DNA was eluted in 100 µL of Tris-containing buffer.

Plasmid DNA was extracted using the QIAprep Spin Miniprep Kit (QIAGEN) according to the manufacturer's instructions available online. Briefly, the DNA preparation kit works on the basis of alkaline lysis of bacterial cells with DNA adsorption to silica membranes in the presence of high salt and elution in a Tris-containing buffer. All DNA was stored at -20 °C for long-term storage.

Purification of agarose gel-bound DNA (Section 2.3.5) was by gel extraction. After electrophoresis and visualised on a UV Transilluminator (FOTODYNE) required bands were carefully excised with a clean scalpel and weighed in a 1.5 mL Eppendorf tube. DNA was extracted using a Wizard® SV Gel and PCR Clean-Up Kit (Promega) according to the manufacturer's instructions available. The kit follows a similar silica membrane DNA binding method to the previous extraction techniques however the gel is dissolved at 60 °C in a membrane binding solution (1 µL per 1 g of gel) before adsorption. Elution was in 30 µL of nuclease-free water. Purification of PCR products was performed using the same kit without the gel dissolving step and the membrane binding solution volume was altered to be of equal volume of the PCR reaction.

2.3.4 DNA Quantification

Quantification of DNA was by the Quant-iT™ PicoGreen® dsDNA Assay Kit (Thermo Fisher) using a Gemini XPS Microplate Reader (Molecular Devices) according to the manufacturer's instructions available online. In brief, the kit utilises an ultrasensitive fluorescent nucleic acid stain that binds selectively to double stranded DNA, (dsDNA) which is excited at 485 nm and has peak fluorescence intensity at 520 nm. A standard curve of Lambda DNA of known concentration is run with all samples and the resultant relative fluorescence units (RFU) are converted to ng/μL using the trendline equation from the standard curve. Due to the stain's ability to bind to double standard DNA only, it is more sensitive and accurate than the typical absorbance at 260 nm based determination method of DNA quantification, which shows significant interference from nucleic acid contaminants.

2.3.5 Agarose Gel Electrophoresis (AGE)

Separation and visualisation of DNA products was performed by AGE on 0.8 – 2% (w/v) agarose gels depending on the length of the expected product. Gels were prepared by dissolving the necessary amount of electrophoresis-grade agarose (Invitrogen) in 1× TAE buffer (containing 40 mM Tris (Invitrogen), 20 mM acetic acid and 1 mM EDTA) by microwave heating for 1 – 2 mins. The gel solutions were left to cool to handling temperature before the addition of ethidium bromide (Sigma-Aldrich) to a final concentration of 0.5 μg/mL. The gel solutions were then poured into gel casts with the appropriate number of well combs and left to set before loading DNA products.

DNA ladders were electrophoresed alongside samples depending on the expected size of the DNA product with products under 1 kb run with 100 bp DNA Ladder (NEB) whilst those above 1 kb were run with 1 kb DNA Ladder (NEB). Samples and DNA ladders were mixed with 6× gel loading dye (NEB), loaded onto the gel and electrophoresed for 30 – 60 mins, depending on product size, in a horizontal electrophoresis system (Bio-Rad) supplied with 70 – 100 V by a PowerPac 300 DC power supply (Bio-Rad). Gels were visualised on a UV/White Light Transilluminator (UVP).

2.3.6 Denaturing Gradient Gel Electrophoresis (DGGE)

Visual and statistical comparisons of microbial community diversity were generated by DGGE of Polymerase Chain Reaction (PCR) amplified microbial DNA as described by Strathdee and Free (2013). The V3 regions of the 16S rRNA gene were used for bacterial and archaeal comparisons. Each PCR reaction (50 µL) contained 34.75 µL nuclease-free PCR grade water, 1× PCR buffer (NEB ThermoPol®), 2.5 mM $MgCl_2$, 200 µM dNTP mix (NEB), 0.4 µM of each primer (see table 2.3), 0.025 U/µL *Taq* polymerase (NEB) and 1 µL of template DNA with an average concentration of 10 ng/µL. Amplification was by a two-stage PCR where 1 µL of the product of the first round was used as the template of the second round. This nested PCR approach reduces the level of non-specific products by amplifying a secondary target within the initial product allowing a larger number of amplification cycles but retaining the specificity of the primers. The second round also utilises primers created with the addition of a GC-clamp, a guanine (G) and cytosine (C) rich length of DNA that remains double stranded irrespective of the concentration of denaturant in the gel (Muyzer, de Waal and Uitterlinden, 1993; Strathdee and Free 2013).

Two 11 mL stock solutions of 8% (v/v) acrylamide/bisacrylamide (37.5:1) (VWR Acrylogel) denaturant gel were prepared in 1× TAE, one with a "low" 0% denaturant and the other with a "high" 80% (relative to the Strathdee and Free (2013) protocol-specific "100%" value), using 0.56 M urea (SLS) and 0.8 M formamide (Thermo Fisher). A 1 mL gel "plug" made from 0% stock was first poured between two glass plates to seal the base of the gel stack, after this had set the two main solutions were mixed and poured using a twin-well gradient mixer with plastic tubing connected to a peristaltic pump; the mixing ensured a linear gradient of 30 to 70% denaturant (relative to the Strathdee and Free (2013) protocol). To ensure a level main gel, 1 mL of water-saturated butanol (Simga) was added on top of the main gel whilst it set to ensure samples started at the same height in the gel before electrophoresis, once set the butanol was poured off and the remnants removed using paper towel. A sample comb was then inserted between the glass plates and a "stacking" gel of 4 mL 0% stock was poured to form the sample wells. A 10% (w/v) stock solution of ammonium persulphate (APS) (Sigma-Aldrich), made in deionised water, and

tetramethylethylenediamine (TEMED) (Sigma-Aldrich) were used as polymerising agents at 0.5 and 0.05% (v/v) respectively prior to pouring the gels with the "plug" and "stacking" gels given double the concentration of polymerising agents. Samples of 20 µL were loaded with 6× gel loading dye (NEB). Electrophoresis was performed using a DCode™ Universal Mutation Detection system (Bio-Rad) and set to run at 75 V for 16 hours with the gel in 60 °C 1× TAE buffer.

Visualisation of bands was by silver nitrate staining. Immediately after electrophoresis the gel was submerged in 200 mL fix solution containing 0.5 % (v/v) glacial acetic acid (Sigma-Aldrich) and 10% ethanol (v/v) (Haymakimia) and shaken gently in a staining tray for 30 mins. The fix was poured off and retained and the gel was then covered with 300 mL of additional fix solution with 0.9 g/L silver nitrate and shaken for 20 mins. After disposal of the stain and washing of the gel several times with deionised water it was then developed in 200 mL of developing solution containing 30 g/L sodium hydroxide (Sigma-Aldrich) and 1.35% (v/v) (Fisher Scientific) until bands could easily be identified on the gel. At this point the developing solution was disposed of and the gel washed again several times with deionised water before a final fix in the retained 200 mL fix solution for at least 30 mins. The gel was then digitally scanned (Perfection V700 PHOTO, EPSON) and the image imported to BioNumerics 6.0 (Applied Maths) for identification, normalisation of band intensities and band-matching. Band data was then output to PRIMER (Quest Research Limited) for multivariate statistical analysis.

2.3.7 Sanger Sequencing

Unknown microbial isolates were submitted for Sanger sequencing (Sanger, Nicklen, and Coulson, 1977) for identification. Pure 16S or 18S rRNA gene fragments were required from the isolate and thus prior to submission for sequencing single colonies of the microorganism were isolated from solid growth medium plates after an overnight incubation at 30 °C and grown overnight again in liquid culture. The following day the cultures were centrifuged for 5 mins at 18 000 × g and the DNA extracted from the pellets (Section 2.3.3). Second round DGGE PCRs (Chapter 2.3.11) were performed on the DNA from unknown isolates with some known

eukaryotic species DNA amplified with dedicated 18S rRNA primers (Chapter 2.3.11). The products were used in a TA cloning kit with pCR™2.1 Vector (Thermo Fisher) according to the manufacturer's instructions available. The kit utilises a one-step cloning strategy that allows for the insertion of *Taq*-amplified PCR products directly into the plasmid vector with ligation via the use of an ExpressLink™ T4 DNA Ligase. The linearised vector is supplied with a single deoxythymidine residue at the 3' end which takes advantage of the *Taq* polymerases mechanism of adding a single deoxyadenosine to the 3' ends of PCR products, thus ensuring efficient ligation.

Transformation was into One Shot® INVF' Chemically Competent *E. coli* with the plasmid vector providing kanamycin resistance and blue/white screening of colonies. A single transformed colony was removed from a LB agar plate using a sterile picker and added to 10 mL LB. The culture was then incubated overnight before isolation and DNA extraction as previously mentioned. The DNA was supplied to Edinburgh Genomics with M13 primers for sequencing the inserted DNA (Table 2.3). Edinburgh Genomics use an ABI 3730XL capillary sequencing instrument with a standard reaction mix and PCR protocol using the BigDye v3.1 Terminator Cycle Sequencing Kit (Thermo Fisher), available online.

2.3.8 Illumina 16S rRNA Sequencing

Next-generation 16S rRNA gene amplicon sequencing was employed for high resolution microbial community analysis. The technique utilises conserved regions within the 16S rRNA gene as primer binding sites flanking hypervariable regions which, when sequenced, can be used to identify the organisms taxonomy. The protocol followed the method described by Caparaso *et al.* (2012) where primers are synthesised with additional sequences as shown in Figure 2.4: a linker sequence that is not homologous to the 16S rRNA sequence directly after the primer binding site, an error-correcting Golay barcode sequence and an Illumina adapter. PCR of sample DNA using these primers yields a library of products that are then pooled and sequenced using an additional three primers that read the forward, reverse and barcode section of each product.

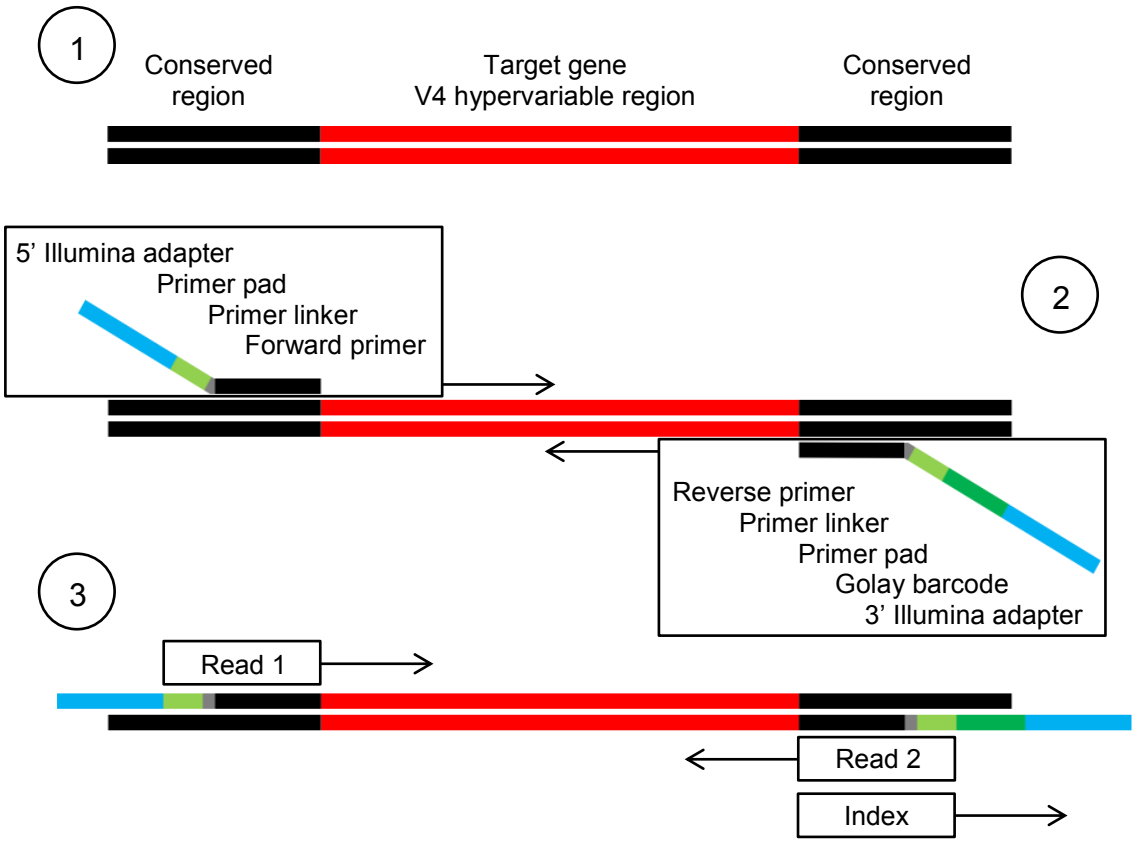

Figure 2.4. Library preparation for Illumina 16S rRNA sequencing. ① The V4 hypervariable region (red) was selected for sequencing and primers were developed for the flanking conserved regions (black). ② Primers consisted of the complimentary forward/reverse sequence of the conserved region (black), a short primer linker (grey), a short primer pad (light green), a Golay barcode sequence (reverse only; dark green) and a 5'/3' Illumina adapter. The fragment was amplified by PCR resulting in a library of barcoded fragments. ③ The resultant fragments consisted of the target gene and additional primer sequences which were amplified using the Illumina protocol with the read 1, 2 and index sequencing primers for the forward, reverse and barcode sequences.

The sequencing takes place on a flow cell coated with oligonucleotides complimentary to the Illumina adapters which are incorporated in the amplification product. The products bind to these sites and serve as a template for PCR amplification of the oligonucleotides. After each round of amplification the

immobilised strand bends to form a bridge to a complimentary adapter site where, after denaturation of the double stranded template, it then acts as the template for further amplification, subsequent extension and denaturation generates a cluster of amplification products at unique locations on the flow cell. Sequencing reagents with fluorescently labelled nucleotides are then added and each cycle of amplification is scanned for incorporation of a nucleotide and thus the fragment sequence.

Samples were extracted as previously described and the DNA was used as the template for PCR amplification of the V4 region of the 16S rRNA gene. Each PCR reaction (25 µL) contained 18.5 µL nuclease-free PCR grade water, 1× PCR buffer (NEB ThermoPol®), 1 mM $MgCl_2$, 200 µM dNTP mix (NEB), 0.25 µM of each primer (see table 2.3), 0.025 U/µL Taq polymerase (NEB) and 1 µL of template DNA. PCR thermal cycles and primers are listed in Table 2.3. It should be noted that the additional barcode sequence was on the reverse primer and thus these were added separately to each sample as opposed to their inclusion in a master mix.

The forward primer was also adapted from the original manuscript to include a greater proportion of archaeal sequences. Using the online SILVA TestPrime 1.0 tool for summarising the taxonomic coverage of primer pairs, it was found that the original 515f primer only covered 52.6% of the known archaeal sequences in the SILVA database. A single nucleotide alteration at the 5' fourth base position from cytosine (C) to either of the pyrimidine bases (Y) was found to increase the coverage to 84.9%. As a consequence the forward read primer for sequencing was also modified for the inclusion of the single nucleotide alteration.

The PCR products were loaded onto an agarose gel and electrophoresed to separate the product (~300 bp plus ~100 bp from additional sequences) from any possible contaminant and primer sequences. Sample DNA was gel extracted (Section 2.3.3), quantified (2.3.4) and pooled such that each sample had identical concentration and then sent for sequencing at Edinburgh Genomics with the three additional sequencing primers.

2.3.9 Illumina Sequence Data Processing

Edinburgh Genomics provided demultiplexed sequences as the output from Illumina sequencing which was analysed using the QIIME 1.9.1 pipeline (Caporaso *et al.*, 2010). Kozich *et al.*, (2013) showed that short amplicons with greater overlap between the forward and reverse reads were more accurate than longer reads with short overlaps, as such the reads were paired with a minimum 250 bp overlap and combined based on the sample, after which low quality (phred <19) and short (<250 bp) reads were filtered out. Chimeric sequences generated during the PCR from multiple templates were identified using the usearch quality filter v10.0.240 (Edgar, 2010) against the SILVA 128 reference database (Quast *et al.*, 2013) and removed. Operational Taxonomic Units (OTUs) were picked '*de novo*' by uclust (Edgar, 2010), assigned taxonomy against the SILVA 128 reference database and aligned using PyNAST (Python Nearest Alignment Space Termination; Caporaso *et al.*, 2009) alignment against the SILVA 128 reference database with sequences that failed to align being removed. Abundant sequences from the control samples that were present in test samples were considered contaminants and removed from the dataset along with singleton OTUs. Alpha rarefaction analysis was performed on the data sets before exporting the OTU table to PRIMER for multivariate analysis.

2.3.10 Single Species PCR Assays

PCR assays were developed for the rapid determination of the presence or absence of a single species in mixed cultures. Individual primer sets and PCR cycling conditions were chosen from the literature and adapted or developed for this project. All PCR reactions (50 µL) contained 41.75 µL nuclease-free PCR grade water, 1× PCR buffer (NEB ThermoPol®), 200 µM dNTP mix (NEB), 0.125 µM of each primer, 0.025 U/µL Taq polymerase (NEB) and 1 µL of template DNA. Individual cycling conditions and primers are detailed in Table 2.3. PCR products were electrophoresed on agarose gels with the presence of a band indicative of presence of the organism.

2.3.11 PCR Conditions

All PCR reactions were set up under sterile conditions in a PCR6 PCR cabinet (LABCAIRE) and sterilised by a 15 minute UV treatment before the addition of

polymerase and template DNA. Standard PCR was performed in a MultiGene™ OptiMax (Labnet International) thermal cycler. Quantitative PCR (qPCR) was performed in a CFX96 Touch™ Real-Time PCR Detection System (Bio-Rad) using the QuantiNova SYBR Green PCR Kit (QIAGEN) according to the manufacturer's instructions available online and analysed using CFX Manager 3.0 (Bio-Rad) software. Gene copy number was quantified against a dilution series of a cloned insert of known concentration with copy number calculated as:

$$Copy\ number = \frac{(amount\ of\ DNA * Avogadro's\ number)}{(length\ of\ DNA * 1 \times 10^9 * average\ weight\ of\ a\ base\ pair)}$$

With units:

$$number = \frac{(ng * number/mole)}{(base\ pairs * ng/g * g/mole\ of\ base\ pair)}$$

Where: Avogadro's number = 6.0221409×10^{23}

Average weight of a base pair = 650

Table 2.3 details the primers sets, cycling conditions and source citations for each of the PCRs.

	Gene	Primer	Thermal Cycling Conditions	Reference
Bacterial Round 1 DGGE	16S rRNA	BactF	94 °C for 5 m; followed by 30 cycles of 94 °C for 1 m, 55 °C for 1 m, 72 °C for 3 m; followed by 72 °C for 7 m	Fernández *et al*., 1999
		BactR		
Bacterial Round 2 DGGE	16S rRNA	341F-GC	94 °C for 5 m; followed by 28 cycles of 94 °C for 1 m, 64 °C for 1 m, 72 °C for 1 m 30 s; followed by 72 °C for 10 m	Muyzer *et al*., 1993
		534R		
Archaeal Round 1 DGGE	16S rRNA	ArchF	94 °C for 2 m; followed by 35 cycles of 94 °C for 30s, 52 °C for 1 m, 72 °C for 3 m; followed by 72 °C for 7 m	Fernández *et al*., 1999
		ArchR		
Archaeal Round 2 DGGE	16S rRNA	rSAf	94 °C for 5 m; followed by 5 cycles of 94 °C for 1 m, 64 °C for 30 s, 72 °C for 1 m; followed by 30 cycles of 92 °C for 30 s, 63 °C for 30 s, 72 °C for 1 m; followed by 72 °C for 10 m	Nicol *et al*., 2005
		PARCH519r		Øvreås *et al*., 1997
Bacillus cereus	motB	BCFomp1	94 °C for 5 m; followed by 30 cycles of 94 °C for 30 s, 545 °C for 1 m, 72 °C for 1 m; followed by 72 °C for 7 m	Oliwa-Stasiak *et al*., 2010
		BCRomp1		
***Halamonas* sp.**	16S	TGOS10F	94 °C for 3 m; followed by 35 cycles of 94 °C for 30 s, 60 °C for 30 s, 72 °C for 1 m; followed by 72 °C for 5 m	Gutierrez *et al*., 2013
		TGOS10R		
***Trichsporon* sp.**	ITS	TRF	94 °C for 3 m; followed by 30 cycles of 94 °C for 30 s, 49 vC for 15 s, 72 °C for 15 s; followed by 72 °C for 10 m	This project
		TRR		
Cupriavidus basilensis	16S rRNA	CbF	94 °C for 3 m; followed by 35 cycles of 94 °C for 30 s, 60 °C for 30 s, 72 °C for 1 m; followed by 72 °C for 5 m	This project
		CbR		
Phanerochaete chrysosporium	ITS	Pchr-F	94 °C for 4 m; followed by 30 cycles of 94 °C for 30 s, 59 °C for 30 s (decrease by 0.1 °C each round), 68 °C for 40 s; followed by 72 °C for 7 m	Lim *et al*., 2007
		ITS4		
Archaeal qPCR	mcrA	mcrA F	94 °C for 5 m; followed by 40 cycles of 94 °C for 1 m, 55 °C for 1 m, 72 °C for 3 m (the first five cycles incorporated a slow ramp rate of 0.1°C s^{-1} between annealing and extension temperatures)	Luton *et al*., 2002 Morris *et al*., 2014
		mcrA R		
Sanger Sequencing	Plasmid vectors	M13F	Performed by Edinburgh Genomics	Messing, 1983
		M13R		
	18S rRNA	EukA	94 °C for 1 m; followed by 36 cycles of 94 °C for 50 s, 55 °C for 50 s, 72 °C for 50 s; followed by 72 °C for 10 m	Diez *et al*., 2001
		P49		Dorigo *et al*., 2002
Illumina sequencing	16S rRNA	a515F	94 °C for 3 m; followed by 25 cycles of 94 °C for 45 s, 527 °C for 1 m, 72 °C for 1 m 30 s; followed by 72 °C for 10 m	Edited from Caporaso *et al*., 2011
		806R		
Caporaso (5')	Illumina PCR products	Read 1	Performed by Edinburgh Genomics	Caporaso *et al*., 2011
Caporaso (3')		Read 2		
Caporaso (Barcode)		Index		

	Gene	Primer	Sequence 5'-3'
Bacterial Round 1 DGGE	16S rRNA	BactF	AGAGTTTGATCCTGGCTCAG
		BactR	AAGGAGGTGATCCAGCCGCA
Bacterial Round 2 DGGE	16S rRNA	341F-GC	CGCCCGCCGCGCCCCGCGCCCGTCCCGCCGCCCCCGCCCGCCTACGGGAGGCAGCAG
		534R	ATTACCGCGGCTGCTGG
Archaeal Round 1 DGGE	16S rRNA	ArchF	TAAGCCATGCRAGTCGAAYG
		ArchR	YCCGGCGTTGAMTCCAATT
Archaeal Round 2 DGGE	16S rRNA	rSAf	CGCCCGCCGCGCGCGGCGGGCGGGGCGGGGGCACGGGGGGCCTAYGGGGCGCAGCAG
		PARCH519r	TTACCGCGGCKGCTG
Bacillus cereus	motB	BCFomp1	ATCGCCTCGTTGGATGACGA
		BCRomp1	CTGCATATCCTACCGCAGCTA
***Halamonas* sp.**	16S	TGOS10F	TGTCAGGCTAGAGTGCAGGA
		TGOS10R	CCAGTCATGAACCACACCGT
***Trichsporon* sp.**	ITS	TRF	AGAGGCCTACCATGGTATCA
		TRR	TAAGACCCAATAGAGCCCTA
Cupriavidus basilensis	16S rRNA	CbF	CCCGAGCTCAACTTGGGAAT
		CbR	TGAACCCTGCCGTGGTAATC
Phanerochaete chrysosporium	ITS	Pchr-F	GAGCATCCTCTGATGCTTT
		ITS4	TCCTCCGCTTATTGATATGC
Archaeal qPCR	mcrA	mcrA F	GGTGGTGTMGGATTCACACARTAYGCWACAGC
		mcrA R	TTCATTGCRTAGTTWGGRTAGTT
Sanger Sequencing	Plasmid vectors	M13F	GTAAAACGACGGCCAGT
		M13R	AACAGCTATGACCATG
	18S rRNA	EukA	AACCTGGTTGATCCTGCCAGT
		P49	AAGCCTGCTTTGAACACTCT
Illumina sequencing	16S rRNA	a515F	AATGATACGGCGACCACCGAGATCTACACTATGGTAATTGTGTGYCAGCMGCCGCGGTAA
		806R	CAAGCAGAAGACGGCATACGAGAT**********AGTCAGTCAGCCGGACTACHVGGGTWTCTAAT
Caporaso (5')	Illumina PCR products	Read 1	TATGGTAATTGTGTGYCAGCMGCCGCGGTAA
Caporaso (3')		Read 2	AGTCAGTCAGCCGGACTACHVGGGTWTCTAAT
Caporaso (Barcode)		Index	ATTAGAWACCCBDGTAGTCCGGCTGACTGACT

Table 2.3. Cycling conditions and primer sets for all PCRs (top) and their 5' – 3' sequences (bottom). The inclusion of ***** indicates a Golay barcode.

2.4 Statistical Methods

2.4.1 Two-Sample T-tests

Statistical significance between two sets of data was calculated using two sample t-tests assuming equal or unequal variance, where the null hypothesis is that the means of the two populations are equal. An F-test was performed prior to this to determine the variances of the populations (Snedecor and Cochran, 1989).

2.4.2 Analysis of Variance (ANOVA)

For three or more sets of data, significant difference was calculated using ANOVA to test the null hypothesis that the means of the populations are all equal (Fisher, 1925).

2.4.3 Two-Sample Kolmogorov-Smirnov Tests

Significant differences between test and control data that displayed a continuous distribution, such as biogas production from anaerobic digesters, was tested by two-sample Kolmogorov-Smirnov tests. The test quantifies the distance between the cumulative distribution functions of each set of data with the null hypothesis being that both data sets have the same distribution (Stephens, 1974).

2.4.4 Multivariate Analysis

Pagaling *et al.*, (2014; 2017) describe the use of the statistical package PRIMER 6 (Plymouth Routines in Multivariate Ecological Research) (Quest Research Limited) for the analysis of DGGE fingerprint and Illumina sequence data for microbial community comparisons, with this project using similar approaches and further utilising the package for analysis of multivariate data sets from mass/intensity lists generated by PetroOrg (Chapter 2.2.1). Microbial communities from environmental sediments and anaerobic digesters are still not well defined with major taxonomic "blind spots" of under-represented microbial clades (Eloe-Fadrosh *et al.*, 2016); as such Bray-Curtis similarity was chosen over a taxonomy-based similarity measurement. Additionally there is also no known method of building relatedness for chemical compounds. Bray-Curtis matrices were constructed and in the case of DGGE data, an initial square root transformation ensured the most abundant species

did not dominate the analysis. Illumina sequencing and FT-ICR MS are such high resolution techniques that the majority of the data is already from less abundant biological and chemical species and as such, the data did not undergo transformation before similarity analysis. The transformation, although useful for smaller datasets, appears to be affected by the sequencing depth of biological samples, which when transformed, drastically effects similarity, presumably due to rarer species missing from low-depth samples. Thus, relative abundance and Bray-Curtis similarity is used without transformation for these large datasets.

Bray-Curtis similarity matrices use a 0 – 100 index of similarity between samples where 0 indicates no shared species (variables) and 100 is an identical species composition with identical abundances. Visualisation of the matrices was by 2D nonparametric multi-dimensional scaling (NMDS) and principal coordinates analysis (PCoA) plots where samples are plotted according to distance dissimilarity from each other (Clarke and Warwick, 2001). The NMDS scaling was performed using 100 random starting configurations and accuracy was determined using the Kruskal stress with a value of < 0.2 considered acceptable (Kruskal, 1964). All Bray-Curtis similarity matrices are available electronically.

Additionally we used permutational analysis of multivariate dispersions (PERMDISP) to test for dispersion differences between groups of samples which can be the sole reason for a positive permutational multivariate analysis of variance (PERMANOVA) test. The latter tests for significant differences between groups of samples based on their Bray-Curtis similarity. By using both tests together it is possible to detect whether differences between groups are due to their location (composition) or dispersion (Anderson, Gorley and Clarke, 2008).

2.5 Aerobic Tests

2.5.1 Bio-oil Toxicity Tests

An initial experiment to test the growth of microbial communities isolated from natural environments was performed in a 48 well plate with each well filled with 1

mL of diluted WP/BO bio-oil to a COD of 1.5 g/l. At this point in the study it was unknown if microorganisms would be capable of utilising bio-oil as the sole source of carbon thus the plate was split between no added glucose in the left four columns and 0.01% glucose in the right. Each of the six rows were allocated an isolated environmental microbial community (100 µL) from each of the initial sites plus a water control. The plate was left to incubate in the dark for 15 days at 24 °C on a platform shaking at 100 RPM. Optical Density at 600 nm (OD600) was measured in each well every two days by a FLUOstar OPTIMA microplate reader (BMG Labtech).

Further tests on the four individual single species were performed using nutrient broth and 1 g/l COD SWP/BO bio-oil in M9 minimal medium. Sealable glass vials were filled with 3 mL of media and inoculated with 10 µL of overnight culture or a water control. The vials were left to incubate horizontally on a platform shaker at 100 RPM at 30 °C in the dark for five days with a daily OD600 reading using a U-1800 UV/VIS Spectrophotometer (Hitachi).

2.5.2 Bio-oil Culture Passaging

Initial test cultures were set up using the six isolated communities from BHB with the aim to observe any differences between the sampling sites communities ability to utilise bio-oil as the sole carbon source. Cultures of 30 mL M9 minimal medium with WP/BO bio-oil at a starting COD of 0.2 g/l were set up in 50 mL Falcon tubes and incubated on a shaking platform at 30 °C. Samples of 500 µL were taken periodically for OD600 readings on a U-1800 UV/VIS Spectrophotometer (Hitachi) and the cultures were left to run until a peak OD600 was reached. Cultures were passaged into new cultures set up with increased concentrations of bio-oil (2 – 4 g/l) and inoculated using the previous test's final cultures (100 µL).

2.6 Anaerobic Digestion (AD)

2.6.1 Hohenheim Biogas Yield Tests

All AD was performed under the guidelines set out by the Fermentation of Organic Materials Standard VDI 4630 with the Hohenheim Biogas Yield Test batch system chosen as the method of monitoring biogas output from AD (Helffrich and Oechsner, 2003). The digesters (Figure 2.5) consisted of a 100 mL glass syringe containing 20 mL wastewater treatment plant anaerobic digestate and any other supplementary compounds required for the individual tests. The plunger was coated with silicone grease to ensure an air-tight fit and inserted to the limit of the contents such that residual air was forced out of the syringe to hasten anaerobic conditions. Each syringe was tipped with a stopcock to allow easy access for sampling the biogas and digestate. The syringes were placed in a rotary mixer and incubated in a temperature control room set to 37 °C. Biogas was monitored daily by checking the distance the plunger had been forced out of the syringe using the scale on the side of the glass and methane concentrations were analysed once sufficient gas for analysis had been generated (≥ 20 mL) using an Advanced Gasmitter® digital infrared methane analyser (PRONOVA).

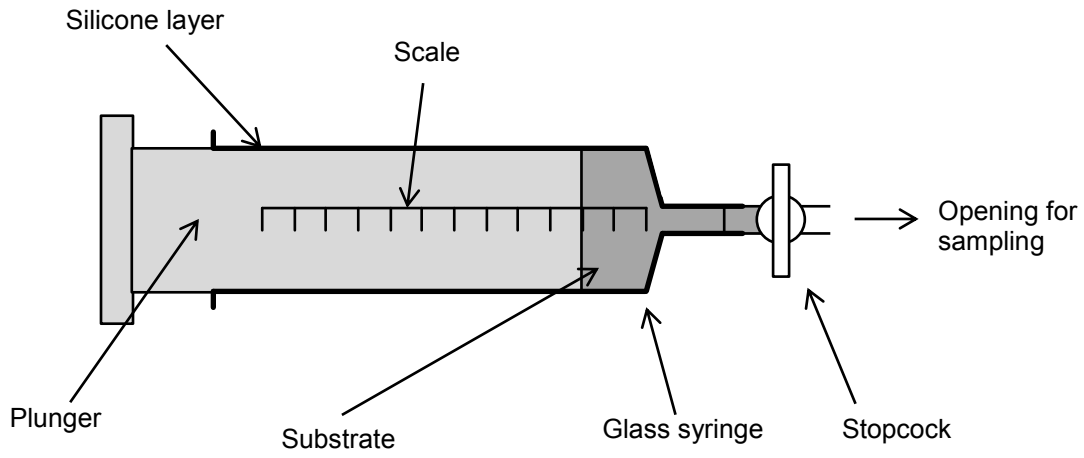

Figure 2.5. Schematic of the Hohenheim biogas yield reactors, as biogas is generated the plunger is forced further out of the syringe.

Additional substrates were added to the digestate to test their impact on biogas production and bio-oil inhibition. Both standard biochar and CreChar® plus a methanogenic inhibitor were investigated for their effects on AD. Both chars were added dry as 2% TS of the reactors and also after pre-incubation in anaerobic digestate for 48 hours. The methanogenic inhibitor sodium 2-bromoethanesulfonate (BES) (Sigma) was added to a final concentration of 50 mM.

CHAPTER 3: BIO-OIL CHARACTERISATION

3.1 Introduction

Bio-oils are complex organic liquids composed of thousands of molecular species, with their composition dependent on the feedstock and pyrolysis conditions. Due to their complexity it is favourable to characterise bio-oils in terms of their total composition as opposed to targeting only a few of their thousands of chemical species. A better understanding of the total composition of bio-oils is also necessary to help comprehend the significant contributions the feedstock and pyrolysis processes have on bio-oil production and potential downstream processing.

Characterisation of bio-oils however is extremely challenging as no single analysis method is capable of identifying every chemical compound they contain, and thus usually requires the combination of several techniques (Garcia-Perez *et al*., 2007). Chromatography techniques such as gas (GC) and liquid chromatography (LC) are routinely used to study volatile and polar compounds within bio-oil and are typically coupled to mass spectrometry (MS) to yield quantitative data on a limited number of selected compounds (Tessini *et al*., 2011; Kraiem *et al*., 2017). The broader scope of infrared (IR) and nuclear magnetic resonance (^{1}H and ^{13}C NMR) spectroscopy allows for the total determination of functional groups present in the sample, and although not able to give individual molecular information, they assist in the characterisation of bio-oil composition by giving detailed information about groups of compounds (Moralı, Yavuzel, and Şensöz 2016; Negahdar *et al*., 2016; Aboulkas *et al*., 2017).

Marshall and Rodgers (2004) denoted the concept of "petroleomics" for the characterisation of the chemical constituents of petroleum utilising ultrahigh-resolution Fourier transform ion cyclotron resonance mass spectrometry (FT-ICR MS). The approach has since been used for the characterisation of bio-oil where the fundamental aims of attempting to understand the molecular composition of complex mixtures apply (Jarvis *et al*., 2012). As previously mentioned, unlike petroleum, bio-oils are dominated by reactive oxygen species due to the thermal depolymerisation of

lignocellulose, which makes identification of these polar components by common MS techniques particularly difficult.

In brief, FT-ICR MS requires ionisation of the organic molecules which are then pulse-fed into a cyclotron where the magnetic field accelerates the ionised analytes to their resonant cyclotron frequencies, inducing an oscillating charge on two electrodes; this charge is converted by a Fourier-transform calculation to a mass/charge ratio (*m/z*) for every ion, giving a full spectrum of the ionised sample (Marshall, Hendrickson and Jackson 1998). The ultrahigh-resolution and mass accuracy of the technique allows for the discrimination and direct assignment of each peak to a unique elemental formula with some structural information elucidated from the atomic ratios. Complex organic mixtures are primarily composed of C, H and O elements and to a lesser degree, N, P and S (Marshall and Rodgers, 2004) thus assignment is made possible by the limited number of potential chemical formulae. The ultrahigh resolution mass accuracy is demonstrated in Figure 3.1 which shows a mass spectrum (200 – 500 *m/z*) from SWP/BO with the inset displaying a 0.1 *m/z* range with five detected signals, each with a corresponding formula assigned within a 0.1 ppm error range; the total peak number was 961.

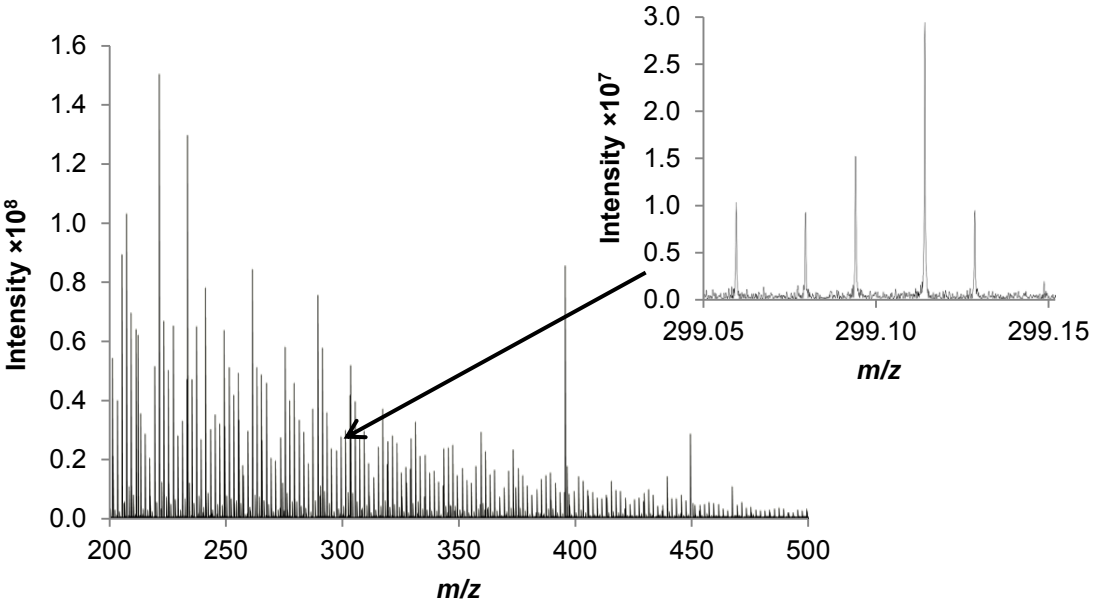

Figure 3.1. Mass spectrum from negative mode ESI FT-ICR MS of SWP/BO bio-oil. The five detected peaks in the 0.1 *m/z* range inset were identified as: $C_{16}H_{12}O_6$ (*m/z* 299.056112 ± 0.04); $C_{13}H_{16}O_8$ (*m/z* 299.077241 ± 0.003); $C_{17}H_{16}O_5$ (*m/z* 299.092497 ± 0.08); $C_{14}H_{20}O_7$ (*m/z* 299.113626 ± 0.01); $C_{18}H_{20}O_4$ (*m/z* 299.128883 ± 0.01).

There are several sources of ionisation which have been studied and combined for greater coverage of the full mass spectrum of bio-oils (Hertzog *et al*., 2016), with this study focusing on negative-mode electrospray ionisation (ESI). ESI is considered a "soft" ionisation technique due to its lower propensity for fragmentation of ions and is commonly used for bio-oil analysis due to its ability to rapidly ionise liquid samples (Jarvis *et al*., 2012), accomplished by applying a high voltage to create an aerosol. ESI also selectively ionises polar, heteroatom-containing compounds such as those that dominate bio-oil composition (Liu *et al*., 2012), with a study by Smith *et al*. (2012) showing the mass-resolving power of ESI being greater for bio-oil than laser desorption ionisation (LDI), another common ionisation method.

Due to the ability of FT-ICR MS to generate data for thousands of compounds, each with an individual chemical formula and intensity, the analysis and visualisation of this data is a challenge. The eponymously-named van Krevelen diagram (van

Krevelen, 1950) is a common method for visualisation of high-resolution mass spectrometric analysis of complex mixtures which plots the H/C (Hydrogen/Carbon) ratio against the O/C (Oxygen/Carbon) ratio for each compound in the sample (Kew *et al*., 2017). The pattern of the plots can aid in the interpretation of such large datasets as regions of the plot are associated with classes of compounds (Kim, Kramer and Hatcher, 2003; Hertkorn *et al*., 2008; Miettinen *et al*., 2015). Figure 3.2 gives an example van Krevelen plot with highlighted regions that denote specific compound classes.

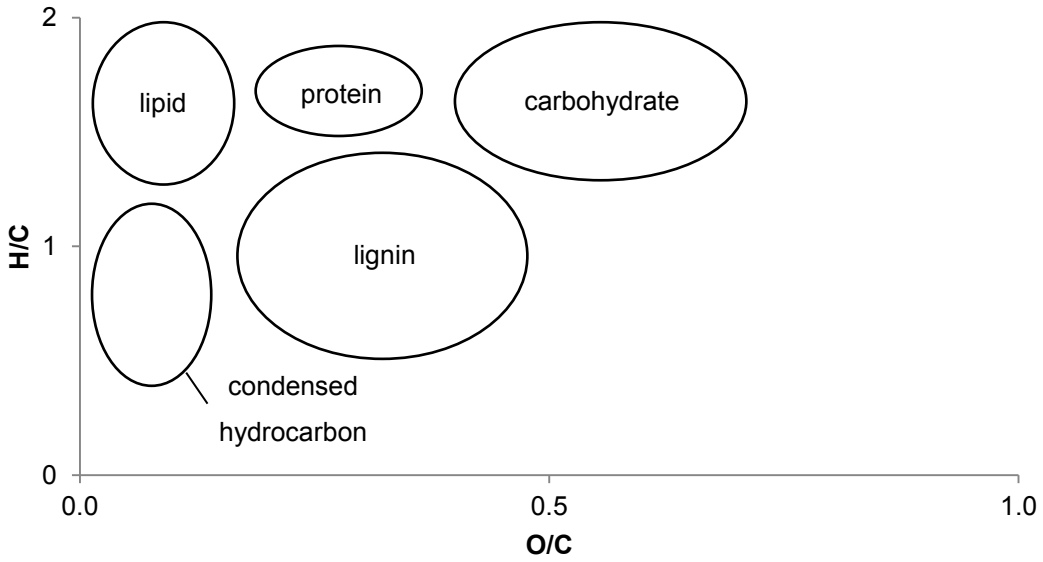

Figure 3.2. Example van Krevelen diagram with regional plots representing elemental compositions of major biomolecular compound classes of interest.

It is also possible to visualise the spread of the heteroatom classes found for each compound assigned using plots of the number of peaks assigned to O_x- and N_xO_y-containing classes. Bio-oils are reported as generally having very high oxygen content (Mohan, Pittman and Steele, 2006), however this is usually reported for bio-oil from lignocellulosic feedstock with little information about the elemental composition of bio-oils from anaerobic digestate and algae. To complete the characterisation of the bio-oils, multivariate statistical analysis can be performed on the ultrahigh resolution data to observe precise differences between the compositions of the bio-oil samples.

The bio-oils analysed with ESI FT-ICR MS for the purposes of this project were those used in anaerobic digestion (AD) tests (Chapter 5), AD/BO, MP/BO and SWP/BO, all of which were pyrolysed from feedstocks at 350 °C and diluted to a similar COD before analysis. The bio-oils used in the four AD tests were produced at the beginning of the first set of experiments and, due to the tendency of bio-oils to age after production, it was important to monitor these changes so that any differences in behaviour of repeated tests could be potentially explained. A sample of each of these bio-oils was additionally sent to the Leibniz-Institut für Agrartechnik und Bioökonomie (ATB) for quantitative analysis by GC-MS and high-performance liquid chromatography (HPLC) of selected C2 – C4 fatty acids, so that the starting concentrations of these potential feedstocks for AD were known, as well as selected phenols, furans and lactic acid which are documented microbial inhibitors known to be present in bio-oils (Lian *et al*., 2010; Hwang *et al*., 2013; Mourant *et al*., 2013). WP/BO bio-oil for use in anaerobic tests (Chapter 4) was supplied by the UKBRC and not characterised by ESI FT-ICR MS or sent for individual compound analysis.

3.2 Results

3.2.1 Pyrolysis

To gain enough bio-oil for the AD tests, both AD/BO and MP/BO bio-oils were produced from two separate runs and pooled together, whereas SWP/BO only required a single run to generate enough material for the tests. As previously described, volatiles and syngas produced as a consequence of the pyrolysis of biomass pass through a series of condensers where the liquid bio-oil collects at different temperatures. Table 3.1 details the percentage mass of each fraction obtained in the pyrolysis equipment after pyrolysis in relation to the starting biomass.

Biomass	HT1	HT2	HT3	Con	CT1	CT2	Char	Gas
SWP	7.91	1.63	2.18	39.98	3.09	1.74	31.73	11.74
AD	6.20	0.86	1.09	13.90	2.39	1.90	37.78	35.88
AD	4.51	2.97	1.22	12.08	3.05	2.13	38.30	35.74
MP	0.40	0.11	0.15	14.88	3.08	4.32	39.75	37.30
MP	0.33	0.00	0.31	11.00	3.53	4.39	40.26	40.17

Table 3.1. Percentage mass distribution after pyrolysis of biomass for bio-oils from anaerobic digestate (AD), *Macrocystis pyrifera* (MP) and softwood pellets (SWP) for use in AD tests. Pyrolysis gases passed through three heated and two cooled condensers where the bio-oil was collected in traps (HT1-3 and CT1-2). The central chamber housed a water-cooled coil condenser (Con) where the majority of bio-oil was collected.

The pyrolysis of softwood pellets produced over double the amount of bio-oil than any other biomass and this is reflected in the lower proportion of both biochar and non-condensable gases. Anaerobic digestate and *M. pyrifera* produced similar amounts of bio-oil; however, the pyrolysis of anaerobic digestate seemed to produce a larger volume of heavier organic phase bio-oils which were collected in HT1-3. These tar-like oils were not produced to such an extent from the pyrolysis of *M. pyrifera* which instead produced a higher amount of aqueous phase oils that were only condensed at sub-zero temperatures. *M. pyrifera* and anaerobic digestate also lost a higher proportion of mass as non-condensable gases which signify distinct differences between these lignin-limited biomasses and the lignocellulosic softwood pellets. As an aside, unlike the other samples, the bio-oil collected in CT2 from *M. pyrifera* could be strongly smelled through the organic vapour filter of a face mask.

It should be noted that wet biomass such as anaerobic digestate and *M. pyrifera* had to be dried before pyrolysis. This was achieved by heating the biomass samples at 60 °C for 48 hours and storing them in desiccation jars until required. The softwood pellets were purchased and had already been through an industrial drying and pelleting process, hence were stored as bought; therefore it is likely they contained a greater volume of water. The COD of the fresh bio-oils showed SWP/BO to contain

a far greater amount of COD than the others (529.67 ± 26.65 g/L COD over 158 ± 11.14 g/L COD for AD/BO and 76.3 ± 13.34 g/L COD for MP/BO (mean ± SD)).

3.2.2 Quantitative Analysis

Samples of the three bio-oils used in the AD tests were sent for quantitative analysis of some of the documented microbial inhibitors that are found in lignocellulosic bio-oils and organic acids that are important intermediate metabolites in AD and also commonly found in bio-oils. Figure 3.3 details the concentration of these compounds; however, due to differences in handling and moisture content between the respective biomasses, the values have been standardised to the COD concentrations of the bio-oils.

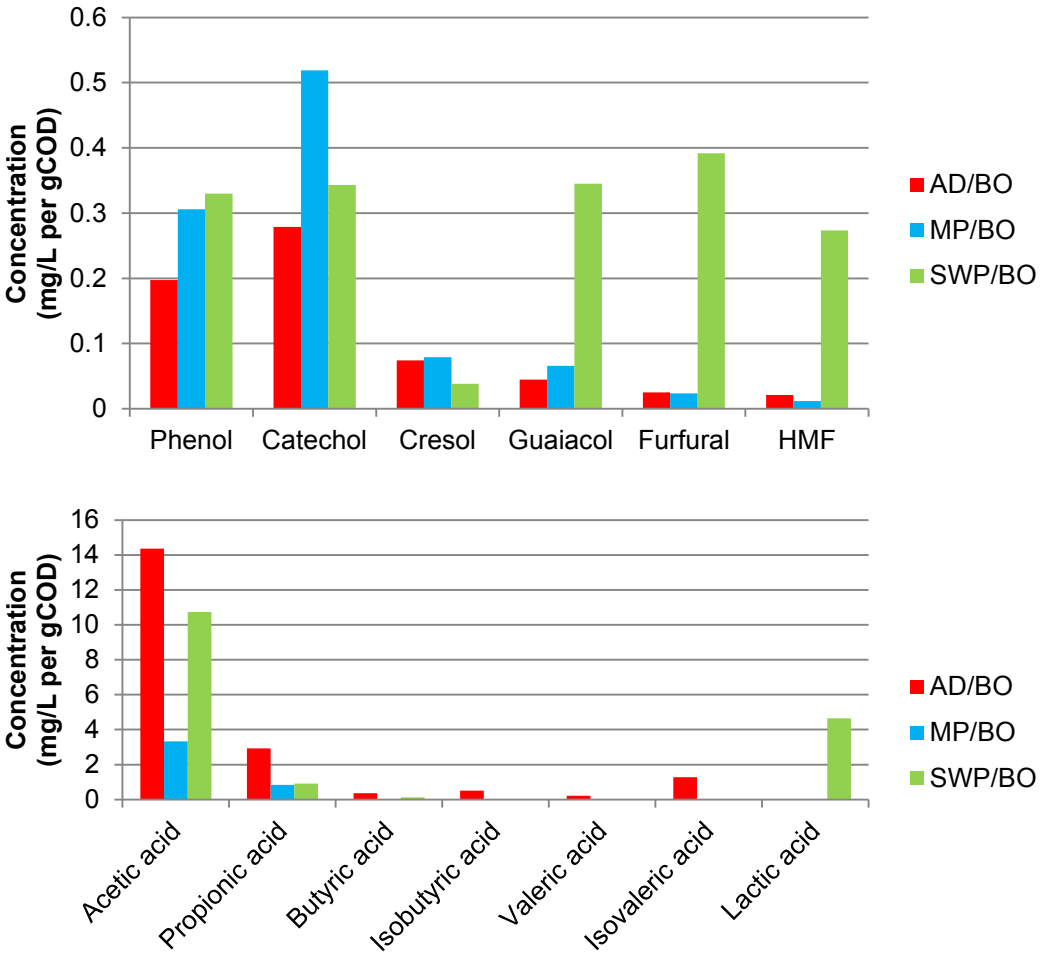

Figure 3.3. Concentrations per gCOD by GC-MS and HPLC of several microbial inhibitors (top) and short chain fatty acids (bottom) of bio-oils pyrolysed from anaerobic digestate (AD), *M. pyrifera* (MP) and softwood pellets (SWP). It should be noted that this data is from single samples and that conclusions based on these findings are subject to a greater degree of uncertainty.

Bio-oil produced from the lignocellulosic biomass of softwood pellets yields a higher concentration of almost all the microbial inhibitors analysed; in fact both AD/BO and MP/BO show almost no presence of the furan compounds furfural and 5-hydroxymethylfurfural (HMF). The same is true for the phenolic compound guaiacol, derived from wood creosotes, which are similarly produced to bio-oils. However with the exception of the low concentration of the phenolic cresol for all bio-oils, the other phenolic compounds, the biologically-ubiquitous phenol and the

common flavonoid catchecol (Machu *et al*., 2015), are present in AD/BO and MP/BO to similarly high levels as SWP/BO. With the exception of acetic acid, all bio-oils showed limited concentrations of fatty acids: MP/BO bio-oil contained the lowest concentrations across all the analytes, while AD/BO bio-oil contained the highest.

3.2.3 ESI FT-ICR MS

Each of the four AD tests (termed AD1 – 4; Chapter 5) used bio-oil produced prior to AD1, with additional samples of each taken before subsequent tests to monitor how the bio-oil had aged. In brief, AD1 and AD2 investigated the AD of the three different bio-oils described previously at differing concentrations, AD3 and AD4 used only SWP/BO bio-oil with a variety of different supplements aimed to test methanogenesis inhibition and biochar addition. The van Krevelen diagrams for the bio-oil spectra prior to AD1 are shown in Figure 3.4, with an additional regional diagram comparing the spread of identified compounds. It should be noted that only a single sample of each bio-oil prior to AD1 was analysed using ESI FT-ICR MS whereas two samples of each were analysed before AD2 and AD4 (AD3 SWP/BO bio-oil was not analysed).

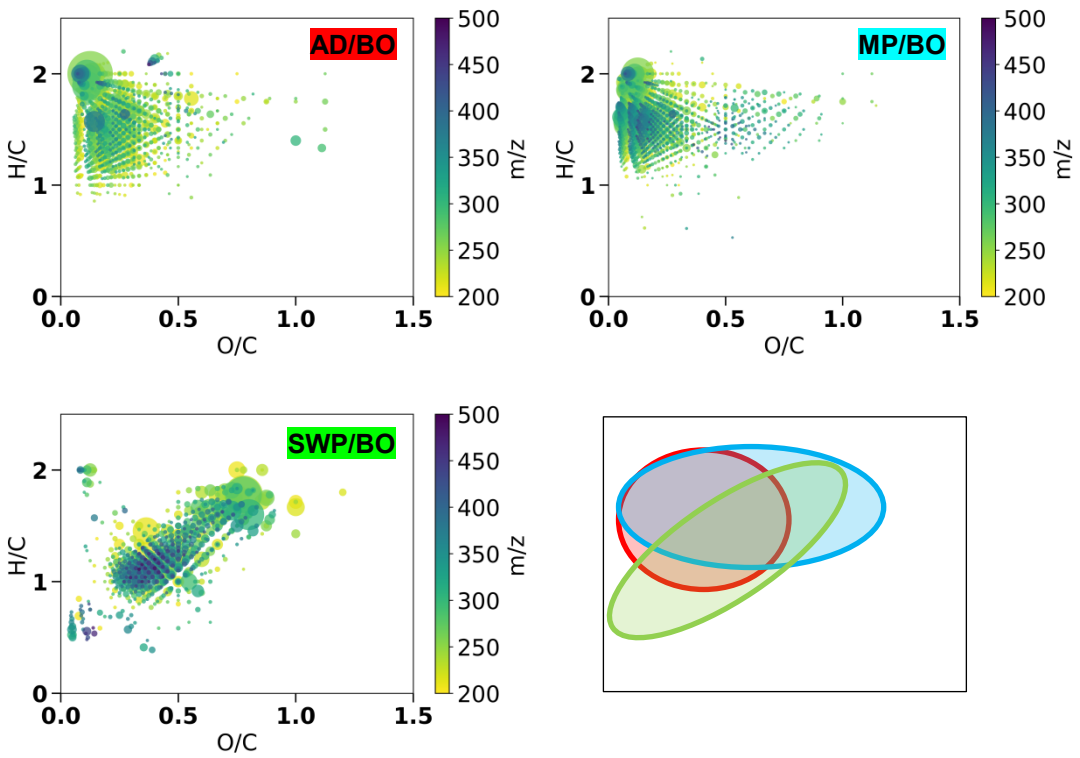

Figure 3.4. Van Krevelen diagrams for pre-AD1 bio-oils from anaerobic digestate (AD/BO; red), *M. pyrifera* (MP/BO; blue) and softwood pellets (SWP/BO; green). Formulae were assigned from ESI FT-ICR MS spectra. Plots are further colour-coordinated by the *m/z* of identified compounds with the relative abundance represented by the size of the point. The regional diagram (bottom right) highlights the differences in the observed spread of compounds' H/C and O/C ratios.

Both AD/BO and MP/BO bio-oils show a similar pattern in the spread of compounds on their corresponding van Krevelen diagrams, whilst SWP/BO shows a distinctly different pattern. The bio-oils pyrolysed from anaerobic digestate show an abundance of low *m/z* compounds with an H/C ratio of 1-2 and an O/C ratio of 0-0.5 indicating a high abundance of small lipids, such as fatty acids, and proteins for these bio-oils. MP/BO also shows clustering in this region and spreads further into the higher O/C range, >1, indicating the presence of carbohydrates. AD/BO also shows its plots extending down to lower H/C values <1, into the range of unsaturated hydrocarbons.

SWP/BO shows abundant clustering in the sugar region of 1.7 H/C and 0.9 O/C ratios indicating the presence of carbohydrates such as cellulose. Unlike the other bio-oils in this project there is also a concentration of high *m/z* compounds in the middle of the plot at H/C ~1 and O/C ~0.5. This region is known for being indicative of pyrolytic lignin compounds (Kim, Kramer and Hatcher, 2003; Marshall and Rodgers, 2004; Miettinen *et al*., 2015; Hertzog *et al*., 2016). Additionally there are an increased number of compounds with an H/C ratio <1 and O/C ratio <0.5 in SWP/BO, indicative of unsaturated hydrocarbons.

While it can be seen from Figure 3.4 that SWP/BO is enriched with high O_x-containing heteroatom classes, the same is not true for AD/BO and MP/BO which both contain only low O_x heteroatom classes. This can be seen more clearly in Figure 3.5 which details the O_x- and N_x-containing heteroatom classes identified in the three bio-oils. It should be noted that peak assignment was based on a compound having at least one O, thus all N_x-containing compounds are also accompanied by an O_x; for the following N_x heteroatom class distribution diagrams the N_xO_y classes are summed to N_x-containing classes.

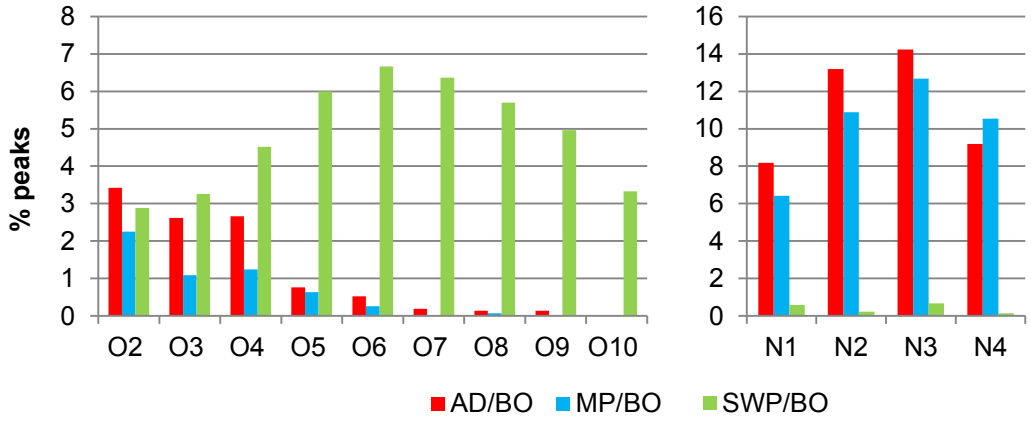

Figure 3.5. Oxygen (left) and nitrogen (right) heteroatom plots of AD1 bio-oils from anaerobic digestate (AD/BO), *M. pyrifera* (MP/BO) and softwood pellets (SWP/BO). Formulae were assigned from ESI FT-ICR MS spectra. N_x classes are the sum of all N_xO_y-containing classes.

The most abundant heteroatom class for SWP/BO belonged to O6-containing compounds with 97.84% of all O_x-containing compounds belonging to O2 to O10. Similarly for AD/BO and MP/BO, the O2- to O10-containing compounds encompassed 100% and 99.1% respectively of all O_x heteroatom classes. However the number of O_x classes identified in AD/BO and MP/BO is much reduced compared to SWP/BO, indeed the O2 class is the most abundant of O_x-containing classes for both these bio-oils. Both AD/BO and MP/BO show a high abundance of N_x-containing classes, with 40.52% and 44.79% of all peaks assigned to an N_x-containing heteroatom class, in comparison to SWP/BO where nitrogen-containing heteroatom classes make up only 1.63% of the total peaks.

3.2.4 Bio-oil Ageing

The bio-oils used for all the tests were produced immediately before the first AD experiment (AD1) and were stored at 4°C between experiments. Storage times of the bio-oils for the remaining tests were approximately 50 days for AD2, 150 days for AD3 and 250 days for AD4. In addition to the bio-oil analysis before AD1, characterisation was performed on the bio-oils before AD2 and AD4. AD2 bio-oils showed almost identical patterns in their van Krevelen diagrams and are therefore available electronically. AD4, however, was started with a significant time delay and this had a considerable effect on the SWP/BO bio-oil used for this experiment. The associated van Krevelen diagram for the bio-oil is shown in Figure 3.6; the replicate sample is not shown due to its high similarity.

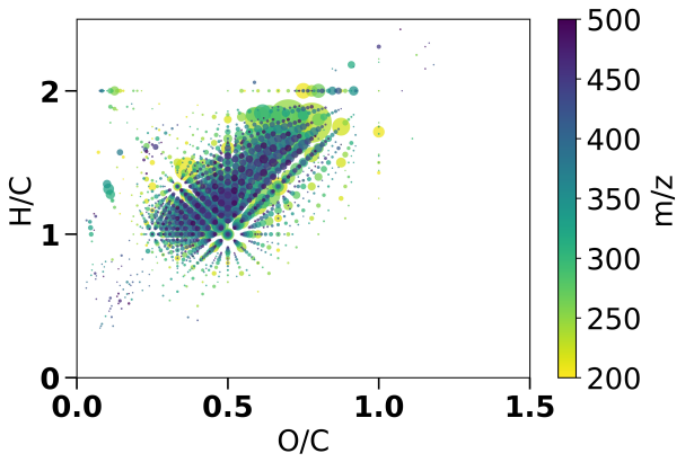

Figure 3.6. van Krevelen diagram for AD4 bio-oil from softwood pellets (SWP/BO). Formulae were assigned from ESI FT-ICR MS spectra. Plots are further colour-coordinated by the *m/z* of identified compounds. The relative abundance of the peaks is represented by the size of the point.

The van Krevelen diagram retains the pattern of the fresh bio-oil (Figure 3.4) with a focus on pyrolytic lignin and carbohydrates; however there is a distinct change in the *m/z* with a shift towards heavier compounds in the older bio-oil. The oxygen heteroatom graph which compares the SWP/BO from AD1 and AD2 to that of AD4 (Figure 3.7) also shows the bio-oil at this later time point displaying a marked shift towards higher O_x-containing heteroatom classes from O6 in the fresher oils to O11. The increase in higher O_x-containing heteroatom classes can also be seen to a lesser extent between AD1 and AD2.

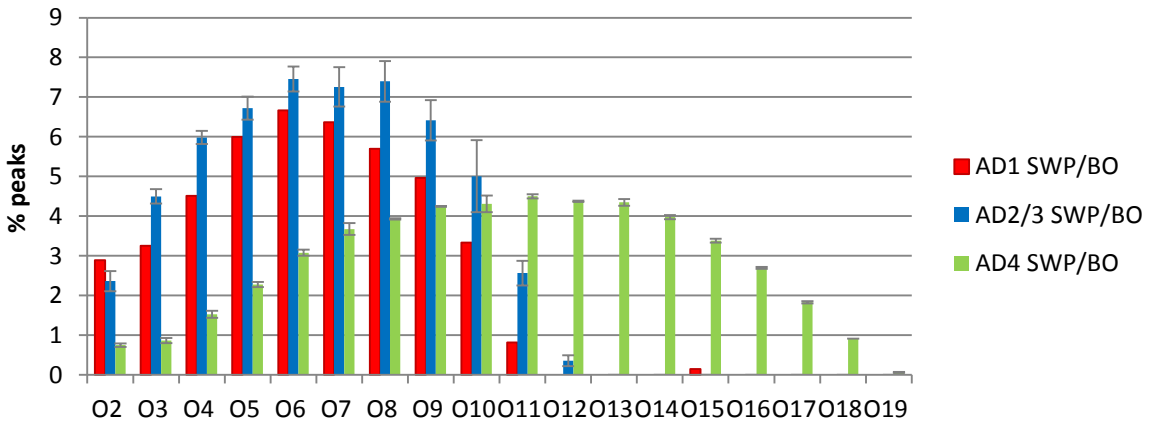

Figure 3.7. Oxygen heteroatom diagrams for AD4 bio-oils from softwood pellets (SWP/BO). SWP/BO bio-oils from AD1 and AD2 are also plotted for comparison. Formulae were assigned from ESI FT-ICR MS spectra.

3.2.5 Multivariate Statistical Analysis

Typically applied to population data for ecological analysis, multivariate statistics techniques were applied to the bio-oil chemistry data in an attempt to also allow the assessment of differences between sample chemistry. ESI FT-ICR MS generates a large amount of highly accurate *m/z* and peak intensity data for thousands of compounds within bio-oil. It is therefore possible to perform multivariate analysis on the data to investigate the statistical differences between the compositions of the bio-oil samples. Below, Bray-Curtis similarity matrices for each of the bio-oil sets from AD1, AD2, AD4 and all the bio-oils together are plotted as 2D or 3D nonparametric multi-dimensional scaling (NMDS) plots where appropriate.

3.2.6 AD1

The fresh AD/BO and MP/BO bio-oils have a Bray-Curtis similarity of 49.24, which is consistent with the similarity of their van Krevelen diagrams (Figure 3.4). Similarly the large difference observed between these bio-oils and SWP/BO corresponds to an average Bray-Curtis similarity of 5.09 ± 0.55 (mean ± SEM). Only a single bio-oil sample from each feedstock was analysed before AD1 and due to the limited number of samples it is not necessary to generate an ordination plot for these bio-oils or check for statistical significance of similarity; however, they are included in the comparison of all the bio-oils (Chapter 3.4.3).

3.2.7 AD2

The Bray-Curtis similarities between AD2 bio-oils mirror those seen in the AD1 samples, with an average similarity between AD/BO and MP/BO of 52.6 ± 0.57 whilst these bio-oils show an average similarity of only 4.84 ± 1.42 to SWP/BO. Replicate bio-oil samples show a high similarity to each other with SWP/BO replicates the least similar at 85.93 compared to the average 93.5 ± 1.31 between AD/BO and MP/BO replicates.

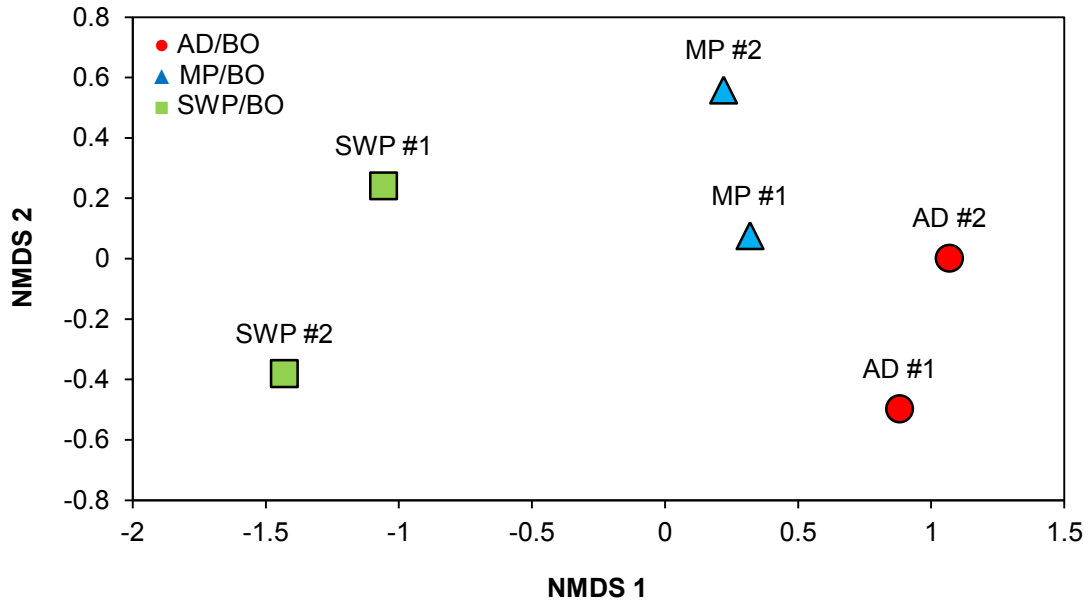

Figure 3.8. 2D NMDS plot generated from the Bray-Curtis similarity matrix for duplicate (#1 and #2) AD2 bio-oils from anaerobic digestate (AD), *M. pyrifera* (MP) and softwood pellets (SWP). 2D stress = 0.

Figure 3.8 plots the similarity between samples and despite the split between bio-oil from lignocellulosic biomass and lignin-limited biomass this difference is not statistically significant (SWP/BO versus AD/BO and MP/BO PERMANOVA P = 0.079; Pseudo-F = 19.012). However this is potentially due to the limited number of samples representing each factor.

3.2.8 AD4 and all Bio-oils

The Bray-Curtis similarity between all the bio-oils is plotted in Figure 3.9. The replicate samples of SWP/BO used in AD4 share a similarity of 95.22 which is likely due to their high dissimilarity with the other bio-oils with an average Bray-Curtis similarity of only 1.47 ± 0.07 to AD/BO and MP/BO bio-oils and 28.31 ± 1.44 to the other SWP/BO bio-oils. This is comparable to the large differences observed in their van Krevelen diagrams (Figure 3.4 and 3.6).

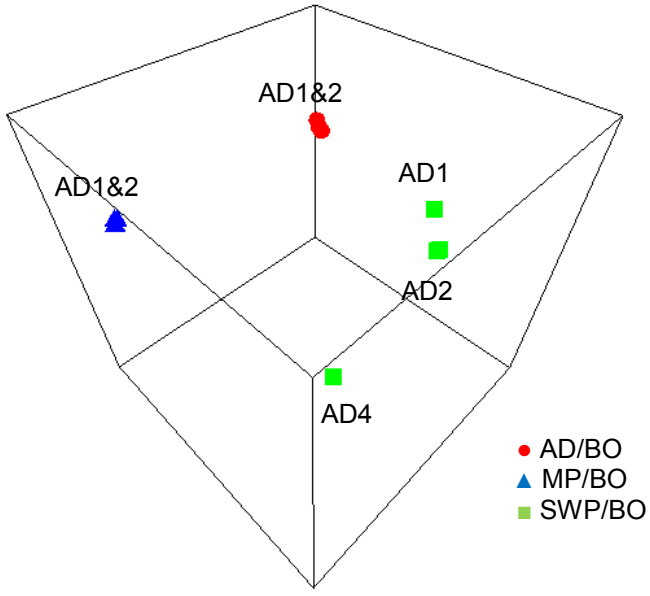

Figure 3.9. 3D NMDS plots generated from the Bray-Curtis similarity matrix for all bio-oils used in AD tests. Bio-oils were produced from anaerobic digestate (AD), *M. pyrifera* (MP) and softwood pellets (SWP). Bio-oils from each AD test are labelled accordingly; AD1, AD2 and AD4. 3D stress = 0.01.

Similarities between the AD1 and AD2 bio-oils are relatively constant with indices of 68.12 ± 0.4, 75.84 ± 0.98 and 69.16 ± 0.56 for AD/BO, MP/BO and SWP/BO bio-oils respectively and therefore cluster together. The large difference between SWP/BO samples between experiments is also evident, with AD1 and AD2 bio-oils clustering together, away from AD4 samples. A PERMANOVA based on bio-oil type for all samples reveals significant differences between pyrolysis feedstocks (P = 0.001; Pseudo-F = 14.402) however a PERMDISP (P = 0.009; F = 18.634) shows

that part of the difference is due to differential variability within the bio-oil groups, presumably due to the dissimilarity of SWP/BO bio-oils between AD tests.

3.3 Discussion

Bio-oils from three different feedstocks were characterised before their use in four AD tests using ESI FT-ICR MS, with additional known microbial inhibitors in these bio-oils quantified by GC-MS and HPLC before their use in the first test. The bio-oils characterised in this chapter were those used in the AD tests (Chapter 5) while the WP/BO bio-oil used in the initial aerobic tests (Chapter 4) was not analysed due to the shift of the project towards AD. WP/BO, however, was produced from the pyrolysis of wood pellets at 650 °C, so although it may share characteristics with SWP/BO, due to being from a similar lignocellulosic biomass, there is evidence that higher temp bio-oils are more toxic to the microbial consortia of AD reactors (Hübner and Mumme, 2015) and as such the composition of this bio-oil could be drastically different.

Anaerobic digestate disposal is a growing waste management concern for AD plants (Bratina, 2016) thus its valorisation is an area of intense research. The coupling of AD with pyrolysis enables the use of digestate as a promising feedstock for bio-oil production and fits within a circular system, where one technology uses the waste products of another. The AD/BO bio-oil used in this project seems to be composed mainly of low mass lipids and proteins, which is to be expected considering that the anaerobic digestate for AD/BO is from an urban wastewater treatment plant which typically treats human waste rich in these compounds (Raunkjær, Hvitved-Jacobsen and Nielsen, 1994). This is supported by the GC/MS data that shows the presence of several short chain fatty acids. Although these compounds are intermediate substrates for methanogenesis in AD, the high nitrogen content, presumably from protein, may cause significant inhibition to AD. There is also the presence of some unsaturated hydrocarbons, possibly from the pyrolysis of the limited amount of lignin in the feedstock, which is indicative of potentially inhibitory aromatic compounds (Jönsson, Alriksson and Nilvebrant, 2013).

Reports on the pyrolysis products of algae and their valorisation by microbial treatment are limited. However, the use of algal biomass for next generation fuels and chemicals is a rapidly growing field of research (Shanmugam *et al*., 2017), thus, characterisation of bio-oils from this biomass is important. The MP/BO bio-oil produced for this project was found to be extremely similar to that produced from anaerobic digestate in that it was composed mainly of lipids and proteins and had high nitrogen content. Algal biomasses are generally abundant in these compounds (Nielfa *et al*., 2015) however only a limited amount of short chain fatty acids were identified by GC/MC and the increased mass of the identified lipids and proteins could indicate larger, lipid compounds such as long chain fatty acids which are reported as being inhibitors of AD (Li *et al*., 2017).

The high number of compounds that were identified as proteins in Figure 3.4 for AD/BO and MP/BO are presumably responsible for the higher nitrogen content of these bio-oils, whose feedstocks are also known to contain high concentrations of proteins and lipids (Aboulkas *et al*., 2017; Jian *et al*., 2017). Protein-rich substrates have been shown to yield high levels of ammonia in AD systems, and are a major cause of process inhibition (Li *et al*., 2017). The presence of nitrogen in these bio-oils may also help explain the clustering of compounds at low O/C on their associated van Krevelen diagrams, as the inclusion of an N_x-containing heteroatom class would decrease the O/C ratio. The finding of high nitrogen levels in these bio-oils highlights a major limitation to this study as ammonia concentrations in the digestates were not analysed and therefore it is not known if inhibition in AD by bio-oil addition was primarily due to high ammonia concentrations in these bio-oils. Any further work on the AD of bio-oils from similar feedstocks should include quantitation of this important inhibitor.

Pyrolysis products from lignocellulosic biomass have been the most extensively researched and have been utilised successfully in AD (Fabbri and Torri, 2016). There are also reports on their characterisation by ultrahigh resolution MS techniques with similar published spectra (Jarvis *et al*., 2012, Liu *et al*., 2012; Kekäläinen, Venäläinena and Jänis, 2014; Miettinen *et al*., 2015). Their van Krevelen diagrams

and associated multivariate analysis show that they are significantly different from the lignin-limited bio-oils use in this project. The majority of compounds seem to be those associated with pyrolytic lignin, which represents a challenging feedstock for microbial conversion; however, there also seems to be a fraction of carbohydrates that could potentially be quickly utilised by a microbial consortium. Acetic acid and lactic acid are commonly produced by the pyrolysis of lignocellulosic biomass and as such are found in SWP/BO. Whilst acetic acid is a direct substrate for acetoclastic methanogenesis, lactic acid is degraded via propionic acid in anaerobic digesters, which has been reported to be a cause of process inhibition (Wang *et al*., 2009).

Pyrolysis of SWP additionally produces furans, known microbial inhibitors that are not present in lignin-limited feedstocks. This is due to these compounds primarily being formed from the dehydration of plant sugars (Iwaki *et al*., 2013). The increased levels of these compounds in addition to a high proportion of unsaturated hydrocarbons in SWP/BO potentially indicate difficulties in its microbial degradation, although the low nitrogen content of the produced bio-oils may be a significant benefit for use in AD.

The lignin-limited bio-oils produced for this project showed a considerably reduced COD and volume yield compared to SWP, presumably due to the increased amount of non-condensable gases produced from their pyrolysis. This has ramifications for the scaling of this technology, as were the production of bio-oils to reach an industrial scale, the biomass of choice would have to satisfy several requirements for its pyrolysis to bio-oil to be financially viable. The loss of so much COD to a non-condensable fraction could have serious implications for the use of these “third-generation” biomasses as a feedstock for bio-oil production.

Also of note is the change in bio-oil composition between tests caused by the ageing of bio-oils which may alter their impact on AD communities and thus produce different results from similar experimental setups. The bio-oils used in the AD tests were made at the start of the first AD test with a ~50 day period separating AD1 from AD2. AD4 was started ~250 days after AD1 and it is with these bio-oils that we

see a large difference between the two dates and evidence of significant bio-oil ageing. This finding is supported in the literature and can be explained by the continuing reactions that occur immediately after the bio-oil is produced (Alsbou and Helleur, 2014), particularly the ongoing reactions of carbohydrates with phenolic compounds that form larger molecules (Sundqvist *et al.*, 2016). This ageing effect has not been studied in regard to its effect on microbial inhibition; however, it is likely that the increase in high molecular weight compounds within the bio-oil will render it more challenging for the microbial communities to degrade. These differences are observed clearly in the SWP/BO van Krevelen diagram with a general increase in the *m/z* of the peaks, indicating continued reactivity of the bio-oil to larger compounds. It is unknown however, how AD/BO and MP/BO age over this period of time as these bio-oils were not used in further tests.

It is important to note that the results from these analyses are only from the initial bio-oils and that this project is investigating their use and impact on AD processes. Further characterisation of the digestate medium and the combined digestate-bio-oil mixture both before and after microbial activity is given in Chapter 6. This initial analysis, however, aids in the understanding of the composition of these bio-oils and their potential impact on AD. It also demonstrates the strength of using ultrahigh resolution MS techniques for the characterisation of complex mixtures and the subsequent application of multivariate analysis to the data.

The ultrahigh resolution and mass accuracy afforded by the use of ESI FT-ICR MS analysis allows for the characterisation of a complex mixture such as bio-oil without focusing on individual compounds. This is beneficial for such mixtures due to the sheer number of compounds present and allows a greater proportion of each bio-oil to be analysed. Although it is possible to infer chemical class data from the elemental compositions of the data, and thus make assumptions on its reactivity, the presence of a class of compounds does not necessarily translate to their expected behaviour. The relative abundance of each peak on the spectrum is not considered accurately quantitative due to some molecules being more easily ionised and therefore skewing the data. The same is also true for the biological characterisation of a sample where it

is reported that bias can be introduced from the polymerase chain reaction (PCR) amplification of sample DNA. With this in mind, assumptions on the potential advantages or disadvantages of a specific bio-oil for bioconversion from its chemical profile, need to be tested.

Similarly to the use of multivariate statistical analysis on biological species data, it is important to note that replication of samples is required for statistical significance to be calculated. The utilisation of these techniques for MS data also requires additional investigation, as the intensity data from FT-ICR MS is not a perfect representation of the abundance of a specific compound and thus there could be an abundance skew of the data. Despite this, it has been shown here that it is possible to use multivariate statistical methods for the analysis of high-resolution MS data, and that by using these techniques it is possible to observe significant differences between bio-oils from different feedstocks, and the same bio-oil over time due to ageing.

CHAPTER 4: AEROBIC

4.1 Introduction

Bio-oil is a complex organic liquid that contains several classes of known microbial inhibitors that make its degradation a significant challenge. There are limited reports in the literature regarding its degradation by aerobic microbial species, all of which require pre-treatment of the bio-oil for the purposes of detoxification or neutralisation (Prosen *et al*., 1993; Bennett, Helle and Duff, 2009; Wang *et al*., 2012; Yang *et al*., 2014).

The majority of these examples also attempt to perform the detoxification or fermentation using single species of microorganisms. Several biotechnological applications desire the use of single strains of species due to the convenience of culturing and the understanding of their metabolic pathways, due to the species generally being well characterised. However, for the degradation of a product with several thousand compounds that changes over time and that is not fully characterised, a single species will be incapable of hosting the myriad metabolic functions required. Studies examining the biodegradation of toxins in the environment show complex communities of microbial species that adapt to environmental conditions with no single species dominating the entire community and previously rare species gaining increased opportunities for growth (Gutierrez *et al*., 2013; Berdugo-Clavijo and Gieg, 2014). This indicates that the species required to fulfil a metabolic role in biodegradation are already present in natural environments.

With this in mind it was hypothesised that the degradation of bio-oil would require a consortium of microorganisms and that a consortium could be isolated from the natural environment. Those bio-oils derived from lignocellulosic feedstock are generally acidic in nature and as such communities from acidic environments would have an advantage in surviving bio-oil toxicity. The wetland area of Benhar Bing in North Lanarkshire, Scotland, was constructed for the treatment of acid drainage from

an ironstone spoil heap (Heal and Salt, 1999) and is characterised by particularly acidic sediments, thus communities isolated from these sediments, and other local natural sediments, were used for testing the potential of aerobic degradation of bio-oil. An initial culture plate with diluted bio-oil was used to assess its toxicity to microbial growth from communities isolated from three natural habitats: freshwater pond sediment from Blackford Pond, intertidal sediment from Cramond beach and remediated wetland sediment from Benhar Bing. Additional isolated communities from Benhar Bing were passaged in an M9 minimal medium with bio-oil as the sole carbon source, with sequential increases in concentration to assess the communities' capability for bio-oil utilisation. In both experiments the starting communities were characterised by DGGE and Illumina sequencing respectively.

The application of single species is still an important strategy for the purposes of bioremediation; the metabolic pathway for the degradation of a particularly recalcitrant compound may not be present, or efficient enough for significant degradation strategies, in the natural community. As such, the addition of a single species that is known to be able to perform the required degradation step can assist in the overall remediation of a toxic compound. Such bioaugmentation approaches are commonly found in examples of remediation strategies of hydrocarbon contaminated sites (Boon and Verstraete, 2010; Shankar *et al*., 2013; Hassanshahian *et al*., 2014; Fuentes *et al*., 2016). In this work, three individual bacterial strains and a single fungal strain, isolated from a contaminated bio-oil culture, were chosen for their potential ability to utilise bio-oil.

The four strains tested for their ability to utilise bio-oil as a sole carbon source were: the Gram-positive facultative anaerobe *Bacillus cereus,* identified as being capable of the degradation of phenolic compounds such as eugenol and guaiacol (Kadakol and Kamanavalli, 2010), both microbial inhibitors found in bio-oil. *Cupriavidus basilensis*, a Gram-negative soil bacterium capable of degrading furan and phenolic compounds (Wang *et al*., 2012; Jiménez, Korenblum and van Elsas, 2013 Shen *et al*., 2015), both common classes of microbial inhibitors found in lignocellulosic-derived bio-oil. A *Halomonas sp*. strain designated TGOS-10 by Gutierrez *et al*. (2013),

capable of producing exopolysaccharides that aid in the solubilisation of aromatic hydrocarbons (Gutierrez *et al*., 2013). And a yeast strain, *Trichosporon sp*. isolated from M9 minimal medium with bio-oil as the sole carbon source. The *Trichosporon* genus contains several species capable of utilising phenols and low-molecular weight aromatic compounds as well as the ability to degrade lignocellulosic hydrolysates and show resistance to inhibition from lignocellulosic degradation compounds (Chen *et al*., 2009; Krastanov, Alexieva and Yemendzhiev, 2013; Cassa-Barbosa *et al*., 2015).

4.2 Results

4.2.1 Environmental Community Analysis

Seven sediment samples were taken from the two overflow pool shores in the Benhar Bing remediation site (BHB1 – 7) and a further two water samples directly from the overflow pool water (BW1 and BW2), additionally three sediments samples were taken from Cramond beach (Cr1 – 3) and one from Blackford Pond (BP). DNA was extracted from these sediment samples and used to generate V3 16S rRNA gene amplification products for DGGE analysis. Figure 4.1 shows the stained DGGE gel image from the bacterial species within each sediment or water sample. First and second-round PCR negative controls were also electrophoresed with the samples. Due to the nature of separation of DNA fragments in a DGGE gel, each band corresponds to a species with a different sequence of the 16S rRNA gene, thus samples that share bands with the same migration along the gel are assumed to have similar compositions of species.

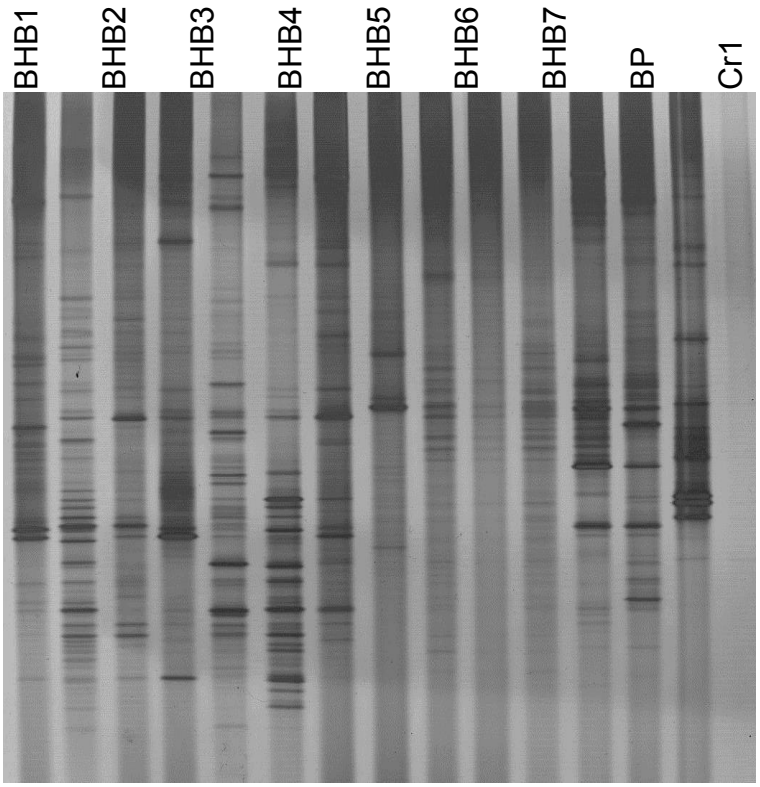

Figure 4.1. DGGE gel image of 16S rRNA gene amplicons amplified from sediment samples. Sediments were collected from Benhar Bing (BHB), Blackford Pond (BP) and Cramond (Cr) with additional water samples from BHB (BW). First and second-round PCR controls (Ctrl) are also shown.

Samples initially seem quite varied in their band profiles however there is a similar banding pattern observed between samples taken from the same locations. In particular the three samples from Cr show almost identical banding whilst samples from BHB, although more varied, do share common bold bands. The band profiles for BP and Cr samples seem fainter than those from BHB. It is also of note that the Ctrl1, which substituted sample DNA with water, shows clear banding, whereas Ctrl2 is clear. Bands identified in the control reactions are searched for on the sample reactions and removed from the analysis.

Figure 4.2 shows the NMDS plot from the Bray-Curtis similarity matrix calculated for the band intensities, after removal of contaminant bands, in each sample following square-root transformation. Distance between samples denotes similarity and it can immediately be seen that the seven BHB samples cluster to the right of the

2D space with the BW samples, taken from the same location. Both Cr and BP samples occupy the left side of the space. It should be noted that there is a high degree of dispersion of the BHB samples. Controls were removed from the plot as the first-round control did not seem to share any common bands with sample DNA on the DGGE gel and the second-round control showed no bands at all.

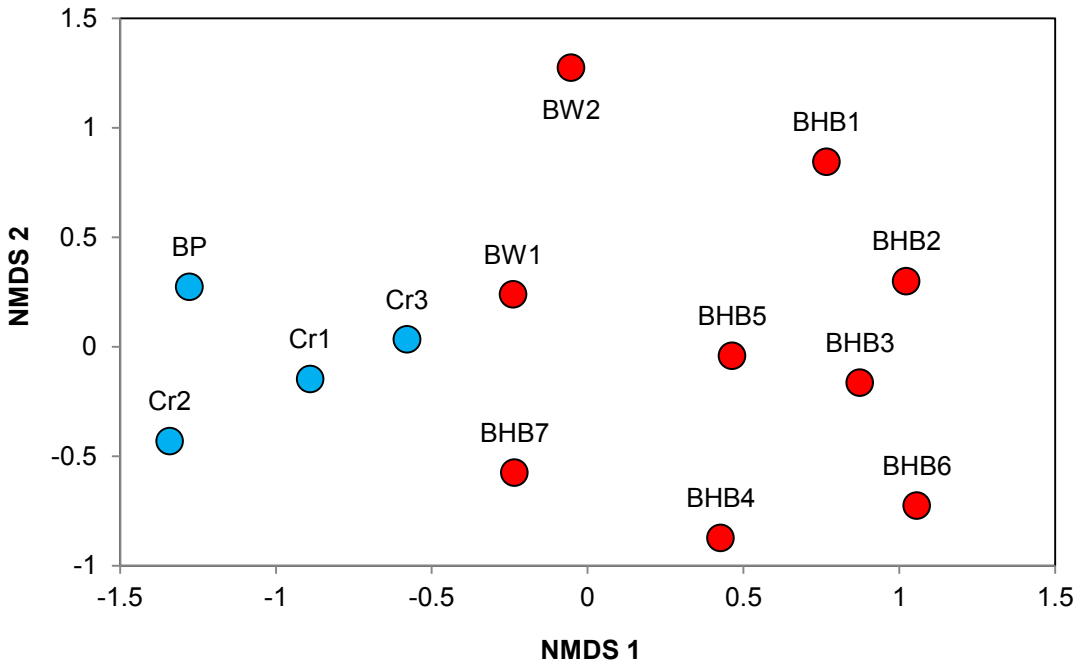

Figure 4.2. 2D NMDS plot of Bray-Curtis similarity of DGGE bands between samples. Samples from natural (BP and Cr) and constructed (BHB and BW) environments are represented by blue and red markers respectively. 2D stress = 0.13.

PERMANOVA and PERMSIDP analyses based on the Bray-Curtis similarity measure were applied to the data sets to find significant differences between groups of samples based on their composition or dispersion in relation to natural environments (Cr and BP) and an "extreme" environment (BHB and BW). A PERMANOVA shows significant variation between the two groups (P=0.003; F=3.128) however a PERMDISP also shows a significant difference (P=0.002; F=22.767). The average inter-replicate Bray-Curtis similarities for the natural environment samples average at 45.4 ± 1.842 (Mean ± SEM) while the more "extreme" environment of BHB average at 36.117 ± 0.969.

4.2.2 Microbial Community Bio-oil Toxicity Tests

It was unknown to what extent the toxicity of bio-oil would inhibit the growth of microbial communities thus the first tests were aimed at probing the viability of the naturally isolated communities under these conditions. Of immediate interest were communities isolated from the constructed wetland site, Benhar Bing, whose low pH soils were expected to harbour acidophilic organisms capable of overcoming the low pH of bio-oil. The pH of the samples were measured at 2.56 for BHB2, 4.02 for BHB4, 2.04 for BHB6, 6.7 for BP and 7.22 for C1; the pH of the WP/BO bio-oil used in the initial tests was 2.78. Diluted WP/BO bio-oil at 0.15 g/L COD was used as the culture medium in each well of a 48-well plate. Five of the microbial communities and a deionised water control added to each row of the plate and monitored for growth using the absorbance at 600 nm of the culture medium to estimate the concentration of microbial cells. Figure 4.3 shows the plate layout and colour change associated with the cultures after 15 days of incubation with the OD600 of the cultures shown in Figure 4.4.

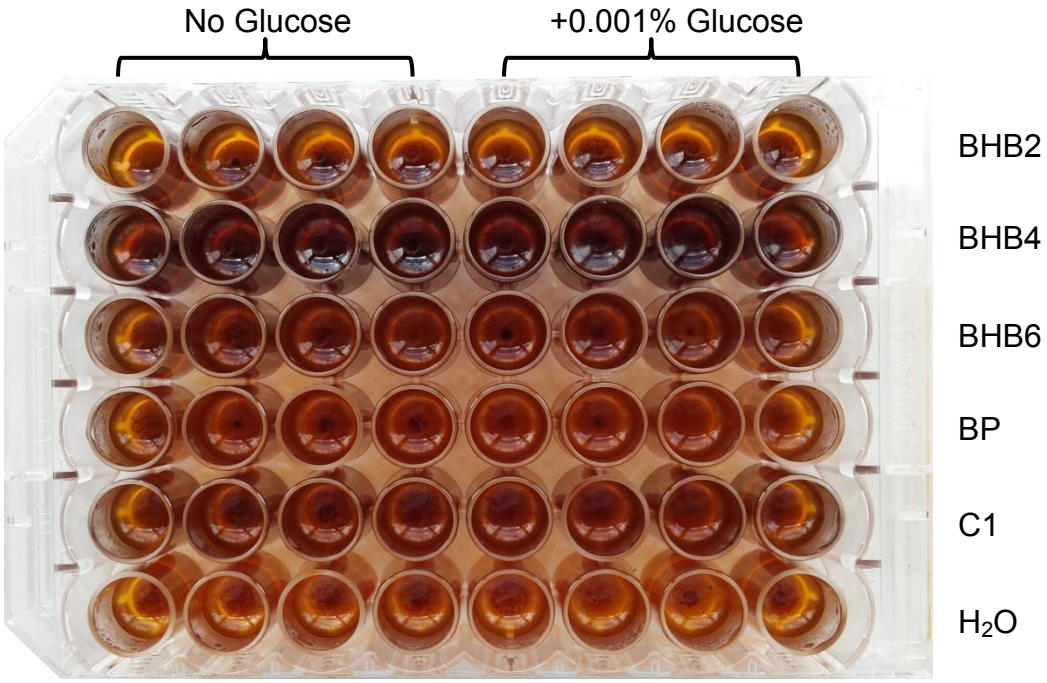

Figure 4.3. Bio-oil cultures in a 48 well plate after 15 days of incubation with inoculation from isolated sediment communities from Benhar Bing (BHB), Blackford Pond (BP), Cramond (C) and a deionised water control (H_2O).

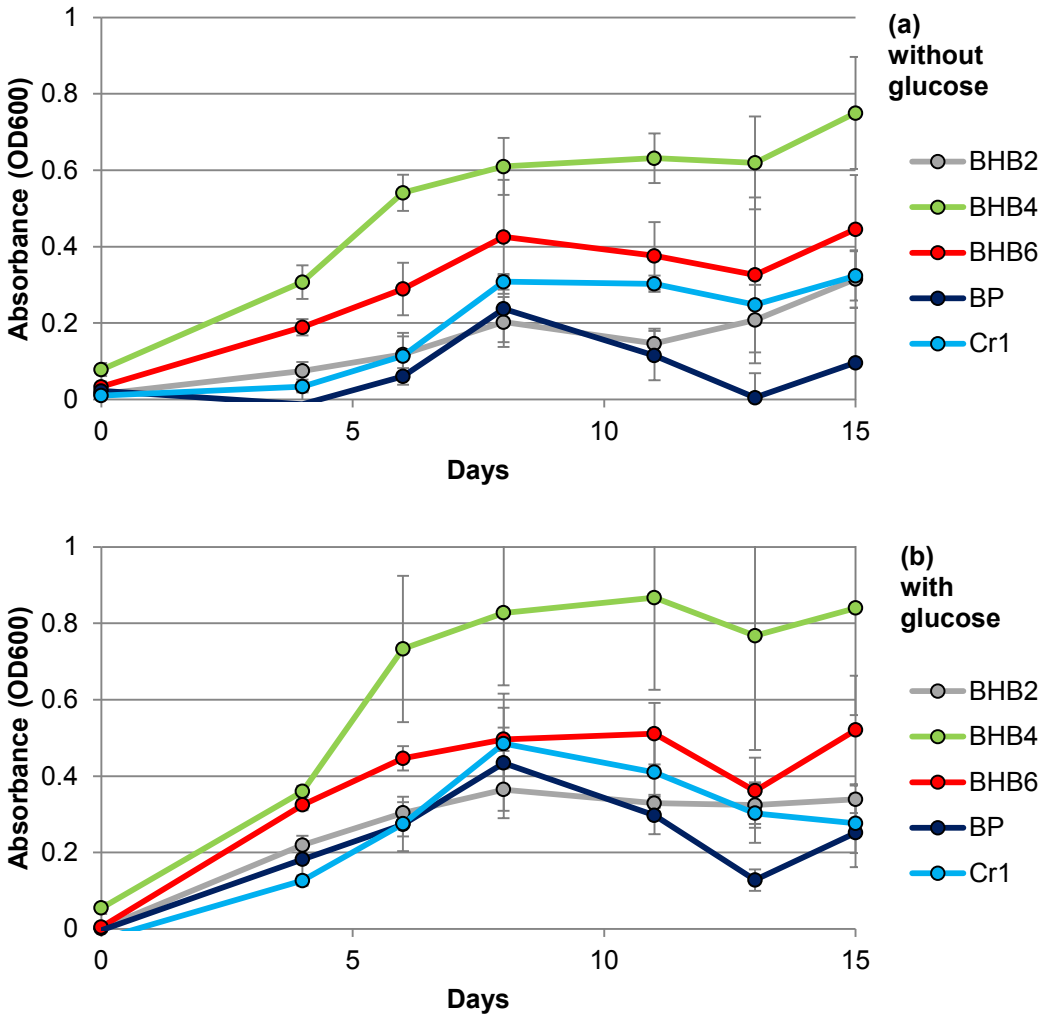

Figure 4.4. Growth curves of bio-oil cultures (a) without and (b) with glucose addition over a 15 day incubation period. Absorbance values are the mean of four replicates across selected microbial communities isolated from Benhar Bing (BHB), Blackford Pond (BP) and Cramond (C). Average standard deviation was 0.064 without glucose and 0.078 with glucose. All samples were performed in triplicate with error bars of standard deviation. Absorbance values are corrected against the deionised water control cultures.

The largest amount of microbial growth was seen in BHB4 as can be observed by the darker culture wells in Figure 4.3 and the higher growth rates in Figure 4.4. There is little difference between the remaining samples, with BHB6 showing slightly higher growth rate and BP showing the least. The water control did show an increase in OD600 over the incubation period however this was due to a loss of volume which

was consistent across all the culture wells due to the volatility of bio-oil, as such the absorbance values of the cultures were all corrected against the water controls so that differences in absorbance are due to microbial growth as opposed to evaporation.

The addition of glucose to the cultures increases the rate at which they reach an optimum OD600 however no significant difference is seen between the final increase in absorbance with an average OD600 increase of 0.44 ± 0.24 (mean ± SD) for the addition compared to 0.35 ± 0.23 for treatment without glucose (two-sample t-test P = 0.26). Both BHB2 and BP do see a significant difference between their respective glucose and non-glucose growth curves (two-sample Kolmogorov-Smirnov test P = 0.028) however these two cultures also exhibited the lowest increase in OD600.

4.2.3 *Trichosporon* sp. Isolation and Identification

In the early stages of attempting aerobic degradation of bio-oil, highly diluted control cultures were occasionally contaminated with an unknown microbial species that was able to utilise bio-oil as a sole carbon source. This contaminant was of great interest and was observed under the microscope as being a yeast species capable of germination into hyphae (Figure 4.5). Sanger sequencing of the 1 – 779 bp region of the 18S rRNA gene revealed the organism had 99% sequence identity with several species of the *Trichosporon* genus of anamorphic fungi, common human commensal yeasts found on the skin and in soils (Sugita, Nishikawa and Shinoda, 1998). A phylogenetic tree composed of the closest alignments is shown in Figure 4.6 (alignments available electronically).

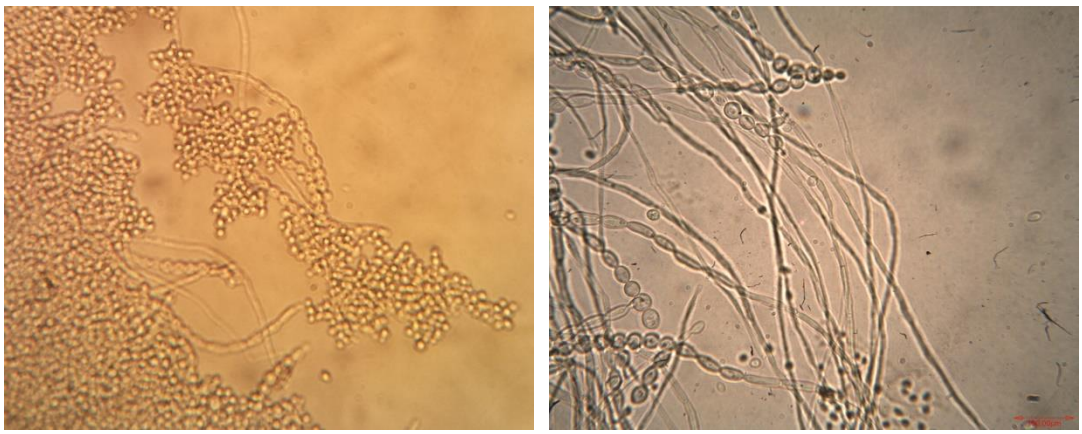

Figure 4.5. Light microscope imaging of a bio-oil control culture contaminant identified as *Trichosporon sp*. at ×40 (left) and ×100 (right) magnification.

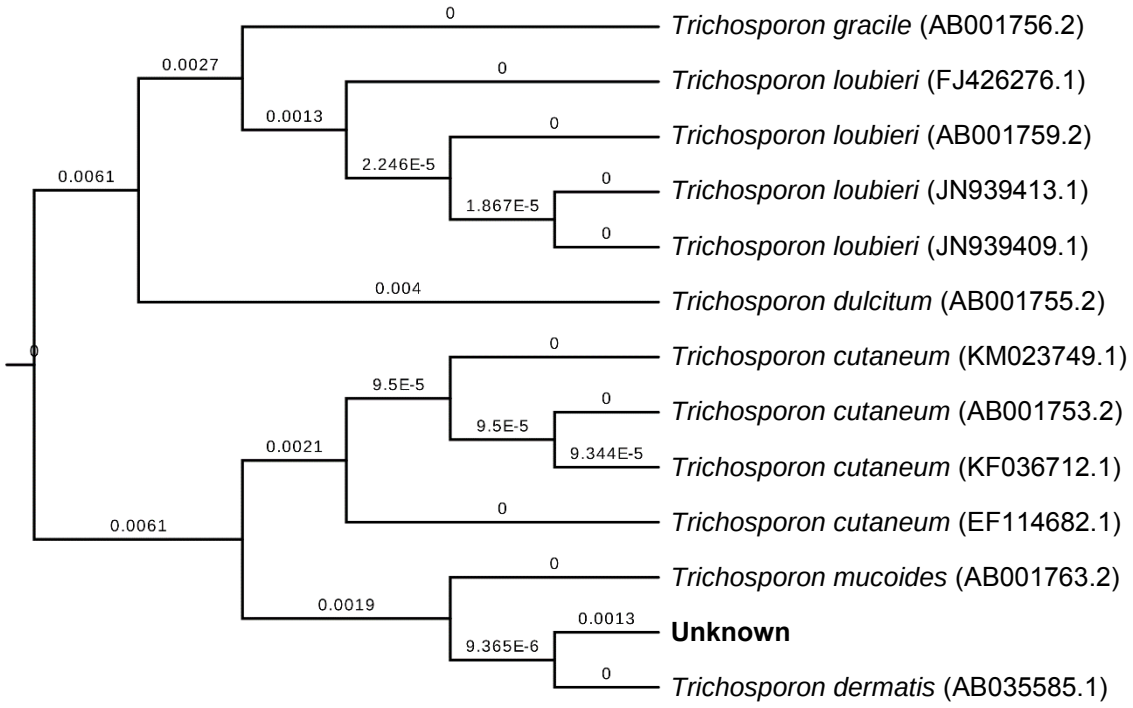

Figure 4.6. Phylogenetic tree of the suspected *Trichosporon* sp. bio-oil control culture contaminant and closest BLAST hits with taxonomic assignment and accession number, from partial 18S rRNA sequences. Branch length is annotated above each branch.

The ability of the *Trichosporon* sp. to utilise bio-oil as a sole carbon source and additional reports on other members of the genus' ability to degrade lignocellulosic degradation products led to its inclusion in the bio-oil toxicity tests on the single species (Matos el al., 2012; Huang el al., 2013; Krastanov, Alexieva and Yemendzhiev, 2013; Xiong el al., 2015).

4.2.4 Single Species Bio-oil Toxicity Tests

Due to the complexity of bio-oil it was not expected that a single species would have a metabolic profile capable of degrading it entirely. However, species of bacteria were chosen from the literature due to their reported ability to degrade some of the more commonly inhibitory chemicals found in bio-oil or similarly complex organic compounds: *B. cereus* was reported as being able to utilise phenols, *C. basilensis* was reported to utilise phenols and furans, and the *Halomonas* sp. was found to aid the degradation of aromatic hydrocarbons. These were in addition to the *Trichospron* sp. which was already observed utilising diluted bio-oil as a sole carbon source.

Overnight cultures of each were grown and diluted to a similar OD600 in nutrient broth (NB) for bacterial cultures and malt extract medium (ME) for yeast and used to inoculate sealed culture tubes to prevent evaporation of the bio-oil medium and prevent contamination during analysis. Cultures were grown in both standard NB/ME and M9 minimal media with SWP/BO bio-oil as the sole carbon source at a concentration of 2.5 g/L COD, which corresponded to the minimum concentration used in the anaerobic tests. Figure 4.7 shows the growth rates of each strain over a five day period in each medium.

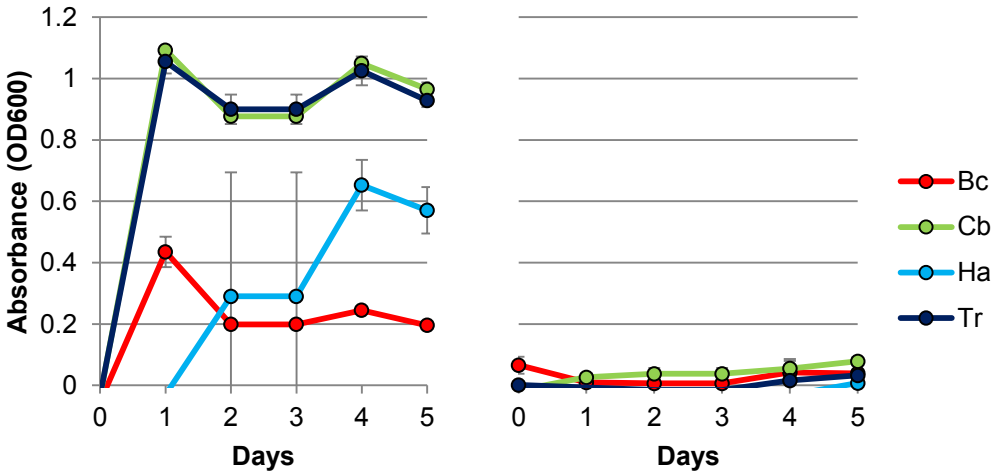

Figure 4.7. Growth curves of single species in NB (bacterial strains) and ME (fungal strains) media (left) and M9 minimal medium (right) with matching absorbance axis values for scale. Selected strains where *Bacillus cereus* (Bc), *Cupriavidus basilensis* (Cb), *Halomonas* sp. strain TGOS-10 (Ha) and *Trichosporon* sp. (Tr). Cultures were in duplicate with error bars of standard deviation. Absorbance values are corrected against a deionised water control culture.

All strains were capable of growth in NB/ME however the absorbance of *B. cereus* cultures were limited to a maximum OD600 of 0.435. *Halomonas* sp. also showed a lower maximum absorbance at 0.653 and also did not reach its peak until day four in contrast to the other cultures that achieved their peaks overnight. None of the cultures were able to grow in M9 minimal medium with 2.5 g/L COD of bio-oil.

4.2.5 Benhar Bing Community Analysis

A second sampling excursion was made specifically for the acidic BHB sediments, six sediment core samples were taken from four sites as described in Table 4.1. DNA was extracted from the isolated communities for 16S rRNA sequence analysis using the Illumina platform providing high-resolution insight into the species composition, diversity and richness of the communities, analysis of the sequence data was with QIIME.

Site	Sample	Description
1	1	Sediment from the shore of the first overflow pool, two samples were taken from the core; one just below the surface and the other ~30 cm deep.
	2	
2	1	Sediment from the shore of the second overflow pool, two samples were taken from the core; one just below the surface and the other ~30 cm deep.
	2	
3	-	Sediment from the overflow pool run-off stream, ~30 cm from surface.
4	-	Sediment from the bottom of a shallow oil-covered pool ~5 m from the second overflow pool.

Table 4.1. Benhar Bing sample identifiers, locations and descriptions for the second sampling excursion for sediments.

Figure 4.8 shows the alpha diversity of the communities using the Shannon index which is commonly used to measure both richness (total OTU count) and evenness (distribution of sequences between the different OTUs) of microbial communities (Prosser, 2012; Haegeman *et al*, 2013). The rarefaction curve is generated by random re-sampling of the sequences multiple times at varying sequencing depths and averaging the total OTUs found; when the curve plateaus the limit of sequences required for any further meaningful increase in diversity has been reached, thus a higher plateau indicates a higher level of diversity. The rarefaction measure takes the sample with the lowest sequencing depth as the limit for all samples, which in this case is 4 770 sequences, however it can be seen that the curve begins to plateau at ~500 sequences thus highlighting the over-abundance of sequences this technique generates according to the Shannon rarefaction measure.

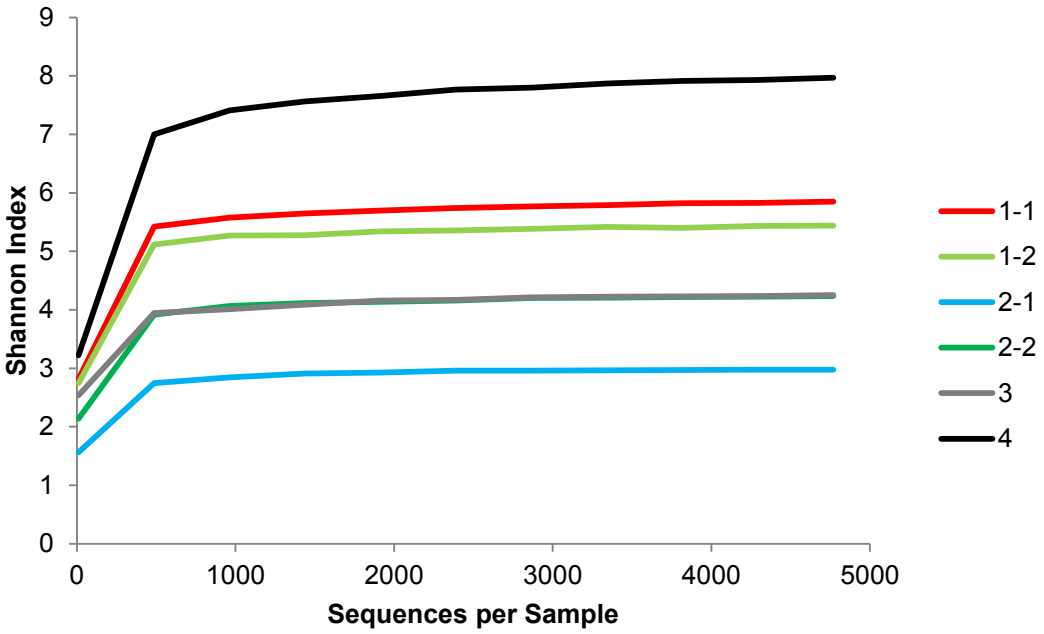

Figure 4.8. Alpha diversity for isolated microbial communities from Benhar Bing sediments as described in Table 4.1. Community compositions are from 16S rRNA gene sequences.

The communities show high variability in their diversity as can be seen in the differences between their Shannon indices. The community from site 4 in particular shows much higher diversity than the others while that from site 2-1 has the lowest along with the remaining sample from site 2 and the sample from site 3, whereas both samples from site 1 show similarly higher levels of diversity.

The relative abundance of each genus assigned to the sequences in each sediment is shown in Figure 4.9. In total there are 715 genera in the dataset however only those that contribute ≥ 0.5% of a samples total relative abundance are included in the figure which reduces the total number to 76, the remaining "rare" genera are therefore absent from the plot however can be seen to have ranged from 1 – 5% of samples from sites 1,2 and 3. For the highly diverse sediment from site 4 it can be seen that the removal of the "rare" genera reduces total abundance to ~73%.

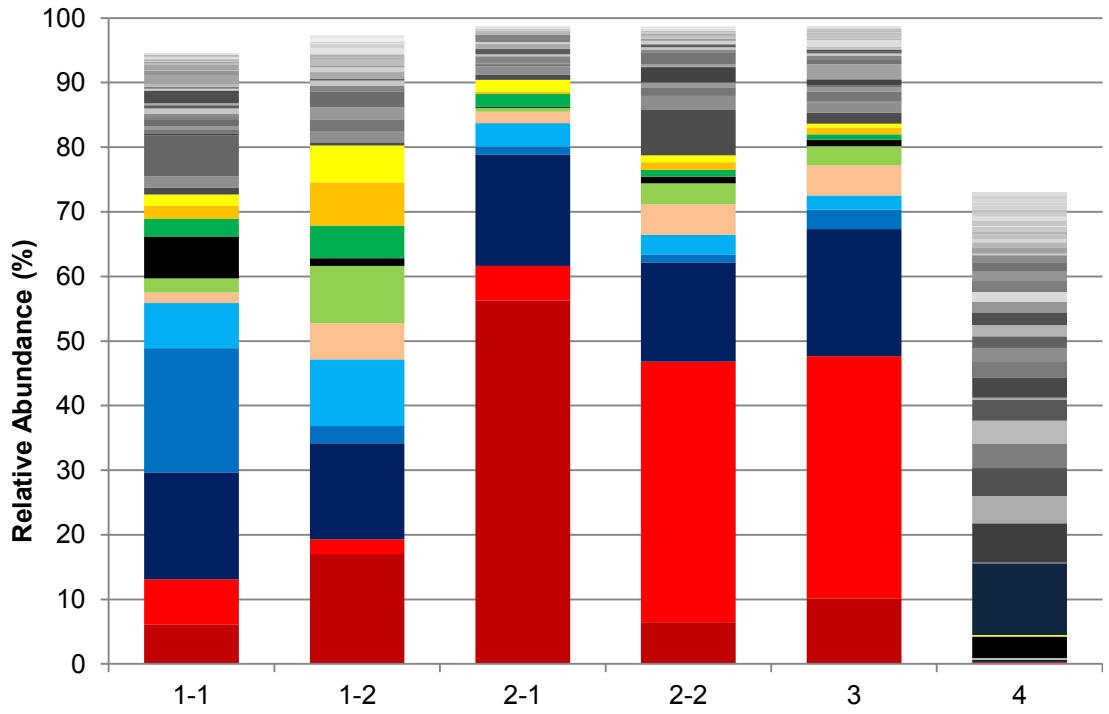

Phylum	Class	Order	Family	Genus
Proteobacteria	*Gammaproteobacteria*	*Xanthomonadales*	*uncultured*	*uncultured*
Proteobacteria	*Gammaproteobacteria*	*Xanthomonadales*	*Xanthomonadaceae*	*Metallibacterium*
Acidobacteria	*Acidobacteria*	*Acidobacteriales*	*Acidobacteriaceae (Subgroup 1)*	*uncultured*
Acidobacteria	*Acidobacteria*	*Acidobacteriales*	*Acidobacteriaceae (Subgroup 1)*	Other
Nitrospirae	*Nitrospira*	*Nitrospirales*	*Nitrospiraceae*	*Leptospirillum*
Proteobacteria	*Gammaproteobacteria*	*Xanthomonadales*	*Xanthomonadales Incertae Sedis*	*Acidibacter*
Actinobacteria	*Acidimicrobiia*	*Acidimicrobiales*	*uncultured*	*uncultured*
Other	Other	Other	Other	Other
Actinobacteria	*Acidimicrobiia*	*Acidimicrobiales*	*Acidimicrobiaceae*	*Ferrithrix*
Chloroflexi	*JG37-AG-4*	*uncultured*	*uncultured*	*uncultured*
Proteobacteria	*Alphaproteobacteria*	*Rhodospirillales*	*Acetobacteraceae*	*uncultured*
Bacteroidetes	*Bacteroidetes vadinHA17*	*uncultured*	*uncultured*	*uncultured*

Figure 4.9. Genus level relative abundance plot of 16S rRNA gene sequences that contributed ≥ 0.5% of the total sequences assigned to the microbial communities isolated from Benhar Bing sediments from sites detailed in Table 4.1. The key to the right of the plot represents the top 11 genera from top to bottom in colour with all other sequences in greyscale. Taxonomy was assigned against the SILVA 128 reference database.

The lack of diversity in sediment 2-1 observed from the alpha rarefaction plot can also be seen in Figure 4.9 with ~56% of the sequences designated to an uncultured *Gammaproteobacterium* of the order *Xanthomonadales* (dark red). Sample 1-1 shows the highest abundance of sequences from two genera (dark blue and blue) from subgroup 1 of the *Acidobacteriaceae*. The second most abundant genus is also a *Xanthomonadales* of the genus *Metallibacterium* (red), and is responsible for 40% and 37% of the sequences in sediment 2-2 and 3 but only 2% to 7% of sediments 2-1 and those from site 1. Also present in high abundance are bacteria of the genus *Leptospirillum* (light blue), particularly in samples from site 1. Archaeal genera account for ~4% of the total abundance of which ~67% are uncultured members of the family Terrestrial Miscellaneous Gp (TMEG), placing them within the acidophilic order *Thermoplasmata*.

Differences between community composition (beta diversity) can be quantified using a Bray-Curtis similarity index where the large difference seen in species diversity in sediment 4 is mirrored; with an average Bray-Curtis similarity to the other sediments of only 2.01 ± 0.29 (Mean ± SEM). This is in contrast to the average similarity between the other sediments at 40.44 ± 1.5 with the exception of sediment 3 which has an 80.77 similarity to sediment 2-2. Visualisation of the index as an NMDS plot is shown in Figure 4.10.

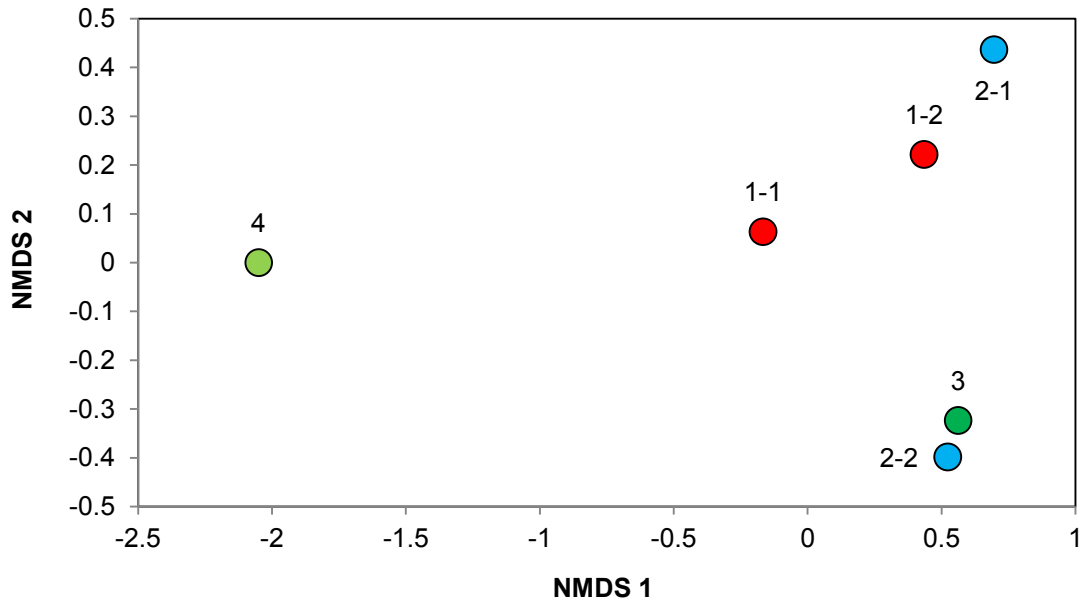

Figure 4.10. 2D NMDS plot generated from the Bray-Curtis similarity matrix for Benhar Bing sediments' community compositions from 16S rRNA gene sequences. Sampling sites are described in Table 4.1. 2D stress = 0.

There is no significant difference observed between Benhar Bing sediment community compositions (PERMANOVA P = 0.23; Pseudo-F = 1.819) however Figure 4.10 does show the community from site 4 as being separate from the other sediment samples. Also of note is the large difference between the samples from site 2.

4.2.6 Bio-oil Culture Passaging

The isolated communities from BHB were used to inoculate M9 minimal medium cultures with bio-oil; this forced the communities to adapt to an environment where bio-oil was the sole carbon source. Any microorganisms that were unable to utilise or survive the toxicity would perish thus the environment would "choose" a community from the starting selection. This process was repeated with each isolated community over three growth periods using the previous final culture as the successive inoculant in new M9 minimal media with increasing concentrations of bio-oil. Figure 4.11 shows the growth curves of each of the communities.

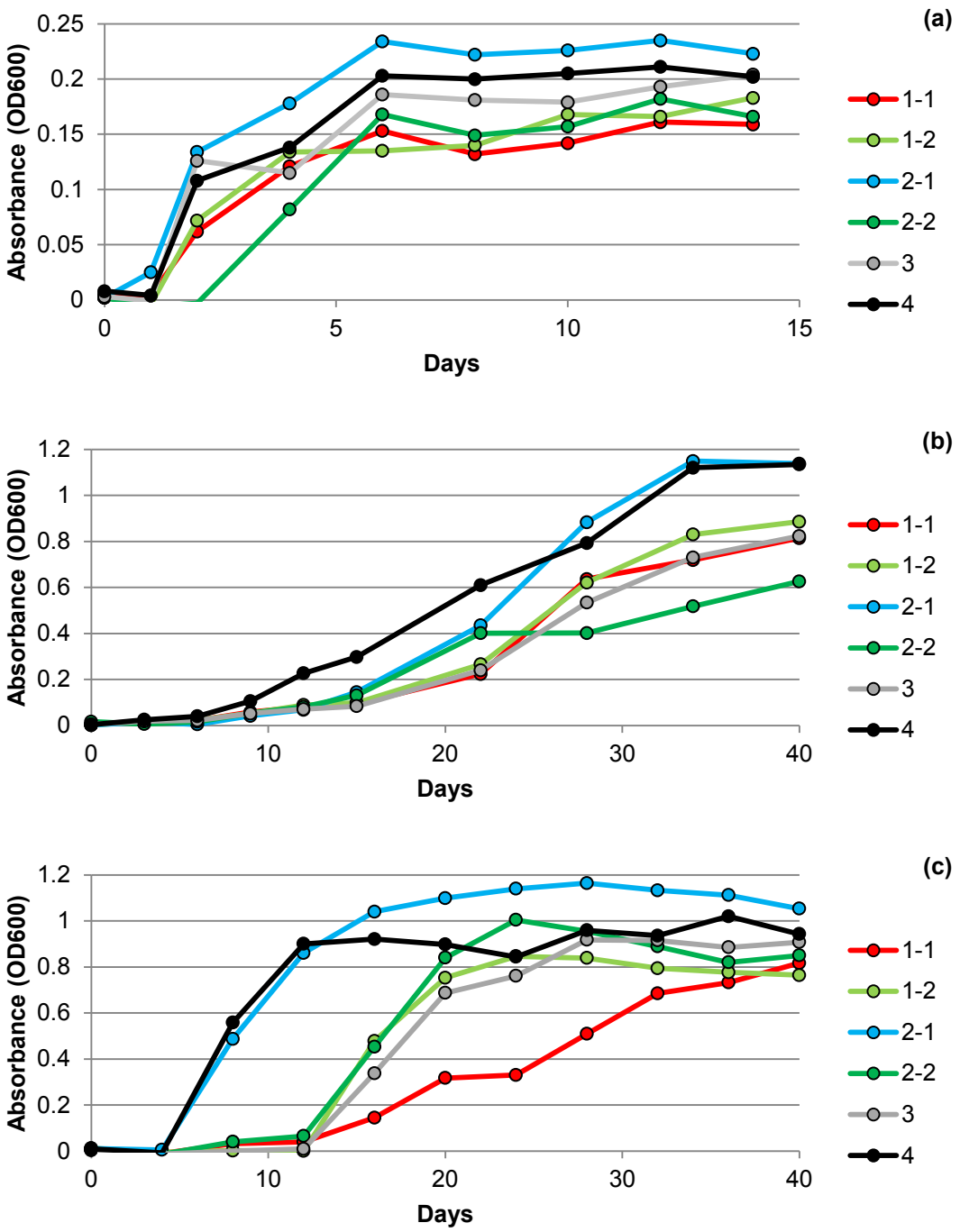

Figure 4.11. Growth curves of isolated microbial communities from BHB sediments over three successive cultures, growing in medium containing increasing concentrations of bio-oil: a) 0.2 g/L COD; b) 2 g/L COD; c) 4 g/L COD. Tests consisted of a single culture for each community with absorbance values corrected against a deionised water control culture.

The initial cultures (a) with the freshly isolated communities saw immediate growth in bio-oil medium with little difference in growth profiles between communities. However the maximum OD600 was limited to ~0.25 and the test was stopped after 14 days due to the curves reaching their plateau. The successive culture (b) which used the previous test's day 14 cultures (a) as the inoculum saw a considerable delay before increases in absorbance were measured. Despite such an increase, the cultures were still able to adapt and utilise the bio-oil for growth with maximum OD600 readings of ~1.2 for communities isolated from sites 2-1 and 4. The site 4 community also seemed to adapt fastest to the bio-oil medium with growth noticeable by day 10 as opposed to day 15 for the other communities. Doubling the bio-oil concentration for the following culture (c) again caused a lag time before growth; however, once overcome the communities reached maximum absorbance earlier than previously, as can be seen by the distinct difference between the two experiments' growth curves. Communities from sites 2-1 and 4 achieved their maximum absorbance before the other cultures and in the case of 2-1 reached a higher absorbance than any other. Curiously, doubling the bio-oil concentration further to 8 g /l COD did not yield growth from these cultures (data not shown).

4.3 Discussion

Bio-oil toxicity is a major obstacle to its aerobic degradation. Species that were chosen for their potential ability to utilise some of the more recalcitrant and inhibitory components of bio-oil were only able to grow in established microbial growth media that supply a wide range of nutrients. The individual microorganisms were unable to grow using bio-oil as a carbon source at a concentration of 2.5 g/L. It must be noted however that the toxicity tests for the single species were not optimised and that further work is required to test the use of these microorganisms to fulfil metabolic functions that might be absent in microbial communities and not as individual cultures, especially at such high concentrations of bio-oil.

The *Trichosporon* sp. contaminant was capable of growth in diluted bio-oil, as this was where it was isolated; however, it was unable to grow in higher concentrations

and as such, 2.5 g/L COD bio-oil in a growth medium for a single species is likely too high. There are reports in the literature of the utilisation of fungal species to pre-treat lignocellulosic biomass before bacterial conversion to value-added products (Camarero, Galletti and Martinez, 1994; Yang *et al*., 2014), due to their enzymatic potential for lignocellulosic degradation. Thus, the bioaugmentation of a microbial community with *Trichosporon* sp. may aid in the degradation of bio-oil in culture.

Analysis of the initial sediments by DGGE showed that the communities from natural sediments generally gave lighter bands compared to those from Benhar Bing, potentially due to a higher diversity of species in these sediments which can cause difficulties in resolving the large number of bands (Pagaling *et al*., 2014). Such richness indicates a diverse community which is expected of highly-diverse natural sediments. Additionally Benhar Bing samples showed a greater degree of variation in composition compared to those from Cramond beach which was presumably the cause for the significant difference observed between the sample sites. The similarity of the Cramond samples is not unexpected as constant mixing of sediments by wave action could predictably maintain a homogenous community structure (Wang *et al*., 2012). The difference in community composition of Benhar Bing sediments from natural sediments and their enhanced utilisation of bio-oil led to additional sediments from this site being used for further bio-oil culturing.

The characterisation of the Benhar Bing sediment communities showed similar taxonomies to other published communities isolated from acid mine drainage sites (Chen *et al*., 2015; Li *et al*., 2017) with high abundances of acidophilic microorganisms and iron-oxidisers. Although some of these microorganisms may not survive the conditions of a bio-oil medium, the acidophilic microorganisms that are capable of the degradation of plant matter potentially could. Communities from site 4 showed the highest diversity and a radically different microbial community composition to the other sites. In contrast, the community from site 2-1 had the lowest diversity however both communities repeatedly showed a higher growth rate than the other isolated communities.

The most abundant genus identified, particularly from site 2-1, was from *Xanthomonadales*, a large and diverse order of bacteria, members of which include major plant pathogens (Naushad *et al*, 2015). Their abundance in sediment from site 2-1 was considerably higher than the other sediments which could be due to the surface location of sampling. Their relative abundance in the community does not explain how it was able to reach a higher OD than the competing communities. Without a clear pattern in the most relatively abundant genera, between the isolated communities of site 2-1 and 4, a limitation of the study is highlighted in that the communities after growth in the bio-oil medium were not sequenced, so it is not possible to know if these two communities eventually began to share common microbial patterns of relative abundance.

Despite the failure of the single species to degrade bio-oil in these tests, successful aerobic growth in bio-oil medium of microbial communities isolated from the environment indicated at least partial degradation of bio-oil up to 4 g/L and promised potential further streamlining of a microbial consortium capable of utilising it. There are still questions that would need to be addressed before further attempts were made at aerobic degradation of bio-oil by microbial consortia. Although the starting communities of the isolated natural sediments are known, it is still unknown how the communities changed after bio-oil degradation and additionally how they changed with successive increases in bio-oil concentration. It may be that bio-oil toxicity drastically reduced the diversity of the communities to a similar threshold which could be further adapted or bioaugmented for more efficient utilisation of bio-oil.

Similarly to the requirement of characterising the microbial communities after bio-oil degradation, the chemical composition of the bio-oil medium needs to be analysed both before, and after aerobic culturing, such that an understanding of how the bio-oil is being utilised is revealed. One of the primary thermal degradation products of cellulose is levoglucosan (1,6-anhydro-b-d-glucopyranose), an anhydrosugar that can be easily hydrolysed to glucose (Bennett, Helle and Duff, 2009) and is a major constituent of lignocellulosic-derived bio-oils (Hwang *et al*., 2013; Mourant *et al*., 2013; Sukhbaatar *et al*., 2014). If the microbial communities were utilising such

sugars and only adapting to tolerate the levels of microbial inhibitors as opposed to metabolising them then there is still a toxic waste product that is not being degraded.

The aerobic tests were the first attempt in this project to convert bio-oil into a value-added product. Despite the ability of some microbial consortia to utilise the bio-oil as a carbon source, the major obstacle to continued efforts was the question of how then to achieve conversion to a value-added product. There are several examples in the literature of neutralised or detoxified bio-oil as a carbon source in liquid media for the growth of pure cultures of organisms modified to utilise pyrolytic sugars for ethanol production (Lian *et al*., 2010; Wang *et al*., 2012; Das and Sarmah, 2015). But the additional pre-treatment steps just to prevent the inhibition of the microorganisms confine the technology to the laboratory as current technologies for fuel and chemical production are still cheaper and more efficient. With that in mind the focus of the project turned towards the application of bio-oil in existing technologies, specifically anaerobic digestion (AD) as a more efficient means of combining degradation and conversion of bio-oil into a product.

CHAPTER 5: ANAEROBIC

5.1 Introduction

Anaerobic Digestion (AD) is a well-established technology for the conversion of various waste streams into renewable energy in the form of biogas. The ability of AD to hydrolyse and ferment feedstocks containing thousands of different carbon-based molecules into single carbon compounds, in the form of methane and carbon dioxide, makes it an attractive platform for the degradation of bio-oils (Fabbri and Torri, 2016). Pyrolysis also alleviates a major barrier to the AD of lignocellulosic material due to the thermal depolymerisation of lignin, which is known to reduce the efficiency of AD (Monlau *et al.*, 2012).

As seen in the aerobic tests, bio-oil is still a particularly difficult feedstock to degrade biologically and contains thousands of compounds including numerous microbial inhibitors that prevent it from being utilised more extensively. Such complexity therefore requires an equally complex set of metabolic pathways which can potentially be found in the microbial consortia of anaerobic digestate. The pairing of pyrolysis and AD is still a relatively novel concept however there does exist in the literature examples of AD of bio-oils (Andreoni *et al.*, 1990; Torri and Fabbri, 2014; Hübner and Mumme, 2015). Microbial inhibition is still encountered however the anaerobic microbial communities are generally capable of adapting to the bio-oil conditions and commencing methanogenesis using bio-oil as a feedstock.

5.1.1 AD1 and AD2

Following the Fermentation of Organic Materials Standard VDI 4630, a standard that provides guidelines on tests for monitoring biogas output of organic materials, I initially utilised a batch AD system to monitor the AD potential of wastewater treatment anaerobic digestate to convert bio-oils to biogas in four separate tests, summarised in Table 5.1. The first tests performed were designed to assess the potential of AD to convert three different bio-oils to biogas, with two experiments using increasing concentrations of bio-oil, AD1 and AD2. The biomasses for the

pyrolysis into bio-oils were chosen for their differing lignocellulosic content, softwood pellets (SWP/BO) as a standard high lignin biomass, wastewater treatment anaerobic digestate (AD/BO) as a mixed biomass from the same wastewater treatment plant as the test digestate, and dried *Macrocystis pyrifera* (MP/BO), a brown algae commonly known as giant kelp, as an example of a non-lignin containing biomass. These first tests were intended to evaluate the limits of bio-oil toxicity to AD, the impact of bio-oils from different feedstocks and the reproducibility of these feedstocks at differing concentrations.

Data published by Hübner and Mumme (2015) suggested that digestates from an on-farm biogas plant, fed with cow manure and maize, were capable of overcoming methanogenesis inhibition from bio-oil at concentrations as high as 12 g/L COD. Due to the general lower COD of sewage sludge digestates (Akhiar *et al*., 2017) and the resultant potential limitations to methanogenesis, the first test reactors were supplemented with only 5 g/L COD bio-oils with the second test reactors supplemented with 15 g/L COD.

5.1.2 AD3

Acetic acid has been described as one of the world's most important chemicals (Ijmker *et al.*, 2014) due to its extensive use in the production of solvents and polymers, with the global market showing an expected compound annual growth rate (CAGR) of ~8.5% between 2016 and 2021 (Zion Research, 2016), compared to ~6.5% for biogas between 2016 and 2026 (Future Market Insights, 2017). With interest in the development of the biorefinery concept, where next generation fuels and chemicals will be derived from biomass as opposed to fossil-derived oil (Cherubini, 2010), there is growing research looking at the use of AD for the production of more than just biogas (Sauer, 2008).

AD3 was performed to investigate the effects of sterilisation of digestate on reactor performance and production of volatile fatty acids (VFAs). Work by Jones *et al*. (2015) utilised dark fermentation of sucrose and grass pellet-fed inoculum from sewage sludge for the production of hydrogen, and recovered the inhibitory VFAs

that accumulated. The process requires the inactivation of methanogenic organisms which is accomplished by heating the inoculum to 120 °C for 40 minutes; the remaining organisms survive these conditions by sporulating (Reilly, Dinsdale and Guwy, 2015). Due to the similarities between the hydrolysis and fermentative processes between AD and dark fermentation, it was hypothesised that the addition of bio-oil to sterilised digestate would still allow for bio-oil degradation to continue by the organisms that had survived the sterilisation however methanogenesis would be absent, thus VFAs could accumulate and potentially be recovered as a value-added product of greater value than biogas.

The experiment was designed for the MSc Biotechnology class of 2016/17 who set up and monitored the reactors during the practical sessions of the Principles of Industrial Biotechnology module. Similarly to the previous experiments, reactors were set up with 20 mL digestate however only half the reactors were supplemented with 10 g/L COD SWP/BO bio-oil. Additionally, the digestate was either 20 mL of "fresh", from the same stock as AD1 and AD2, "autoclaved", where the digestate has been autoclaved prior to use, or a 1:1 (v:v) mixture of fresh or autoclaved digestate with a "seed" digestate from the day 102 SWP/BO reactors from AD2. Of interest was whether it was possible to "rescue" the methanogenic capabilities of a digestate by mixing autoclaved digestate with a "seed" digestate that already had a microbial consortium capable of degrading the bio-oil used in the experiment; thus it was expected that bio-oil-supplemented reactors with this digestate might not display as much of an inhibited biogas production curve as fresh digestate reactors with bio-oil.

5.1.3 AD4

The addition of the solid fraction of biomass pyrolysis, biochar, to AD systems is a subject of increasing interest (Mumme *et al.*, 2014; Sunyoto *et al.*, 2016; Lü *et al.*, 2016; Fagbohungbe *et al.*, 2017; Wang *et al.*, 2017) and the limited literature for its inclusion in bio-oil-supplemented reactors does report a reduction in inhibition and an increase in biogas production (Torri and Fabbri, 2014; Hübner and Mumme, 2015). Biochar has been utilised as a catalyst for several industrial applications such as soil improvement and wastewater treatment due to advantageous physical

properties such as a large surface area, high porosity and long term stability (Chen *et al*., 2015). However there is little information regarding the microbial associations with biochar surfaces, which is surprising considering the aforementioned properties of biochar are similarly advantageous to microbial attachment (Feng *et al*., 2015).

The inclusion of biochar in anaerobic digesters supplemented with bio-oil is a natural progression of the research considering both are products from the same technology, and were interest in this coupling to increase, a use would have to be found for both as they are made simultaneously. The benefits of including biochar in anaerobic digesters are due to their ability to sequester toxins through adsorption and for their porous structure to harbour microorganisms and promote syntrophy by mediating interspecies electron transfer (Torri and Fabbri, 2014; Fabbri and Torri, 2016; Lü *et al*., 2016).

Surface topology plays a significant role in microbial attachment and biofilm formation where surface roughness generates crevices for microorganisms to attach and be protected from external environmental pressures (Mitik-Dineva *et al*., 2008). Microorganisms in biofilms are also more likely to survive unfavourable conditions and can trap other species that do not form biofilms, assisting in their survival (Hsu *et al*., 2013). Coupled with this, biochar has been shown to promote direct interspecies electron transfer (DIET) between microorganisms growing on the char surface (Chen *et al*., 2015). DIET is an important strategy for interspecies electron transfer which does not require the usual diffusion of electron carriers between species. It has been suggested that the production of cellular components for such extracellular transfer of electrons requires time that DIET does not and as such, the inclusion of conductive materials, such as biochar, in anaerobic digesters can shorten lag times before methanogenesis (Zhao *et al*., 2015).

Two biochars were utilised for the purpose of AD4, a standard biochar from softwood pellets and CreChar® from waste paper cups. In an effort to standardise the production of biochars for industrial or commercial usage, the UK Biochar Research Centre (UKBRC) have a Standard Biochar list of 10 biochars from five feedstocks,

made using their pilot-scale pyrolysis unit, giving them a high level of control over the pyrolysis process thus enabling high reproducibility of their chars. For this test the UKBRC supplied SWP550 made from softwood pellets pyrolysed at 550 °C. Carbogenics Ltd are a spin-out company from the UKBRC that supplied their biochar product, CreChar®, made from waste paper cups pyrolysed at 450 °C. Combined research interests in AD supplements facilitated the inclusion of CreChar® in the test as a comparison against a standard biochar.

It was further hypothesised that the pre-incubation of biochars with the microorganisms that would be present in the system could aid the catalytic effect of biochar addition. The microorganisms that were expected to adhere to the biochar surfaces would gain the advantage of a stable micro-environment that would offer some protection from bio-oil toxicity (Watnick and Kolter, 2000). The documented lag period observed in bio-oil-supplemented reactors is most likely due to the microbial communities having to adapt to its presence (Hübner and Mumme, 2015), therefore, if a stable community of microorganisms was already established, the total community could begin degradation of bio-oil sooner and shorten the lag period. As such, for AD4, both chars were additionally pre-incubated with anaerobic digestate for 48 hours, gently washed with deionised water and used in the reactors.

The examination of methanogenesis inhibition for the purposes of organic acid accumulation was also continued in AD4, initially two compounds were chosen for their ability to completely inhibit methanogenesis, sodium 2-bromoethanesulfonate (BES) and alamethicin. BES is a structural analog of coenzyme M (CoM), a cofactor present only in methanogenic archaea that is responsible for the terminal step of methane biosynthesis, where it carries a methyl group to methyl-CoM reducatase for conversion to methane. BES competitively inhibits the reductive step and so is specific only to methanogens (Liu *et al.*, 2011) with a reported complete inhibition accomplished with a concentration of 50 mM.

Alamethicin is an antibiotic produced by the fungal species *Trichoderma viride* and belongs to the peptiabol group of polypeptides. These peptides are amphiphilic and

therefore surfactants, due to the presence of the non-essential amino acid 2-aminoisobutyrate, which induces an alpha-helical peptide structure able to reduce the interfacial tension between cell lipid layers and create holes in cell membrane structures (Ionov *et al.*, 2004). As such, the method of inhibition is not specific to methanogens. However Zhu *et al.* (2015) reported methanogenesis inhibition and the promotion of acetogenesis in bioelectrical systems, similar to the mixed cultures found in anaerobic digesters, at concentrations of 25 µg/mL. It was theorised that the thinner protein envelopes of methanogenic species are more sensitive to the surfactant-effect of alamethicin. The use of this concentration in our reactors however did not cause any inhibition of methanogensis and supplemented reactors displayed similar levels of biogas production to the controls reactors. Therefore these data are not shown below.

Methanogenic potential has been shown to be closely related to the *mcrA* copy number of a sample (Morris *et al*., 2014; Narihiro and Sekiguchi 2011) as a proxy for methanogenic archaeal abundance. Therefore quantitative PCR (qPCR) of the *mcrA* gene was utilised to measure the number of these DNA sequences in the reactors at the sampling time points of AD4. Additionally, biochar surfaces were analysed for *mcrA* copy number before and after the experiment. Biochars were separated from the digestate and washed with deionised water upon completion of the experiment and from a sample taken from the initial pre-incubation before DNA extraction. Due to the washing it was presumed that DNA extracted from the biochars would predominantly be from organisms that were attached to the biochar surface.

By AD4 it was known from the previous tests that the microbial communities in the Seafield waste water treatment anaerobic digestate were capable of degrading SWP/BO; however, reactors were still inhibited at the beginning of the test to such an extent that fresh digestate needed to be added in all instances. As such it was unknown if the digestates were capable of overcoming the toxicity of SWP/BO at concentrations of 10 g/L COD without reinoculation, and so the concentration of bio-oil was reduced to 5 g/L COD for the test. In addition, a new digestate batch was obtained from Seafield wastewater treatment plant. AD4 was designed for an MSc

Biotechnology project undertaken by Sabrina Yeo who aided in the set up and monitoring of the experiment.

Test	Bio-oils	COD (g/L)	Test Parameters	Notes
AD1	AD/BO MP/BO SWP/BO	2.5	Three different bio-oil feedstocks at low concentration	20 mL digestate added at day 6 to overcome inhibition
AD2	AD/BO MP/BO SWP/BO	10	Three different bio-oil feedstocks at high concentration	10 mL digestate added at day 20 to overcome inhibition
AD3	SWP/BO	10	Unsterilised, sterilised, mixed & seed digestates	Seed digestate was from AD2 SWP/BO-reactors
AD4	SWP/BO	5	Standard biochar CreChar® Incubated biochars Methanogenic inhibitor	Digestate was from a second sampling batch

Table 5.1. Anaerobic digestion tests of sewage sludge digestate from Seafield wastewater treatment plant, supplemented with bio-oils from anaerobic digestate (AD/BO), *Macrocystis pyrifera* (MP/BO) and softwood pellets (SWP/BO). Details are given of the specific test parameters and notable alterations.

5.2 Results

5.2.1 AD1

After 6 days of complete inhibition of bio-oil-supplemented reactors, a further 20 mL of digestate was added to every reactor thereby halving the bio-oil concentration to 2.5 g/L COD. The addition of fresh digestate immediately saw biogas generated from the bio-oil-supplemented reactors as can be seen in Figure 5.1.

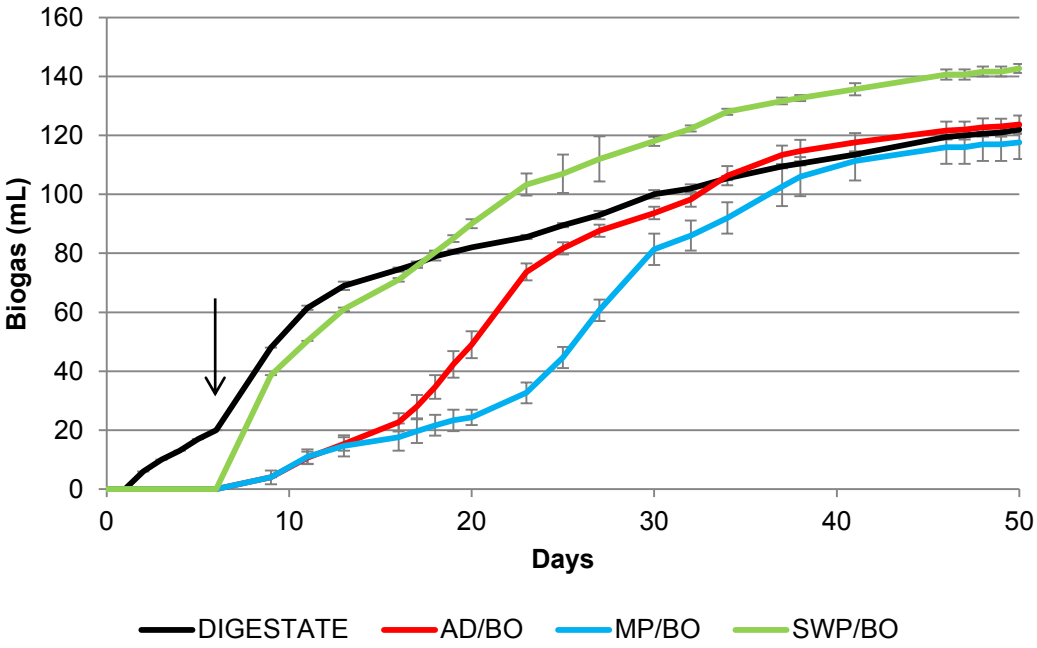

Figure 5.1. Biogas generation from test AD reactors with 2.5 g/L COD bio-oils from anaerobic digestate (AD/BO), *Macrocystis pyrifera* (MP/BO) and softwood pellets (SWP/BO) in 40 mL sewage sludge digestate, the additional 20 mL was added on day 6 (arrow) due to complete biogas inhibition. All conditions were performed in triplicate with the exception of the digestate-only control where one replicate was removed due to setup error. Each curve is a mean of the replicates with error bars of standard deviation.

Digestate-only control reactors began generating biogas from the second day of the test whilst all those that were supplemented with any kind of bio-oil were completely inhibited until the addition of more digestate. The addition of new digestate alleviated the inhibition caused by the SWP/BO whose reactors rapidly began generating biogas. Reactors with AD/BO and MP/BO were still partially inhibited until day 16 and 23 respectively; however, by then the community had overcome the inhibition and begun biogas generation.

The additional COD from the bio-oil caused SWP/BO-supplemented reactors to have an increased total biogas volume over the control reactors (142.67 ± 5.68 mL over 122 ± 1.41 mL (mean ± SD)), overtaking the controls by day 17. With the only difference in COD between test conditions being the presence of bio-oil, the bio-oil

must have been degraded to biogas. Of note is that this was only seen in SWP/BO reactors with AD/BO and MP/BO reactors generating an equal or lesser volume of biogas compared to the controls (123.67 ± 3.06 mL and 117.67 ± 1.53 mL respectively).

Biogas from sewage treatment anaerobic digestate typically has a methane content of 60 – 65% by volume (Liebetrau *et al.*, 2017) with the rest made up mainly of carbon dioxide. Methane concentration was monitored over the course of the experiment with measurements taken at day 6, 20 and 34 for reactors that had generated > 20 mL biogas. Biogas volumes remaining at the end of the experiment that were below the 20 mL threshold used estimated methane concentrations based on their previous measurement. The biogas generated from the test reactors over the course of the experiment averaged slightly higher than typically reported for sewage treatment anaerobic digestate at 69.33 ± 5.33%. There were however differences in the methane content between the test conditions; control digestate had an average methane content of 65.2 ± 1.18% similar to that of biogas from SWP/BO reactors at 63.65 ± 1.24% whereas biogas from the AD/BO and MP/BO reactors contained 74.48 ± 1.34% and 73.98 ± 2.43% methane respectively.

It is possible to see the rate of bio-oil degradation by observing the changes in COD of the aqueous fraction of the digestate. Figure 5.2a shows the start (d0) and end (d50) COD concentrations of the reactors. Immediately obvious is the increased COD that bio-oil-supplemented reactors have over the digestate-only controls; it is important to note that the concentration difference between the digestate control reactors and bio-oil-supplemented reactors is ~2.5 g/L COD as it was unknown if it would be immediately sequestered by any solid material in the digestate and therefore give a reduced reading. Digestate-only control reactors show a limited reduction in COD of the aqueous phase (9.79 ± 5.22%) with greater reductions of 23.5 ± 0.61%, 16.38 ± 0.71% and 32.5 ± 1.03% for AD/BO, MP/BO and SWP/BO respectively.

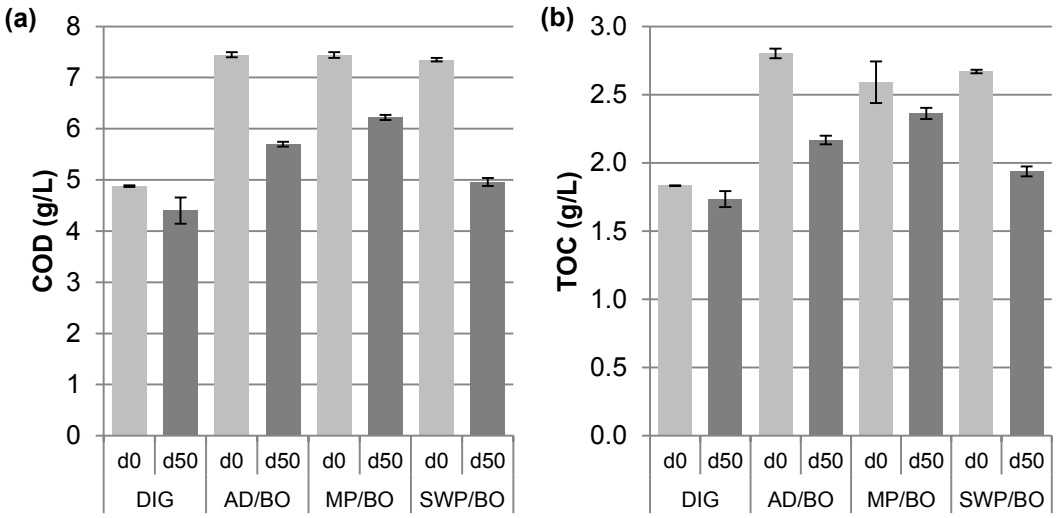

Figure 5.2. (a) COD and (b) TOC of aqueous phase digestate at d0 (light grey) and d50 (dark grey) of AD reactors with 2.5 g/L COD bio-oils from anaerobic digestate (AD/BO), *Macrocystis pyrifera* (MP/BO) and softwood pellets (SWP/BO) in 40 mL sewage sludge digestate. All conditions were performed in triplicate with the exception of the digestate-only control (DIG) where one replicate was removed due to setup error. Each measurement is a mean of the replicates with error bars of standard deviation.

The TOC of the reactors is additionally shown in Figure 5.2b. Whereas COD measures the amount of oxidisable carbon in a sample; the TOC test purges the inorganic fraction of carbon and so only measures the organic fraction of a sample. Similarly to reported values on wastewater treatment (Dubber and Gray, 2010), the TOC shows a similar pattern to the COD of the reactors; with a limited reduction for the controls (5.38 ± 3.24%) and increasing reductions for the bio-oil reactors from MP/BO (8.78 ± 1.58%), AD/BO (22.65 ± 1.13%) to SWP/BO (27.44 ± 1.35%).

Changes in COD and TOC of the reactors are independent of the reductions in organic acid concentrations as can be seen in Figure 5.3. AD/BO bio-oil has a greater concentration of organic acids compared to the other bio-oils; in fact SWP/BO seems to have the least despite producing more biogas during the experiment.

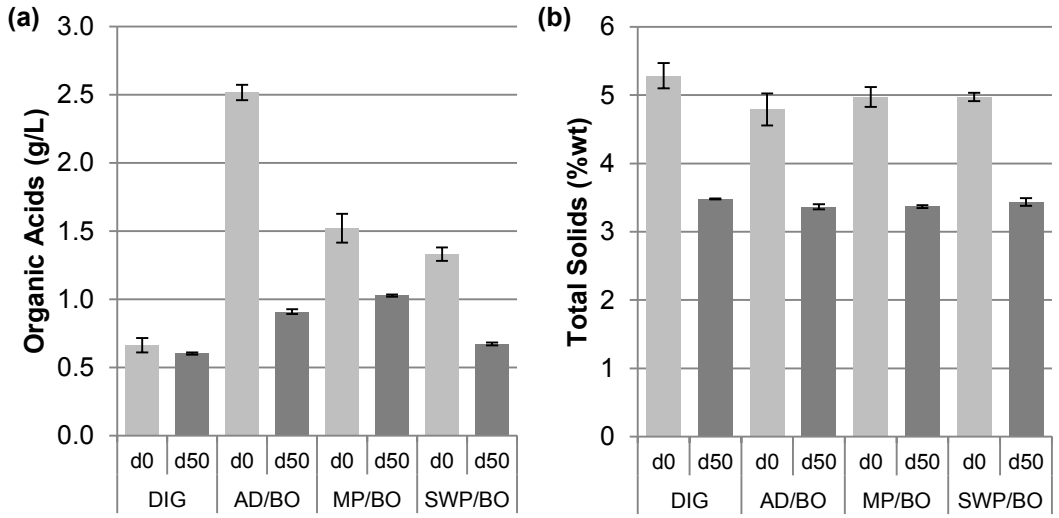

Figure 5.3. (a) Organic acids of aqueous phase digestate and (b) total solids of digestate at d0 (light grey) and d50 (dark grey) of AD reactors with 2.5 g/L COD bio-oils from anaerobic digestate (AD/BO), *Macrocystis pyrifera* (MP/BO) and softwood pellets (SWP/BO) in 40 mL sewage sludge digestate. All conditions were performed in triplicate with the exception of the digestate-only control (DIG) where one replicate was removed due to setup error. Each measurement is a mean of the replicates with error bars of standard deviation.

Digestate-only controls reduced their initial levels of organic acids by 8.68 ± 1.07% while SWP/BO reactors saw a 49.5 ± 0.78% reduction down to a similar end value. Meanwhile AD/BO reactors reduced their organic acid levels by 63.88 ± 0.5% but still had greater end concentrations than controls and SWP/BO reactors. This pattern is more pronounced for the MP/BO reactors that saw only a 32.46 ± 0.5% reduction in organic acid concentration and show an end concentration almost double that of controls.

Figure 5.3b shows the reduction in TS of the reactors as the solid organic material is eventually converted to water and gas as part of the AD process. It can be seen that despite differences in biogas output, the reactors show a similar decrease in their TS. The addition of the diluted bio-oils is noticeable at the start of the test with a slight decrease in TS (an average difference of -0.37 ± 0.1% to controls) however day 50

samples all exhibit similar TS levels with an average loss of 31.76 ± 1.88% across all conditions.

Although bio-oils are typically acidic, those derived from sewage sludge anaerobic digestate or macroalgae are more basic, with pHs of 9.37 and 9.3 respectively. This is mirrored in the digestates supplemented with them, (Figure 5.4a) as can be seen by the slight increase in pH to 8.72 and 8.75 above digestate-only controls at 8.45. In contrast, the bio-oil derived from lignocellulosic biomass that had a pH of 2.39 lowered the pH of the digestate to 8.33. After the 50 days of anaerobic digestion we see all the reactors reduce their pHs by a similar amount (ΔpH = -0.68 ± 0.04).

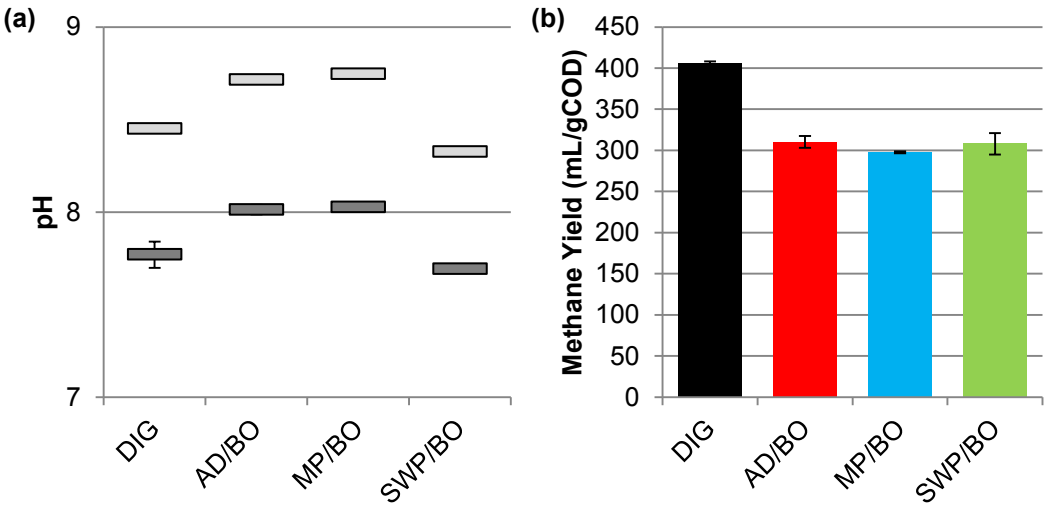

Figure 5.4. (a) pH of digestate at d0 (light grey) and d50 (dark grey) and (b) methane yields of AD reactors with 2.5 g/L COD bio-oils from anaerobic digestate (AD/BO), *Macrocystis pyrifera* (MP/BO) and softwood pellets (SWP/BO) in 40 mL sewage sludge digestate. All conditions were performed in triplicate with the exception of the digestate-only control (DIG) where one replicate was removed due to setup error. Each measurement is a mean of the replicates with error bars of standard deviation.

Figure 5.4b shows the methane yield per starting amount of COD for the reactors. This can give an impression of the efficiency of these reactors at producing methane based on the starting material. All the bio-oil-supplemented reactors show a

decreased methane yield relative to the digestate-only controls. There is no considerable difference in yield based on the feedstock as, although the largest producer of biogas, SWP/BO reactors produced biogas with the lowest concentration of methane.

5.2.2 AD2

After 20 days of limited methane production, another 10 mL of digestate was added to each reactor decreasing the final concentration of bio-oil to 10 g/L COD.

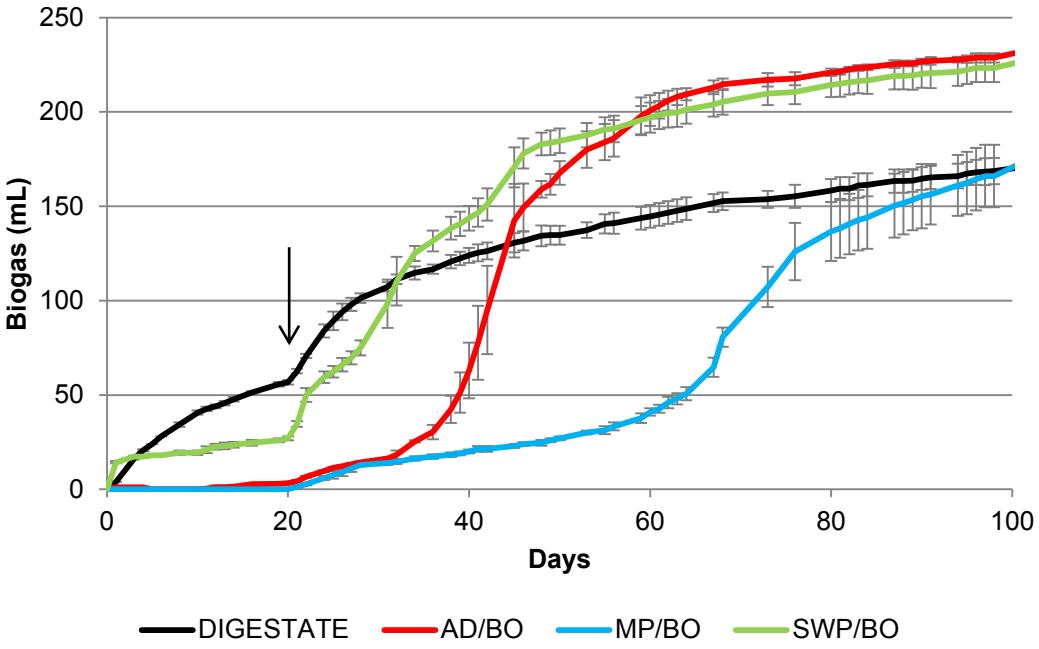

Figure 5.5. Biogas generation from test anaerobic digestion reactors with 10 g/L COD bio-oils from AD (AD/BO), *Macrocystis pyrifera* (MP/BO) and softwood pellets (SWP/BO) in 30 mL sewage sludge digestate, the additional 10 mL was added on day 20 (arrow) due to complete biogas inhibition. All conditions were performed in triplicate with each curve as a mean of the replicates with error bars of standard deviation.

Similarly to AD1, the digestate-only control reactors immediately began to produce biogas (Figure 5.5); however SWP/BO-supplemented reactors also saw a sudden burst of 20 mL biogas over the first 10 days. Once analysed, the gas was found to contain only a maximum of 1% methane over the three replicates. This effect is not

seen in the other, basic, bio-oils and after the initial release of this gas, biogas generation is as low as the other bio-oil-supplemented. Once fresh digestate had been added all the bio-oil-supplemented reactors began producing biogas to a similar pattern as in AD1. SWP/BO reactors showed no further inhibition after reinoculation whereas AD/BO and MP/BO reactors were further inhibited until days 32 and ~63 respectively.

Again we see increased biogas generated from SWP/BO reactors over the digestate-only control reactors (226.67 ± 7.51 mL over 171.33 ± 7.09 mL), overtaking the control biogas generation at day 32. We also however see AD/BO reactors do likewise (232 ± 2 mL) by day 45 and then overtaking SWP/BO reactors at day 59, to become the reactors that produced the highest volume of biogas. Although the pattern of inhibition is similar to AD1, we did not observe such a high level of biogas output from the AD/BO-supplemented reactors in that experiment. MP/BO reactors show a significantly shorter biogas generation curve before it begins to plateau in comparison to AD1. Of note is that MP/BO-supplemented reactors still managed to produce, on average, a larger amount of biogas than control reactors by the end of the experiment at 175 mL (± 16.7mL). Also the rate of biogas produced per day in the last 10 days of the experiment was still higher for MP/BO-supplemented reactors than for the other reactor conditions at 2.46 ± 0.26 mL over 0.76 ± 0.98 mL.

The methane content of the biogas also follows similarly to AD1, with digestate controls producing biogas with an average 69.51 ± 1.33% methane while the methane contents of biogas from AD/BO and MP/BO reactors were again higher at 75.91 ± 3.61% and 76.4 ± 4.63% respectively. Even disregarding the initial release of carbon dioxide at the beginning of the test, SWP/BO reactors still produced the lowest proportion of methane, with it being an average 66.01 ± 10.83% of the biogas. The large standard deviation in SWP/BO reactor methane content is due to the second sampling period at day 28, where reactors still seemed to have been releasing further carbon dioxide with an average methane content of 48.32 ± 0.95% of the biogas.

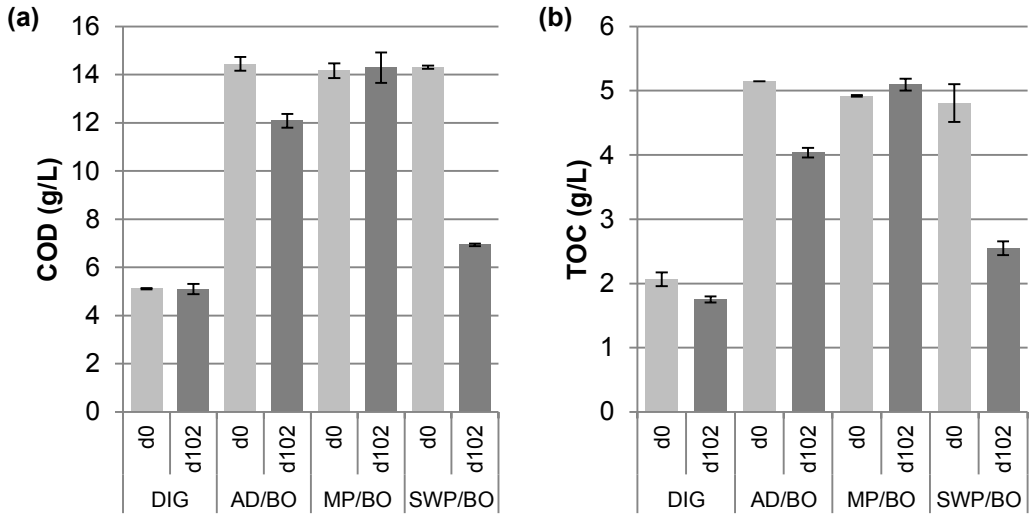

Figure 5.6. (a) COD and (b) TOC of aqueous phase digestate at d0 (light grey) and d102 (dark grey) of AD reactors with 10 g/L COD bio-oils from anaerobic digestate (AD/BO), *Macrocystis pyrifera* (MP/BO) and softwood pellets (SWP/BO) in 30 mL sewage sludge digestate (DIG). All conditions were performed in triplicate with each measurement as a mean of the replicates with error bars of standard deviation.

Figure 5.6a and b show the changes in COD and TOC of the aqueous phase of the digestates at day 0 and day 102 of the experiment and similarly to AD1 we see little-to-no discernible change in COD and TOC of the control reactors. This is not the case when bio-oils are added however; both AD/BO- and SWP/BO-supplemented reactors see a COD reduction of 16.16 ± 1.22% and 51.56 ± 0.38% respectively with SWP/BO reactors almost reaching control levels of final COD. Unlike AD1, MP/BO-supplemented reactors do not show a decrease in COD or TOC, but instead produce similar levels of biogas to digestate-only controls. It is important to note that these reactors had not reached a plateau of biogas production similar to the other reactors, and so there was likely more biogas to be generated.

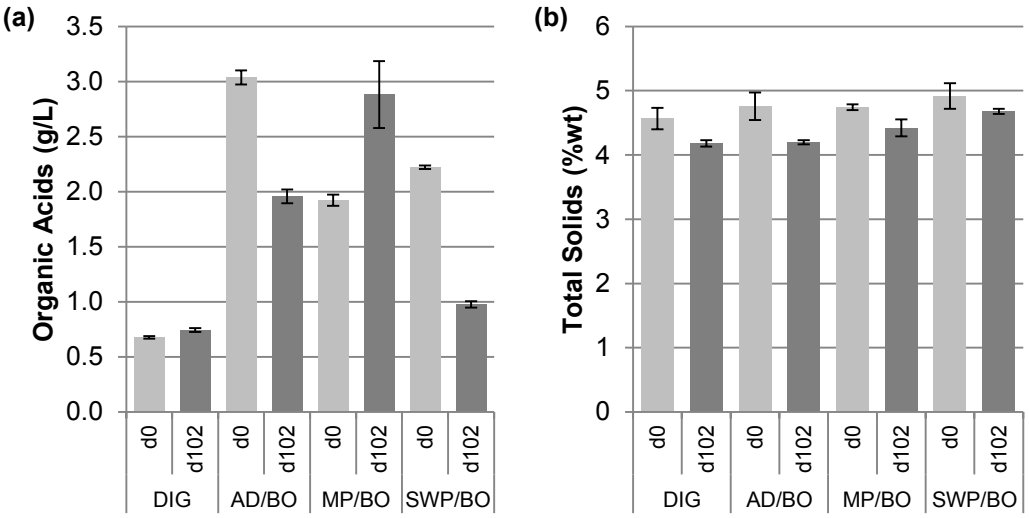

Figure 5.7. (a) Organic acids of aqueous phase digestate and (b) total solids of digestate at d0 (light grey) and d102 (dark grey) of AD reactors with 10 g/L COD bio-oils from anaerobic digestate (AD/BO), *Macrocystis pyrifera* (MP/BO) and softwood pellets (SWP/BO) in 30 mL sewage sludge digestate (DIG). All conditions were performed in triplicate with each measurement as a mean of the replicates with error bars of standard deviation.

The initial concentration of AD/BO organic acids is, similarly to AD1, greater than the other bio-oil-supplemented reactors. And unlike AD1, the SWP/BO-supplemented reactors reduce the concentration of their organic acids by the greatest amount, with a 56.05 ± 1.48% reduction to a value similar to that of the digestate-only control. In comparison, AD/BO reactors reduced their organic acid concentration by 35.57 ± 1.09% to a value still over double that of the final controls. MP/BO reactors increased their organic acid concentration by 49.77 ± 13.13% by day 102; however, the rate of biogas production at this point was higher than the other reactors.

Figure 5.7b shows the limited reduction in TS across all the reactors and illustrates a major difference between AD1 and AD2. Whereas AD1 reactors' TS were reduced by ~30%, the greatest reduction seen in AD2 reactors was from those supplemented with AD/BO bio-oil at 11.77 ± 0.64%. In contrast, the digestate-only controls lost

8.48 ± 1.11% TS followed by MP/BO at 6.77 ± 2.75% and finally SWP/BO at 4.9 ± 0.81%.

The pH of the reactors at day 0 and 102 is shown in Figure 5.8a. Initial digestate pH remains similar to AD1 at 8.55 while the increased concentration of bio-oils has a stronger effect on the starting pHs of the supplemented reactors. The basic bio-oils, AD/BO and MP/BO, with pHs of 9.71 and 9.8 respectively, altered the digestate pHs to 9.18 and 9.39, while SWP/BO bio-oil with a pH of 2.39 caused the digestate pH to drop to 7.39. At the end of the experiment we see a similar reduction of pH across the digestate controls and those reactors with basic bio-oils (a pH reduction of 0.62 ± 0.13); however, the pHs of AD/BO- and MP/BO-supplemented reactors do not reduce to the same level as the digestate-only controls. We observe an increase in pH of the SWP/BO-supplemented reactors (an increase in pH of 0.45 ± 0.14) to a value similar to the digestate-only controls.

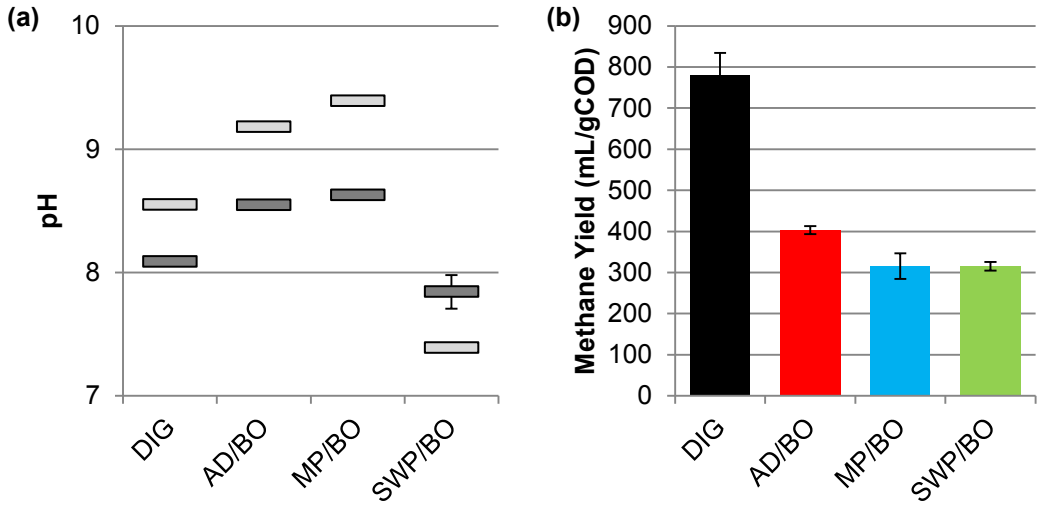

Figure 5.8. (a) pH of digestate at d0 (light grey) and d102 (dark grey) and (b) methane yields of AD reactors with 10 g/L COD bio-oils from anaerobic digestate (AD/BO), *Macrocystis pyrifera* (MP/BO) and softwood pellets (SWP/BO) in 30 mL sewage sludge digestate (DIG). All conditions were performed in triplicate with each measurement as a mean of the replicates with error bars of standard deviation.

Figure 5.8b shows the control reactors for AD2 with the highest methane yield of 779.42 ± 55.7 mL/gCOD after 102 days. The bio-oil-supplemented reactors show a pattern of methane yield similar to in AD1 with AD/BO-supplemented reactors generating the largest amount of methane at 403.17 ± 9.72 mL/gCOD, followed by MP/BO and SWP/BO at 315.62 ± 31.27 mL/gCOD and 315.45 ± 10.48 mL/gCOD respectively.

5.2.3 AD3

Figure 5.9 shows the biogas production of the reactors and immediately noticeable is that all reactors supplemented with bio-oil were significantly inhibited. Therefore, at day 40, 1 mL of each test inoculum, or mix of inocula, was added to stimulate biogas production. Just as the previous tests had shown, the reinoculation with fresh digestates stimulated biogas production in inhibited reactors (with the exception of autoclaved). However, unlike previous tests, there was a ~5 to ~13 day delay until it was observed.

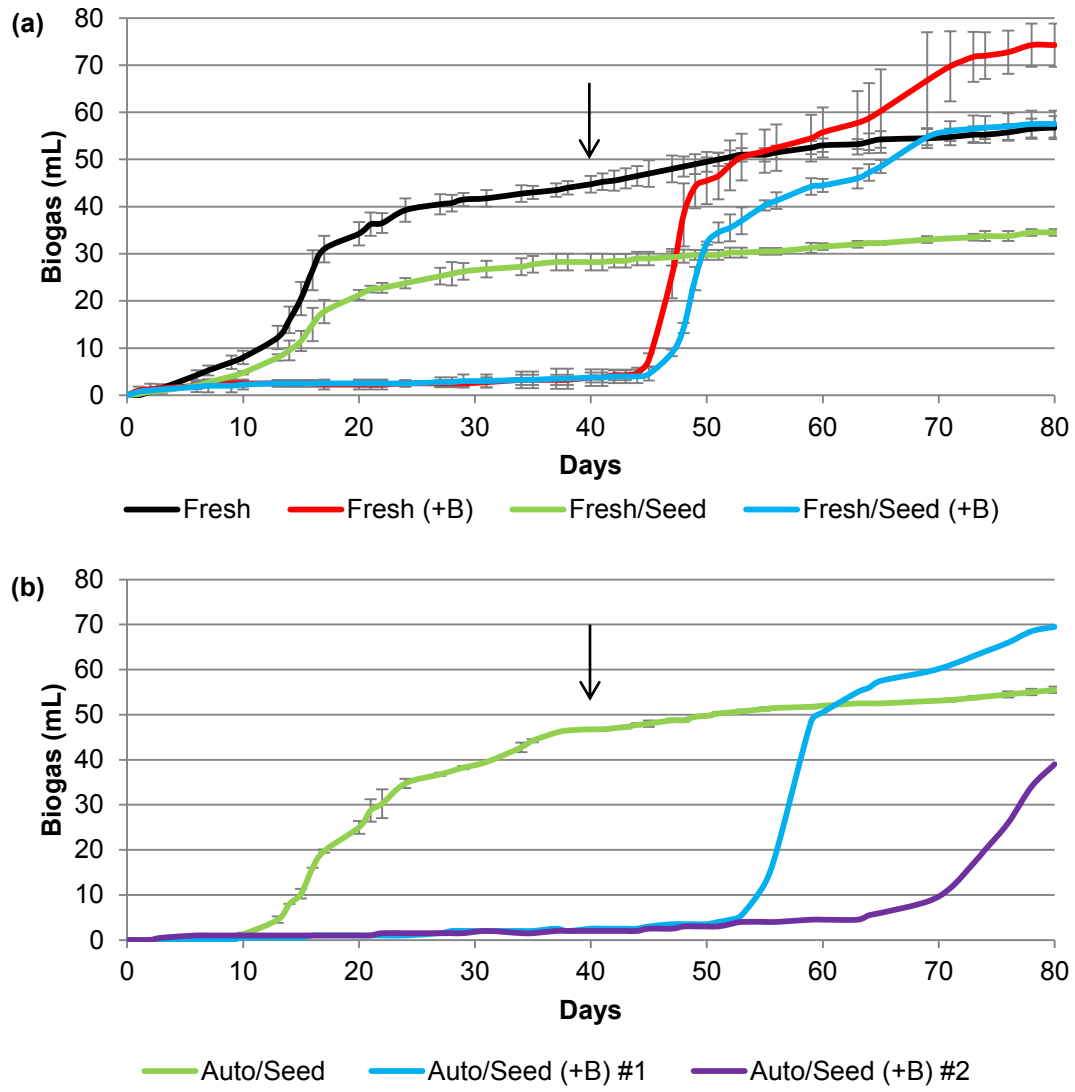

Figure 5.9. Biogas generation from test AD reactors with (+B) and without 10 g/L COD bio-oil from softwood pellets (SWP/BO). The 20 mL of digestate was composed of either (a) fresh or (b) autoclaved sewage sludge digestate with or without 1:1 (v:v) seed digestate from d102 SWP/BO reactors from AD2. Reinoculation of 1 mL of each test inoculum, or mix of inocula, was performed to stimulate biogas production at day 40 (arrow). Both autoclaved and autoclaved with bio-oil reactors produced no biogas and are therefore excluded from Figure 5.9b. All conditions were performed in duplicate with each curve as a mean of the replicates with error bars of standard deviation however due to the significant difference in biogas production from autoclaved/seed digestates with bio-oil replicates, their individual curves are shown.

Of note is that digestate-only controls produced an average 56.75 ± 2.47 mL of biogas over 80 days of AD compared to 122 ± 1.41 mL from AD1 after 50 days and 158.33 ± 6.11 mL from AD2 by the same time point. There is also a distinct difference in the shape of the curve for the control reactors, which require ~13 days of acclimatisation before significant biogas production is observed. This was not seen in AD1 and AD2, where the curves immediately start with a high rate of biogas production having made 69 ± 1.41 mL and 45.67 ± 1.15 mL respectively by day 13 compared to 12.25 ± 2.47 mL from AD3 digestate controls.

Also noticeable in the biogas curves is the difference in biogas production of reactors with different digestates. Autoclaved digestates without the seed digestate do not produce biogas. However, autoclaved digestate mixed with seed digestate produce 37.84% more biogas than fresh digestate with the seed. Additionally seed digestates produce a reduced amount of biogas, with fresh/seed reactors producing 39.21% less than just fresh digestate.

After reinoculation, the fresh digestates recovered fastest. As seen in previous tests, the addition of bio-oil to the fresh digestate produced more biogas than the control reactors (74.25 ± 4.6 mL over fresh digestate controls at 56.75 ± 2.47 mL) with an increased rate of biogas production over fresh/seed digestates. Fresh/seed reactors with bio-oil also produced an average biogas volume greater than the controls at 57.5 ± 2.83 mL.

An important note to make regarding the autoclaved/seed digestates amended with bio-oil is that the replicates exhibited extremely different biogas production, and as such are presented as two separate curves in Figure 5.9b. Due to the inter- replicate variability, any conclusions derived are therefore subject to a higher degree of uncertainty. The two reactors differ not only in their inhibition profile but also in the eventual rate of biogas production. The first autoclaved/seed digestate reactor with bio-oil (ASB1) shows a further 9 days of inhibition compared to the fresh digestate equivalents while the second autoclaved/seed digestate reactor with bio-oil (ASB2) required 25 additional days before significant biogas production began. Once the

curve does begin to climb, it is clear that the rate of biogas production is lower for ASB2 with a maximum rate of 3.06 mL/day, between days 71 – 80, compared to the maximum of ASB1 at 7.17 mL/day between days 53 – 59. It can also be seen that ASB1 overtakes the autoclaved/seed digestate reactors total biogas output at day 60.

Figures 5.10a and b show the change in COD of the reactors with fresh and autoclaved digestate respectively. The autoclaving process did increase the amount of soluble organic material as can be seen by the overall increase in starting COD of the aqueous fractions of these digestates. All reactors with fresh digestate (Figure 5.10a) continued the trend seen from the previous tests where there is little change in COD of the aqueous phase of the digestates without bio-oil addition and a large reduction in COD, close to control values, when it is present. The presence of the seed digestate had no impact on the changes in the fresh digestate reactors. However, those reactors with autoclaved digestates (Figure 5.10b) behave very differently. The absence of biogas production in autoclaved digestate reactors (A) causes a 41.52 ± 19.15% total increase in the COD of the aqueous fraction while reactors with autoclaved digestate plus bio-oil (A+B) see little increase in COD (3.11 ± 3.9% increase). Autoclaved/seed digestates (AS) however see a decrease of 37.08 ± 2.23% while those with bio-oil (AS+B) see a similar 38.45 (± 10.21% decrease. These trends are mirrored by the change observed in TOC (Figure 5.10c and d), as also seen in the previous tests.

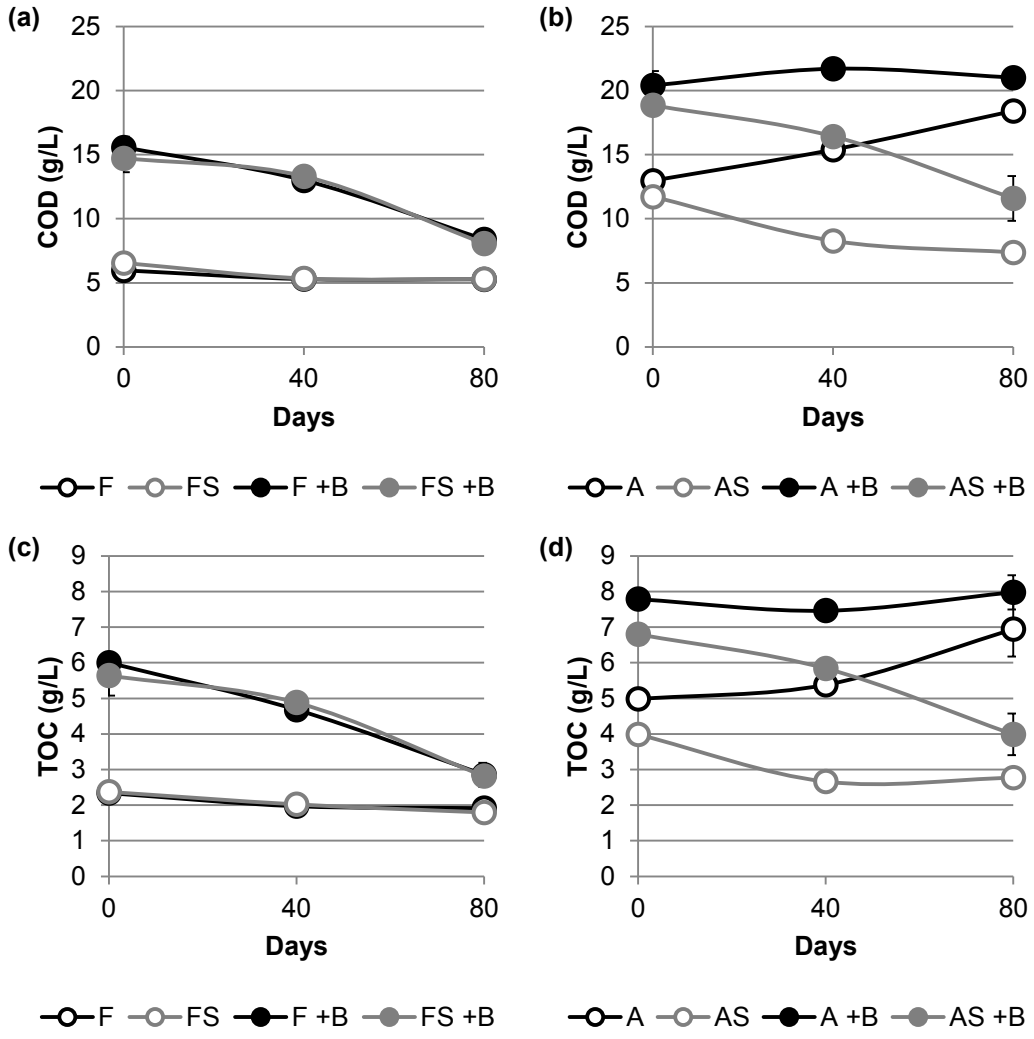

Figure 5.10. (a+b) COD and (c+d) TOC of aqueous phase digestates at d0, d40 and d80 of AD. Half the reactors were supplemented with 10 g/L COD bio-oil (+B) from softwood pellets (SWP/BO). The 20 mL of digestate was composed of either fresh (F) or autoclaved (A) sewage sludge digestate with or without 1:1 (v:v) seed (S) digestate from d102 SWP/BO reactors from AD2. All conditions were performed in duplicate with each measurement as a mean of the replicates with error bars of standard deviation.

We see a different pattern emerge from the changes in organic acid concentrations of these reactors. Similarly to previous tests, the addition of SWP/BO bio-oil increases the initial concentration of organic acids in the aqueous phase of the digestates (Figure 5.11). However, we also see an increase from the autoclaving of the digestate similarly to the COD and TOC. Fresh digestates with no bio-oil (F and FS) see no

change in their organic acid concentrations while the inhibition of biogas production causes an increase of 56.15 ± 7.65% and 80.67 ±7.52% of the starting concentrations for fresh digestate with bio-oil (F+B) and fresh/seed digestate with bio-oil (FS+B) respectively. Once biogas production begins these values then drop by 70.59 ± 1.66% and 69.98 ± 0.45% to values close to the non-bio-oil reactors. The autoclaved digestates show a similar pattern if they are mixed with seed digestate where AS organic acid concentrations do not notably change over the course of the experiment, whereas AS +B show an increase of 38.58 ± 8.33% before biogas generation and then a reduction of 52.5 ± 12.67% after. Both A and A+B displayed complete inhibition of biogas production however the digestate without the addition of bio-oil increased its total organic acid concentration by 397.54 ± 16.79% while the addition of bio-oil caused only a total increase of 38.93 ± 11.63%.

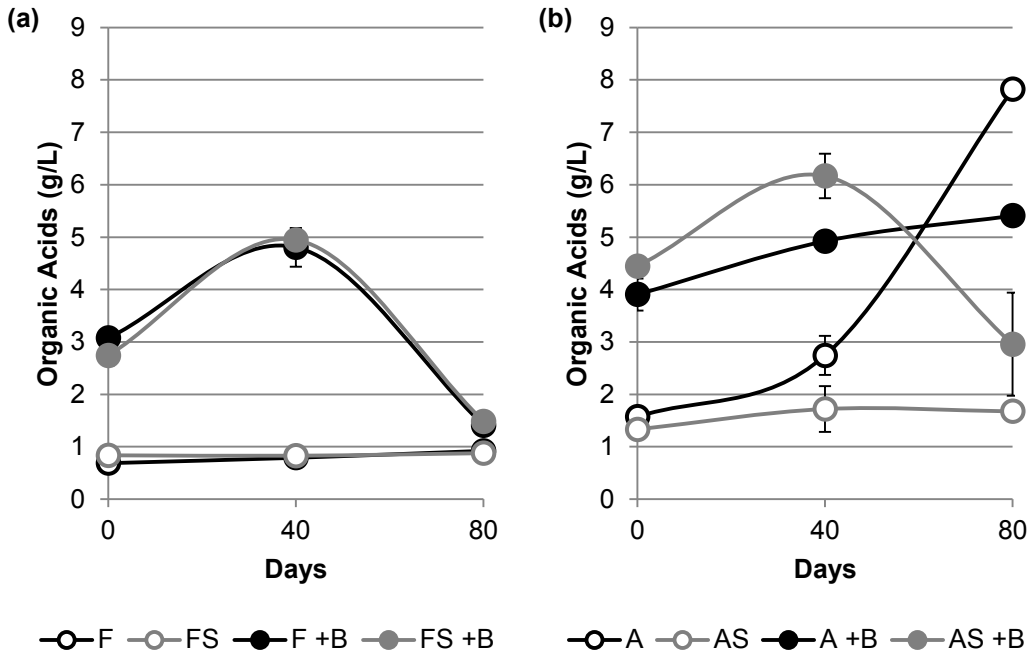

Figure 5.11. Organic acid concentrations of aqueous phase digestates at d0, d40 and d80 of AD. Half the reactors were supplemented with 10 g/L COD bio-oil (+B) from softwood pellets (SWP/BO). The 20 mL of digestate was composed of either fresh (F) or autoclaved (A) sewage sludge digestate with or without 1:1 (v:v) seed (S) digestate from d102 SWP/BO reactors from AD2. All conditions were performed in duplicate with each measurement as a mean of the replicates with error bars of standard deviation.

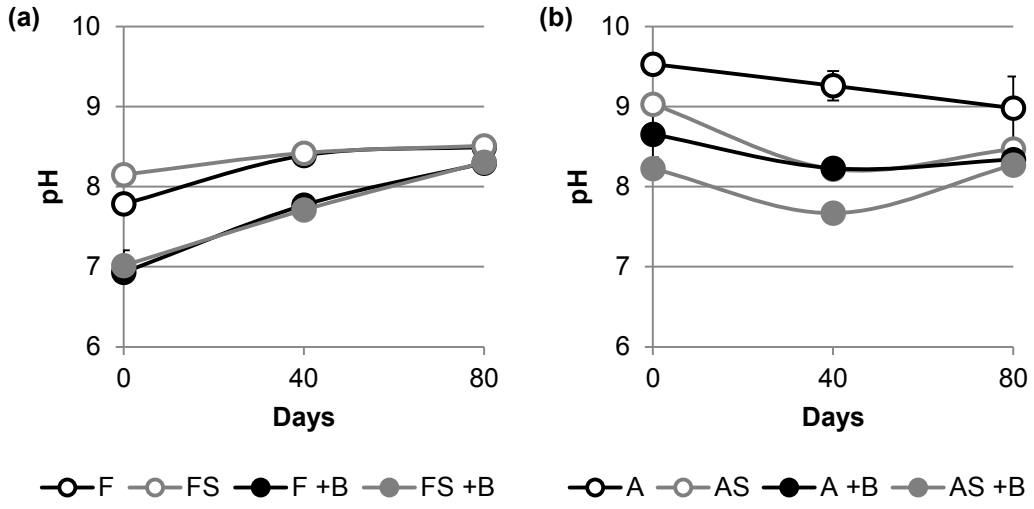

Figure 5.12. Change in pH of AD reactor digestates at d0, d40 and d80 of anaerobic digestion. Half the reactors were supplemented with 10 g/L COD bio-oil (+B) from softwood pellets (SWP/BO). The 20 mL of digestate was composed of either fresh (F) or autoclaved (A) sewage sludge digestate with or without 1:1 (v:v) seed (S) digestate from d102 SWP/BO reactors from AD2. All conditions were performed in duplicate with each measurement as a mean of the replicates with error bars of standard deviation.

Figure 5.12 shows the pH change in the fresh (a) and autoclaved (b) digestates over the course of the experiment, with a general trend for digestates to converge on a similar pH of ~8.5. Bio-oil-supplemented reactors show an initial reduction in pH however in fresh digestates, pH steadily climbs back to control levels. Of note is that the rise in pH at day 40 occurs before the bio-oil-supplemented reactors displayed their rapid production of biogas at ~day 44. This is not the case with the autoclaved digestates, which see acidification before an eventual rise in pH, with the exception of non-supplemented autoclaved digestates which only see acidification.

The methane yield pattern of these reactors (Figure 5.13) shows similarity to the previous tests with the highest yield achieved by digestate alone and the addition of bio-oil COD decreasing the methane potential. Autoclaved digestates without the seed produced no biogas whereas the addition of seed digestate to fresh reduces the

yield. In contrast, seed addition to autoclaved digestate improves the methane yield to levels comparable to fresh digestate plus seed.

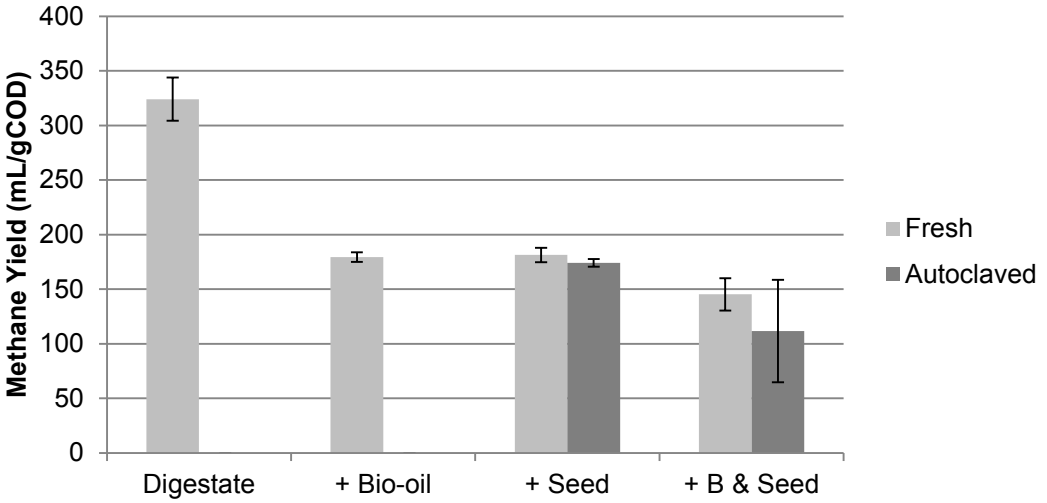

Figure 5.13. Methane yields per gCOD of starting material for AD reactors. Half the reactors were supplemented with 10 g/L COD bio-oil (+B) from softwood pellets (SWP/BO). The 20 mL of digestate was composed of either fresh (light grey) or autoclaved (dark grey) sewage sludge digestate with or without 1:1 (v:v) seed digestate from d102 SWP/BO reactors from AD2. Absent bars are due to total inhibition of biogas production. All conditions were performed in duplicate with each measurement as a mean of the replicates with error bars of standard deviation.

5.2.4 AD4

Figure 5.14a and b show the biogas production from the reactors without (N) and with bio-oil (B) respectively. None of the reactors supplemented with BES (Be) produced enough biogas for methane quantification over the course of the experiment. Similarly to previous tests all reactors with bio-oil displayed a lag phase before substantial biogas production however there was no requirement to reinoculate these reactors as biogas was produced from all conditions by day 3.

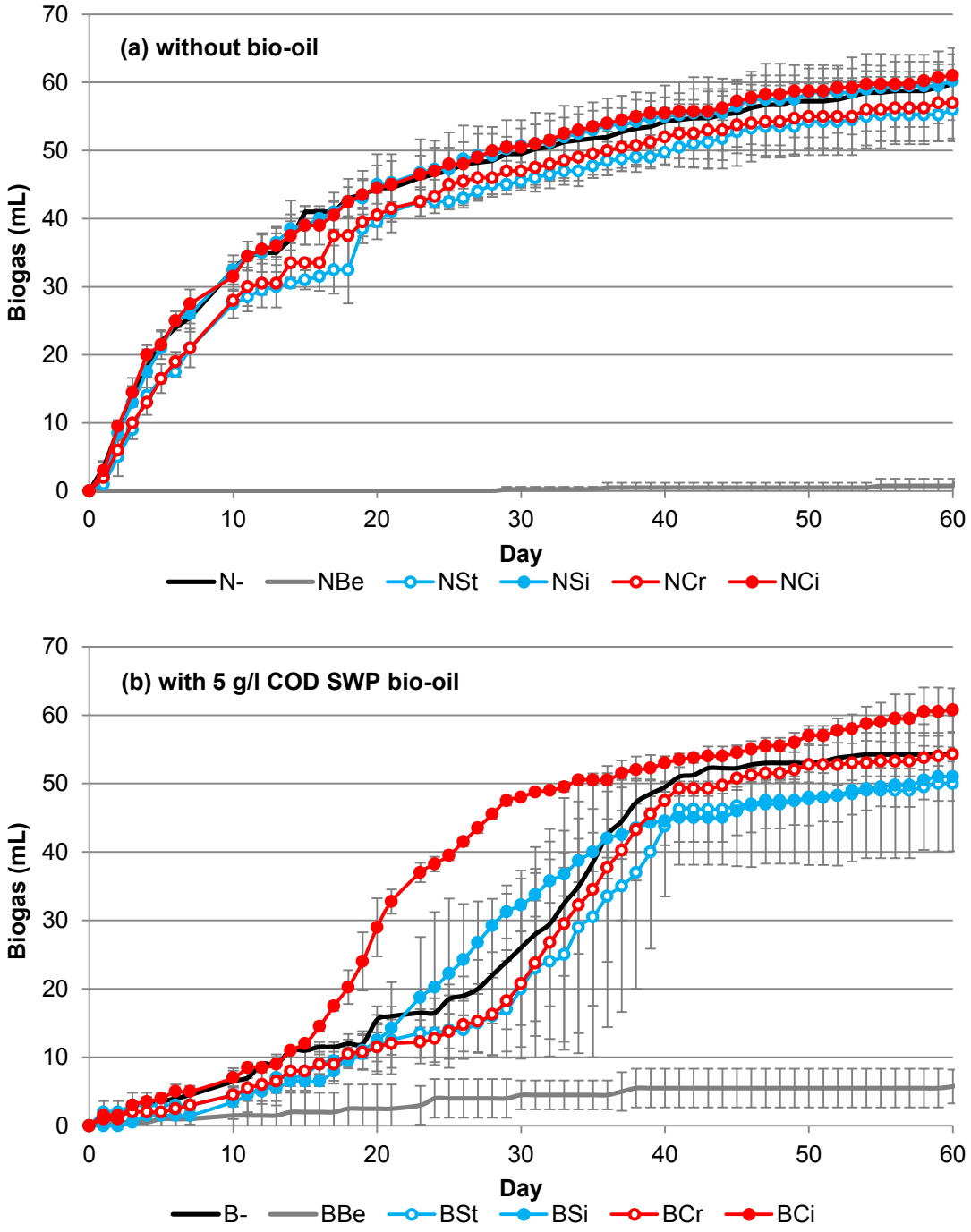

Figure 5.14. Biogas generation from test AD reactors without (a/N) and with (b/B) the addition of 5 g/L COD bio-oil from softwood pellets (SWP/BO). The 20 mL of digestate was supplemented with BES (Be), standard biochar (St), pre-incubated standard biochar (Si), CreChar® (Cr) and pre-incubated CreChar® (Ci). Control reactors were not supplemented (-). All conditions were performed in duplicate with each curve as a mean of the replicates with error bars of standard deviation.

Despite the reduction of bio-oil concentration, we still do not observe bio-oil-supplemented reactors overtaking the control reactors in total biogas output, with the exception of BCi. This is the first example of this behaviour from the AD experiments as the addition of SWP/BO bio-oil in all the previous tests has caused an increase in total biogas over the controls.

Reactors without the addition of bio-oil or BES produce a similar amount of methane at a similar rate irrespective of biochar addition, with an average total of 58.8 mL (± 3.82 mL) over the course of the experiment. The addition of bio-oil to the reactors causes a far greater degree of variation between the reactor conditions. Bio-oil-supplemented reactors show a significantly higher average standard deviation of 3.67 ± 13.33 mL compared to 3 ± 4.66 mL for non-bio-oil reactors (two-sample t-test $P < 0.001$). The bio-oil-supplemented reactors still exhibit the characteristic lag phase before substantial biogas production; however the duration of the lag phase differs between biochar supplements. B- reactors begin substantial biogas production at ~day 24 whereas both the non-incubated reactor sets, BSt and BCr, show a further delay of ~4 days before they begin rapid biogas production. Meanwhile the reactors containing incubated biochars, BSi and BCi, begin their substantial production of biogas at days 16 for standard and 14 for CreChar®.

By the end of the test, both standard biochar-supplemented sets of reactors, BSt and BSi, showed a slightly lower total biogas volume than B- (50.5 ± 6.1 mL compared to 54.25 ± 3.18 mL) while BCr reactors produced an equal amount of biogas (54.25 ± 1.06 mL). Showing significant difference from the bio-oil-supplemented control reactors' biogas production (two-sample Kolmogorov–Smirnov test $P < 0.05$), BCi reactors display, not only a decreased inhibitory phase, but an eventual increase in total biogas produced over the bio-oil and non-bio-oil control reactors (60.75 ± 3.18 mL compared to 59.75 ± 5.3 mL).

Methane concentrations fluctuated between the two sets of data, with non-bio-oil reactors producing biogas with an average 65.14 ± 1.21% methane at day 20, while the biogas from bio-oil-supplemented reactors averaged at 50.8 ± 4.17% methane at

the same time point. For non-bio-oil reactors the concentration then dropped to an average 46.59 ± 1.46% by the end of the test, whereas the methane concentration of biogas from bio-oil-supplemented reactors seemed to increase over time to 57.23 ± 0.93% by day 34 and then 60.47 ± 5.3% by the end of the test. Both N- and NCi reactors produced the highest total volume of methane over the course of the experiment (38.65 ± 0.59 mL and 38.03 ± 3.25 mL respectively) with NSt and NCr reactors producing the least of the non-bio-oil reactors (34.78 ± 2.33 mL). The average total methane produced from the bio-oil-supplemented reactors, excluding BCi (34.9 ± 3.81 mL), was 30.49 ± 1.26 mL.

Changes to the COD and TOC of the aqueous phase of the digestates are shown in Figure 5.15 for non-bio-oil (a and c) and bio-oil-supplemented (b and d) reactors. Immediately noticeable is the considerable deviation of BES-treated reactors to the rest of the tests. The addition of BES causes these reactors to start with over double the COD and a third more TOC than the other reactor conditions. These values then rise by 42.6 ± 0.31% COD and 13.42 ± 2.44% TOC for reactors with no bio-oil and 20.39 ± 1.11 COD and 5.55 ± 0.16% TOC for bio-oil-supplemented reactors.

For the reactors that did produce biogas we see a similar pattern to previous tests with significantly greater reduction of both COD and TOC from bio-oil-supplemented reactors over those reactors with no bio-oil (36.09 ± 3.1% over 25.19 ± 6.22% for COD and 29.99 ± 2.18% over 20.33 ± 6.27% for TOC; two-sample t-tests $P < 0.001$). Although these reactors show a similar pattern in the decrease of both COD and TOC, the BCi reactors ability to overcome bio-oil inhibition before the other bio-oil-supplemented conditions causes an increased rate of COD and TOC reduction. This translates to BCi reactors showing a 19.37 ± 5.1% reduction in COD and 13.68 ± 7.29% reduction of TOC between the start of the test and day 20, compared to an average reduction of 4.93 ± 7.56% and a slight average increase of 2 ± 3.78% for the other bio-oil-supplemented conditions for the same time period. With the exception of BCi however, there is no discernible effect of biochar type or pre-incubation on the digestate COD or TOC.

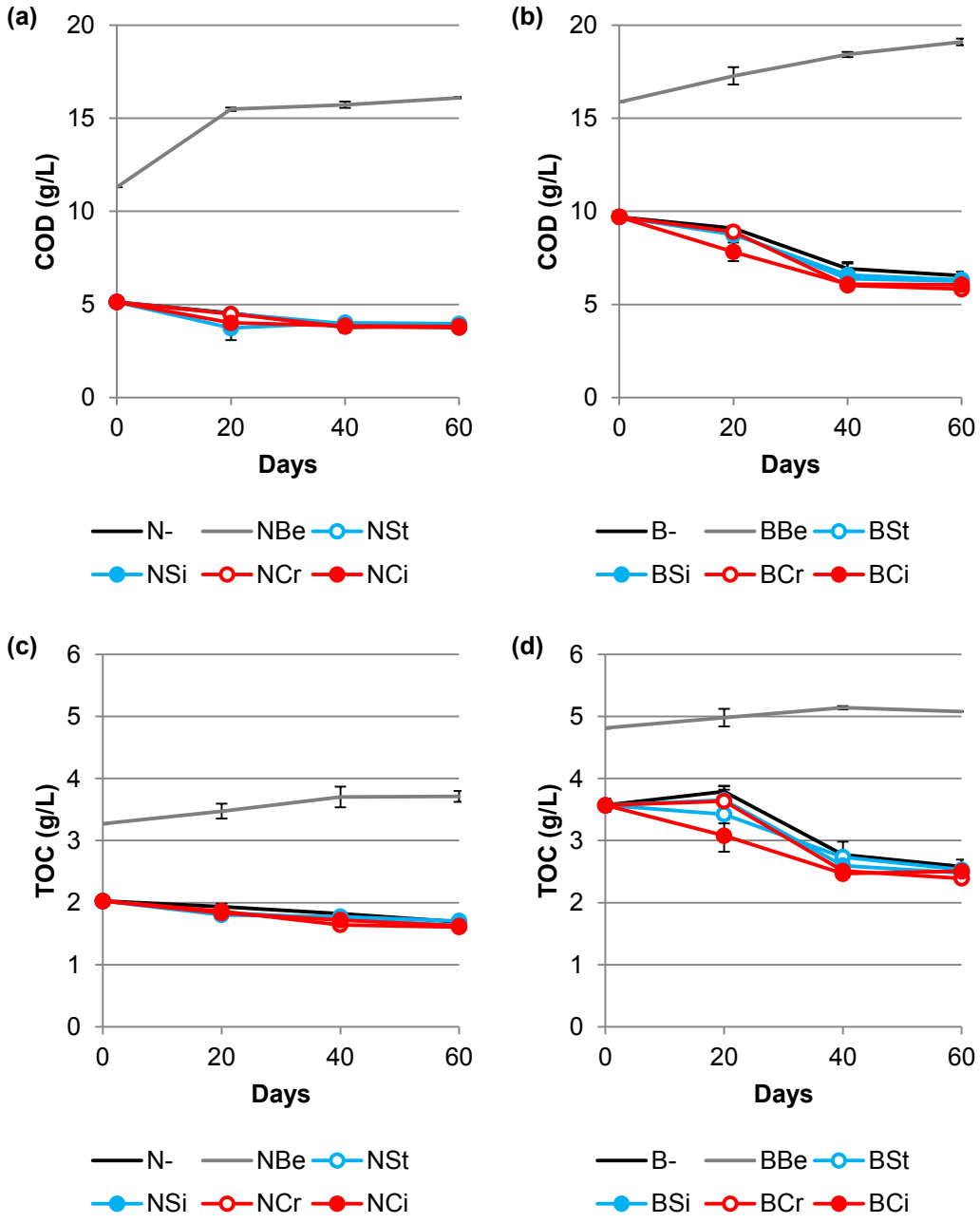

Figure 5.15. Change in (a+b) COD and (c+d) TOC of aqueous phase digestates over 60 days of AD in reactors without (N) and with (B) the addition of 5 g/L COD bio-oil from softwood pellets (SWP/BO). The 20 mL of digestate was supplemented with BES (Be), standard biochar (St), pre-incubated standard biochar (Si), CreChar® (Cr) and pre-incubated CreChar® (Ci). Control reactors were not supplemented (-). All conditions were performed in duplicate with each measurement as a mean of the replicates with error bars of standard deviation.

The change in organic acid concentrations (Figure 5.16) mirrors the COD and TOC changes with a significant increase observed for BES-treated reactors (two-sample t-test $P < 0.001$). Again this effect is more pronounced without the addition of bio-oil (an increase of 133.51% ± 33.61% in non-bio-oil reactors over 46.03% ± 2.89% for bio-oil-supplemented). The remaining non-bio-oil-supplemented reactors show little change in their organic acid concentrations which reflects the similar pattern observed in the previous tests. The pattern of change in organic acid concentration for bio-oil-supplemented reactors is much more distinct, with a clear initial increase in the concentration of organic acids for all tests excluding BCi. Whereas the rest of the bio-oil-supplemented conditions' organic acid concentrations rise and then fall, BCi reactors do not show this initial increase.

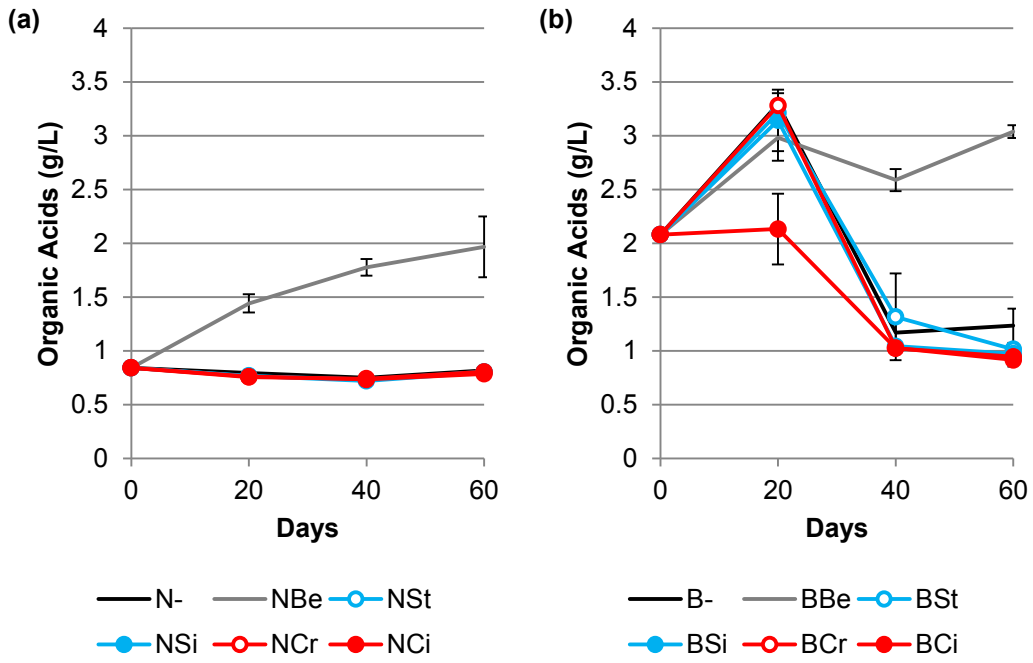

Figure 5.16. Change in organic acid concentrations of the aqueous phase digestates over 60 days of AD in reactors (a) without and (b) with the addition of 5 g/L COD bio-oil from softwood pellets (SWP/BO). The 20 mL of digestate was supplemented with BES (Be), standard biochar (St), pre-incubated standard biochar (Si), CreChar® (Cr) and pre-incubated CreChar® (Ci). Control reactors were not supplemented (-). All conditions were performed in duplicate with each measurement as a mean of the replicates with error bars of standard deviation.

Figure 5.17 shows the change in pH of the reactors over the course of the experiment. There appears to be some variability in the readings based on when the measurements were taken as, despite steady changes in COD, TOC and organic acid concentrations, there is a fluctuation in pH across all the reactors depending on the sampling date. It can still however be seen that BES-treated reactors show an increase in acidity compared to the other reactor conditions. Bio-oil-supplemented reactors also start with a decreased pH.

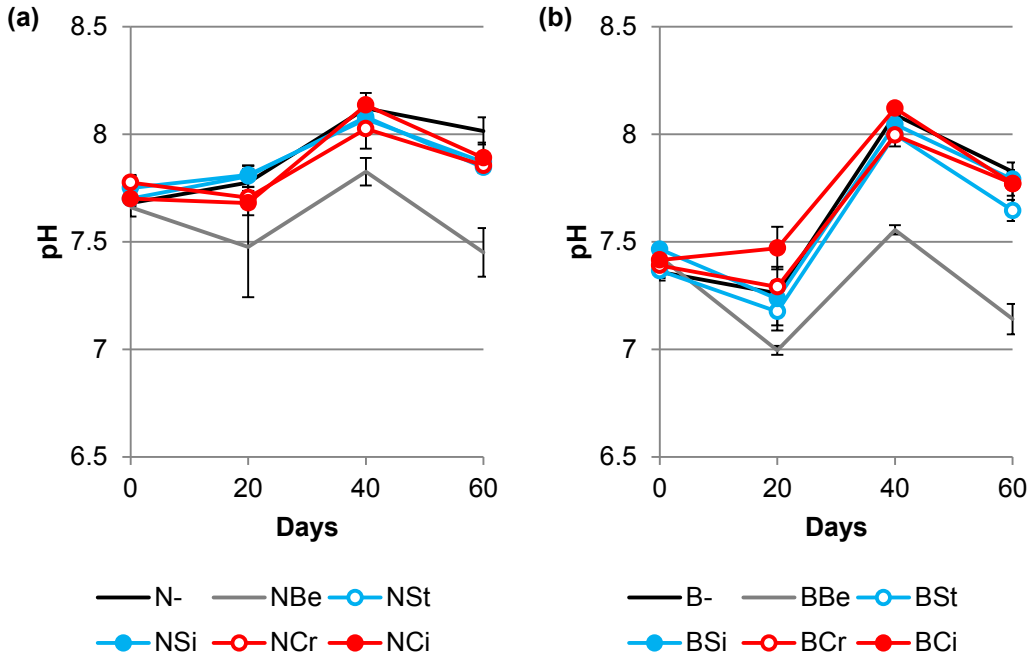

Figure 5.17. Change in pH of digestates over 60 days of AD in reactors (a) without and (b) with the addition of 5 g/L COD bio-oil from softwood pellets (SWP/BO). The 20 mL of digestate was supplemented with BES (Be), standard biochar (St), pre-incubated standard biochar (Si), CreChar® (Cr) and pre-incubated CreChar® (Ci). Control reactors were not supplemented (-). All conditions were performed in duplicate with each measurement as a mean of the replicates with error bars of standard deviation. Of note is the sampling date-dependant fluctuation in pH, highlighting analysis uncertainty.

Loss of TS from the reactors is shown in Figure 5.18. Whereas non-bio-oil-supplemented reactors lost an average 22.29% (± 3.79%) total solids over the course

of the experiment, those reactors with bio-oil lost significantly less (two-sample t-test $P < 0.001$) with an average loss of 8.57% (± 4.60%). This is a considerable difference from the previous tests where loss in TS has been relatively similar, irrespective of bio-oil addition.

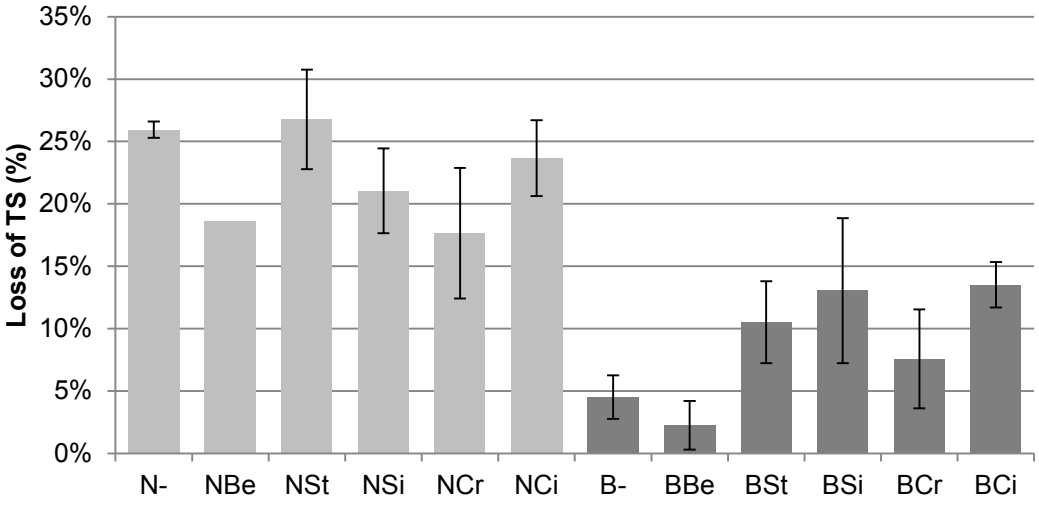

Figure 5.18. Change in total solids of digestates over 60 days of AD in reactors without (N) and with (B) the addition of 5 g/L COD bio-oil from softwood pellets (SWP/BO). The 20 mL of digestate was supplemented with BES (Be), standard biochar (St), pre-incubated standard biochar (Si), CreChar® (Cr) and pre-incubated CreChar® (Ci). Control reactors were not supplemented (-). All conditions were performed in duplicate with each measurement as a mean of the replicates with error bars of standard deviation. Of note is that NBe data is from a single replicate due to loss of the sample.

Differences in TS reduction between the biochar-supplemented reactors are not clear due to inter-replicate variation; however, we do observe BES-treated reactors displaying a lower reduction in TS compared to the other conditions.

Changes in the gene copy number of *mcrA* are shown in Figure 5.19. After 20 days of anaerobic digestion in both non-bio-oil and bio-oil-supplemented reactors, the gene copy number of *mcrA* decreases compared to that of the starting material. For

non-bio-oil reactors the number of gene copies remains constant throughout the experiment with no significant difference observed between sampling dates (one-way ANOVA $P = 0.49$). However for bio-oil-supplemented reactors there is a significant increase in gene copy at day 40 of the experiment (one-way ANOVA $P < 0.05$).

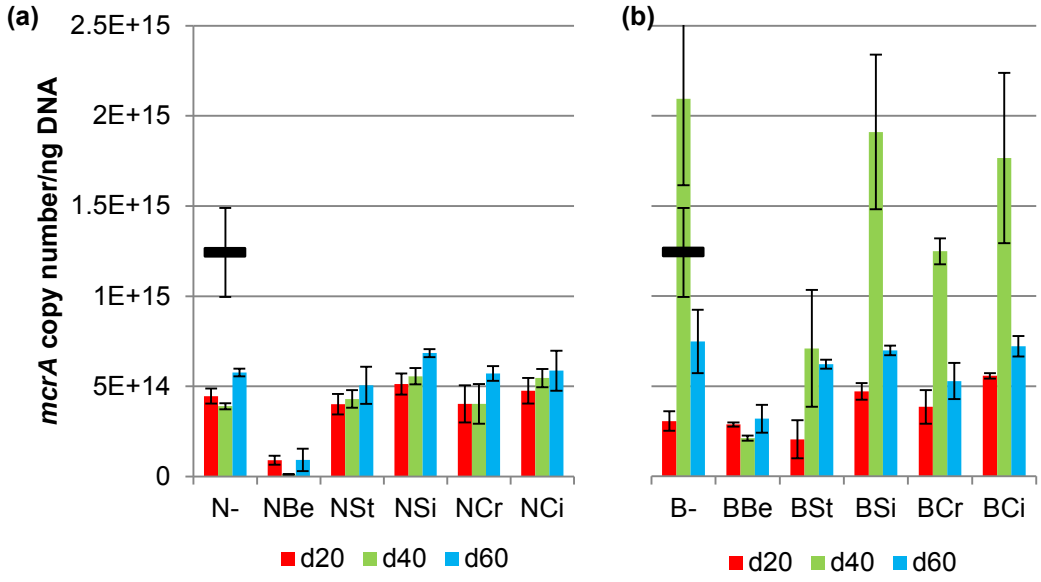

Figure 5.19. Change in the abundance of *mcrA* gene copy number over 60 days of AD in reactors without (a) and with (b) the addition of 5 g/L COD bio-oil from softwood pellets (SWP/BO). The 20 mL of digestate was supplemented with BES (Be), standard biochar (St), pre-incubated standard biochar (Si), CreChar® (Cr) and pre-incubated CreChar® (Ci). Control reactors were not supplemented (-). The initial digestate copy number is represented by the single black bar. All conditions were performed in duplicate with each measurement as a mean of the replicates with error bars of standard deviation.

Also noticeable is the lower *mcrA* copy number in BES-treated reactors; however, the difference in *mcrA* copy number between BES-treated reactors and the control reactors is only significant for non-bio-oil reactors (two-sample t-test $P < 0.05$). Figure 5.20 shows the number of *mcrA* genes in the extracted samples from biochar surfaces.

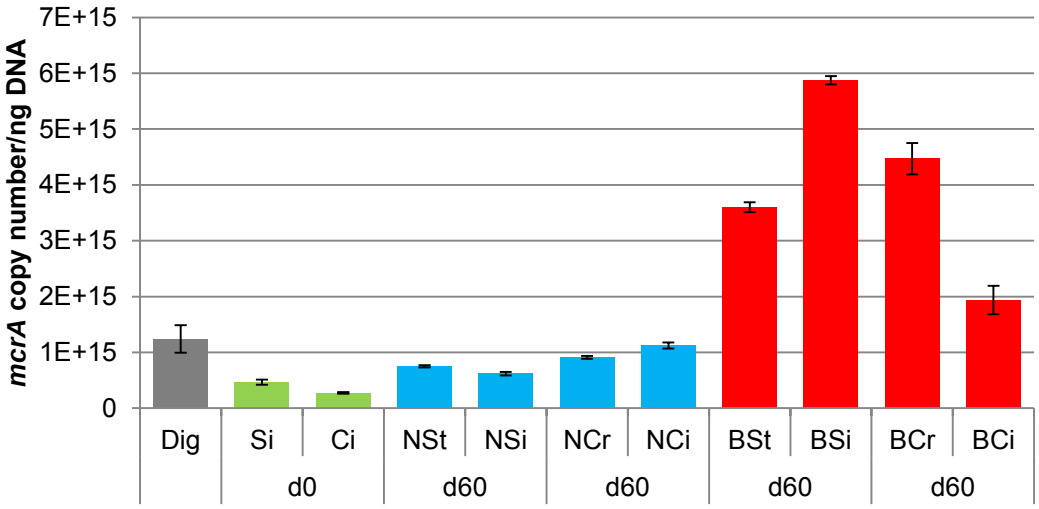

Figure 5.20. Change in the abundance of mcrA gene copy number from biochar samples after pre-incubation (d0/green) and at the conclusion of the test (d60) in reactors without (N/blue) and with (B/red) the addition of 5 g/L COD bio-oil from softwood pellets (SWP/BO). Biochars used for the supplementation of 20 mL of digestate were: standard biochar (St), pre-incubated standard biochar (Si), CreChar® (Cr) and pre-incubated CreChar® (Ci). The initial digestate copy number (Dig) is represented by the single grey bar. All conditions were performed in duplicate with each measurement as a mean of the replicates with error bars of standard deviation.

Pre-incubation of the chars did seem to facilitate growth of methanogenic archaea on the biochar surface however the number of *mcrA* gene copies per ng of DNA is lower than the digestate it was incubated in. By day 60 it is possible to see a similar pattern to the digestate copy number data in that *mcrA* gene abundance is low for non-bio-oil-supplemented reactors and greater for reactors supplemented with bio-oil. Bio-oil-supplemented digestates showed peak *mcrA* gene abundance at day 40 which then drops to background levels by day 60; however, for the biochars, the increased abundance of *mcrA* genes relative to the starting digestate is still found at day 60.

5.3 Discussion

Bio-oils were successfully converted to biogas as a value-added product in AD however bio-oil addition never increased the yield per gCOD over control digestates. Thus, inhibition of AD was encountered with all bio-oil additions, the level of which was dependant on the feedstock of the bio-oil. It is important to note that although different inhibition profiles were observed for each bio-oil and that the changes in digestate chemistry before and after AD indicate their degradation; there are several limitations to the experiments.

Chemical analysis was only performed on the aqueous phase of the digestates due to inconsistent results when the solid fraction was included in the tests. Bio-oil is completely soluble in water and due to the limited reduction in COD of control aqueous phase digestates, any significant COD reductions in bio-oil supplemented reactors are attributed to bio-oil degradation. This does however highlight a limitation of the experiment in that a vast amount of digestate COD is omitted from the analysis. It is also the reason why we observe methane yields per gCOD above theoretical limits as the calculation does not take the total COD of the digestate. Ageing of the digestate between experiments was also not quantified as the COD of the solid fraction was not measured and it is in this solid fraction that the majority of hydrolysis occurs. It is recommended for future work that a method for accurate determination of the COD of digestate solids is utilised to more precisely analyse changes in digestate chemistry.

There was no neutralisation of the bio-oil or its mix with digestate so that as little pre-treatment was performed on the bio-oils before their use in AD, in an effort to more realistically mimic its potential use as a feedstock. However, the addition of bio-oil to the digestates drastically altered their pH before each test and represents an uncontrolled variable in each experiment and a limitation to the experimental design. Due to the log scale of pH, the differences between the starting digestates translate as considerable differences in their hydrogen ion concentrations. As such, for future

work, a standardised starting pH should be used across all reactors so that differences in reactor performance can more accurately be attributed to bio-oil chemistry.

There was a general trend for loss of activity from the digestate acquired at the start of AD1, with reduced biogas potential and change in TS. The reduced biogas productivity is most likely due to a loss in the amount of available organic material due to storage at 4 °C, which is preferable to freezing as there is less chance of physical disruption of microbial cells. Although metabolic functions are slowed at 4 °C, they are not stopped, as witnessed by the occasional requirement to vent the digestate containment vessels due to the accumulation of biogas. Thus over time it is expected that digestates stored at 4 °C will naturally lose a portion of the available organic material due to, albeit slowed, continued microbial activity which has an impact on the eventual biogas production in tests. Due to the continuation of microbial activity, this also has an impact on the starting consortium of microorganisms which could also affect biogas production rates (Chapter 7). Ideally, the digestate acquired for seeding reactors should be from the same source and as fresh as possible for each experiment with any potential ageing analysed.

Throughout the AD tests performed on bio-oil-supplemented sewage sludge digestate, it was found that bio-oils from a common lignocellulosic feedstock were least challenging to degrade. Reactors with SWP/BO bio-oil consistently showed increased biogas production over non-supplemented reactors and displayed a shorter inhibitory phase compared to bio-oils pyrolysed from anaerobic digestate and *M. pyrifera*. AD of SWP/BO bio-oils also showed the greatest reduction in COD, TOC and organic acids concentration in the aqueous phase of the digestate as well as a change in pH closest to control reactors. The COD, TOC and organic acid levels were never reduced completely to control levels however; suggesting that there is still a fraction of this bio-oil that cannot be degraded by the communities in the digestate and as such could potentially accumulate and cause complete process inhibition were these reactors to be continuously fed with SWP/BO bio-oil.

The inhibitory phase observed in all reactors with bio-oil could be shortened with the addition of fresh digestate and digestate that had been previously supplemented with bio-oil. The reduction in biogas productivity of the digestate caused variability between the tests as observed by the requirement to reinoculate AD1, AD2 and AD3 reactors that had bio-oil COD concentrations of 2.5 and 10 g/L, to stimulate biogas production, but not AD4 reactors with 5 g/L COD bio-oil. Additionally control AD4 reactors with bio-oil were the only ones to demonstrate a lower total biogas output than non-bio-oil controls. Of note is that although the bio-oil and digestates used in AD4 were from the same sources as previous tests, the digestate was from a different sampling batch and the bio-oil had been stored for ~250 days so it is possible that either the microbial community in the digestate, or the compounds in the SWP/BO bio-oil, had significantly changed between tests.

AD/BO bio-oil, produced from anaerobic digestate, was able to be degraded in the anaerobic reactors and exhibited some benefits over the use of SWP/BO. Over the course of AD1 and AD2, reactors supplemented with AD/BO bio-oil produced biogas with ~7% higher methane content, and in the case of AD2, produced slightly more biogas in total than SWP/BO. The increased methane content was attributed to the increased initial levels of organic acids in the bio-oil, some of which can be directly utilised by methanogens for methane production. These organic acids were presumed to be mainly acetic acid due to the increased concentration observed in this bio-oil (Figure 3.3).

The lower methane content for SWP/BO-supplemented reactors was attributed to acidification of the digestate which caused the release of dissolved carbon dioxide as seen in similar published work (Hübner and Mumme, 2015). Acidification did not occur in AD/BO- and MP/BO- supplemented reactors due to their basic pHs. Despite the increased methane yields from the addition of AD/BO, reactors supplemented with this bio-oil exhibited a longer lag phase before biogas production and by the end of AD1 and AD2, were left with ~30% and ~75% of the bio-oil COD remaining respectively. This is in contrast to SWP/BO-supplemented reactors that were left with ~3% and ~20% bio-oil COD remaining for the respective tests. The inability to

reduce COD to control levels plus the apparent lack of utilisation of such a high initial concentration of acetic acid indicates inhibition from AD/BO.

The bio-oil produced from the brown algae *M. pyrifera* showed a similar average methane concentration to AD/BO however produced substantially less biogas in total during both AD1 and AD2. Reactors supplemented with this bio-oil also suffered an even greater lag time before biogas production, were left with ~60% and ~100% of the bio-oil COD remaining by the end of AD1 and AD2 respectively and showed increased organic acid concentrations by the end of the test. It is still unknown what compounds in MP/BO cause such a high level of inhibition, particularly since it does not contain high levels of lignin-derived microbial inhibitors such as furans. The higher nitrogen composition of the bio-oil however, as observed in Chapter 3, could lead to the formation of ammonia which is a common inhibitor of AD systems (Yenigün and Demirel, 2013) and again highlights the need for analysis of this inhibitor in future work.

It was not clear whether it was also possible to utilise bio-oil as a feedstock for digesters showing complete methanogenic inhibition. Organic acid accumulation was achieved however the process was still inhibited in bio-oil-supplemented reactors suggesting it has a broad inhibitory spectrum across all AD processes. The slopes of the concentration of organic acids were continuing to climb by the end of AD3 and AD4 and so it is possible that the process of converting bio-oil COD into VFAs for potential removal and recovery requires a greater period of time. There will be a threshold however, when it is no longer thermodynamically possible to continue organic acid production by the microorganisms in the reactor (Siegert and Banks, 2005). The process requires inhibition of methanogenesis which can be accomplished by heat and pressure treatment or with the addition of 50 mM BES. Despite the findings by Zhu *et al*. (2015), alamethicin at 25 μg/mL was not capable of inhibiting methanogenesis in the anaerobic digesters used in this project.

The process of autoclaving had the additional effect of increasing the aqueous phase starting COD of the digestate and showed greater biogas potential. Autoclaving can

be compared to thermal heat treatment of digestate which is routinely performed on an industrial scale in waste water treatment plants before the sludge is introduced to an anaerobic digester. The Thermal Hydrolysis Process (THP) assists in the degradation of the feedstock by increasing the fraction of soluble organic material (Jolis, 2008), which can explain why autoclaved digestates with seed produce an increased amount of biogas compared to their fresh equivalents. Conversely, seed digestates produced less biogas as can be expected from biomass that had already been through AD.

Neither standard SWP biochar nor CreChar® addition on their own seemed to contribute to increased biogas yields or a decrease in the inhibitory period for bio-oil-supplemented reactors. The pre-incubation of CreChar®, and to a non-statistically significant extent, standard biochar, in anaerobic digestate did however reduce bio-oil inhibition and increase biogas production, presumably by the addition of a stable community of AD microorganisms that was able to survive bio-oil toxicity due to biofilm formation. It can be hypothesised that the microbial community of an AD reactor is dynamic and rapidly changes with its environment and that biochar-associated communities seem more rigid and require a greater period of time to adapt. This is further investigated in Chapter 6 and 7.

The *mcrA* gene abundance data from AD4 shows that methanogens were present on the surface of biochar both before and after AD. However, there was a reduced abundance on day 0 biochar surfaces compared to the starting digestate, indicating that the other microbial species are able to colonise the surface of biochars more rapidly than methanogens. This is not surprising considering the slower growth rate of methanogens (Thauer, 2008); however, over the course of the experiment we only observe day 40 for bio-oil supplemented reactors as the period where *mcrA* gene abundance is considerably greater than other sampling time points. With a 20 day period between sampling points, this indicates that methanogen abundance is transient, rapidly increases during significant biogas production. This highlights a limitation in the methods of sampling and for future tests it will be important to more

regularly sample the digestate for *mcrA* abundance, so that the peaks are not missed, as the case is for the non-bio-oil control reactors.

To further elucidate on these queries and to gain a better understanding of bio-oil inhibition of AD reactors and their conversion to biogas, both the chemical and biological changes that are occurring in AD1 and AD2 are analysed in Chapter 6 with AD3 and AD4 analysed in Chapter 7.

CHAPTER 6: BIOLOGICAL AND CHEMICAL CHARACTERISATION OF AD/BIO-OIL REACTORS WITH BIO-OILS FROM DIFFERENT FEEDSTOCKS

6.1 Introduction

It has been possible to utilise the microbial processes of AD to convert bio-oil into methane as a value-added product; however, supplementation of reactors drastically affects their ability to produce biogas. As seen from AD1 and AD2, bio-oils from different feedstocks inhibit AD processes to a different extent. The indirect and direct inhibition of methanogenesis in AD3 and AD4 caused an accumulation of organic acids, with the process still inhibited by bio-oil. Additionally, the inclusion of different biochars in AD4, both incubated and non-incubated, caused changes in the reactors' ability to overcome bio-oil inhibition. To better understand the biological processes and adaptations that are occurring in the digestate due to the addition of these supplements, Illumina 16S rRNA gene sequencing was employed to identify the microbial community of the digestate at each sampling point of each test. Additionally the chemical changes were monitored by ESI FT-ICR MS so that the aqueous fraction of the digestate was characterised at each sampling point.

The microbial characterisation of anaerobic digesters is a major field of study, in order to attempt to control the biological processes of an AD reactor; an understanding is required of the ecology and function of the microbial community (Vanwonterghem *et al*., 2014). With the introduction of culture-independent next-generation sequencing technologies it is now possible to explore the "unculturable" fraction of a microbial community and gain a more definitive picture of the total community. This increase in the use of molecular techniques for analysing community diversity has also highlighted the distinct lack of cultivable representatives for several phyla (Keller and Zengler, 2004). As such, despite the great depth and resolution of these techniques, we are still limited in the assignment of sequences that have no cultured and sequenced representatives and thus can only

infer characteristics from their potential synergies with other microorganisms or close relatives.

Nonetheless, there are numerous studies that characterise the microbial community of wastewater and sewage sludge anaerobic digesters which highlight some key microbial divisions that show consistent reoccurrence. The most abundant bacterial populations tend to be in the following phyla: *Proteobacteria, Firmicutes, Bacteroidetes, Chloroflexi,* (Narihiro and Sekiguchi, 2007; Rivière *et al*., 2009; Guo *et al*., 2015).

Several classes of *Proteobacteria* are reported in digestates including *Alpha-*, *Beta-*, *Gamma-* and *Deltaproteobacteria,* covering a wide range of metabolic functions. Specifically however, members of these classes have been identified as important acidogenic and acetoclastic syntrophs capable of utilising acetate, butyrate, propionate and glucose (Ariesyady, Ito and Okabe, 2007). A major class of *Firmicutes,* common to anaerobic digesters, is *Clostridia* that contain members capable of degrading various VFAs and are involved in acidogenesis, syntrophic acetogenesis and hydrolysis (Zitomer *et al*., 2016). Similarly, *Bacteroidetes* members are known to be proteolytic thus aiding in hydrolysis and have the ability to ferment amino acids to acetate (Rivière *et al*., 2009). The *Chloroflexi* are a diverse phylum of bacteria identified in numerous anaerobic digestates; their members have, however, only recently been identified as being important in the primary degradation of carbohydrates and cellular material and in the utilisation of glucose (Ariesyady, Ito and Okabe, 2007; Narihiro and Sekiguchi, 2007).

Generally present in lower abundances, members of the phyla *Synergistetes*, *Spirochaetae*, *Actinobacteria* and the candidate bacterial phylum *Cloacimonetes* (WWE1) are common to anaerobic digesters treating wastewater and sewage sludge (Narihiro and Sekiguchi, 2007; Pelletier *et al*., 2008; Guo *et al*., 2015). *Synergistetes* species are reported to be capable of the fermentation of organic materials such as carbohydrates and organic acids (Vartoukian, Palmer and Wade, 2007; Dodsworth *et al*., 2013). *Spirochaetae* species are reported as syntrophic acetate oxidisers,

particularly in ammonia stressed conditions (Poirier *et al*., 2016), and members of *Actinobacteria* are heterotrophic fermenters capable of lipid degradation (FitzGerald *et al*., 2015). The *Cloacimonetes* candidate phylum contains only one cultured representative in "*Candidatus Cloacamonas acidaminovorans*" (Pelletier *et al*., 2008); however uncultured bacterial sequences related to *Cloacimonetes* have been identified in several anaerobic sludge digesters (Eloe-Fadrosh *et al*., 2016; Hao *et al*., 2016; Müller *et al*., 2016) and are thought to be hydrogen-producing syntrophs capable of cellulose hydrolysis.

The bacterial contribution to AD ends after acetogenesis, with the final conversion of acetate, carbon dioxide and hydrogen to methane via Archaeal-dependant methanogenesis. Methanogenesis is accomplished mainly by two pathways: the acetoclastic, which coverts acetate to acetyl-CoA and then to a methyl group before conversion to methane, and the hydrogenotrophic, which utilises hydrogen for the reduction of carbon dioxide through a series of intermediate methyl compounds to methane. The majority of Archaeal sequences observed in AD reactors are from the phylum *Euryarchaeota*, which contains the main methanogenic classes and the class *Thermoplasmata*, containing acidophilic and thermophilic species, which also regularly have representatives in anaerobic digesters (Chouari *et al*., 2005; Fitamo *et al*., 2017). It is possible to divide the methanogenic Archaea into sub-groups depending on their mechanisms of methanogenesis with genera such as *Methanosaeta* being strictly acetoclastic and *Methanospirillum* and *Methanoculleus* hydrogenotrophic. Members of the genus *Methanosarcina* are capable of performing both pathways depending on the available substrate (Ariesyady, Ito and Okabe, 2007; Guo *et al*., 2015).

Microbial characterisation data in the event of bio-oil addition to anaerobic digesters is scarce (Andreoni *et al*., 1990) and due to the complexity of bio-oil and the range of microbial inhibitory effects it is generally capable of, it is unknown what effect its addition has on the digestate communities. It can be hypothesised however that the large proportion of organic acids could cause inhibition from VFA accumulation and the higher N/C ratio observed in the basic bio-oils, from lignocellulosic-limited

feedstocks, could contribute to ammonia inhibition, both common inhibitory events in AD reactors (Lerm *et al*., 2012; Fotidis *et al*., 2013; Zhang, Yuan and Lu, 2014; Gao *et al*., 2015). In fact, ammonia is considered the foremost environmental factor causing inhibition of methanogenesis (Chen, Cheng and Creamer, 2008) due to free ammonia diffusing across cell membranes to disrupt the proton balance inside the cell (Zhang, Yuan and Lu, 2014). Coupled with this, it is still unknown what the direct effect of the high concentrations of phenols and furans in bio-oil have on AD communities; however they will no doubt play a significant role in inhibition of numerous AD processes (Monlau *et al*., 2014).

Reports of ammonia- and VFA-inhibited AD reactors show patterns in their microbial responses. In fact, there is a wealth of literature regarding the Archaeal response to environmental stress in AD reactors. The general principle is that acetoclastic methanogens are less resistant to environmental stresses than hydrogenotrophic methanogens due to the hydrogenotrophs syntrophy with bacterial species, that are able to oxidise intermediate compounds, and then utilise the produced hydrogen to keep a low hydrogen partial pressure (Sung and Liu, 2003; Munk, Guebitz and Lebuhn, 2017). During periods of stress, the abundances of these two groups switch accordingly (Zhang, Yuan and Lu, 2014; Gao *et al*., 2015; Regueiro, Carballa and Lema, 2016). It is also reported that in the event of inhibition of acetoclastic methanogenesis, syntrophic acetate-oxidisers show increased abundance. Syntrophic acetate-oxidisers are able to convert acetate to carbon dioxide and hydrogen which is then directly utilised by hydrogenotrophic methanogens to continue methanogenesis (Westerholm *et al*., 2011; Westerholm, Leven and Schnurer, 2012). The loss of balance between the two forms of methanogenesis is, however, detrimental to the operating of the reactor and it has been shown that bioaugmentation of acetoclastic-inhibited reactors with acetoclastic methanogens significantly aids total methanogenesis (Li *et al*., 2017). An exception to this trend in resistance is found in species of the phylum *Methanosarcina* that can utilise both forms of methanogenesis. Their shorter doubling times in comparison to other methanogens (1.0 – 1.2 compared to 4 – 6 days) also lends them a slight advantage in reactors shocked with sudden increases in environmental stresses (Yun *et al*., 2016).

Bacterial responses to ammonia and VFA stress are more ambiguous, as the vast range of bacterial species capable of performing the metabolic function of another means that significant differences between the microbial components of reactors do not always translate to a difference in behaviour. However, there are repeating patterns in the literature regarding taxa commonly found in wastewater and sewage sludge anaerobic digesters. An increased abundance of the *Cloacimonetes* candidate phylum has been reported with increasing ammonia stress in several AD reactors (Gao *et al*., 2015; Hao *et al*., 2016; Müller *et al*., 2016). And although members of this phylum are thought to be hydrogen-producing syntrophs, there are still a large proportion of associated genes with no known annotation. Other reports indicate shifts at the phylum level from *Bacteroidetes*-dominated communities to *Firmicutes*-dominated, particularly members belonging to the *Clostridia* class (Zhang, Yuan and Lu, 2014). The reason behind this shift is thought to be due to a significant portion of syntrophic acetate-oxidising bacterial species belonging to the *Firmicutes* phylum that show increased resistance to environmental stresses (Gao *et al*., 2015).

It can therefore be hypothesised that the addition of bio-oil to digestate will cause similar shifts in the archaeal and bacterial abundances. The bio-oils used in this project with a high nitrogen content, those from anaerobic digestate (AD/BO) and macroalgae (MP/BO), may cause an increased amount of inhibition to the microbial communities due to the degradation of the nitrogenous compounds to ammonia. AD/BO also had a large proportion of organic acids (Figure 3.3) which have the potential to cause inhibition by accumulation. The van Krevelen plot from MP/BO (Figure 3.4) indicated a high proportion of large lipid and protein compounds which, when degraded, form ammonia and long chain fatty acids (LCFA). LCFAs are also important inhibitors of AD due to adsorption onto cell membranes, interfering with membrane transport functions (Rinzema *et al*., 1994) and as such cause acute toxicity towards Gram-positive bacteria and methanogens, which share similar membrane characteristics (Chen *et al*., 2014). The van Krevelen plot of the bio-oil from softwood pellets SWP/BO (Figure 3.4) showed a larger proportion of lignin-related compounds which, although reported to cause toxicity to microbial communities in

AD, require very high concentrations to inhibit methanogenesis (Chen, Cheng and Creamer, 2008). However, the presence of inhibitory furan compounds observed in this bio-oil (Figure 3.3) indicates another potential inhibitory effect to AD.

Both biological and chemical data were obtained from the AD tests summarised as follows. AD1 and AD2 were designed to assess the impact different bio-oil feedstocks had on their AD at 2.5 and 10 g/L COD concentrations respectively. Samples were taken at the beginning and end of the 50 and 102 day tests for both microbial and chemical characterisation.

6.2 AD1 – Effects of Bio-oils from Different Feedstocks at 2.5 g/L COD

6.2.1 Overview

Variable	Unit	Digestate	AD/BO	MP/BO	SWP/BO
Total Biogas	**mL**	122.00 (1.41)	123.67 (3.06)	117.67 (1.53)	142.67 (5.69)
Lag Phase	**days**	0	16	23	6
CH_4 Content	**% CH_4**	65.23 (1.91)	74.48 (1.34)	73.98 (2.43)	63.65 (1.24)
COD/TOC	**% Diff.**	-9.79/-5.38 (5.22/3.24)	-23.50/-22.65 (0.61/1.13)	-16.38/-8.78 (0.71/1.58)	-32.50/-27.44 (1.03/1.35)
Organic acids	**% Diff.**	-8.68 (1.07)	-63.88 (0.50)	-32.46 (0.50)	-49.50 (0.78)
Total solids	**% Diff.**	-34.12 (0.12)	-29.74 (0.79)	-32.25 (0.42)	-30.94 (1.12)
pH	**from→to**	8.45→7.77 *→(0.07)	8.72→8.01 *→(0.03)	8.75→8.03 *→(0.02)	8.33→7.69 *→(0.02)

Table 6.1. Details of analysed variables between day 0 and day 50 of AD reactors with 2.5 g/L COD bio-oils from anaerobic digestate (AD/BO), *Macrocystis pyrifera* (MP/BO) and softwood pellets (SWP/BO) in 40 mL sewage sludge digestate, the additional 20 mL was added on day 6 due to complete biogas inhibition. The lag phase is the estimated time before significant biogas production is seen from the reactors. All conditions were performed in triplicate with the exception of the digestate-only control (Digestate) where one replicate was removed due to setup error. Each measurement is a mean of the replicates with the standard deviation given in brackets. *Day 0 pH measurements were not replicated.

AD1 was designed to assess the toxicity limits of bio-oils from different feedstocks when added to digestate. Table 6.1 details the results of the analysed variables of the test. Complete inhibition of biogas production was observed for the first 6 days until a further 20 mL digestate was added. This immediately prompted SWP/BO-supplemented reactors to begin biogas production. It took a further 10 and 17 respective days for AD/BO- and MP/BO-supplemented reactors to begin their

significant production of biogas. Over the course of the test, AD/BO reactors produced an equal volume of biogas to controls, but showed an almost 10% higher methane content. MP/BO reactors produced less biogas than controls but also displayed higher methane content, while SWP/BO reactors produced a higher volume of biogas with a similar methane concentration compared to controls. All reactors saw a reduction in COD/TOC, organic acid concentration, total solids (TS) and pH. However, SWP/BO-supplemented reactors showed the greatest reductions and the closest day 50 values to control reactors, followed by AD/BO- and MP/BO-supplemented reactors.

6.2.2 Results – Biological Characterisation

An initial sample of the digestate used in AD1 was taken at the beginning of the tests with subsequent samples taken from reactors at the culmination of the test at day 50. Since only a single day 0 sample was taken and analysed there is no average abundance data for this time point and as such, comparisons between the day 0 sample and the replicate day 50 samples are subject to a degree of uncertainty.

DNA extracted from the digestates was amplified with barcoded primers and sent for Illumina 16S rRNA gene sequencing at Edinburgh Genomics who returned the demultiplexed sequences for further processing. There were a total of 1 145 425 sequences between the samples which, after removing short reads, chimeras, PyNAST failures and singletons using the QIIME package, was reduced to 815 441 sequences. Sample rarefaction reduced the sequencing depth to ~32 000 reads for all samples, however the calculation of the Shannon index of diversity generates a plateau at 3 166 sequences which is enough to predict the diversity of the samples.

d0 DIG	d50 DIG	d50 AD/BO	d50 MP/BO	d50 SWP/BO
4.68	3.61 (0.06)	3.66 (0.22)	3.57 (0.07)	3.33 (0.15)

Table 6.2. Shannon indices at 3 166 sequences from isolated microbial communities from anaerobic digestates from sewage sludge with 2.5 g/L COD bio-oils from anaerobic digestate (AD/BO), *M. pyrifera* (MP/BO) and softwood pellets (SWP/BO), plus a digestate only control (DIG). The digestates were sampled at the start (d0) and end of the test (d50). All conditions were performed in triplicate with the exception of the day 0 digestate which was only sampled once. Each measurement is a mean of the replicates with the standard deviation in brackets.

Table 6.2 shows the Shannon indices as the quantitative measurement for the alpha diversity of the digestate communities at day 0 and day 50. The microbial community in the digestate sample at the beginning of the test shows a greater diversity to the digestates at day 50. The day 50 samples show a similar diversity with the exception of those communities from digestates supplemented with SWP/BO. SWP/BO reactors show a significantly lower Shannon diversity, to a 95% confidence, than the day 50 digestate control communities at the start of the plateau at 3 166 sequences (two-sample t-test $P = 0.0335$), no other set of reactors at day 50 show significant difference from each other.

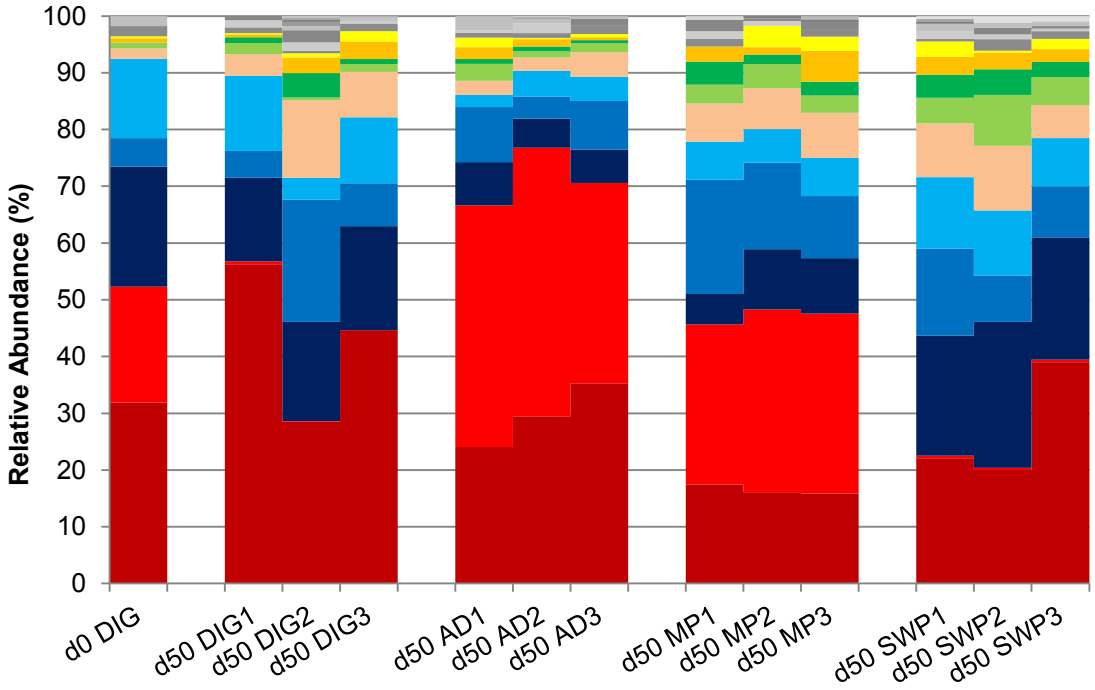

Phylum	Class	Order	Family	Genus
Euryarchaeota	*Methanobacteria*	*Methanobacteriales*	*Methanobacteriaceae*	*Methanobacterium*
Euryarchaeota	*Methanomicrobia*	*Methanosarcinales*	*Methanosarcinaceae*	*Methanosarcina*
Euryarchaeota	*Methanomicrobia*	*Methanosarcinales*	*Methanosaetaceae*	*Methanosaeta*
Euryarchaeota	*Methanobacteria*	*Methanobacteriales*	*Methanobacteriaceae*	*Methanobrevibacter*
WSA2	*WCHA1-57*	*uncultured*	*uncultured*	*uncultured*
Lokiarchaeota	*uncultured*	*uncultured*	*uncultured*	*uncultured*
Euryarchaeota	*Methanomicrobia*	*Methanomicrobiales*	*Methanomicrobiaceae*	*Methanoculleus*
Lokiarchaeota	*uncultured*	*uncultured*	*uncultured*	*uncultured*
Lokiarchaeota	*uncultured*	*uncultured*	*uncultured*	*uncultured*
Euryarchaeota	*Thermoplasmata*	*Thermoplasmatales*	*Marine Benthic Group D and DHVEG-1*	*uncultured*

Figure 6.2. Genus level relative abundance plot of 16S rRNA gene sequences assigned to the archaeal community in anaerobic digestates from sewage sludge with 2.5 g/L COD bio-oils from anaerobic digestate (AD), *M. pyrifera* (MP) and softwood pellets (SWP). The digestate (DIG) was sampled at the start (d0) and in triplicate at the end of the test (d50). The key below the plot represents the top 10 genera from top to bottom in colour with all other sequences in greyscale. Taxonomy was assigned against the SILVA 128 reference database.

The relative abundances of each genus assigned to the sequences derived from the digestate samples are shown in Figure 6.1 for the archaeal and Figure 6.2 for the bacterial proportions of the sequences. The total number of archaeal operational taxonomic units (OTUs) assigned to specific taxonomic groups make up an average 0.46% ± 0.21% (mean ± SD) of the total. There is no significant variation observed between the archaeal proportions of the total OTUs. Due to the lower number of archaeal taxonomic assignments to bacterial (21 different taxonomic groups as opposed to 353), the total archaeal abundance is shown in Figure 6.1 whereas only taxonomic groups that contributed ≥ 0.5% of the total assigned bacterial OTUs are shown in Figure 6.2.

Although there is clear variation between the replicate archaeal abundances in Figure 6.1, particularly the day 50 digestate controls, there are patterns of similarity amongst replicate assignments. Most striking is the almost total loss of the *Methanosarcina* genus from both the day 50 digestate control and SWP/BO-supplemented reactors with an average loss of 98.99% ± 1.28% and 97.87% ± 0.12% respectively. This is in contrast with AD/BO- and MP/BO-supplemented reactors which saw an increase of 104.31% ± 29.64 and 50.27% ± 10.72% of this genus respectively. Also noticeable is the reduction in the relative abundance of *Methanosaeta* in both AD/BO- and MP/BO-supplemented reactors with average reductions of 70.62% ± 5.91% and 59.46% ± 13.27% respectively. In regards to the other methanogens, the genus with the highest total abundance was *Methanobacterium* which, on average, was slightly reduced for all conditions apart from the digestate controls; however, there is high variation of this genus between replicates. *Methanobrevibacter* and *Methanoculleus* show increased abundance across all the day 50 conditions however *Methanospirillum* and the uncultured representatives of the *WSA2* (also referred to as *Arc I*) phylum were reduced across all conditions. The majority of other archaeal sequences were assigned to uncultured representatives of the Phylum *Lokiarchaeota*. It is important to note however, that this is a measurement of relative abundance so the differences observed between samples are relative to the total number of sequences in the sample.

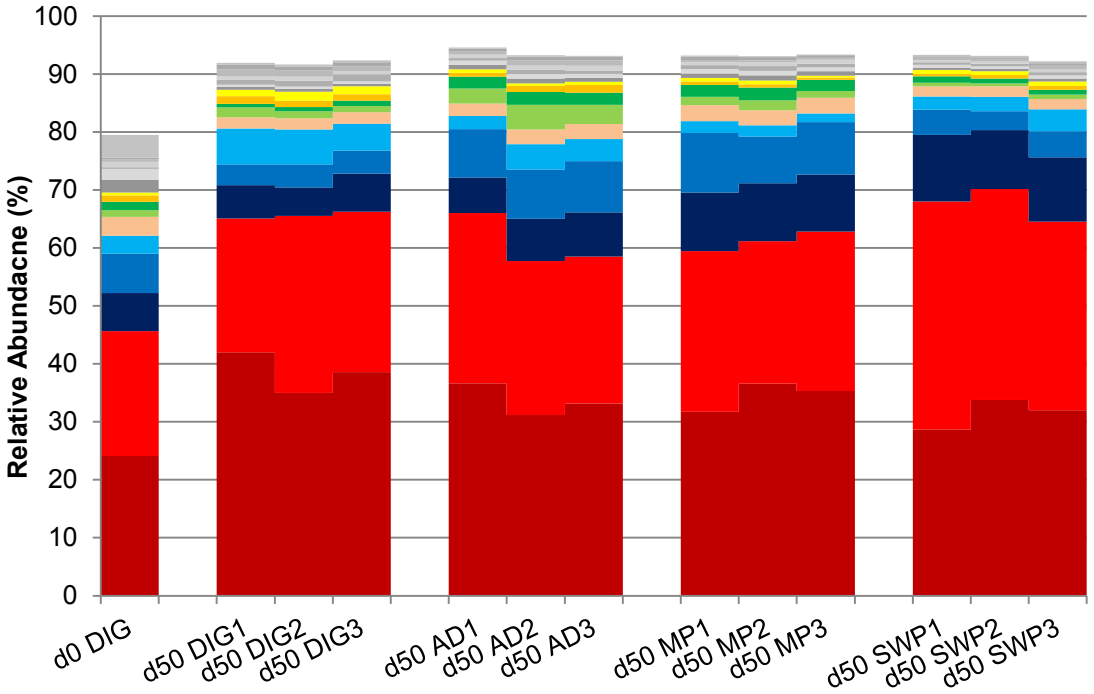

Phylum	Class	Order	Family	Genus
Thermotogae	*Thermotogae*	*Petrotogales*	*Petrotogaceae*	*Defluviitoga*
Cloacimonetes	*W5*	*uncultured*	*uncultured*	*uncultured*
Bacteroidetes	*Sphingobacteriia*	*Sphingobacteriales*	*Lentimicrobiaceae*	*uncultured*
Bacteroidetes	*Bacteroidia*	*Bacteroidales*	*Porphyromonadaceae*	*Proteiniphilum*
Firmicutes	*Clostridia*	*D8A-2*	*uncultured*	*uncultured*
Firmicutes	*Clostridia*	*Thermoanaero-bacterales*	*Thermoanaero-bacteraceae*	*Gelria*
Firmicutes	*Clostridia*	*Clostridiales*	*Family XI*	*uncultured*
Bacteroidetes	*Bacteroidia*	*Bacteroidales*	*Porphyromonadaceae*	*uncultured*
Synergistetes	*Synergistia*	*Synergistales*	*Synergistaceae*	*Anaerobaculum*
Aminicenantes	*uncultured*	*uncultured*	*uncultured*	*uncultured*

Figure 6.4. Genus level relative abundance plot of 16S rRNA gene sequences that contributed ≥ 0.5% of the total sequences assigned to the bacterial community in anaerobic digestates from sewage sludge with 2.5 g/L COD bio-oils from anaerobic digestate (AD), *M. pyrifera* (MP) and softwood pellets (SWP). The digestate (DIG) was sampled at the start (d0) and in triplicate at the end of the test (d50). The key below the plot represents the top 10 genera from top to bottom in colour with all other sequences in greyscale. Taxonomy was assigned against the SILVA 128 reference database.

Figure 6.2 shows the bacterial abundances of those taxonomic groups that contributed ≥ 0.5% of the total assigned bacterial OTUs. Immediately noticeable is the greater proportion of absent OTUs in the day 0 digestate control, again showing the greater alpha diversity of this sample compared to the day 50 samples. There is less variation seen amongst the bacterial abundances than that seen in the archaeal graph, although there are some noticeable differences between the reactor conditions. The genus *Defluviitoga* and the uncultured representatives of the candidate phylum *Cloacimonetes* make up ~60% of the assigned sequences in the day 50 reactors, with general increases across all reactor conditions compared to day 0 control reactors of 43.55% ± 12.24% for *Defluviitoga* and 25.16% ± 1.38% for *Cloacimonetes* (this is excluding SWP/BO-supplemented reactors that show a 67.67% ± 15.9% increase in *Cloacimonetes*).

Contributing a further ~15% of the total bacterial OTUs, to encompass almost 80% of the total, are an uncultured genus of the *Lentimicrobiaceae* family and a *Proteiniphilum* genus. *Lentimicrobiaceae* abundance is increased in SWP/BO-supplemented reactors up to 65.81% ± 10.48% and in MP/BO- by 51.52% ± 1.91% while AD/BO-supplemented reactors and digestate only controls see varied fluctuations at 6.01% ± 11.74% and -13.31% ± 12.46% respectively. An average reduction in *Proteiniphilum* of 42.01% ± 1.95% was observed in digestate only control and SWP/BO-supplemented reactors however both AD/BO- and MP/BO-supplemented reactors saw an average 30.41% ± 6.13% increase in the abundance of the *Proteiniphilum* genus. Although it is possible to observe changes in the most abundant taxonomic groups in the reactor as has been shown here; there remain hundreds of other groups of organisms that display fluctuations between the sampling time points that are low in abundance and share no discernible pattern in their relative abundance profiles between samples.

It is possible to view the beta diversity between the samples by calculating the Bray-Curtis similarity of their abundance data from the total OTUs and plotting this as a distance on an NMDS plot. The inter-replicate variability observed in the archaeal community shows the day 50 digestate-only control reactors having the highest

variability with a Bray-Curtis similarity of 72 ± 6.79 (mean ± SEM) compared to the average of the other day 50 replicate samples at 84.13 ± 1.13. MP/BO-supplemented reactors show the lowest similarity to the day 0 digestate sample with a significantly lower average similarity score of 61.62 ± 0. 9 compared to an average 68.29 ± 1.54 for the other replicate reactors to a 95% confidence (two-sample t-test P = 0.0378).

There is no significant difference between the inter-replicate variability of the bacterial abundances for each day 50 reactor condition, with a total average similarity score of 93.09 ± 0.49. There is, however, a 99.9% confident significant difference between the digestate-only control and SWP-supplemented reactors and the AD/BO- and MP/BO-supplemented reactors (two-sample t-test P = 0.0001). The AD/BO and MP/BO reactors show a higher similarity in their bacterial abundances to the day 0 digestate (76.57 ± 0.5) than the control and SWP/BO reactors (72.23 ± 0.42).

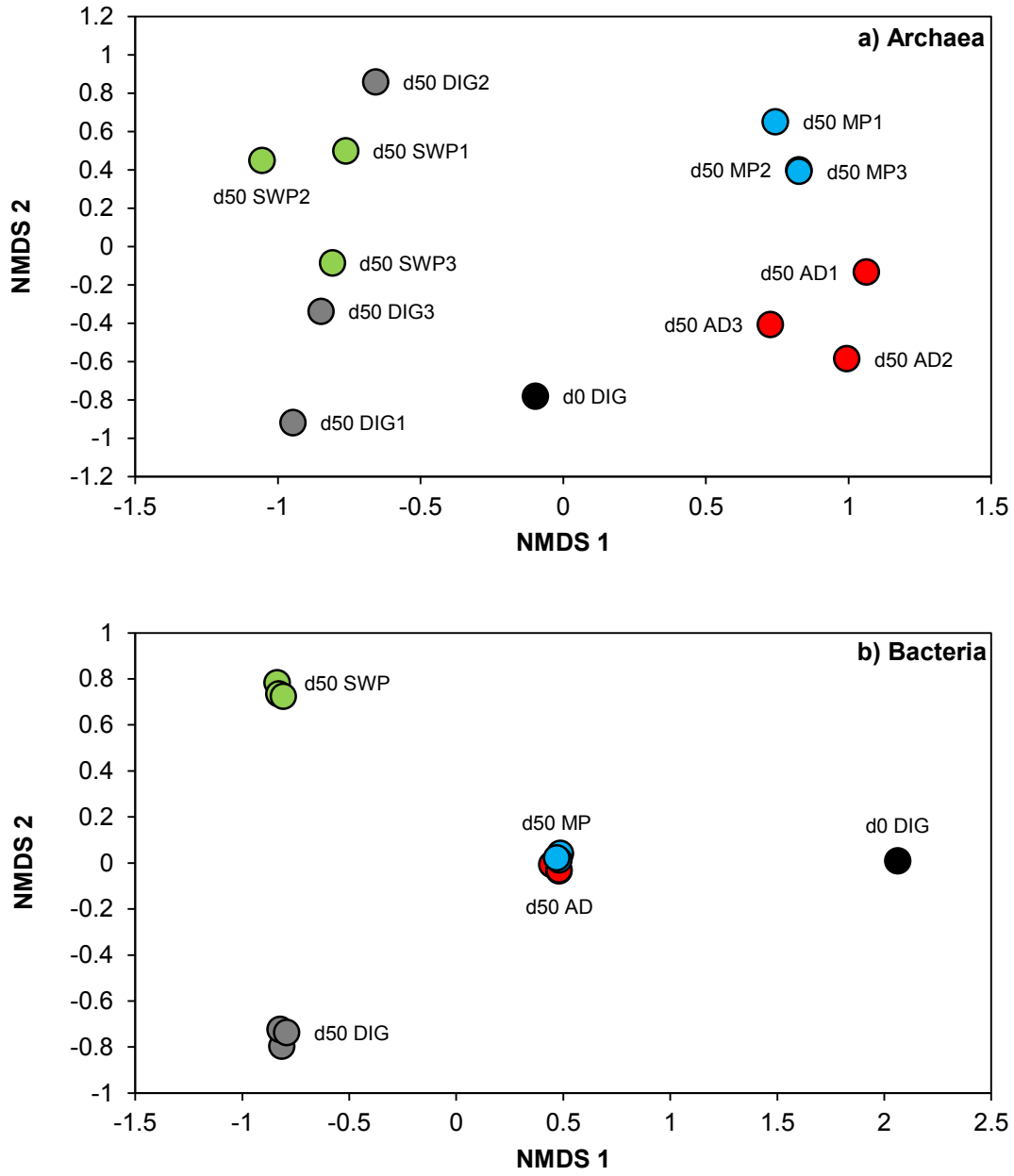

Figure 6.3. 2D NMDS plots generated from the Bray-Curtis similarity matrices for (top/a) archaeal and (bottom/b) bacterial OTU abundances assigned to 16S rRNA gene sequences from sewage sludge anaerobic digestates with 2.5 g/L COD bio-oils from anaerobic digestate (AD/red), *M. pyrifera* (MP/blue) and softwood pellets (SWP/green), plus a digestate only control (DIG/grey). A single sample was taken at the start of the test (d0/black) with all day 50 samples in triplicate (d50). The high inter-replicate similarity of the bacterial samples allows for a single annotation of the replicates. 2D stress (a) = 0.06 and (b) = 0.01.

Figure 6.3a shows an NMDS plot of the archaeal Bray-Curtis similarity index for the AD1 reactors. The high inter-replicate variation observed for the digestate-only controls is evident with the second replicate clustering closer to SWP/BO-supplemented reactors than to its other replicates. There is also a clear division between the digestate-only control and SWP/BO reactors on the left of the 2D space and the MP/BO and AD/BO reactors on the right, with the single day 0 digestate sample in the middle. In addition to this divide a significant difference with 99.9% confidence is observed between the day 50 reactor conditions (PERMANOVA P = 0.001; Pseudo-F = 8.03) that is not due to dispersion differences (PERMDISP P = 0.32; F = 3.71).

A comparable pattern is seen for the bacterial similarity (Figure 6.3b); however the differences between the digestate-only controls and SWP/BO reactors are far greater than the MP/BO and AD/BO dissimilarity, which cluster on top of each other. The greater similarity of AD/BO and MP/BO reactors to the day 0 digestate is also clearly seen, with the SWP/BO and digestate-only control reactors clustering further away from the day 0 digestate sample. Again a significant difference with 99.9% confidence is observed between the day 50 reactor conditions (PERMANOVA P = 0.001; Pseudo-F = 11.04) that is also not due to differences in dispersion (PERMDISP P = 0.39; F = 1.32).

6.2.3 Results – Chemical Characterisation

In Chapter 3, the mass spectrometry technique ESI FT-ICR was used to characterise the chemistry of the bio-oils used in the AD tests. Similarly, the aqueous phases of the digestates were analysed using the same methods. A sample for chemical analysis was taken from each starting digestate, after bio-oil addition, in addition to the day 50 samples from each of the 12 reactors.

Figure 6.4 shows the van Krevelen diagrams for the day 0 digestate-only control and bio-oil-supplemented reactors. Unfortunately, due to the additional peaks associated with digestate compounds, the contribution of bio-oil peaks is almost completely

masked and therefore difficult to observe. There is also very little visually discernible difference between the day 0 and day 50 samples. As such, the day 50 van Krevelen diagrams are available electronically.

It is however still possible to see differences between the van Krevelen diagrams. AD/BO-supplemented reactors seem to contain a greater proportion of smaller compounds, particularly in the lipid region of the diagram (H/C = 1.5 – 2.0; O/C = 0 – 0.3). SWP/BO reactors seem to have a greater proportion of compounds clustering in the lignin region (H/C = 0.7 – 1.5; O/C = 0.1 – 0.67) and the digestate itself seems to contain a mixture of lipids, proteins (H/C = 1.5 – 2.2; O/ C = 0.3 – 0.67) and lignin compounds.

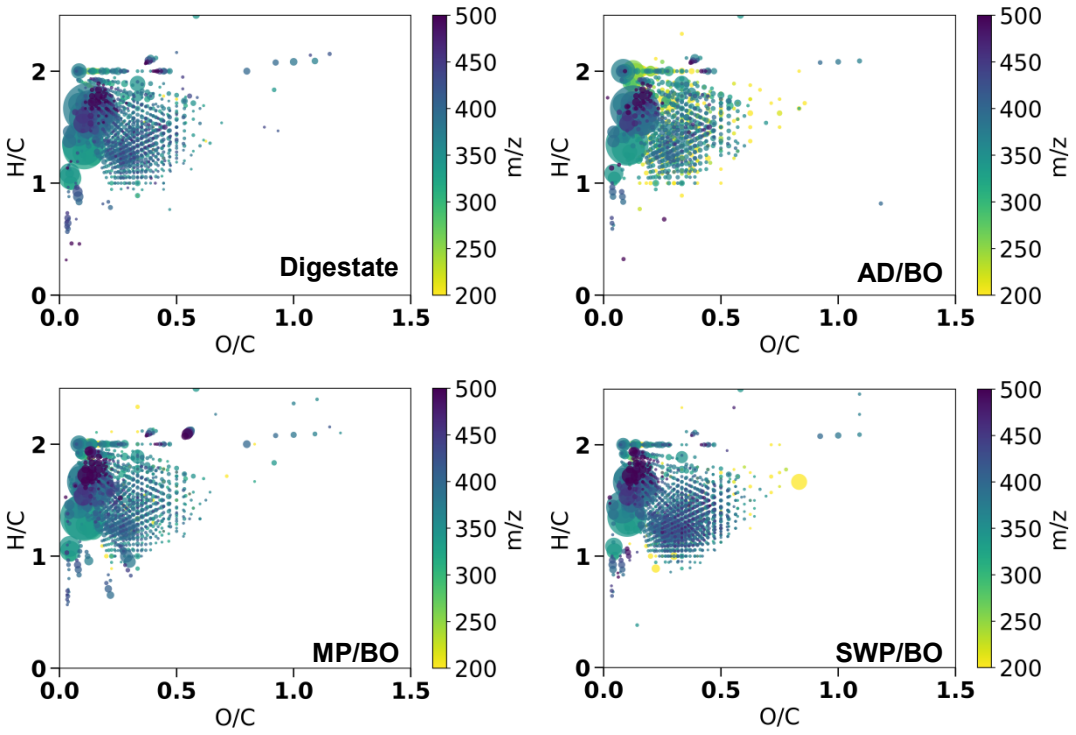

Figure 6.4. van Krevelen diagrams for AD1 day 0 digestates with 2.5 g/L COD bio-oils from anaerobic digestate (AD/BO), *M. pyrifera* (MP/BO) and softwood pellets (SWP/BO) plus a digestate-only control. Formulae were assigned from ESI FT-ICR MS spectra. Plots are further colour-coordinated by the *m/z* of identified compounds with the relative abundance represented by the size of the point.

Although it is not possible to observe changes in the digestate chemistry from the van Krevelen diagrams during the experiment, the changes to heteroatom frequency and distribution between the two sampling dates can be plotted. Figure 6.5 shows the average change in the relative abundance of oxygen heteroatom classes between the day 0 samples and the day 50 replicates. There is a general increase in O_3 and O_4 heteroatom-containing compounds. In the case of the digestate-only control we also observe a decrease in O_5 to O_8 heteroatom-containing compounds and thus a shift from higher oxygen states to lower, which is also observed in the SWP/BO-supplemented reactors from O_8 and O_9 heteroatom classes.

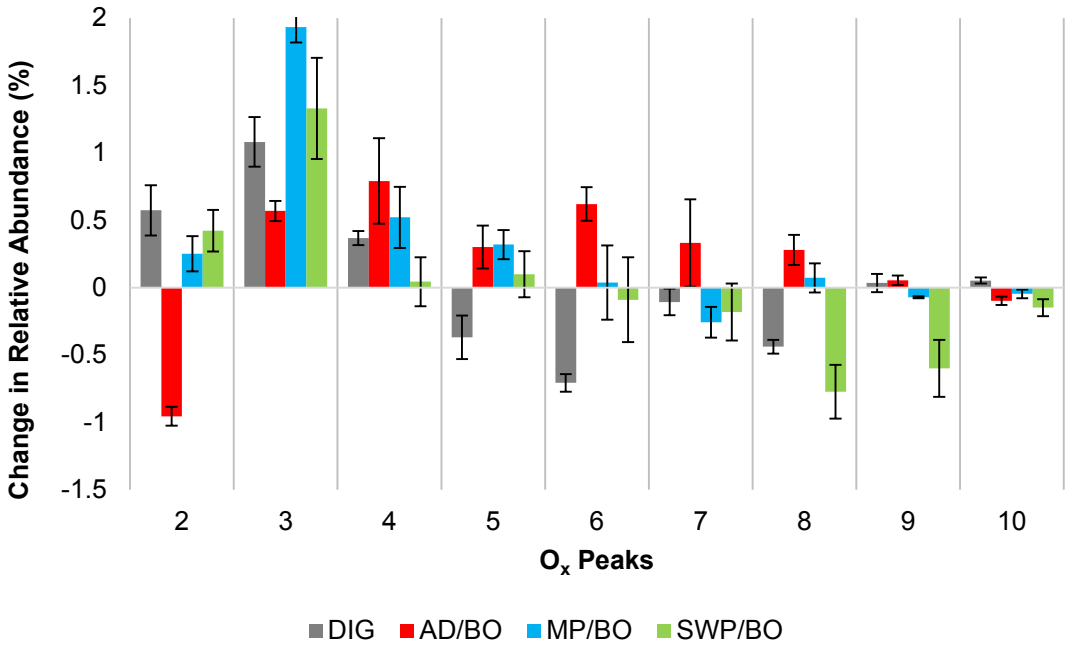

Figure 6.5. Change in oxygen heteroatom relative abundance plots of AD1 digestates with 2.5 g/L COD bio-oils from anaerobic digestate (AD/BO), *M. pyrifera* (MP/BO) and softwood pellets (SWP/BO) plus a digestate-only control (DIG). Formulae were assigned to peaks generated from ESI FT-ICR MS spectra.

A similar pattern is observed in the nitrogen heteroatom-containing compounds as seen in Figure 6.6. With the exception of SWP/BO bio-oil-supplemented reactors, all the digestates show a decreased relative abundance of higher N_x heteroatom-

containing compounds and increases in lower N_x heteroatom-containing compounds. The addition of SWP/BO only causes a slight increase in the initial nitrogen heteroatom-containing species however there is a relative loss across N_1 – N_4 heteroatom-containing compounds.

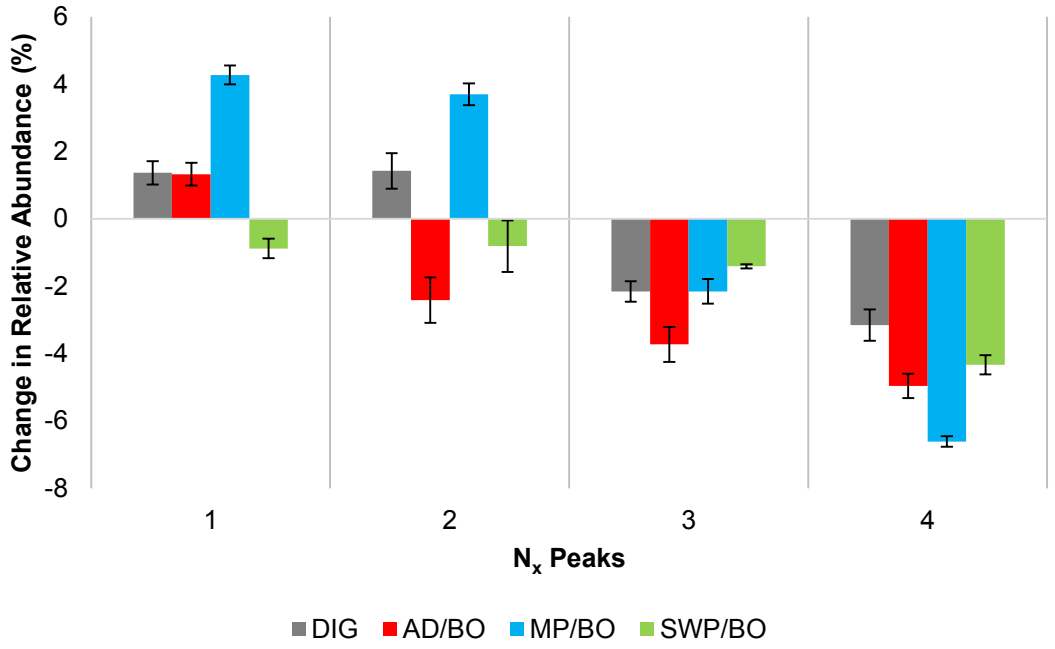

Figure 6.6. Change in nitrogen heteroatom relative abundance plots of AD1 digestates with 2.5 g/L COD bio-oils from anaerobic digestate (AD/BO), *M. pyrifera* (MP/BO) and softwood pellets (SWP/BO) plus a digestate-only control (DIG). Formulae were assigned to peaks generated from ESI FT-ICR MS spectra. N_x classes are the sum of all N_xO_y containing classes.

The ultrahigh resolution afforded by the use of ESI FT-ICR MS generates a comparably large set of chemical formulae to bacterial taxa from the 16S rRNA gene Illumina sequencing. As such, it is possible to analyse the chemical data in the same way as the biological, and compare the patterns observed between them. Bray-Curtis similarity was calculated for the formula abundances from the peak assignments of the digestates at the start and end of the test. The inter-replicate variability was similar across all the day 50 digestates at 87.05 ± 0.29 indicating little difference between the replicate samples for each reactor condition. However, the day 50 digestate-only controls show a significantly higher similarity, to a 95% confidence,

to their respective day 0 sample at 67.21 ± 0.71 compared to the day 50 bio-oil supplemented reactors to their day 0 samples (two-sample t-test AD/BO P = 0.025; MP/BO P = 0.002; SWP/BO P = 0.024).

Figure 6.7 is the NMDS plot of the Bray-Curtis similarities and immediately noticeable is the considerable difference between the day 0 samples and the day 50 samples, the latter clustering to the bottom-right of the 2D space. Although the difference in time points is significant to a 99.9% confidence (PERMANOVA P = 0.001; Pseudo-F = 5.572), this can be explained by the difference in distribution of the groups (PERMDISP P = 0.001; F = 22.264). The lack of technical replicates of the day 0 digestates makes comparisons between each condition start and end chemical compositions difficult; therefore, despite the clear separation between the day 0 and day 50 samples, no significant difference can be extrapolated. In spite of this distribution dissimilarity, the difference in sample type for all digestates (DIG, AD, MP and SWP) is still significant to a 95% confidence (PERMANOVA P = 0.006; Pseudo-F = 2.472. PERMNDISP P = 0.964; F = 0.056).

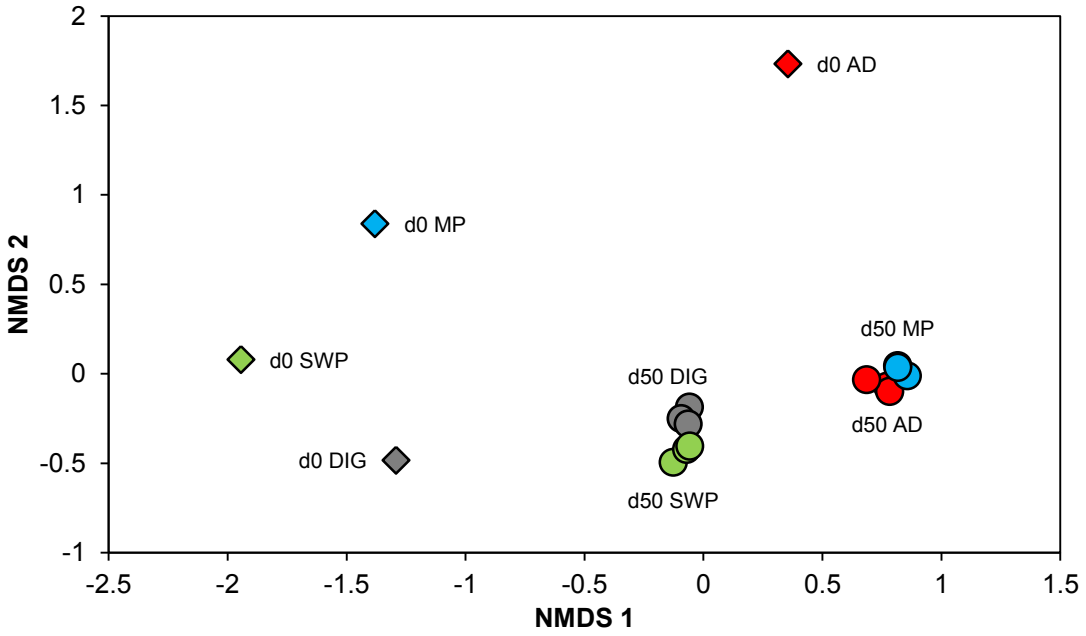

Figure 6.7. 2D NMDS plot generated from the Bray-Curtis similarity matrices for chemical formulae assigned to ESI FT-ICR MS peaks from sewage sludge anaerobic digestates with 2.5 g/L COD bio-oils from anaerobic digestate (AD/red), *M. pyrifera* (MP/blue) and softwood pellets (SWP/green), plus a digestate only control (DIG/grey). The high inter-replicate similarity of the chemical samples allows for a single annotation of the replicates. 2D stress = 0.05.

The day 50 digestates show two distinct clusters; digestate-only controls and SWP-supplemented reactors are separated from AD/BO- and MP/BO-supplemented reactors. The difference between these two groups of day 50 conditions is found to be significant to a 99% confidence (PERMANOVA P = 0.003; Pseudo-F = 16.367) and cannot be explained by differences in dispersion (PERMDISP P = 0.067; F = 2.863).

6.2.4 Relatedness

The division observed between the day 50 digestate-control plus SWP/BO-supplemented reactors and day 50 AD/BO- plus MP/BO-supplemented reactors in the chemistry data is mirrored by the biological data. A comparative test on the

similarity using a Spearman's rank correlation coefficient shows that there is a 0.717 similarity between the relationships observed between the two matrices to a 99% confidence, where a score of 1 indicates identical and 0 is no similarity. This shows that both the biological and chemical data analysed for the day 50 samples share a ~70% agreement on the differences observed between the reactor conditions.

6.3 AD2 – Effects of Bio-oils from Different Feedstocks at 10 g/L COD

6.3.1 Overview

Variable	Unit	Digestate	AD/BO	MP/BO	SWP/BO
Total Biogas	**mL**	171.33 (7.09)	232 (2)	175 (16.7)	226 (7.51)
Lag Phase	**days**	0	36	67	20**
CH_4 Content	**% CH_4**	69.51 (1.33)	75.91 (3.61)	76.4 (4.63)	52.81 (10.83)
COD/TOC	**% Diff.**	-0.18/-15.16 (7.7/2.04)	-16.36/-21.6 (1.22/1.44)	+1.01/+18.74 (6.11/28.21)	-51.56/-46.96 (0.38/2.57)
Organic acids	**% Diff.**	+9.96 (4.24)	-35.57 (1.09)	+49.77 (13.13)	-56.05 (1.48)
Total solids	**% Diff.**	-8.48 (1.11)	-11.77 (0.64)	-6.77 (2.75)	-4.9 (0.81)
pH	**from→to**	8.55→8.09 *→(0.03)	9.18→8.55 *→(0.03)	9.39→8.63 *→(0.01)	7.39→7.84 *→(0.14)

Table 6.3. Details of analysed variables between day 0 and day 102 of AD reactors with 10 g/L COD bio-oils from anaerobic digestate (AD/BO), *M. pyrifera* (MP/BO) and softwood pellets (SWP/BO) in 30 mL sewage sludge digestate, the additional 10 mL was added on day 20 due to complete biogas inhibition.. The lag phase is the estimated time before significant biogas production is seen from the reactors. All conditions were performed in triplicate. Each measurement is a mean of the replicates with the standard deviation given in brackets. *Day 0 pH measurements were not replicated. **SWP/BO lag phase does not include the day 0 production of 40 mL CO_2 from acidification of the digestate.

AD2 was set up identically to AD1 however the concentration of each bio-oil added to the digestates was increased to 10 g/L COD. Table 6.3 details the analysed variables of the test. Again, complete inhibition of biogas production was observed until day 20 when a further 10 mL of digestate were added to stimulate biogas production. SWP/BO reactors immediately began production of biogas at this point with a further 16 and 47 days required for AD/BO and MP/BO reactors to overcome

their respective inhibition phases and begin significant production of biogas. Despite the increased total biogas output and higher average methane concentration obtained from AD/BO-supplemented reactors, the lower reduction in COD/TOC and organic acid concentrations combined with an increased inhibitory phase compared to SWP/BO reactors gave a similar profile to the respective AD1 reactors. MP/BO-supplemented reactors showed an even greater inhibition profile with increases in the COD/TOC and organic acid concentrations of the aqueous phase digestate compared to the day 0 values; however, these reactors continued to produce biogas with higher methane content than SWP/BO reactors. All the bio-oil-supplemented reactors produced more biogas than the control reactors, which showed little reduction in COD/TOC and a slight increase in organic acid concentration. All the reactors lost a fraction of their total solids however it was drastically less than the AD1 reactors. Additionally, the increase in bio-oil COD amplified the respective increases and decreases of starting digestate pHs. Control, AD/BO and MP/BO reactors became more acidic while SWP/BO became more basic, with the greatest change in pH, close to digestate controls.

6.3.2 Results – Biological Characterisation

Three technical replicates were taken at the start of AD2 to allow for significant differences between time points to be calculated. Illumina 16S rRNA sequencing of digestate DNA provided a total of 4 929 973 sequences which, after the removal of short reads, chimeras, PyNAST failures and singletons was reduced to 2 500 548 sequences. The Shannon indices at day 0 and day 102 are shown in Table 6.4 as the quantitative measurement for the alpha diversity of the digestate communities. The sequencing depth after sample rarefaction was similar to AD1 at ~32 000 reads for all samples with the curves plateauing at 3 276 sequences.

d0 DIG	d102 DIG	d102 AD/BO	d102 MP/BO	d102 SWP/BO
5.82 (0.04)	3.06 (0.14)	4.00 (0.12)	4.28 (0.05)	3.60 (0.82)

Table 6.4. Shannon indices at 3 276 sequences from isolated microbial communities from anaerobic digestates from sewage sludge with 10 g/L COD bio-oils from anaerobic digestate (AD/BO), *M. pyrifera* (MP/BO) and softwood pellets (SWP/BO), plus a digestate only control (DIG). The digestates were sampled at the start (d0) and end of the test (d102). All conditions were performed in triplicate. Each measurement is a mean of the replicates with the standard deviation in brackets.

The alpha diversities of the AD2 samples are similar to those see in AD1, with greater diversity observed in the day 0 digestate compared to the end of the test. The inclusion of technical replicates allows for the significance of the change over time to be calculated. There is a significant difference seen between the day 0 digestate samples diversity at the start of the plateau, at 3 276 sequences, and the next highest diversity sample, MP/BO, to a 99.9% confidence (two-sample t-test $P = 1.9\times10^{-6}$). Unlike AD1, the day 102 digestate-only samples show the lowest diversity with a significant difference between these reactors and AD/BO reactors to a 99.9% confidence (two-sample t-test $P = 0.001$). Two of the SWP/BO reactors share a similar average diversity to day 102 controls (3.14 ± 0.19 for the SWP/BO reactors compared to 3.06 ± 0.14 for day 102 controls) however the first SWP/BO replicate shows greater diversity (4.53) and thus causes high variation for this condition's diversity measure.

Figure 6.8 and 6.9 are the relative abundance plots of the archaeal and bacterial communities at the start and end of AD2. The archaeal OTUs contribute an average $1.55\% \pm 1.26\%$ of the total OTUs for each sample with the exception of the first SWP/BO reactor with a total archaeal abundance of 29.85%. This drastic difference in total abundance is paired with the higher alpha diversity observed in this sample, and with no indication from the test data that this replicate sample was particularly

different from the other replicates, these differences are likely due to a sequencing error. Despite the increased abundance of archaeal sequences, the relative abundance profile of this sample's archaea is very similar to the other replicates.

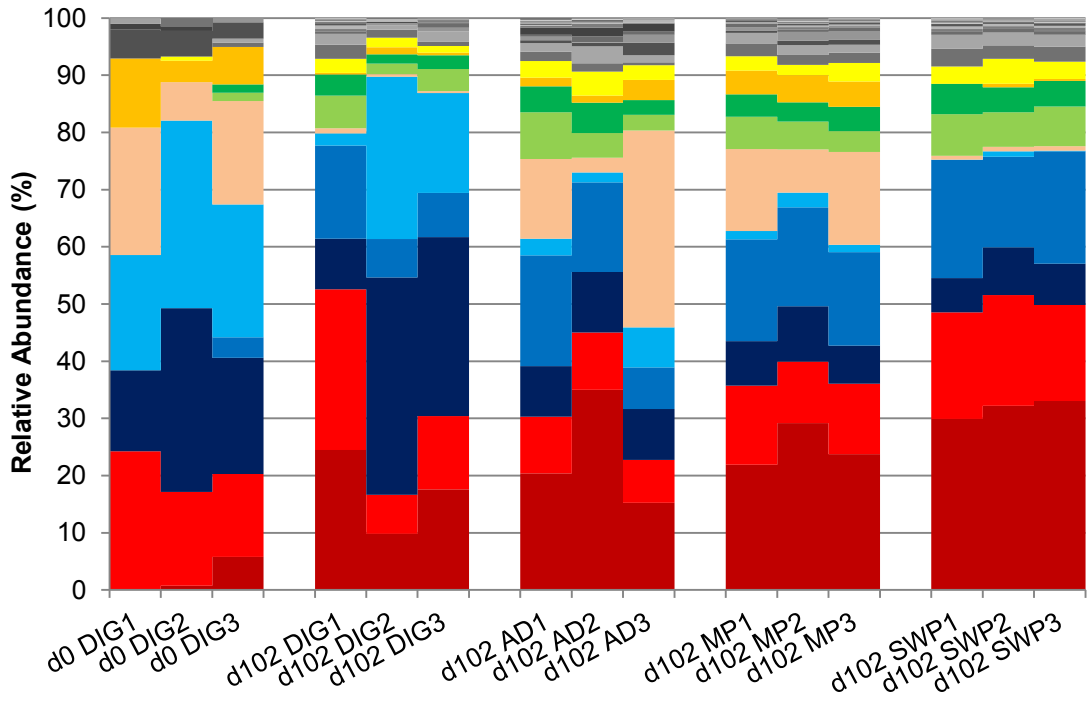

Phylum	Class	Order	Family	Genus
Euryarchaeota	*Methanobacteria*	*Methanobacteriales*	*Methanobacteriaceae*	*Methanobrevibacter*
Euryarchaeota	*Methanomicrobia*	*Methanosarcinales*	*Methanosaetaceae*	*Methanosaeta*
Euryarchaeota	*Methanobacteria*	*Methanobacteriales*	*Methanobacteriaceae*	*Methanobacterium*
Lokiarchaeota	*uncultured*	*uncultured*	*uncultured*	*uncultured*
WSA2	*WCHA1-57*	*uncultured*	*uncultured*	*uncultured*
Euryarchaeota	*Methanomicrobia*	*Methanosarcinales*	*Methanosarcinaceae*	*Methanosarcina*
Lokiarchaeota	*uncultured*	*uncultured*	*uncultured*	*uncultured*
Lokiarchaeota	*uncultured*	*uncultured*	*uncultured*	*uncultured*
Euryarchaeota	*Methanomicrobia*	*Methanomicrobiales*	*Methanomicrobiaceae*	*Methanoculleus*
Euryarchaeota	*Thermoplasmata*	*Thermoplasmatales*	*Marine Benthic Group D and DHVEG-1*	*uncultured*

Figure 6.8. Genus level relative abundance plot of 16S rRNA gene sequences assigned to the archaeal community in anaerobic digestates from sewage sludge with 10 g/L COD bio-oils from anaerobic digestate (AD), *M. pyrifera* (MP) and softwood pellets (SWP). The digestate (DIG) was sampled at the start (d0) and end of the test (d102). The key below the plot represents the top 10 genera from top to bottom in colour with all other sequences in greyscale. Taxonomy was assigned against the SILVA 128 reference database.

Out of the top ten archaeal genera, there are five methanogenic groups which, although showing a slightly altered abundance profile, are the same five as those observed in AD1. Similar patterns are observed in the abundance profile of the AD2 archaeal community as those seen in AD1, particularly the loss of the *Methanosarcina* genus from the digestate-only controls (a loss of 96.3% ± 1.72%) and SWP/BO-supplemented reactors (a loss of 95.28% ± 0.44%). Similarly, the abundance of *Methanoculleus* drops an average 93.28% ± 3.21% for digestate-only and SWP/BO reactors while only dropping 56.01% ± 22.18% for AD/BO and MP/BO reactors.

Unlike AD1, AD/BO and MP/BO reactors did not see a dramatic increase in the abundance of *Methanosarcina*. In fact there is a general loss of all the known methanogenic genera with bio-oil addition, despite no significant difference in the average archaeal percentage assignment of the sequences (ANOVA P = 0.228 F = 4.347). The increase in bio-oil COD has also caused differences to arise between the digestate-only control and the SWP/BO reactors. Although there is high variation between replicates, the digestate-only controls see increases in the *Methanobacterium* genus (17.61% ± 68.84%) whereas this group is reduced in abundance for all bio-oil supplemented reactors (62.86% ± 5.23%). Additionally, the uncultured representatives of the WSA2 phylum were reduced by 37.14% ± 51.75% in the digestate-only controls but by an average 92.1% ± 4.85% for the bio-oil supplemented reactors.

The abundances of bacterial OTUs that contribute ≥ 0.5% of the total OTUs for the AD2 reactors are shown in Figure 6.9 and again, there is similarity between the two tests' most abundant organisms. Indeed, the top 6 genera are identical in their abundance order and account for 72.84% of the total bacterial sequences. The increased alpha diversity of the first SWP/BO replicate reactor is evident from the plot, with a decreased total abundance of genera that contribute ≥ 0.5% to the total OTUs. Also of note is the reduced total abundance of OTUs that contribute ≥ 0.5% of the total for the day 0 digestate compared to the sample from AD1 (an average total of 70.1% ± 0.92% for AD2 compared to 79.48% for AD1).

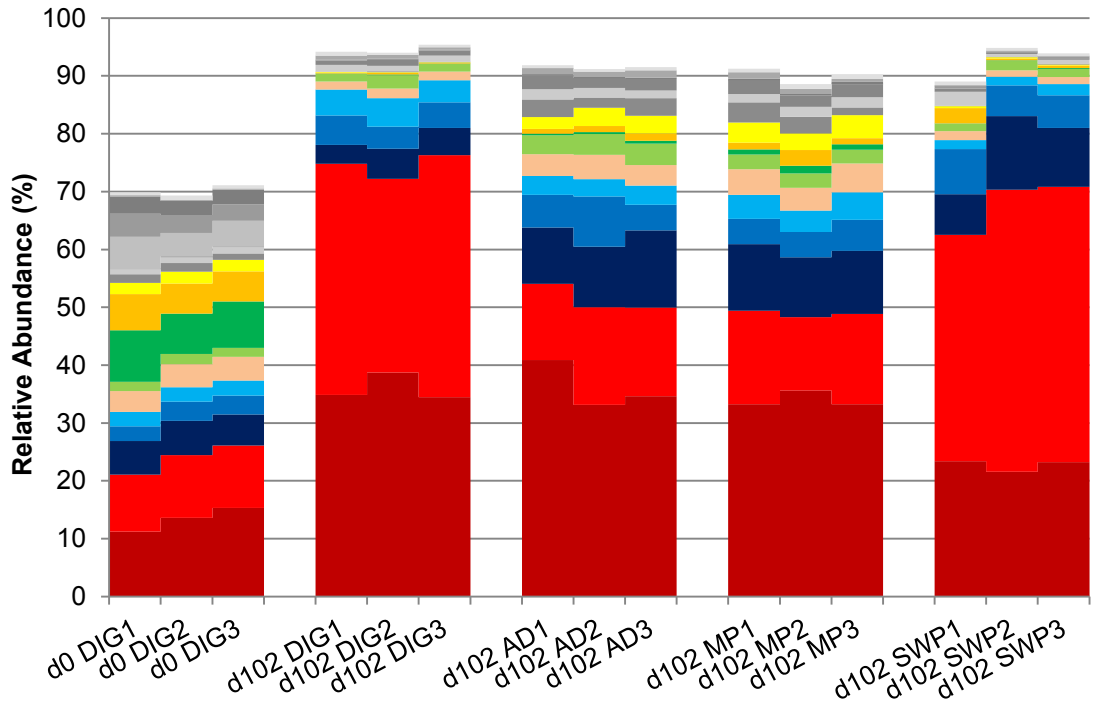

Phylum	Class	Order	Family	Genus
Thermotogae	*Thermotogae*	*Petrotogales*	*Petrotogaceae*	*Defluviitoga*
Cloacimonetes	*W5*	*uncultured*	*uncultured*	*uncultured*
Bacteroidetes	*Sphingobacteriia*	*Sphingobacteriales*	*Lentimicrobiaceae*	*uncultured*
Bacteroidetes	*Bacteroidia*	*Bacteroidales*	*Porphyromonadaceae*	*Proteiniphilum*
Firmicutes	*Clostridia*	*D8A-2*	*uncultured*	*uncultured*
Firmicutes	*Clostridia*	*Thermoanaero-bacterales*	*Thermoanaero-bacteraceae*	*Gelria*
Bacteroidetes	*Bacteroidia*	*Bacteroidales*	*Porphyromonadaceae*	*uncultured*
Proteobacteria	*Gammaproteobacteria*	*Pseudomonadales*	*Pseudomonadaceae*	*Pseudomonas*
Firmicutes	*Clostridia*	*Clostridiales*	*Caldicoprobacteraceae*	*Caldicoprobacter*
Firmicutes	*BSA1B-03*	*uncultured*	*uncultured*	*uncultured*

Figure 6.9. Genus level relative abundance plot of 16S rRNA gene sequences that contributed ≥ 0.5% of the total sequences assigned to the bacterial community in anaerobic digestates from sewage sludge with 10 g/L COD bio-oils from anaerobic digestate (AD), *M. pyrifera* (MP) and softwood pellets (SWP). The digestate (DIG) was sampled at the start (d0) and end of the test (d102). The key below the plot represents the top 10 genera from top to bottom in colour with all other sequences in greyscale. Taxonomy was assigned against the SILVA 128 reference database.

Both the genus *Defluviitoga* and the uncultured representatives of the candidate phylum *Cloacimonetes* contribute 71.16% ± 4.64% of the total abundance of bacterial sequences for the day 102 digestate-only and SWP/BO reactors and 50.09% ± 1.76% of the total for AD/BO and MP/BO reactors. This represents increases of 140.98% ± 46.22% in all the reactor conditions for *Defluviitoga* and 297.76% ± 53.95% and 42.26% ± 15.88% increases in *Cloacimonetes* for digestate-only with SWP/BO reactors and AD/BO with MP/BO reactors respectively. This pattern in the two largest taxonomic groups is similar to that observed in AD1; however, the digestate-only controls also now show a significantly higher abundance of *Cloacimonetes* along with the SWP/BO reactors, at higher than 99.9% confidence, compared to AD/BO and MP/BO reactors (two-sample t-test $P = 3.14 \times 10^{-5}$).

Lentimicrobiaceae increase in abundance in all bio-oil-supplemented reactors (88.08% ± 32.03%) however see a reduction in digestate-only controls by 22.87% ± 17.64%. In AD1, *Proteiniphilum* only saw increases in abundance in the AD/BO and MP/BO reactors however in AD2 we observe the largest increases in abundance in AD/BO and SWP/BO (an average increase of 105.77% ± 53.77% compared to 76.06% ± 44.78% for digestate-only and MP/BO reactors). The difference in *Proteiniphilum* abundance increase between these two groups is however not significant (two-sample t-test $P = 0.055$), as there is a large amount of variation between replicates.

The Bray-Curtis similarity was calculated for archaeal and bacterial relative abundances. Inter-replicate variability between samples was similar to AD1 values with an increased amount of variance observed in the archaeal community compared to bacterial and the highest archaeal variability observed in the day 102 digestate-only controls. Compared to the archaeal community inter-replicate variation of day 0 control reactors, MP/BO and SWP/BO reactors have a significantly lower inter-replicate variability, to a 99% confidence (two-sample t-test MP/BO $P = 0.009$; SWP/BO $P = 0.002$) whereas both day 102 control and AD/BO reactors show a non-significant drop in inter-replicate variation.

The similarity of day 102 archaeal abundances to the day 0 digestate shows the opposite of AD1, where the lowest similarity was observed in MP/BO reactors. In AD2, SWP/BO reactors show a significantly lower similarity of archaeal abundance to the day 0 digestate to a 99% confidence (two-sample t-test P = 0.0012).

Similarly to AD1, there is no significant difference in the inter-replicate variability of the bacterial communities between samples. However, both AD/BO and MP/BO show significantly higher similarity to the day 0 digestates at an average 55.33 ± 2.12 compared to the day 102 digestate controls at 43.11 ± 1.03 similarity, with above a 99.9% confidence (two-sample t-test AD/BO P = 7.82×10^{-7}; MP/BO P = 1.52×10^{-7}). SWP/BO reactors show a comparable level of similarity to the day 102 digestate controls at 45.23 ± 1.04.

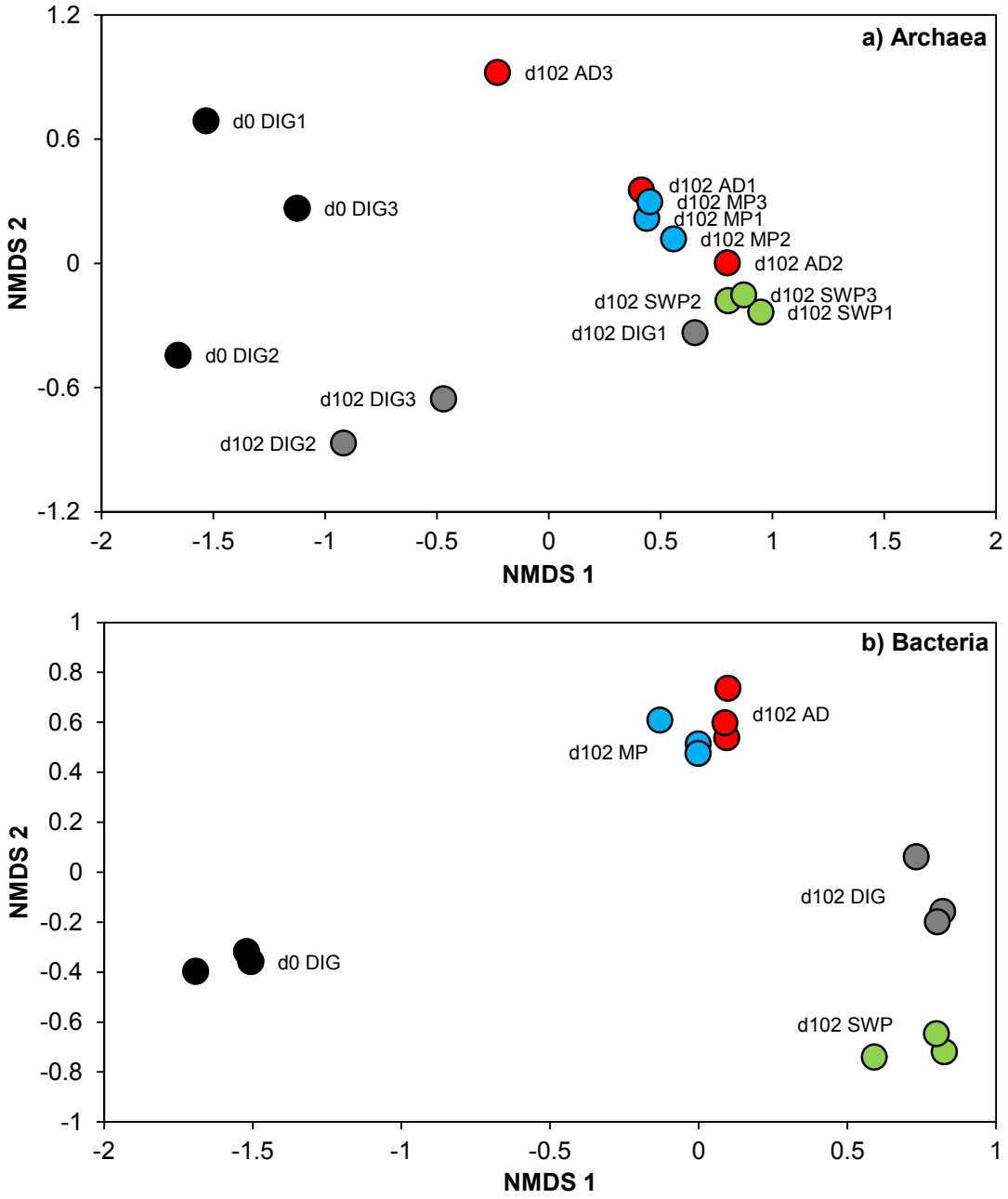

Figure 6.10. 2D NMDS plots generated from the Bray-Curtis similarity matrices for (top/a) archaeal and (bottom/b) bacterial OTU abundances assigned to 16S rRNA gene sequences from sewage sludge anaerobic digestates with 10 g/L COD bio-oils from anaerobic digestate (AD/red), *M. pyrifera* (MP/blue) and softwood pellets (SWP/green), plus a digestate only control (DIG/grey). The digestates (DIG) were sampled at the start (d0) and end of the test (d102). The high inter-replicate similarity of the bacterial samples allows for a single annotation of the replicates. 2D stress (a) = 0.04 and (b) = 0.02.

The similarity of the archaeal communities is shown in Figure 6.10a, plotted using NMDS. High inter-replicate variation can be seen for both day 0 and day 102 digestate-only samples and also for AD/BO-supplemented reactors, which show a spread of samples. Despite what seems like an overlap between the different conditions, a significant difference to a 95% confidence is observed between the reactor groups based on both the reactor condition and time (PERMANOVA based on condition P = 0.002; Pseudo-F = 6.738, and based on time P = 0.002; Pseudo-F = 11.69), that cannot be explained by the dispersion of the samples (PERMDISP based on condition P = 0.2; F = 4.231, and based on time P = 0.678; F = 0.559).

Despite the suspected sequencing error that caused SWP/BO replicate one to have ~30% archaeal abundance, after calculating for the percentage abundance of the samples' archaeal communities, the similarity between this conditions replicates is similar to the other replicates, although still slightly removed as can be seen in the plot. The division between digestate-only plus SWP/BO and AD/BO plus MP/BO reactors observed in the archaeal NMDS plots in AD1, can still be seen in the AD2 plots however there is a larger gap between the day 102 digestate-only and SWP/BO reactors than that seen in AD1.

A very similar pattern is seen in the bacterial abundance data, with clustering of the AD/BO and MP/BO reactors at the top of the 2D space and the day 102 digestate controls and SWP/BO reactors nearer the bottom; again with a larger gap between the day 102 controls and SWP/BO-supplemented reactors. The tight clustering of the different reactor conditions causes a significant difference, with a 99.9% confidence, between the reactor types (PERMANOVA P = 0.001; Pseudo-F = 47.825) that is not explained by dispersion (PERMDISP P = 0.642; F = 1.332). Additionally, there is a significant difference based on the time of sampling (PERMANOVA P = 0.002; Pseudo-F = 18.839) but again, due to the high similarity of the replicates and the significant difference between reactor conditions, the difference due to time can be explained by the change in dispersion of the samples (PERMDISP P = 0.003; F = 41.047).

6.3.3 Results – Chemical Characterisation

Figure 6.11 shows the van Krevelen diagrams for the chemical analysis of the AD2 day 0 digestates and a single replicate from the respective day 102 samples. There is little variation in the plots between the day 102 replicates, so the additional replicates are available electronically. The additional bio-oil COD makes differences between the start and end digestates more evident. A noticeable difference between the two time points can be seen in the higher intensity of some common, high *m/z*, peaks that cluster in the lipid region of the van Krevelen diagrams for day 102 samples (H/C = 1.5 – 2.0; O/C = 0 – 0.3).

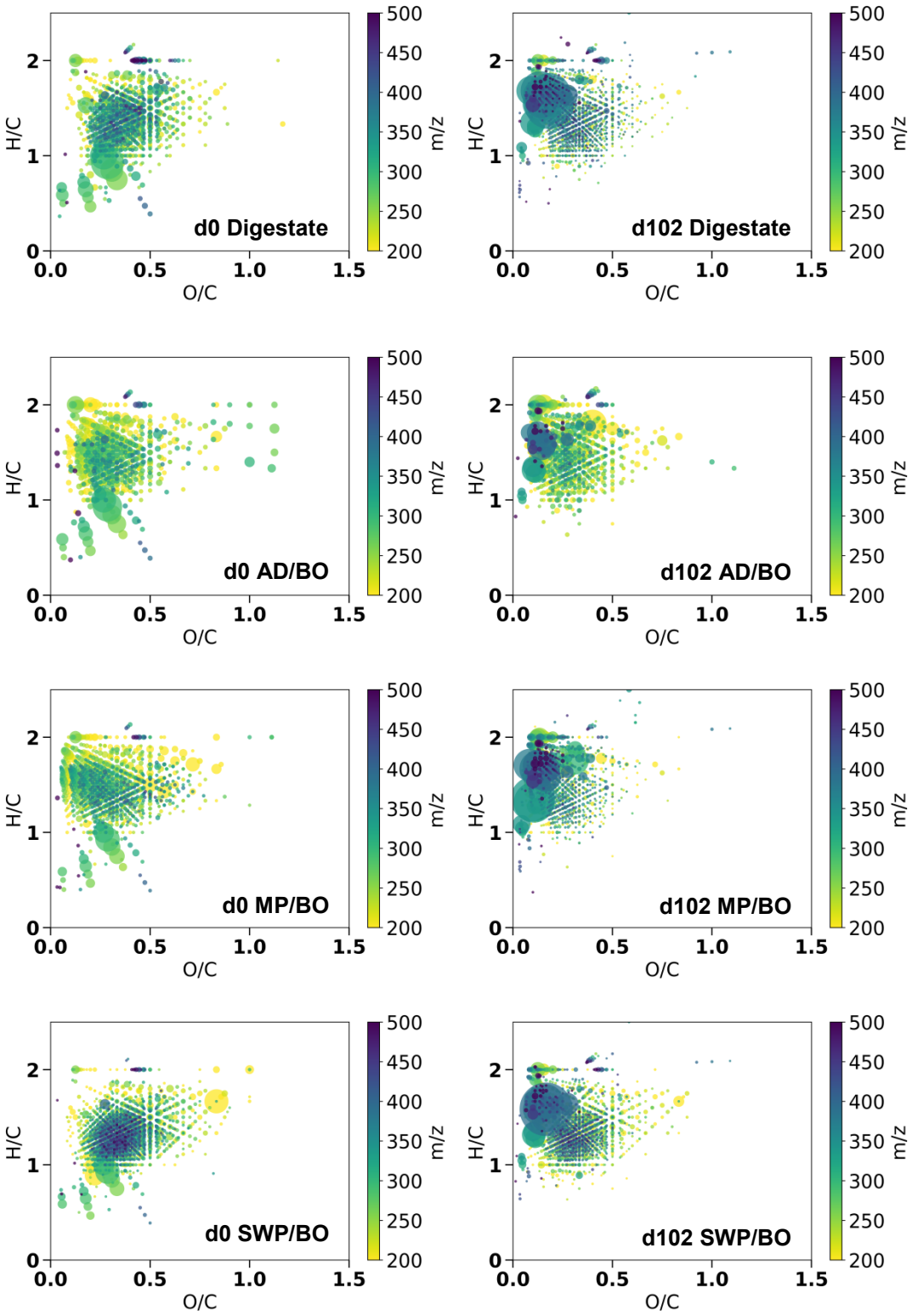

Figure 6.11. van Krevelen diagrams for AD2 day 0 and day 102 digestates with 10 g/L COD bio-oils from anaerobic digestate (AD/BO), *M. pyrifera* (MP/BO) and softwood pellets (SWP/BO) plus a digestate only control. Formulas were assigned from ESI FT-ICR MS spectra. Plots are further

colour-coordinated by the *m/z* of identified compounds with the relative abundance represented by the size of the point.

There is also a general reduction in the spread of the peaks between the day 0 and day 102 samples with a loss of some peaks in the protein region of the diagrams (H/C = 1.5 – 2.2; O/C = 0.3 – 0.67) coupled with a loss of condensed aromatic compounds (H/C = 0.2 – 0.7; O/C = 0 – 0.67). The differences between the day 0 samples are similar to those seen in AD1; however, there appear to be a greater proportion of lower *m/z* compounds in all the AD2 digestates. Despite this, the pattern of clustering for lipid and protein compounds can still be seen in the AD/BO- and MP/BO-supplemented reactors whilst SWP/BO-supplemented reactors show a clustering of larger compounds in the lignin region of the diagram (H/C = 0.7 – 1.5; O/C = 0.1 – 0.67).

The patterns of compound types remain similar for the bio-oils between tests however there is a significantly lower average molecular weight of AD2 compounds (326.52 ± 96.86 M_n) compared to AD1 (401.13 ± 49.67 M_n), to above a 99.9% confidence (two-sample t-test $P = 4.24 \times 10^{-6}$). Of note is that the digestates used for both of these tests were from the same sampling trip with a ~50 day storage time at 4 °C between the start of the first and second tests.

The changes to oxygen heteroatom abundance between day 0 and day 102 is plotted in Figure 6.12 and shows similarity to those changes observed in AD1. Digestate controls and SWP/BO reactors show a decrease in $O_7 – O_{10}$-containing species and all reactors see an increase in $O_2 – O_5$ heteroatom-containing compounds. Of note is that day 0 AD/BO- and MP/BO-supplemented reactors have greatly reduced abundances of oxygen-containing compounds compared to digestate controls and SWP/BO reactors; however, there is still a shift from higher O_x-containing compounds to lower O_x.

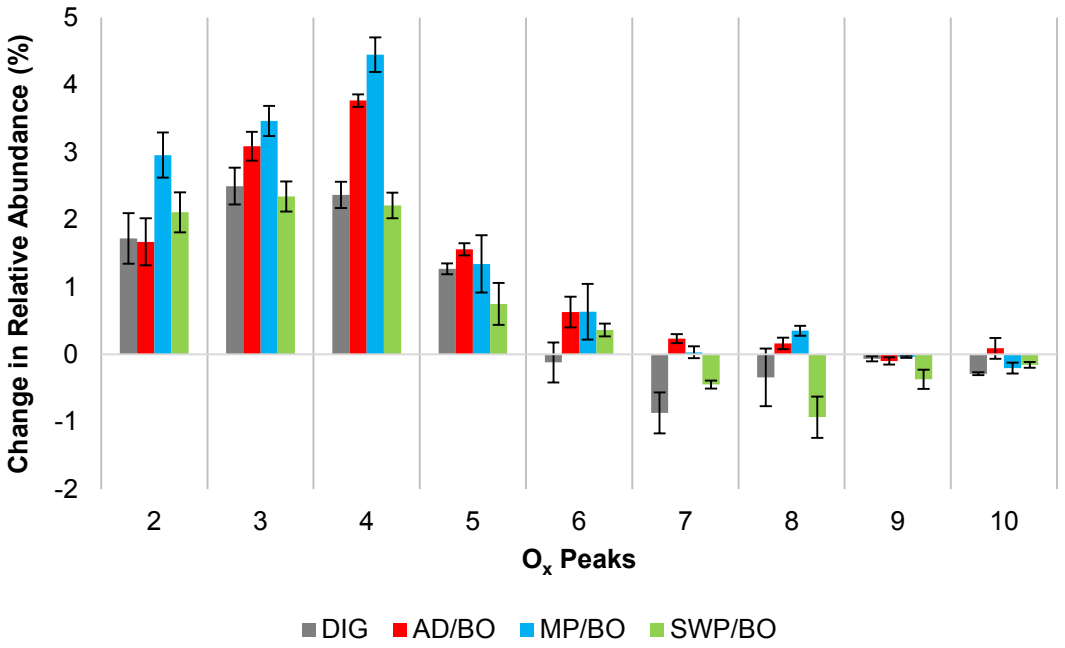

Figure 6.12. Change in oxygen heteroatom relative abundance plots of AD2 digestates with 10 g/L COD bio-oils from anaerobic digestate (AD/BO), *M. pyrifera* (MP/BO) and softwood pellets (SWP/BO) plus a digestate-only control (DIG). Formulae were assigned to peaks generated from ESI FT-ICR MS spectra.

The abundances of nitrogen heteroatom-containing classes in the digestates are shown in Figure 6.13 and are similar to the respective AD1 plots. With the exception of digestate-only controls, there is an overall reduction in N_3 – N_4-containing compounds with an increase in N_1 – N_2-containing compounds for both AD/BO- and MP/BO-supplemented reactors. SWP/BO reactors show the greatest reduction in total nitrogen-containing compounds across all classes.

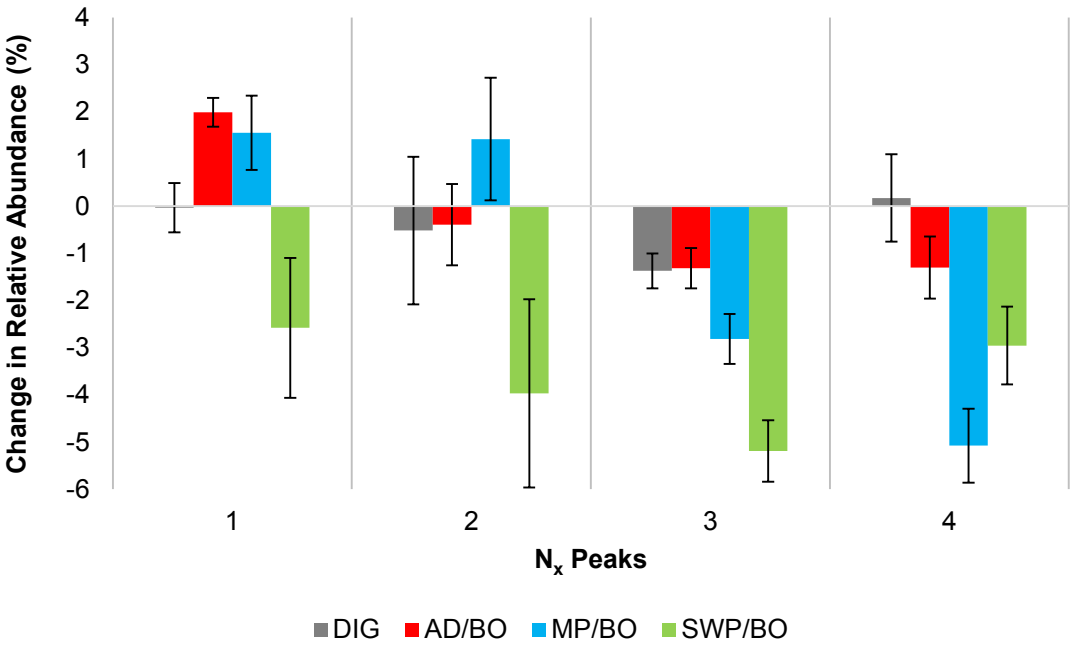

Figure 6.13. Change in nitrogen heteroatom relative abundance plots of AD2 digestates with 10 g/L COD bio-oils from anaerobic digestate (AD/BO), *M. pyrifera* (MP/BO) and softwood pellets (SWP/BO) plus a digestate-only control (DIG). Formulae were assigned to peaks generated from ESI FT-ICR MS spectra. N_x classes are the sum of all N_xO_y containing classes.

The Bray-Curtis similarities were calculated for the AD2 chemical formula abundances from the peak assignments of the digestates at the start and end of AD2. Inter-replicate variability averages at 72.94 ± 2.99 for all the day 102 conditions which is significantly lower than the similarity observed in AD1 day 50 samples (two-sample t-test P = 0.001). There is also significantly reduced similarity of the day 102 samples to their respective day 0 digestates compared to the variation observed in AD1 (an average 39.13 ± 8.46 for AD2 reactors compared to 64.08 ± 2.67 for AD1), to above a 99.9% confidence (two-sample t-test P = 2.44×10^{-7}). No significant differences are observed between the conditions' similarities to their respective day 0 samples whereas in AD1, the day 50 digestate-only control samples were significantly more similar to their day 0 samples than the other conditions.

The NMDS plot of the Bray-Curtis similarities for the AD2 reactors is shown in Figure 6.14. The increased variation among replicate samples is evident by the

increased spread of samples however it is still possible to see the clustering of each reactor condition and the separation of the day 0 and day 102 samples. Both the reactor starting conditions and time of sampling cause significant differences between the samples to a 99.9% and 95% confidence respectively (PERMANOVA for reactor conditions P = 0.001; Pseudo-F = 3.469 and time P = 0.002; Pseudo-F = 6.362). Neither of these results can be explained by differences in the dispersion of the samples (PERMIDSP for reactor conditions P = 0.884; F = 0.378 and time P = 0.388; F = 1.652).

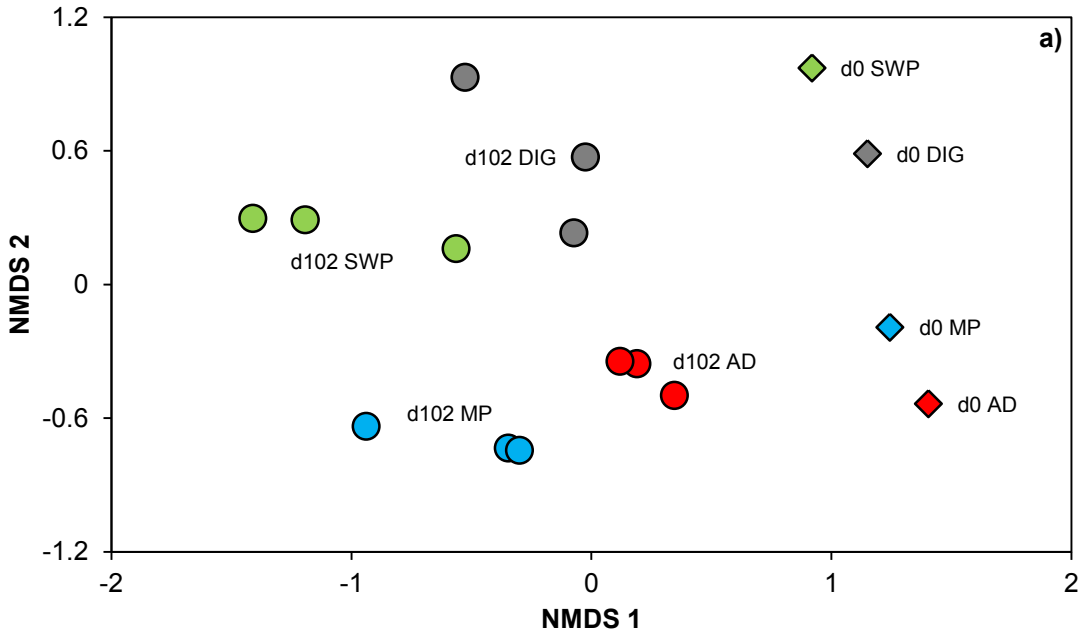

Figure 6.14. 2D NMDS plot generated from the Bray-Curtis similarity matrices for chemical formulae assigned to ESI FT-ICR MS peaks from sewage sludge anaerobic digestates with 10 g/L COD bio-oils from anaerobic digestate (AD/red), *M. pyrifera* (MP/blue) and softwood pellets (SWP/green), plus a digestate only control (DIG/grey). All samples were in triplicate with a single annotation on the graph for each condition. 2D stress = 0.09.

Separation of AD/BO with MP/BO and SWP/BO with digestate-only controls is observed as a split between the top and bottom of the 2D space; however, the clusters

are no longer as easily-identifiable as those in the AD1 chemistry (Figure 6.7) and no significant difference is found between these two sets of day 102 conditions.

6.3.4 Relatedness

Using the same statistical methods as those used in AD1 to compare both the biological and chemical matrices, it is found that the AD2 matrices show a 0.405 similarity to a 95% confidence. Thus the separation of the day 102 samples on the biological and chemical matrices shares ~40% similarity.

6.4 Discussion

AD1 and AD2 show that it is possible to anaerobically digest certain bio-oils for the production of a higher volume of biogas than control reactors without bio-oil addition. The main finding from these experiments was, however, that bio-oil from macroalgae and anaerobic digestate as feedstocks show a significant inhibitory effect on AD whereas the use of bio-oil from a lignocellulosic source is less inhibitory. It was presumed that the control digestates used in all of the tests represent an optimised AD reactor and so both the biological and chemical data associated with the controls are used as the comparison for bio-oil-supplemented reactors. AD1 sees SWP/BO-supplemented reactors cluster with the control reactors in both the chemical and biological data, which are found to be highly relatable in terms of similarity of observed patterns, while the AD/BO and MP/BO reactors both showed a significantly different clustering for both data sets.

AD2 shows very similar patterns to AD1, which is to be expected due to the similarity of the test; however, the increase in bio-oil concentration and the increased time period between the sampling dates do create some observable differences. Whereas AD1 reactors see a definitive split between the digestate control reactors with SWP/BO reactors, and between AD/BO with MP/BO reactors, the increased concentration of bio-oil further splits these groups apart in both their biological and chemical similarity matrices. The increased time period of the experiment also presumably contributes to this divide and to the decreased similarity between the

patterns observed in the chemical and biological data, which shows a reduced relatedness compared to that seen in AD1.

The alpha diversity of the isolated communities at the end of each test is lower across all reactors compared to the starting digestate. And although in AD1 the addition of bio-oil does not significantly reduce the diversity any more or less than control reactors, in the case of AD2, the pattern of diversity reduction for the day 102 reactors follows the inverse of the observed inhibition. The greater the inhibition, the higher the final diversity.

There are also similar patterns in the relative abundances of methanogenic archaea between the experiments. Of the identified methanogenic archaea in both AD1 and AD2, only species of *Methanosaeta* are capable of acetoclastic methanogenesis, while the other known methanogens are hydrogenotrophic. *Methanosarcina* are capable of adopting both metabolic pathways. Based on the method of methanogenesis, digestate-only control reactors and those supplemented with SWP/BO show an increased abundance of those methanogens solely capable of hydrogenotrophic methanogenesis. This is due to the relative reduction of *Methanosarcina* members which are instead enriched in AD/BO- and MP/BO-supplemented reactors. These two reactor conditions performed the worst in regards to the lag time before biogas production and the reduction of COD in the aqueous phase of the digestate. Thus, the abundance increase of *Methanosarcina* members may be an indicator of an inhibited reactor. In these datasets the majority of other archaeal sequences were assigned to the Phylum *Lokiarchaeota* (Da Cunha *et al*., 2017) of which there are no cultured representatives and whose metabolic abilities are still unknown.

As previously mentioned, acetoclastic methanogens are less resistant to the inhibitors commonly found in AD reactors and this can be seen in the reduction of *Methanosaeta* in the AD/BO- and MP/BO-supplemented reactors. The fact we see such similarity between the digestate-only controls and SWP/BO-supplemented

communities indicates that SWP/BO is less toxic to the archaeal communities than AD/BO and MP/BO bio-oils.

Characterisation of the bacterial communities also reveals similar patterns between AD1 and AD2. Both experiments showed increased relative abundances of *Defluviitoga* and *Cloacimonetes* across all reactors between the two sampling points. Members of both these groups are thought to be syntrophic partners with hydrogenotrophic methanogens and are common components of anaerobic digester microbial communities (Maus *et al*., 2016; Maus *et al*., 2016; Pelletier *et al*., 2008). In AD2 specifically, the relative abundance of *Cloacimonetes* was increased in the digestate-only and SWP/BO-supplemented reactors which also showed a higher proportion of methanogens solely capable of hydrogenotrophic methanogenesis.

The relative abundance of *Proteiniphilum* in AD1 was also observed to increase in reactors supplemented with AD/BO and MP/BO. *Proteiniphilum acetatigenes* gen. nov., sp. nov. was identified and described as being able to utilise saccharides and proteinaceous substances in anaerobic digesters (Chen and Dong *et al*., 2005). Both of these bio-oils show a high proportion of proteinaceous compounds that clustered in their associated van Krevelen diagrams and as such the increased abundance of *Proteiniphilum* in these reactors at the end of the test potentially indicates ongoing degradation of these compounds.

AD/BO- and MP/BO-supplemented reactors appear similarly inhibited in their microbial profile compared to digestate controls and SWP/BO-supplemented reactors. The increased bio-oil concentration caused SWP/BO reactors to show a higher dissimilarity to the digestate-only controls at day 102 than in AD1 at day 50. Although both the archaeal and bacterial communities in these reactors are more similar compared to the other day 102 reactors, the increased difference compared to that seen in AD1 does suggest that the SWP/BO is having an inhibitory effect on the microbial communities. However, considering the dramatic increase in COD added to these reactors, the digestate was still able to reduce COD/TOC to similar levels as the control reactors and produce additional biogas without a drastic effect on the

microbial communities, unlike the AD/BO and MP/BO reactors. Thus, although the addition of 10 g/L COD of SWP/BO bio-oil may be too high, there is definitely scope for its successful bioconversion to a value-added product in AD. Of note is that the similarity of AD/BO and MP/BO microbial communities through both tests is high despite the very different inhibition profiles observed in their biogas production, with MP/BO reactors exhibiting far greater inhibition.

The individual bio-oil chemistries can be seen in the day 0 digestates with increased amounts of lignin peaks in SWP/BO reactors and more protein and lipid peaks in the AD/BO and MP/BO reactors. Ageing of the digestate can also be seen as a reduction of average molecular weight of compounds in AD2 controls compared to AD1. This ageing can potentially explain the reduced biogas potential of AD2 reactors as ongoing degradation of the digestate occurs during storage. Inter-replicate variability and the variability between the two sampling dates are also greater for AD2 reactors compared to AD1 and are likely due to the doubling of the incubation time for these reactors as the increased time scale of the experiment allows for further divergence of the digestate chemistry.

Through both sets of tests there is also a pattern for an increase in the amount of compounds with lower oxygen and nitrogen heteroatom-containing states and a reduction of those with higher states. This reduction is likely the result of successful degradation of bio-oil compounds as the majority of heteroatom changes are in bio-oil-containing digestates.

It should be noted that these conclusions are based on a single time point after these reactors have completed their significant production of biogas. As such it is likely that a great deal of adaptation has occurred in the microbial community that has been missed, and similarly so for the chemistry of the digestate. This highlights a limitation of the study and for future work it is recommended that additional sampling periods are analysed particularly when there is notable biogas production.

CHAPTER 7: BIOLOGICAL AND CHEMICAL CHARACTERISATION OF AD/SWP/BO BIO-OIL REACTORS WITH ADDITIONAL DIGESTATE TREATMENTS AND SUPPLEMENTS

7.1 Introduction

Volatile fatty acids (VFAs) have been identified as a more valuable product than biogas, particularly acetic acid, which is also the terminal substrate for acetoclastic methanogenesis. If it were possible to prevent this step, then it could lead to the accumulation of VFAs which could be further isolated and recovered. Similar work has been performed on dark fermentation broths for hydrogen production that see the accumulation of VFAs as inhibitory to hydrogen production (Jones *et al*., 2015). Dark fermentation is similar to AD however relies on no biogas production from methanogens that would utilise the hydrogen. Thus, the inoculum is generally heat treated to ensure their inactivity, relying on bacterial hydrolysers, which are capable of sporulating at high temperatures, to recover after the treatment and continue hydrolysis. The use of heat treatment of digestate is investigated in AD3 for the Seafield wastewater digestates' ability to accumulate VFAs, both with and without bio-oil addition.

The addition of biochar has also been reported to affect both the microbial populations and the chemistry of anaerobic digestate. Biochar supplementation is thought to aid AD by the adsorption of inhibitory compounds, similar to the application of activated carbon, which has also been used for the adsorption of bio-oil inhibitory compounds (Chen *et al*, 2014; Shanmugam *et al*., 2017). There are several proposed methods of adsorption to biochar surfaces from simple physical adsorption and pore filling to ion exchange and hydrophobic attraction (Fagbohungbe *et al*., 2017). It has been reported that several common inhibitory compounds can adsorb onto biochars and that AD reactors supplemented with biochar exhibit reduced lag from inhibition and increased methane yield (Mumme *et al*., 2014).

The impact of biochar addition on the microbial communities in AD is also well documented. Similarly to other solid carbonaceous material, its inclusion in AD allows for the adhesion of microbial communities that gain environmental protection from inhibitory compounds due to the nature of the biochar surface. The pyrolysis of biomass causes volatilisation of the organic matter, increasing pore size as the structure is rearranged (Lua, Yang and Guo, 2004). The porosity of biochars confers a high surface area for the immobilisation of microbial cells and biofilm growth. Microorganisms in biofilms show increased resistance to environmental stresses and can assist in the survival of other non-biofilm-forming species by immobilising them (Hsu *et al*., 2013).

Biochars are also partially conductive to the flow of electrons and are thus capable of supporting direct interspecies electron transfer (DIET) between microorganisms situated on the biochar surface. DIET is thought to aid in syntrophy between DIET-capable microorganisms by allowing the transfer of electrons from different species to occur without physical contact and has been demonstrated on a number of conductive materials such as carbon cloth, granular activated carbon and biochar (Chen *et al*., 2014; Zhao *et al*., 2016). It is reported that species from the *Geobacter* genus of *Deltaproteobacteria* are capable of DIET with methanogenic Archaea from the genera of *Methanosaeta* and *Methanosarcina* (Chen *et al*., 2015; Cooney *et al*., 2016; Wang *et al*., 2016). It is therefore likely that biochar surfaces in anaerobic digesters are enriched with microorganisms that are capable of DIET as this would give them a significant advantage over competing microorganisms that have to expend energy to produce extracellular biological electrical connections.

Similarly to AD1 and AD2, both biological and chemical data were obtained from the AD tests which are summarised as follows. AD3 utilised only bio-oil from softwood pellets (SWP/BO) at 10g/L COD and assessed the impact different digestate treatments had on biogas production. Samples were taken at the beginning, middle and end of the 80 day test and only the microbial community was analysed. AD4 used SWP/BO at 5 g/L COD and was designed to assess the impact a microbial inhibitor and different biochars, both dry and pre-incubated, had on biogas

production. Samples were taken at the start, day 20, day 40 and day 60 of the test and were analysed for both the biological and chemical components.

7.2 AD3 – Digestate Treatment Effects on AD/Bio-Oil Reactors

7.2.1 Overview

Variable	Unit	Fresh Autoclaved	+Bio-oil	+Seed	+Bio-oil & Seed
Total Biogas	mL	56.75 (2.47) 0 (0)	74.25 (4.6) 0 (0)	34.5 (0.71) 55.5 (0.71)	57.5 (2.83) 54.25 (21.57)
Lag Phase	days	13 -	44 -	14 13	45 53 & 71*
CH_4 Content	% CH_4	69.18 (1.27) -	75.14 (0.35) -	70.18 (0.57) 79.33 (0.78)	77 (1.98) 76.88 (0.57)
COD	% Diff.	-11.71 (2.3) +41.52 (19.15)	-46.09 (2.02) +3.11 (3.9)	-19.06 (4.11) -37.08 (2.23)	-45.01 (6.37) -38.45 (10.21)
TOC	% Diff.	-17.92 (4.76) +39.51 (17.71)	-52.43 (5.61) +2.48 (4.97)	-24.34 (1.51) -30.5 (0.83)	-49.97 (3.51) -41.51 (6.18)
Organic acids	% Diff.	+34.41 (8.12) +397.54 (16.79)	-54.14 (0.35) +38.93 (11.63)	+5.13 (8.05) +26.28 (13.18)	-45.74 (3.07) -33.65 (21.52)
pH	From → to	7.79→8.5 (0.09)→(0.08) 9.53→9.98 (0.11)→(0.4)	6.93→8.3 (0.11)→(0.05) 8.66→8.34 (0.29)→(0.01)	8.15→8.51 (0.01)→(0.07) 9.03→8.47 (0.06)→(0)	7.02→8.31 (0.19)→(0.04) 8.23→8.27 (0.01)→(0.01)

Table 7.1. Details of analysed variables between day 0 and day 80 of AD reactors with 20 mL of digestates plus supplements. Half the reactors were supplemented with 10 g/l COD bio-oil (+B) from softwood pellets (SWP/BO). The 20 mL of digestate was composed of either fresh (blue) or autoclaved (red) sewage sludge digestate with or without 1:1 (v:v) seed digestate from AD2 d102 SWP/BO reactors. The lag phase is the estimated time before significant biogas production is seen from the reactors. All conditions were performed in duplicate with each measurement as a mean of the replicates with the standard deviation given in brackets. *The two replicate autoclaved digestates plus bio-oil and seed reactors showed considerably different lag times and are thus displayed individually.

The third AD test utilised autoclaving to permanently inhibit the methanogenic potential of the digestates so that the ability of the surviving microbial community to continue anaerobic digestion of bio-oil for VFA accumulation could be assessed. Included in the test was seed digestate from AD2 day 102 SWP/BO-supplemented reactors which was used at a 1:1 (v:v) ratio with fresh or autoclaved digestate to assess what impact it had on reactors' ability to utilise bio-oil. The results of the tested parameters are summarised in Table 7.1; it should be noted that samples were not taken for chemical analysis by FT-ICR MS. Autoclaving successfully prevented methanogenesis in reactors that were not supplemented with seed digestate and resulted in a marked increase in COD, TOC and organic acids.

Bio-oil-supplemented reactors were completely inhibited of biogas production until day 40 when a further 1 mL of the reactor's respective digestate was added. The reinoculation prompted biogas production 4 – 5 days later in reactors with the seed digestate. Fresh digestate with bio-oil produced the most amount of biogas whilst the addition of seed digestate caused a reduction in total biogas due to its reduced COD. Autoclaved digestates were found to contain a greater COD in their aqueous fraction, presumably due to the pressure and heat treatment of autoclaving. Although the addition of seed digestate to autoclaved allowed for biogas production, there was no significant reduction in the lag phase for seeded reactors to overcome bio-oil inhibition. Thus, the microbial community from the seed digestate was not sufficient for alleviating bio-oil inhibition.

Organic acid accumulation did occur in bio-oil supplemented reactors with autoclaved digestate and the concentration was still increasing by the end of the test. Non-bio-oil reactors showed an increased rate of organic acid accumulation however, indicating continued bio-oil inhibition of the surviving microbial communities.

7.2.2 Results – Biological Characterisation

Samples were taken for all duplicate reactor conditions at the start, day 40 and day 80 of the test. Table 7.2 shows the alpha diversity of the reactors using the Shannon index. Rarefaction reduced the number of reads to a sequencing depth of 48 910;

however, the curves begin to plateau at 4 900 sequences per sample. The fresh control digestate reactors (F) show a general reduction in their diversity over time with the exception of those supplemented with seed only (FS) which show little variation in their diversity. These FS reactors start with a reduced diversity compared to the control reactors however this difference is not significant (two-sample t-test P = 0.073). The reduced diversity is presumably due to the inclusion of the day 102 SWP/BO seed digestate from AD2, which can be seen to have a Shannon diversity of ~3.5 (Figure 6.13).

d0 F	d40 F	d80 F	d0 FB	d40 FB	d80 FB	d0 FS	d40 FS	d80 FS	d0 FSB	d40 FSB	d80 FSB
5.72	4.28	3.47	6.18	5.64	4.84	4.47	4.14	4.43	5.54	4.19	3.56
(0.05)	(0.19)	(0.06)	(0.11)	(0.63)	(0.13)	(0.37)	(0.07)	(0.16)	(0.06)	(0.55)	(0.04)

d0 A	d40 A	d80 A	d0 AB	d40 AB	d80 AB	d0 AS	d40 AS	d80 AS	d0 ASB	d40 ASB	d80 ASB
5.87	6.17	4.60	4.61	4.45	4.47	5.88	5.70	3.81	5.97	3.88	3.47
(0.05)	(0.24)	(0.32)	(0.10)	(0.46)	(0.38)	(0.05)	(0.18)	(1.75)	(0.04)	(1.64)	(2.31)

Table 7.2. Shannon indices at 4 900 sequences from isolated microbial communities from sewage sludge anaerobic digestates. The 20 mL of digestate was composed of either fresh (F) or autoclaved (A) digestate with or without 1:1 (v:v) seed digestate (S) from AD2 d102 SWP/BO reactors. Reactors were sampled at day 0, day 40 and day 80 of the test. Half the reactors were supplemented with 10 g/L COD bio-oil (B/grey) from softwood pellets (SWP/BO). Each measurement is a mean of two replicates with the standard deviation in brackets.

Fresh digestate samples with bio-oil (FB) show increased diversity compared to the fresh digestate controls, with significance observed in their day 80 samples to above a 95% confidence (two-sample t-test P = 0.009) compared to day 80 F reactors. The reduction of diversity observed in the seeded reactors and the increase due to bio-oil additional causes the reactors with both (FSB) to show a balance, where there is no significant difference in diversity from the control reactors.

The autoclaved digestates show a different pattern, with the autoclaved-only control reactors (A) showing little difference in diversity of the day 0 and day 40 reactors but then a significant reduction, to a 95% confidence, in the day 80 sample (two-sample t-test P = 0.048). The autoclaved digestate with bio-oil reactors (AB) show a reduced diversity across all time points compared to controls. Both autoclaved with seed (AS) and autoclaved with seed and bio-oil (ASB) reactors have a single replicate that deviates considerably from the other samples. A day 80 AS replicate shows an extremely low diversity compared to the other sample which shows little variation across the time points for this reactor condition and is responsible for the increased standard deviation. Similarly one ASB reactor shows little variation throughout the experiment; however, the second ASB replicate exhibits an extremely low diversity starting at day 40 and continually reducing into day 80.

Archaeal OTUs account for 0.3% ± 0.27% of the total sequencing reads with their relative abundances shown in Figures 7.1 and 7.2 for each reactor with fresh and autoclaved digestates respectively. The fresh digestate reactors show some similar patterns in their relative abundances, irrespective of the addition of seed digestate or bio-oil, with an increased abundance of *Methanobacterium* and a slightly decreased abundance of *Methanosaeta* in all F reactors compared to A reactors, with the exception of FS reactors, which show little variation in their archaeal community. Of note is that the increase over time in *Methanobacterium* observed in the FB and FSB reactors coincides with these reactors' significant biogas generation period. Additionally, Both F and FSB reactors show a reduced abundance of *Methanosarcina* in their day 80 reactors, similarly to the digestate-only controls of AD1 and AD2.

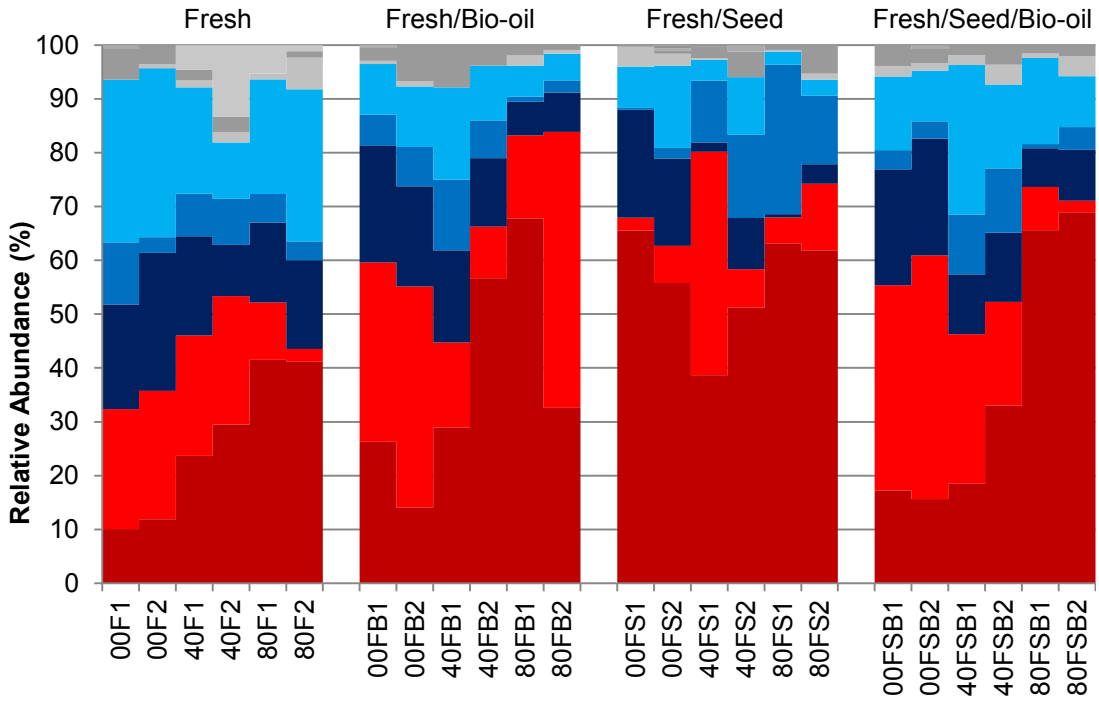

Phylum	Class	Order	Family	Genus
Euryarchaeota	*Methanobacteria*	*Methanobacteriales*	*Methanobacteriaceae*	*Methanobacterium*
Euryarchaeota	*Methanomicrobia*	*Methanosarcinales*	*Methanosarcinaceae*	*Methanosarcina*
Euryarchaeota	*Methanomicrobia*	*Methanosarcinales*	*Methanosaetaceae*	*Methanosaeta*
Euryarchaeota	*Methanomicrobia*	*Methanomicrobiales*	*Methanomicrobiaceae*	*Methanoculleus*
WSA2	*WCHA1-57*	*uncultured*	*uncultured*	*uncultured*

Figure 7.1. Genus level relative abundance plot of 16S rRNA gene sequences assigned to the archaeal community in anaerobic digestates. The 20 mL of digestate was composed of fresh (F) sewage sludge digestate with or without 1:1 (v:v) seed digestate (S) from AD2 d102 SWP/BO. Reactors were sampled at the start (00), day 40 and day 80 of the test. Half the reactors were supplemented with 10 g/L COD bio-oil (B) from softwood pellets (SWP/BO). The key below the plot represents the top five genera from top to bottom in colour with all other sequences in greyscale. Taxonomy was assigned against the SILVA 128 reference database.

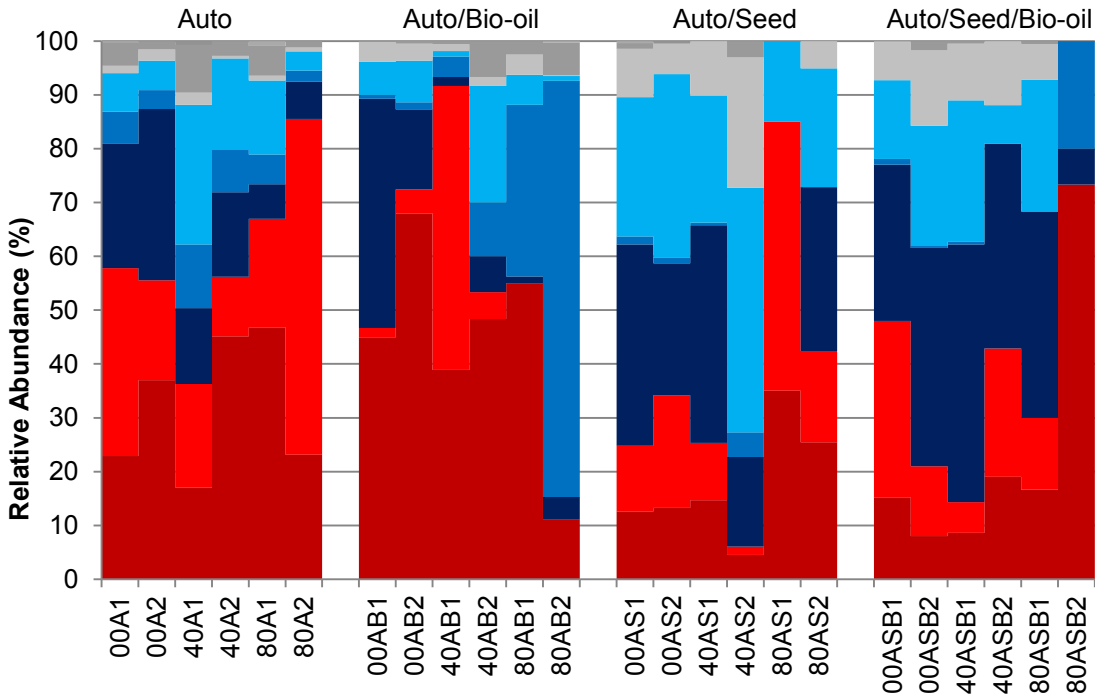

Phylum	Class	Order	Family	Genus
Euryarchaeota	*Methanobacteria*	*Methanobacteriales*	*Methanobacteriaceae*	*Methanobacterium*
Euryarchaeota	*Methanomicrobia*	*Methanosarcinales*	*Methanosarcinaceae*	*Methanosarcina*
Euryarchaeota	*Methanomicrobia*	*Methanosarcinales*	*Methanosaetaceae*	*Methanosaeta*
Euryarchaeota	*Methanomicrobia*	*Methanomicrobiales*	*Methanomicrobiaceae*	*Methanoculleus*
WSA2	*WCHA1-57*	*uncultured*	*uncultured*	*uncultured*

Figure 7.2. Genus level relative abundance plot of 16S rRNA gene sequences assigned to the archaeal community in anaerobic digestates. The 20 mL of digestate was composed of autoclaved (A) sewage sludge digestate with or without 1:1 (v:v) seed digestate (S) from AD2 d102 SWP/BO. Reactors were sampled at the start (00), day 40 and day 80 of the test. Half the reactors were supplemented with 10 g/L COD bio-oil (B) from softwood pellets (SWP/BO). The key below the plot represents the top five genera from top to bottom in colour with all other sequences in greyscale. Taxonomy was assigned against the SILVA 128 reference database.

Autoclaving the digestates completely inhibited methanogenesis and unless reactors were seeded, no biogas was produced. However, archaeal DNA was still detected in A and AB reactors. Although it is unknown what is happening at the absolute abundance level, a pattern is observable in the abundance data for A and AB reactors with what seems to be a decrease in *Methanosaeta* and an increase in hydrogenotrophic methanogens such as *Methanoculleus* over time, despite no biogas being generated from these reactors. Regardless of biogas production, the autoclaved digestates vary considerably in their archaeal abundances with no clear pattern of increase or decrease in the relative abundances of specific genera.

The bacterial relative abundances are shown in Figure 7.3 and 7.4 for the fresh and autoclaved digestate reactors respectively. Again the largest contributing genera are the genus *Defluviitoga* and the uncultured representatives of the candidate phylum *Cloacimonetes*. These two genera are, however, reduced in abundance in almost every condition's day 0 samples compared to later sampling periods, but then see an immediate increase in abundance at day 20. The starting samples instead show an abundance of *Pseudomonas* which has not been a major component of the starting digestate in the previous tests. This genus is almost completely lost from fresh, day 20, digestate reactors onwards.

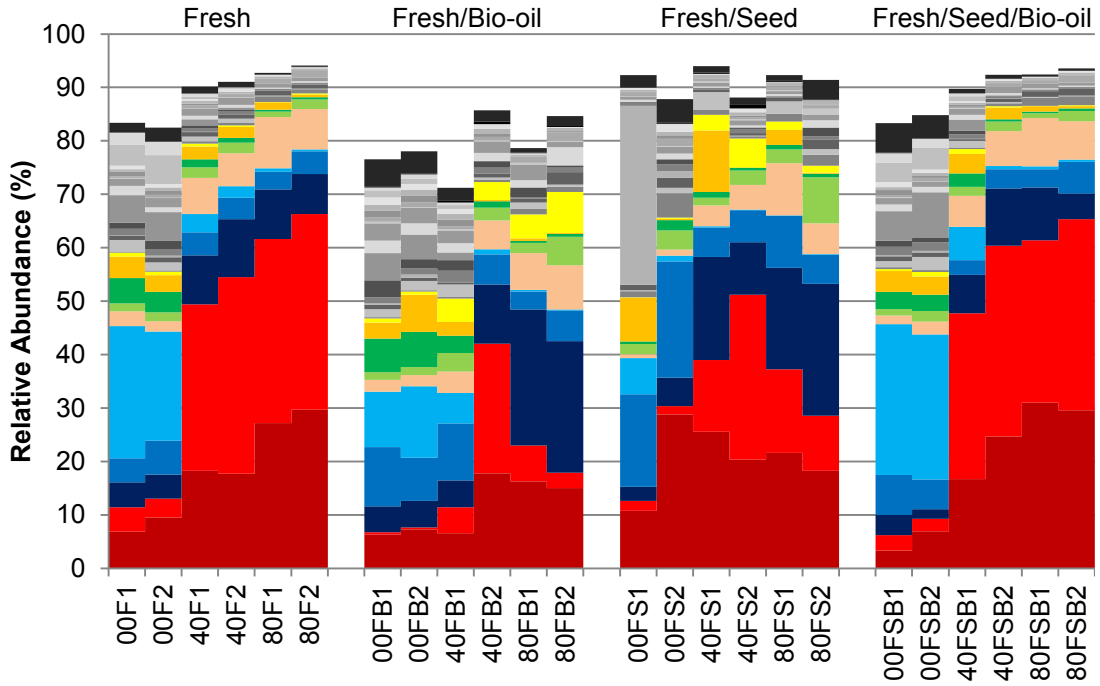

Phylum	Class	Order	Family	Genus
Thermotogae	*Thermotogae*	*Petrotogales*	*Petrotogaceae*	*Defluviitoga*
Cloacimonetes	*W5*	*uncultured*	*uncultured*	*uncultured*
Bacteroidetes	*Sphingobacteriia*	*Sphingobacteriales*	*Lentimicrobiaceae*	*uncultured*
Firmicutes	*Clostridia*	*D8A-2*	*uncultured*	*uncultured*
Proteobacteria	*Gammaproteobacteria*	*Pseudomonadales*	*Pseudomonadaceae*	*Pseudomonas*
Bacteroidetes	*Bacteroidia*	*Bacteroidales*	*Porphyromonadaceae*	*Proteiniphilum*
Firmicutes	*Clostridia*	*Thermoanaerobacterales*	*Thermoanaerobacteraceae*	*Gelria*
Firmicutes	*Clostridia*	*Clostridiales*	*Caldicoprobacteraceae*	*Caldicoprobacter*
Proteobacteria	*Gammaproteobacteria*	*Pseudomonadales*	*Pseudomonadaceae*	*Thiopseudomonas*
Firmicutes	*BSA1B-03*	*uncultured*	*uncultured*	*uncultured*

Figure 7.3. Genus level relative abundance plot of 16S rRNA gene sequences that contributed ≥ 0.5% of the total sequences assigned to the bacterial community in anaerobic digestates. The 20 mL of digestate was composed of fresh (F) sewage sludge digestate with or without 1:1 (v:v) seed digestate (S) from AD2 d102 SWP/BO. Reactors were sampled at the start (00), day 40 and day 80 of the test. Half the reactors were supplemented with 10 g/L COD bio-oil (B) from softwood pellets (SWP/BO). The key below the plot represents the top 10 genera from top to bottom in colour with all other sequences in greyscale. Taxonomy was assigned against the SILVA 128 reference database.

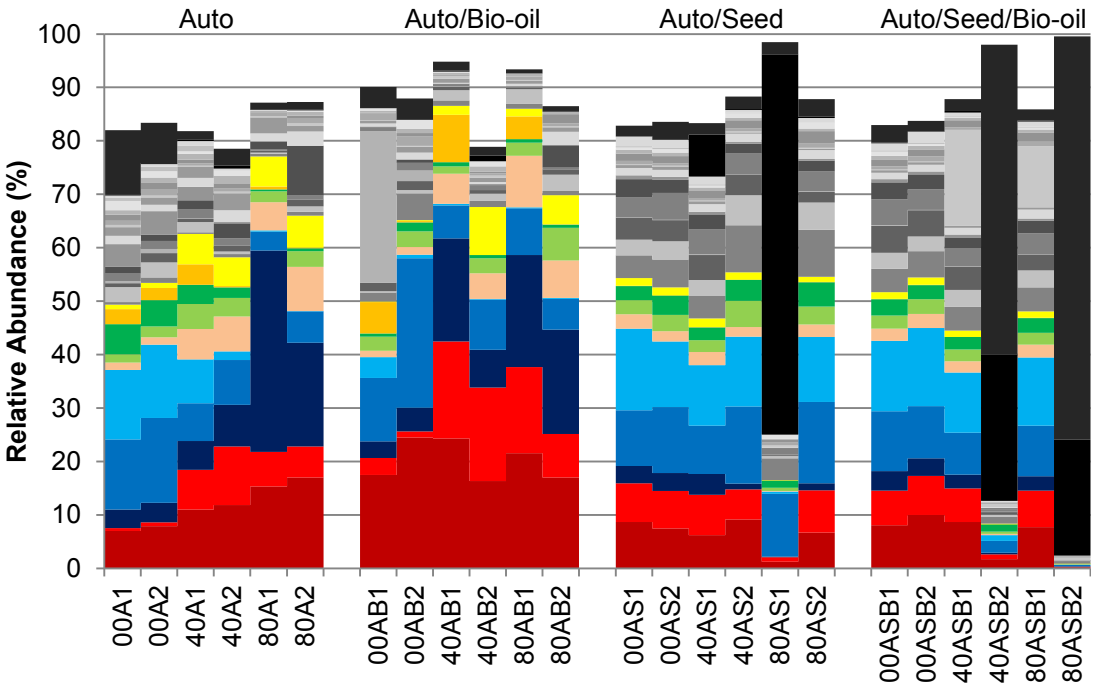

Phylum	Class	Order	Family	Genus
Thermotogae	*Thermotogae*	*Petrotogales*	*Petrotogaceae*	*Defluviitoga*
Cloacimonetes	*W5*	*uncultured*	*uncultured*	*uncultured*
Bacteroidetes	*Sphingobacteriia*	*Sphingobacteriales*	*Lentimicrobiaceae*	*uncultured*
Firmicutes	*Clostridia*	*D8A-2*	*uncultured*	*uncultured*
Proteobacteria	*Gammaproteobacteria*	*Pseudomonadales*	*Pseudomonadaceae*	*Pseudomonas*
Bacteroidetes	*Bacteroidia*	*Bacteroidales*	*Porphyromonadaceae*	*Proteiniphilum*
Firmicutes	*Clostridia*	*Thermoanaerobacterales*	*Thermoanaerobacteraceae*	*Gelria*
Firmicutes	*Clostridia*	*Clostridiales*	*Caldicoprobacteraceae*	*Caldicoprobacter*
Proteobacteria	*Gammaproteobacteria*	*Pseudomonadales*	*Pseudomonadaceae*	*Thiopseudomonas*
Firmicutes	*BSA1B-03*	*uncultured*	*uncultured*	*uncultured*

Figure 7.4. Genus level relative abundance plot of 16S rRNA gene sequences that contributed ≥ 0.5% of the total sequences assigned to the bacterial community in anaerobic digestates. The 20 mL of digestate was composed of autoclaved (A) sewage sludge digestate with or without 1:1 (v:v) seed digestate (S) from AD2 d102 SWP/BO. Reactors were sampled at the start (00), day 40 and day 80 of the test. Half the reactors were supplemented with 10 g/L COD bio-oil (B) from softwood pellets (SWP/BO). The key below the plot represents the top 10 genera from top to bottom in colour with all other sequences in greyscale. Taxonomy was assigned against the SILVA 128 reference database.

The top three contributing genera *Defluviitoga, Cloacimonetes* and an uncultured representative of the *Lentimicrobiaceae,* show an increase in abundance both immediately before and after the significant production of biogas for each fresh digestate reactor set.

Of note is the similarity between the fresh digestate-only controls and FSB reactors whose day 40 replicate samples have abundance profiles that show an average standard deviation of 0.19% ± 0.36% between the genera that contribute ≥ 0.5% of the total sequences. Additionally, FSB reactors by day 20 had not produced a significant amount of biogas, whereas the fresh controls had, yet both the archaeal and bacterial abundance profiles show a high similarity. A similar pattern is observed in the autoclaved control and AB digestates with an increased abundance of the top three contributing genera over time. This is despite any biogas production from these reactors but observed increases in organic acid concentration. The abundances of both *Defluviitoga* and *Cloacimonetes* in the autoclaved digestates are generally reduced, particularly in AS and ASB reactors that did produce biogas.

The AS and ASB reactors show little variation in their bacterial community between the sampling dates, even with or without the addition of bio-oil. Both conditions see an almost complete domination of the microbial community by one or two genera in their first and second replicates respectively. Regarding the AS reactors, this domination occurs after completion of biogas production however, in ASB reactors the failure occurs before biogas production and coincides with the significantly reduced biogas output of the replicate as seen in Chapter 5. These reactors are dominated by two genetically distinct, enigmatic members of the *Family XI,* of the order *Clostridiales*, of which there are no cultured representatives and are denoted on the plots by the black and dark grey bars. Of note is that the respective archaeal communities show a general loss of *Methanosaeta* and an increase in *Methanosarcina* after these time points.

The Bray-Curtis similarity matrices for the total archaeal and bacterial abundances are available electronically. The average Bray-Curtis similarity of all the replicate

reactor communities was 71 ± 16.09 and 70.65 ± 23.92 for archaea and bacteria respectively, which is comparable to the inter-replicate variability seen in AD2; however, these reactors still show lower similarity between replicates than AD1 replicates. The average Bray-Curtis similarity for the archaeal communities in fresh digestates is 80.53 ± 9.42, whereas in autoclaved digestates this drops to 61.46 ± 15.94, a significantly higher amount of inter-replicate variation to a 95% confidence (two-sample t-test P = 0.002). Despite the two reactors that were dominated by *Clostridiales* in autoclaved digestates, there is no significant difference in the average Bray-Curtis similarity for the bacterial communities between fresh and autoclaved digestates (with average Bray-Curtis similarities between replicates of 78.78 ± 13.31 and 62.52 ± 29.57 for fresh and autoclaved digestates respectively and a two-sample t-test P = 0.1).

Figure 7.5 shows the total archaeal and bacterial Bray-Curtis similarity matrices plotted on NMDS plots, with samples grouped by date (colour) and digestate (shape). There is little discernible variation between the groups of samples in the archaeal plot with no significant differences observed between samples based on the digestate type or presence of bio-oil or the seed. The only significant difference between the samples is when they are grouped by the date of sampling (PERMANOVA P = 0.004; Pseudo-F = 3.773), and this difference cannot be explained by the sample dispersion (PERMDISP P = 0.312; F = 1.336).

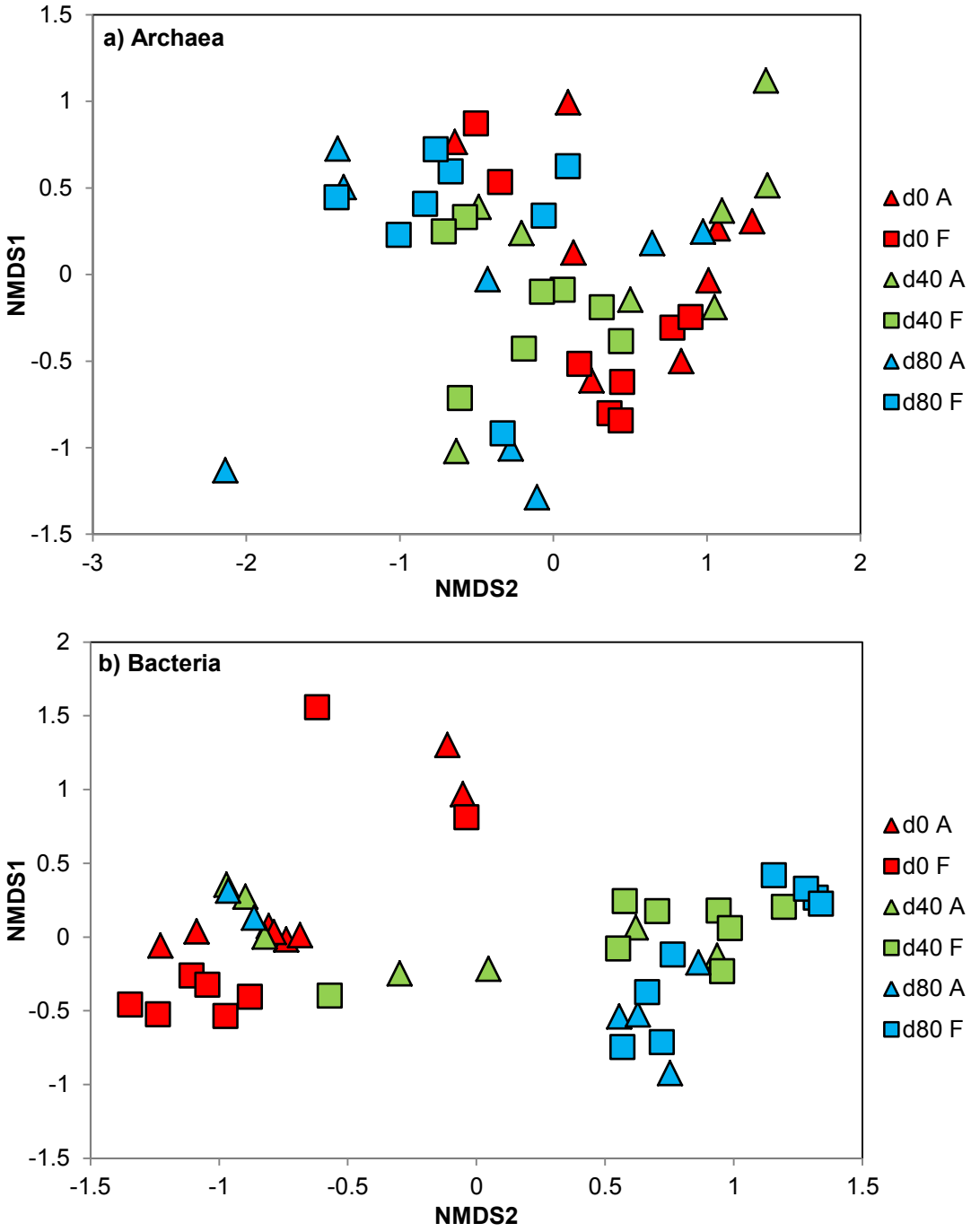

Figure 7.5. 2D NMDS plots generated from the Bray-Curtis similarity matrices for total (a) archaeal and (b) bacterial abundances assigned to 16S rRNA gene sequences from sewage sludge anaerobic digestates. The 20 mL of digestate was composed of either fresh (F) or autoclaved (A) digestate with or without 1:1 (v:v) seed digestate from AD2 d102 SWP/BO. Reactors were sampled at the start (d0), day 40 (d40) and day 80 (d80) of the test.

Half the reactors were supplemented with 10 g/l COD bio-oil from softwood pellets. Presence of seed digestate and bio-oil are not annotated due to no significant differences found between samples based on these variables. The three samples that showed reactor failure (d80AS1, d40ASB2 and d80ASB2) are omitted from the bacterial plot due to the extreme difference in bacterial community composition. 2D stress (a) = 0.13 and (b) = 0.11.

The same is true for the bacterial plot with a significant difference found between sampling date (PERMANOVA P = 0.001; Pseudo-F = 8.718), which also cannot be explained by the sample dispersion (PERMDISP P = 0.903; F = 0.155). This pattern however, can be observed in the plot, with a general transition of samples from the left of the 2D space to the right with time. Unlike the archaeal plot, the bacterial plot does show significant differences between the samples based on either fresh or autoclaved digestate (PERMANOVA P = 0.004; Pseudo-F = 4.579), which cannot be explained by the sample dispersion (PERMDISP P = 0.191; F = 2.019). This difference is difficult to see on the plot; however, is potentially due to the large cluster of autoclaved digestate samples on the left of the 2D space. This cluster consists mostly of day 0 and 40 samples.

7.3 AD4 - Digestate Supplementation Effects on AD/Bio-Oil Reactors

7.3.1 Overview

Variable	Unit	N Ctrl	N BES	NSt	N Si	N Cr	N Ci
Total Biogas	**mL**	59.75 (5.3)	0.75 (1.06)	56 (4.24)	60.25 (3.89)	57 (5.66)	61 (0.71)
Lag Phase	**days**	0	∞	0	0	0	0
CH_4 Content	**% CH_4**	56.4 (0.21)	-	54.88 (1.59)	56.63 (0.25)	54.9 (0.99)	56.53 (0.25)
COD	**% Diff.**	-24.46 (2.48)	+42.6 (0.31)	-26.66 (3.79)	-22.76 (3.1)	-26.66 (0.34)	-25.44 (2.07)
TOC	**% Diff.**	-16.6 (2.68)	+13.42 (2.44)	-19.45 (2.23)	-15.79 (0.98)	-20.63 (0.56)	-19.84 (0.28)
Organic acids	**% Diff.**	-2.79 (4.8)	+133.51 (33.61)	-4.34 (0.84)	-4.93 (2.52)	-6.71 (2.52)	-4.34 (1.68)
pH	**From → to**	7.68 → 8.02 (0.01) → (0.06)	7.66 → 7.45 (0.04) → (0.11)	7.7 → 7.85 (0.01) → (0.01)	7.75 → 7.87 (0.06) → (0.01)	7.78 → 7.86 (0.04) → (0.01)	7.7 → 7.89 (0.01) → (0.07)

Table 7.3. Details of analysed variables between day 0 and day 60 of AD control reactors with 20 mL of digestates plus supplements that were not supplemented with bio-oil (N). Reactors were supplemented with the methanogenic inhibitor: Sodium 2-bromoethanesulfonate (BES), two biochars: Standard biochar (St) and CreChar® (Cr) and pre-incubated versions of the two biochars (Si and Ci). Pre-incubation was achieved by incubating the biochars in digestate for 48 hours anaerobically. The lag phase is the estimated time before significant biogas production is seen from the reactors, of note is that there was no significant production of biogas from BES-supplemented reactors. All conditions were performed in duplicate with each measurement as a mean of the replicates with the standard deviation given in brackets.

Variable	Unit	B Ctrl	B BES	B St	B Si	B Cr	B Ci
Total Biogas	**mL**	54.25 (3.18)	5.75 (2.47)	50 (9.90)	51 (3.54)	54.25 (1.06)	60.75 (3.18)
Lag Phase	**days**	27	∞	27	16	27	15
CH_4 Content	**% CH_4**	62.35 (0)*	-	57.1 (1.38)	58.13 (0.35)	59.2 (0)*	63.2 (0)*
COD	**% Diff.**	-32.52 (1.35)	+20.39 (1.11)	-34.83 (0)	-35.6 (0.36)	-39.98 (1.82)	-37.53 (4.19)
TOC	**% Diff.**	-27.65 (0.91)	+5.55 (0.16)	-29.04 (2.06)	-30.55 (0.71)	-32.96 (1.43)	-29.76 (1.98)
Organic acids	**% Diff.**	-40.64 (9.06)	+46.03 (2.89)	-51.2 (1.36)	-53.25 (0.17)	-56.01 (0)	-54.57 (4.42)
pH	**From → to**	7.36 → 7.83 (0.03) → (0.01)	7.43 → 7.14 (0.01) → (0.07)	7.37 → 7.65 (0.01) → (0.05)	7.47 → 7.79 (0.01) → (0.04)	7.39 → 7.77 (0.07) → (0.1)	7.42 → 7.77 (0.05) → (0.06)

Table 7.4. Details of analysed variables between day 0 and day 60 of AD control reactors with 20 mL of digestates plus supplements with 5 g/L COD bio-oil (B) from softwood pellets (SWP/BO). Reactors were supplemented with the methanogenic inhibitor: Sodium 2-bromoethanesulfonate (BES), two biochars: Standard biochar (St) and CreChar® (Cr) and pre-incubated versions of the two biochars (Si and Ci). Pre-incubation was achieved by incubating the biochars in digestate for 48 hours anaerobically. The lag phase is the estimated time before significant biogas production is seen from the reactors, of note is that was no significant production of biogas from BES-supplemented reactors. All conditions were performed in duplicate with each measurement as a mean of the replicates with the standard deviation given in brackets. *indicates missing methane values for one replicate.

The final AD test built on the idea of using methanogenic inhibition for the accumulation of organic acids as an alternative value-added product from AD systems with the addition of bio-oil. Table 7.3 and 7.4 detail the test variables for non-bio-oil (N) and bio-oil (B) supplemented reactors respectively. Methanogenic inhibition was achieved by the addition of a methanogen-specific inhibitor, Sodium 2-bromoethanesulfonate (BES). Additionally, the test utilised the solid fraction of

biomass pyrolysis, biochar, to investigate its ability to reduce bio-oil toxicity and increase biogas production in AD systems. Two biochars were selected for the experiment with the UKBRC supplying a standard biochar from softwood pellets pyrolysed at 550 °C and Carbogenics supplying their CreChar® pyrolysed from paper cups at 450 °C. Both the biochars were added dry and after a pre-incubation period of 48 hours, followed by gentle washing with deionised water. All the reactor conditions were set up with and without the addition of bio-oil. The addition of biochars did little to increase biogas yield of N reactors and did not contribute to a lessening of the lag time before biogas production in B reactors, unless pre-incubated in digestate. The pre-incubation seemed to have significantly shortened the lag time caused by bio-oil inhibition, particularly for CreChar®-supplemented reactors.

In addition to sequencing the digestate communities, attempts were made to isolate the communities associated with the surfaces of the biochars. Before and after the test, the biochars were gently washed with deionised water, and the washed biochars subjected to the same DNA extraction technique as the digestate. The yield of DNA was expected to be low, due to the small biochar sample sizes and the limited surface area for microbial attachment, and as such, the final day samples were pooled between replicates for DNA extraction. There are therefore two technical replicates for each of the day 0 incubated biochars but only an individual sample for each reactor condition at day 60.

The addition of BES was a massive influx of a pure chemical that could change the digestate chemistry depending on its reactivity with the digestate and bio-oil, additionally the final step of AD was completely inhibited and therefore supplemented reactors began to accumulate organic acids. Biochar addition to AD is also able to change the digestate chemistry in two ways. Firstly chemicals can be directly adsorbed onto the porous biochar surface and thus sequestered, reducing any potential inhibitory effects associated with the chemical. Secondly the biochar surface acts as an excellent adherence point for biofilm-forming microbial species; which have been shown to be more resistant to environmental stresses, thus achieving degradation of more recalcitrant chemicals.

The bio-oil chosen for the experiment was from the lignocellulosic softwood pellets, which has been shown from AD1 and AD2 to be a bio-oil readily degradable in AD. However as the chemical characterisation of the bio-oils used in these experiments has shown, distinct changes occurred to the chemistry of the bio-oil over time as it aged. Additionally, AD4 marked the first AD experiment where the SWP/BO bio-oil-supplemented reactors did not produce a substantially larger volume of biogas compared to control reactors with no bio-oil and as such the remaining COD in the reactors may be too recalcitrant to be efficiently degraded by AD. It is therefore possible that SWP/BO has aged to a point where it is no longer a viable source of additional COD in AD reactors.

Although all the duplicate reactors were sampled for analysis by ESI FT-ICR MS, the high similarity of the chemical data between the replicates justifies the use of a single replicate for the following analyses. Biochar chemistry was not analysed however represents further work that could help explain their effects on the digestates.

7.3.2 Results – Biological Characterisation

Rarefaction of the digestate samples for alpha diversity analysis reduces the total sequences per sample to ~18 000, with a plateau at 1 804 sequences per samples. Using the Shannon index at a sequence depth of 1 804 for the microbial communities in the digestate, reveals no significant differences between the supplements in non-bio-oil control (N) and bio-oil-supplemented (B) reactors when all sampling dates are included (two-sample t-test N $P = 0.488$; B $P = 0.443$). However, a significant difference is observed between N and B reactor samples at this sequencing depth above a 99.9% confidence (two-sample t-test $P = 0.0002$), with B reactors showing a significantly lower average diversity. Table 7.5 shows the average Shannon index across the N and B samples.

d0 Dig	N d20	N d40	N d60	B d20	B d40	B d60
4.49 (0.20)	4.17 (0.34)	4.29 (0.32)	3.97 (0.33)	3.94 (0.16)	3.96 (0.18)	3.61 (0.32)

Table 7.5. Shannon indices at 1 804 sequences from isolated microbial communities from sewage sludge anaerobic digestates without (N) and with (B) 5 g/L COD bio-oils from softwood pellets (SWP/BO). The digestate was sampled at the start (d0 Dig) with reactors sampled at day 20, 40 and 60. All conditions were performed in duplicate with each measurement a mean of the replicates with the standard deviation in brackets.

The standard deviations show clear variation between the samples at each time point, and although the average indices for N samples at day 20, 40 and 60 are not significantly different compared to the day 0 digestate (two-sample t-tests day 20 P = 0.223, day 40 P = 0.411 and day 60 P = 0.05), the bio-oil samples, averaged at each time point, have significantly lower diversity than the day 0 digestate (two-sample t-tests day 20 P = 0.001, day 40 P = 0.003 and day 60 P = 0.003).

A greater sequencing depth was available for the biochar data with the samples rarefied to ~80 000 sequences and the plateau at 7 861 sequences. An opposite pattern is seen with the biochar data, with a slight increase in diversity between the communities on the biochar surfaces at day 0 and at day 60 at the start of the plateau, however, these differences are not significant. Table 7.6 shows the Shannon indices for the day 60 N and B biochars compared to the d0 digestate. Due to only having a single sample for each of the different biochar conditions it is also not possible to calculate an average or significance of the differences between them.

d0 Dig	d60 NSt	d60 NSi	d60 NCr	d60 NCi	d60 BSt	d60 BSi	d60 BCr	d60 BCi
4.58 (0.22)	4.92	5.28	5.48	5.08	5.56	4.96	5.11	4.37

Table 7.6. Shannon indices at 7 861 sequences for microbial communities isolated from biochar surfaces incubated in anaerobic digestates from sewage sludge without (N) and with (B) 5 g/L COD bio-oils from softwood pellets (SWP/BO). The digestate was sampled at the start (d0 Dig), with the biochars recovered and sampled at day 60. Biochars were pooled between duplicate reactors. Two biochars were used: Standard biochar (St) and CreChar® (Cr) with pre-incubated versions of the two biochars (Si and Ci) also utilised. Pre-incubation was achieved by incubating the biochars in digestate for 48 hours anaerobically. Duplicate initial digestate values are as a mean value with the standard deviation in brackets.

Of note is the greater amount of variation between the curves in the B reactors and that the reduction in diversity follows the order of increasing biogas output and reduced lag time before biogas production. No such pattern is observable in the N reactors; however, all these reactors performed similarly in terms of biogas output and lag time. BCi biochar seems to have the lowest diversity of the biochars and is the only one with diversity lower than the starting digestate.

Plots of the archaeal abundances for N and B digestates are shown in Figure 7.6 and 7.7 respectively. Archaea account for an average 0.25% ± 0.13% of the total microbial abundance of the digestate dataset, and some slight trends are observable in total archaeal abundance across reactor conditions. NBe reactors see a marked decrease in their total archaea compared to the N control reactor (0.06% ± 0.04% compared to 0.30% ± 0.09%); however although there is also a reduction in BBe archaeal abundance, it is not as dramatic as its control (0.21% ± 0.06% for BBe compared to 0.28% ± 0.17% for B controls).

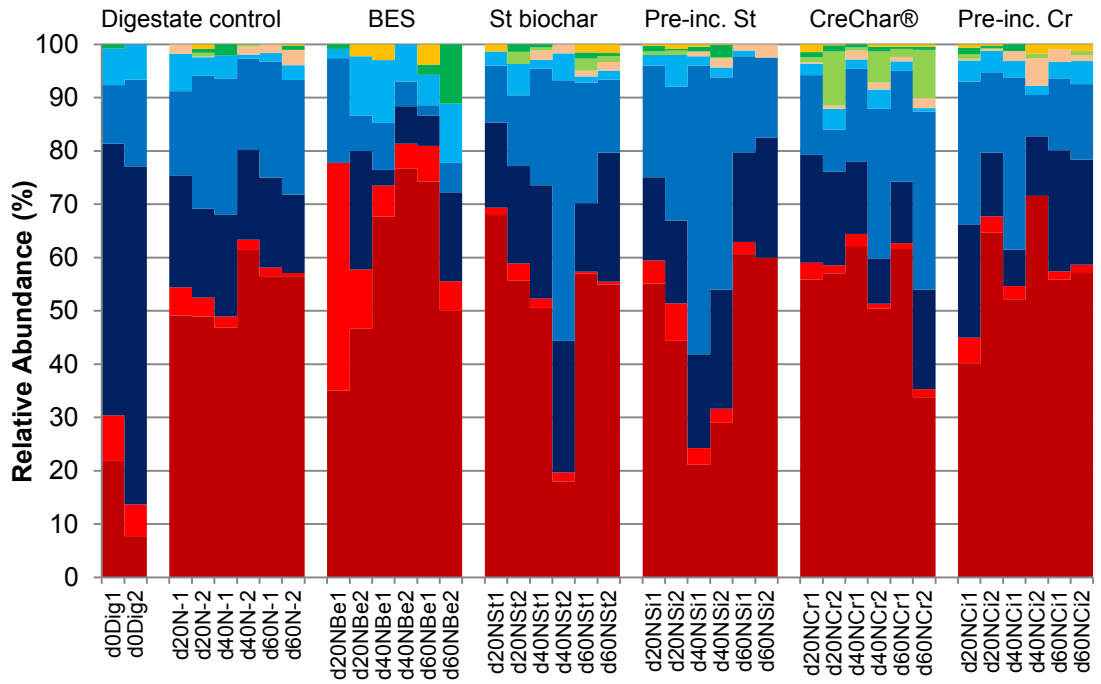

Phylum	Class	Order	Family	Genus
Euryarchaeota	*Methanomicrobia*	*Methanosarcinales*	*Methanosaetaceae*	*Methanosaeta*
Euryarchaeota	*Methanomicrobia*	*Methanosarcinales*	*Methanosarcinaceae*	*Methanosarcina*
Euryarchaeota	*Methanomicrobia*	*Methanomicrobiales*	*Methanomicrobiaceae*	*Methanoculleus*
Euryarchaeota	*Methanobacteria*	*Methanobacteriales*	*Methanobacteriaceae*	*Methanobacterium*
Euryarchaeota	*Thermoplasmata*	*Thermoplasmatales*	*Thermoplasmatales Incertae Sedis*	*Methanomassiliicoccus*
Euryarchaeota	*Thermoplasmata*	*Thermoplasmatales*	*Thermoplasmatales Incertae Sedis*	*Candidatus Methanoplasma*
Euryarchaeota	*Thermoplasmata*	*Thermoplasmatales*	*Thermoplasmatales Incertae Sedis*	*uncultured*
Euryarchaeota	*Methanomicrobia*	*Methanomicrobiales*	*Methanospirillaceae*	*Methanospirillum*
WSA2	*WCHA1-57*	*uncultured*	*uncultured*	*uncultured*

Figure 7.6. Genus level relative abundance plot of 16S rRNA gene sequences assigned to the archaeal community in 20 mL of sewage sludge digestates plus supplements from AD control reactors that were not supplemented with bio-oil (N). Samples were taken at the start (d0), day 20, 40 and 60. Reactors were supplemented with the methanogenic inhibitor: Sodium 2-bromoethanesulfonate (Be), two biochars: Standard char (St) and CreChar® (Cr) and pre-incubated versions of the two biochars (Si and Ci). The key below the plot ranks the genera from their total abundances from top to bottom. Taxonomy was assigned against the SILVA 128 reference database.

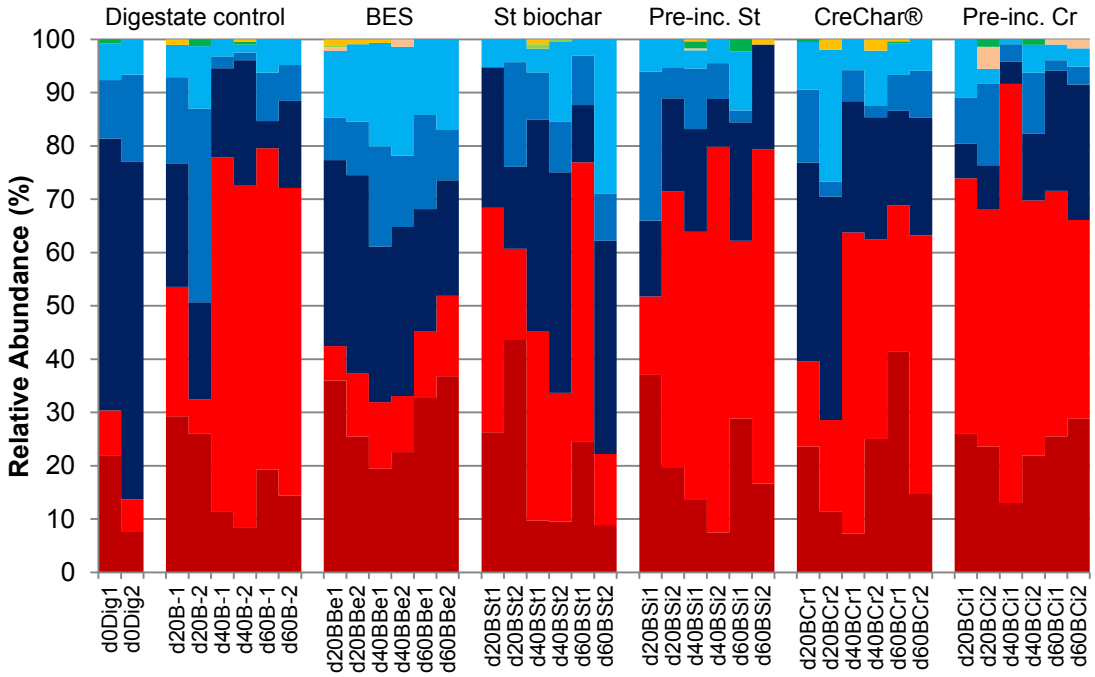

Phylum	Class	Order	Family	Genus
Euryarchaeota	*Methanomicrobia*	*Methanosarcinales*	*Methanosaetaceae*	*Methanosaeta*
Euryarchaeota	*Methanomicrobia*	*Methanosarcinales*	*Methanosarcinaceae*	*Methanosarcina*
Euryarchaeota	*Methanomicrobia*	*Methanomicrobiales*	*Methanomicrobiaceae*	*Methanoculleus*
Euryarchaeota	*Methanobacteria*	*Methanobacteriales*	*Methanobacteriaceae*	*Methanobacterium*
Euryarchaeota	*Thermoplasmata*	*Thermoplasmatales*	*Thermoplasmatales Incertae Sedis*	*Methanomassiliicoccus*
Euryarchaeota	*Thermoplasmata*	*Thermoplasmatales*	*Thermoplasmatales Incertae Sedis*	*Candidatus Methanoplasma*
Euryarchaeota	*Thermoplasmata*	*Thermoplasmatales*	*Thermoplasmatales Incertae Sedis*	*uncultured*
Euryarchaeota	*Methanomicrobia*	*Methanomicrobiales*	*Methanospirillaceae*	*Methanospirillum*
WSA2	*WCHA1-57*	*uncultured*	*uncultured*	*uncultured*

Figure 7.7. Genus level relative abundance plot of 16S rRNA gene sequences assigned to the archaeal community in 20 mL of sewage sludge digestates plus supplements from AD reactors with 5 g/L COD bio-oil (B) from softwood pellets (SWP/BO). Samples were taken at the start (d0), day 20, 40 and 60. Reactors were supplemented with the methanogenic inhibitor: Sodium 2-bromoethanesulfonate (Be), two biochars: Standard char (St) and CreChar® (Cr) and pre-incubated versions of the two biochars (Si and Ci). The key below the plot ranks the genera from their total abundances from top to bottom. Taxonomy was assigned against the SILVA 128 reference database.

Additionally, despite little difference observed in biogas production from N reactors, those supplemented with CreChar® show a significantly higher total archaeal abundance (0.39% ± 0.14%) compared to supplementation with standard biochar (0.23% ± 0.06%) to >99% confidence (two-sample t-test P = 0.002). This significance is not seen in the B reactors (0.23% ± 0.20% for CreChar®-supplemented compared to 0.18% ± 0.08% for standard biochar-supplemented).

Similarly to the previous tests we see the distinctive increase of *Methanosaeta* and loss of *Methanosarcina* from control reactors with no bio-oil. Unlike the previous tests, even though only 5 g/L COD of SWP/BO bio-oil was added, we still see the domination of the B reactors by *Methanosarcina*. It should also be noted that AD4 B reactors generally did not produce more biogas than their respective N reactors, despite the almost doubling of digestate COD.

The N reactors show a great deal of similarity between their archaeal relative abundance profiles which mirrors the similarity of their biogas output curves (Figure 5.14). Despite the inhibition of biogas production by BES, these reactors do show altered archaeal abundance compared to the starting digestate. BES reactors seem to retain a larger population of *Methanosarcina* than the other N reactors and show a reversal of the general increase in *Methanobacterium* and decrease in *Methanomassiliicoccus*, observed in the other N reactors. There is also a relative increase in abundance over time of *Methanosaeta* in the BES reactors.

The archaeal profile of the B reactors looks more similar to the inhibited reactors of AD1 and AD2 that had the addition of AD/BO and MP/BO bio-oils. Although we see a slight increase in *Methanosaeta* compared to day 0 digestates, it is far less than that seen in N reactors. B reactors also see a decreased abundance of *Methanobacterium* and a slight increase in the amount of *Methanomassiliicoccus* as the two most abundant hydrogenotrophic methanogens after *Methanoculleus* which does not show a general pattern of abundance change. This pattern is the opposite of the profiles observed for N reactors.

The bacterial abundance plots for the digestates are shown in Figure 7.8 and 7.9. Immediately noticeable is the loss of *Cloacimonetes* from the bio-oil samples and the N sample with BES. *Lentimicrobiaceae* abundance also shows a distinct difference between the two reactor conditions with a general decrease in N reactors but a relatively stable population in B reactors. There are also more *Gelria* and *Proteiniphilum* in the B reactors and the N BES reactors which also show high total similarity in their relative abundance profiles. Of note is that there is little difference in both bacterial and archaeal abundance between the different biochars or between the incubated and non-incubated-biochars.

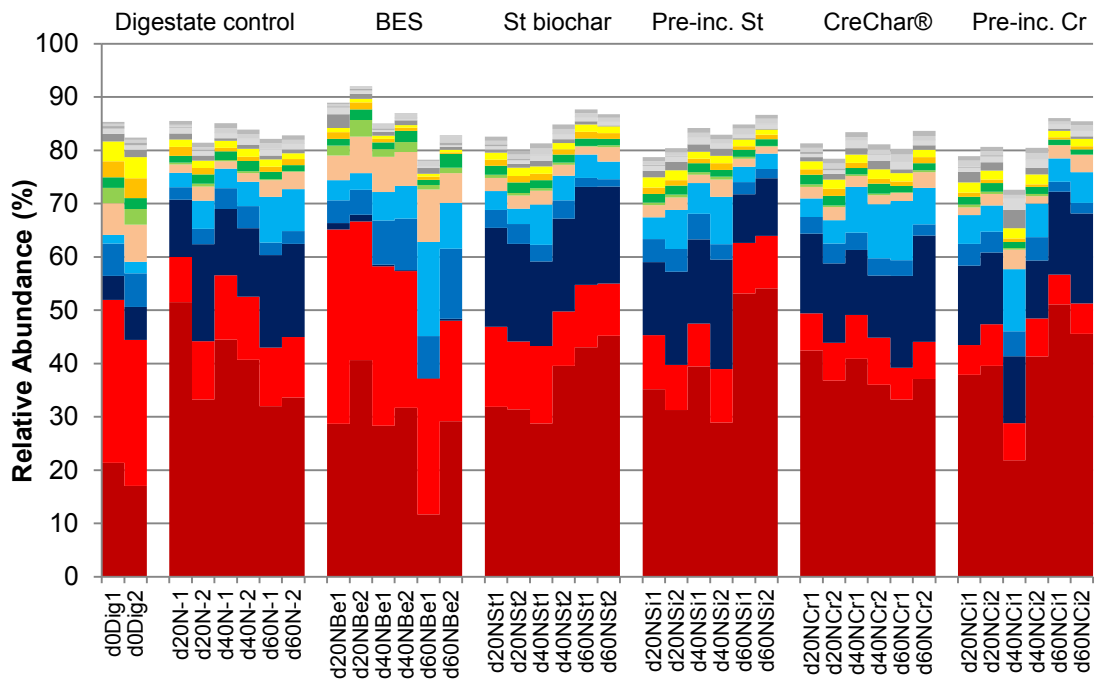

Phylum	Class	Order	Family	Genus
Thermotogae	*Thermotogae*	*Petrotogales*	*Petrotogaceae*	*Defluviitoga*
Bacteroidetes	*Sphingobacteriia*	*Sphingobacteriales*	*Lentimicrobiaceae*	*uncultured*
Cloacimonetes	*W5*	*uncultured*	*uncultured*	*uncultured*
Firmicutes	*Clostridia*	*Thermoanaerobacterales*	*Thermoanaerobacteraceae*	*Gelria*
Chloroflexi	*Anaerolineae*	*Anaerolineales*	*Anaerolineaceae*	*Ornatilinea*
Bacteroidetes	*Bacteroidia*	*Bacteroidales*	*Porphyromonadaceae*	*Proteiniphilum*
Firmicutes	*BSA1B-03*	*uncultured*	*uncultured*	*uncultured*
Firmicutes	*Clostridia*	*Clostridiales*	*Syntrophomonadaceae*	*Syntrophomonas*
Bacteroidetes	*Bacteroidia*	*Bacteroidales*	*Porphyromonadaceae*	*uncultured*
Firmicutes	*Clostridia*	*Clostridiales*	*Caldicoprobacteraceae*	*Caldicoprobacter*

Figure 7.8. Genus level relative abundance plot of 16S rRNA gene sequences that contributed ≥ 0.5% of the total sequences assigned to the bacterial community in 20 mL of sewage sludge digestates plus supplements from AD control reactors that were not supplemented with bio-oil (N). Samples were taken at the start (d0), day 20, 40 and 60. Reactors were supplemented with the methanogenic inhibitor: Sodium 2-bromoethanesulfonate (Be), two biochars: Standard char (St) and CreChar® (Cr) and pre-incubated versions of the two biochars (Si and Ci). The key below the plot ranks the top 10 genera from their total abundances from top to bottom in colour with all other sequences in greyscale. Taxonomy was assigned against the SILVA 128 reference database.

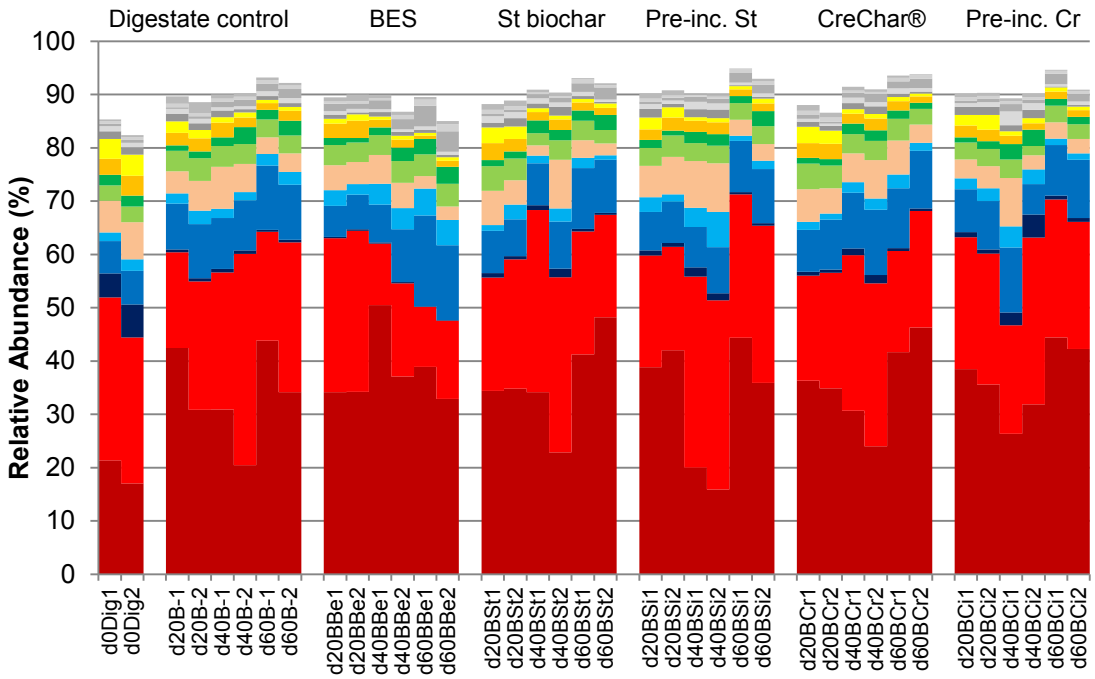

Phylum	Class	Order	Family	Genus
Thermotogae	*Thermotogae*	*Petrotogales*	*Petrotogaceae*	*Defluviitoga*
Bacteroidetes	*Sphingobacteriia*	*Sphingobacteriales*	*Lentimicrobiaceae*	*uncultured*
Cloacimonetes	*W5*	*uncultured*	*uncultured*	*uncultured*
Firmicutes	*Clostridia*	*Thermoanaerobacterales*	*Thermoanaerobacteraceae*	*Gelria*
Chloroflexi	*Anaerolineae*	*Anaerolineales*	*Anaerolineaceae*	*Ornatilinea*
Bacteroidetes	*Bacteroidia*	*Bacteroidales*	*Porphyromonadaceae*	*Proteiniphilum*
Firmicutes	*BSA1B-03*	*uncultured*	*uncultured*	*uncultured*
Firmicutes	*Clostridia*	*Clostridiales*	*Syntrophomonadaceae*	*Syntrophomonas*
Bacteroidetes	*Bacteroidia*	*Bacteroidales*	*Porphyromonadaceae*	*uncultured*
Firmicutes	*Clostridia*	*Clostridiales*	*Caldicoprobacteraceae*	*Caldicoprobacter*

Figure 7.9. Genus level relative abundance plot of 16S rRNA gene sequences that contributed ≥ 0.5% of the total sequences assigned to the bacterial community in 20 mL of sewage sludge digestates plus supplements from AD reactors with 5 g/L COD bio-oil (B) from softwood pellets (SWP/BO). Samples were taken at the start (d0), day 20, 40 and 60. Reactors were supplemented with the methanogenic inhibitor: Sodium 2-bromoethanesulfonate (Be), two biochars: Standard char (St) and CreChar® (Cr) and pre-incubated versions of the two biochars (Si and Ci). The key below the plot ranks the top 10 genera from their total abundances from top to bottom in colour with all other sequences in greyscale. Taxonomy was assigned against the SILVA 128 reference database.

The inclusion of biochar DNA extracts has enabled the specific microorganisms associated with their surfaces to be revealed. Figure 7.10 and 7.11 show the archaeal and bacterial abundance profiles of the biochars after the initial incubation (if pre-incubated) and after the experiment at day 60. It should be noted however that these observations are based on a single sample, and so there is a greater degree of uncertainty during analysis.

Pre-incubation of the biochars immediately sees a large increase in the relative abundance of *Methanosaeta* and *Methanobacterium*, an exception being d0 St2 with a large abundance of *Methanospirillum*. By the end of the test at day 60, biochars from the N reactors are almost completely dominated by *Methanosaeta* and, similarly to the B digestates, the B biochars by *Methanosarcina*.

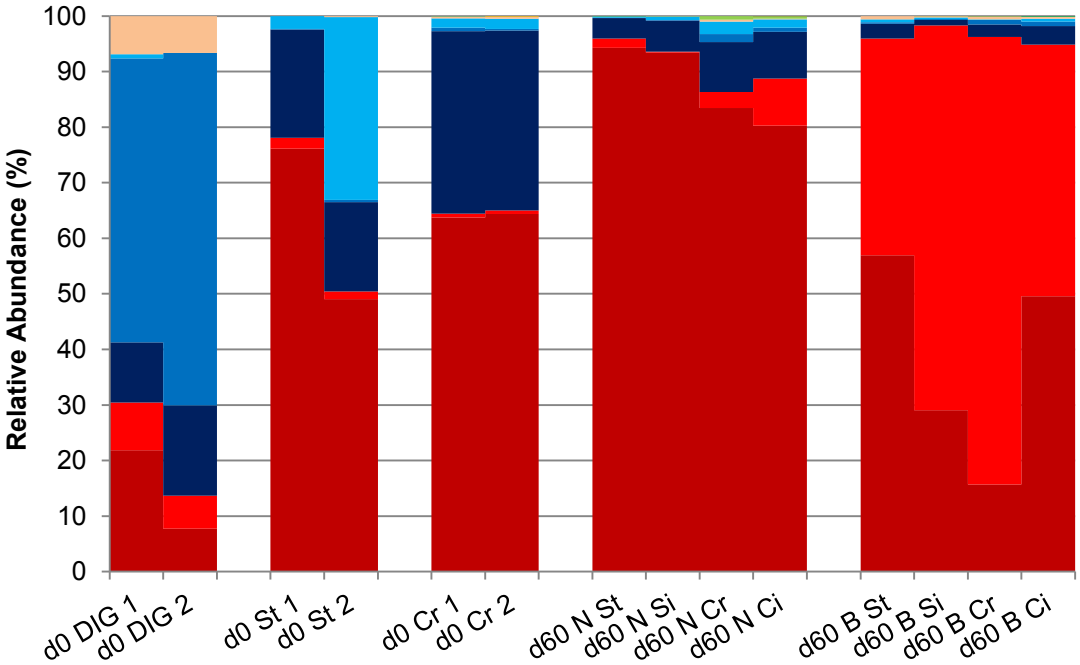

Phylum	Class	Order	Family	Genus
Euryarchaeota	*Methanomicrobia*	*Methanosarcinales*	*Methanosaetaceae*	*Methanosaeta*
Euryarchaeota	*Methanomicrobia*	*Methanosarcinales*	*Methanosarcinaceae*	*Methanosarcina*
Euryarchaeota	*Methanobacteria*	*Methanobacteriales*	*Methanobacteriaceae*	*Methanobacterium*
Euryarchaeota	*Methanomicrobia*	*Methanomicrobiales*	*Methanomicrobiaceae*	*Methanoculleus*
Euryarchaeota	*Methanomicrobia*	*Methanomicrobiales*	*Methanospirillaceae*	*Methanospirillum*
Euryarchaeota	*Thermoplasmata*	*Thermoplasmatales*	*Thermoplasmatales Incertae Sedis*	*Methanomassiliicoccus*
Euryarchaeota	*Thermoplasmata*	*Thermoplasmatales*	*Thermoplasmatales Incertae Sedis*	*uncultured*
WSA2	*WCHA1-57*	*uncultured*	*uncultured*	*uncultured*
Euryarchaeota	*Thermoplasmata*	*Thermoplasmatales*	*Thermoplasmatales Incertae Sedis*	*Candidatus Methanoplasma*

Figure 7.10. Genus level relative abundance plot of 16S rRNA sequences assigned to the Archaeal community on biochar surfaces incubated in anaerobic digestates from sewage sludge without (N) and with 5 g/L COD bio-oil (B) from softwood pellets (SWP/BO). The digestate was sampled at the start (d0 DIG), with the biochars recovered and sampled at day 0 and 60. Day 60 biochars were pooled between duplicate reactors. Two biochars were used: Standard char (St) and CreChar® (Cr) with pre-incubated versions of the two biochars (Si and Ci) also utilised. The key below the plot ranks the genera from their total abundances from top to bottom. Taxonomy was assigned against the SILVA 128 reference database.

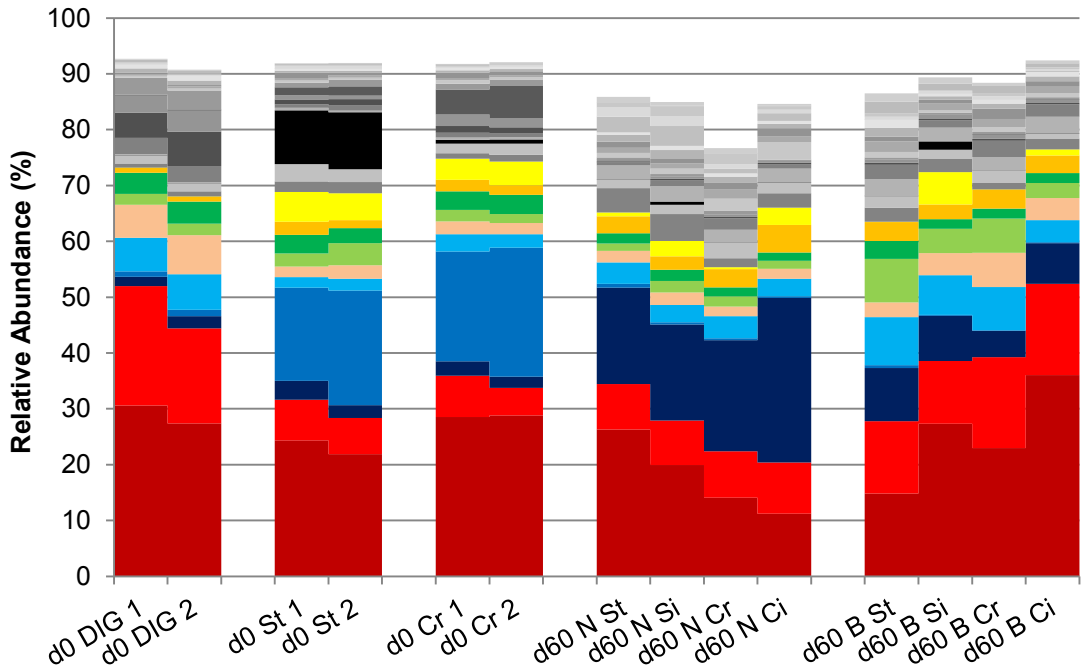

Phylum	Class	Order	Family	Genus
Bacteroidetes	*Sphingobacteriia*	*Sphingobacteriales*	*Lentimicrobiaceae*	*uncultured*
Thermotogae	*Thermotogae*	*Petrotogales*	*Petrotogaceae*	*Defluviitoga*
Chloroflexi	*Anaerolineae*	*Anaerolineales*	*Anaerolineaceae*	*Ornatilinea*
Proteobacteria	*Gammaproteobacteria*	*Pseudomonadales*	*Pseudomonadaceae*	*Pseudomonas*
Firmicutes	*Clostridia*	*Thermoanaerobacterales*	*Thermoanaerobacteraceae*	*Gelria*
Bacteroidetes	*Bacteroidia*	*Bacteroidales*	*Porphyromonadaceae*	*Proteiniphilum*
Firmicutes	*Clostridia*	*Clostridiales*	*Syntrophomonadaceae*	*Syntrophomonas*
Firmicutes	*Clostridia*	*Clostridiales*	*Caldicoprobacteraceae*	*Caldicoprobacter*
Synergistetes	*Synergistia*	*Synergistales*	*Synergistaceae*	*Anaerobaculum*
Firmicutes	*Bacilli*	*Bacillales*	*Paenibacillaceae*	*Desulfuribacillus*

Figure 7.11. Genus level relative abundance plot of 16S rRNA sequences assigned to the bacterial community on biochar surfaces incubated in anaerobic digestates from sewage sludge without (N) and with 5 g/L COD bio-oil (B) from softwood pellets (SWP/BO). The digestate was sampled at the start (d0 DIG), with the biochars recovered and sampled at day 0 and 60. Day 60 biochars were pooled between duplicate reactors. Two biochars were used: Standard char (St) and CreChar® (Cr) with pre-incubated versions of the two biochars (Si and Ci) also utilised. The key below the plot ranks the top 10 genera from their total abundances from top to bottom in colour with all other sequences in greyscale. Taxonomy was assigned against the SILVA 128 reference database.

The bacterial abundances associated with the biochars (Figure 7.11) show a very different pattern from the digestates, with the disappearance of some of the previously seen most abundant genera. The top two most abundant genera, *Defluviitoga* and *Lentimicrobiaceae* are still present however there is a loss of *Cloacimonetes*, which formed a large part of the digestate abundances in all the AD experiments. The abundance of *Lentimicrobiaceae* in N reactors reduces from St to Cr and Si to Ci biochars with the opposite seen in B reactors, where Si- and Ci-supplemented reactors see an increased abundance of this taxon over the biochars that were not pre-incubated.

There are some similarities with the digestate as can be seen by the increased abundances of *Gelria* and *Proteiniphilum* in the B reactors, whereas the N reactors see a large proportion of *Ornatilinea* which is reduced in B reactors. Additionally, *Geobacter* were found in high abundance on the day 0 N standard biochars only (indicated by the black bars) and then are greatly reduced on the day 60 biochars. Pre-incubation of biochars does not seem to confer a particular bacterial abundance profile however we do see an increase in *Desulfuribacillus* on all pre-incubated biochars, irrespective of bio-oil addition.

Patterns of archaeal and bacterial abundances between the reactor conditions are difficult to observe. As such, multivariate analysis of the similarities of the abundance profiles can help in the determination of differences between conditions. Bray-Curtis similarity matrices for the archaeal and bacterial abundances in both the digestate and on the biochar surfaces are available electronically. Inter-replicate variability of the duplicate reactors' digestates for their archaeal and bacterial populations are 79.67 ± 12.07 and 89.16 ± 5.89 respectively, these values are higher than those seen in AD3. There is also no significant difference of the inter-replicate variability between the N and B reactors for either archaea or bacteria.

What we do see is a significant difference between the N and B reactors' digestate community abundance similarities, to the d0 digestates. N reactors show an average archaeal similarity of 48.87 ± 8.86 whereas B reactors have a significantly higher

similarity, to a 95% confidence, at 55.33 ± 14.11 (two-sample t-test P = 0.0013). The same is true for the bacterial community but with a higher confidence of significance, with similarities of 58.38 ± 6.89 and 73.13 ± 7.01 for the N and B reactors respectively (two-sample t-test $P = 2.97\times10^{-25}$). The same pattern is observed for the biochar-associated bacterial communities regarding similarity to the day 0 digestates with those biochars in B reactors showing a significantly higher similarity to day 0 digestates at 68.18 ± 5.97 compared to those in N reactors at 50.13 ± 5.87 (two-sample t-test $P = 2.76\times10^{-5}$). This is not the case for the archaeal communities which show an average similarity between N and B reactors of 25.08 ± 0.55.

NMDS plots of the total archaeal and bacterial abundance profiles of the digestate matrices are shown in Figure 7.12. The N and B reactors see a clear divide in their archaeal and bacterial compositions with N samples (circles) clustering to the left and B samples (triangles) to the right of the 2D space in both plots. The archaeal communities seem to show an equal amount of dissimilarity to the initial digestates irrespective of bio-oil addition however the bacterial communities that were from B reactors show a greater similarity to the starting digestates.

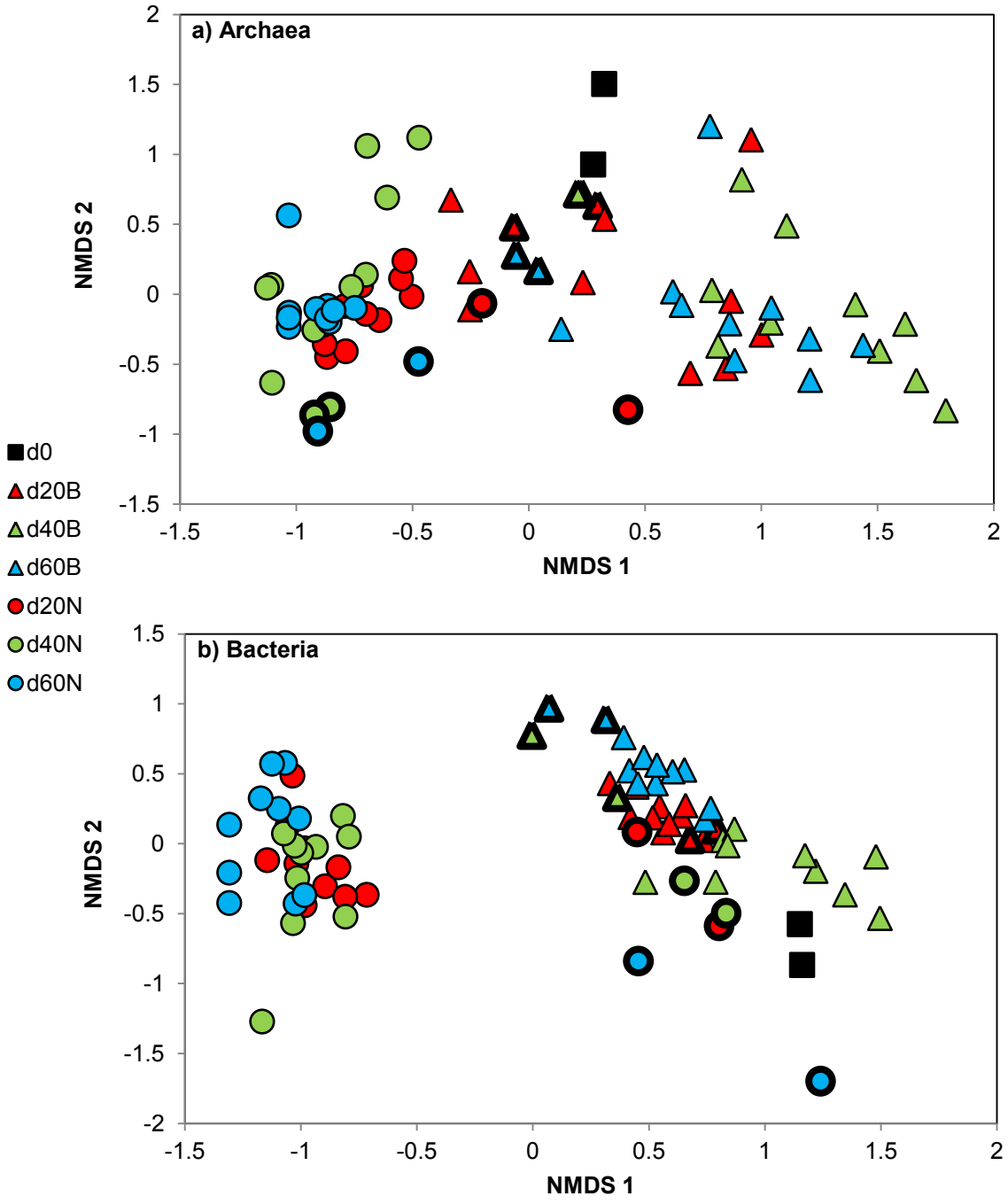

Figure 7.12. 2D NMDS plots generated from the Bray-Curtis similarity matrices for total (a) archaeal and (b) bacterial abundances assigned to 16S rRNA gene sequences from sewage sludge anaerobic digestates without (N/circles) and with (B/triangles) 5 g/L COD bio-oil from softwood pellets (SWP/BO). Samples were taken at the start (d0/black), day 20 (red), 40 (green) and 60 (blue). Reactors were supplemented with the methanogenic

inhibitor, BES, which is indicated by a thick black outline. Two sets of biochars were also used as supplements; however, there is no significant difference observed at this level of analysis and so these factors are not annotated. 2D stress (a) = 0.1 and (b) = 0.1.

In both plots some BES-supplemented reactors do not cluster with their fellow N or B samples. In the archaeal plot there is a collection of B samples that show a greater similarity to N samples and the initial digestate located at the centre of the plot. The bacterial plot shows the opposite effect with a collection of N samples clustering with the B and initial digestate samples. It is found that in both plots the presence of bio-oil causes significant differences among the samples (PERMANOVA archaea P = 0.001; Pseudo-F = 34.924 and bacteria P = 0.001 Pseudo-F = 29.216); however, the significance can be explained by the dispersion of the samples in the archaeal plot (PERMDISP P = 0.001; F = 7.76) and almost by the dispersion in the bacterial (PERMDISP P = 0.054; F = 4.418); however, there is still clearly an effect of composition effect in both. This is likely due to the clusters of the aforementioned BES reactors. No significant differences can be found based on the day of sampling or the reactor supplements.

NMDS plots based on the biochar-associated archaea and bacteria are shown in Figure 7.13. The samples cluster based on the date and the presence of bio-oil, and due to the lack of replicate samples, no meaningful conclusion can be gained based on the type of biochar or whether it was incubated or not. The archaeal communities (Figure 7.13a) on the biochar surfaces at day 60 when subjected to bio-oil show a clear difference from those from N reactors and this difference is found to be significant (PERMANOVA P = 0.001; Pseudo-F = 6.9), however, it can be partly explained by differences in the dispersion of the samples, most likely from the variation seen in the B reactors (PERMDISP P = 0.013; F = 15.76). The difference between the day 0 samples and day 60 samples also shows significance (PERMANOVA P = 0.001; Pseudo-F = 6.9), and cannot be explained by differences in dispersion (PERMDISP P = 0.52; F = 0.582). The N reactor biochars show a high similarity in their archaeal abundance profile to the initial pre-incubated biochars.

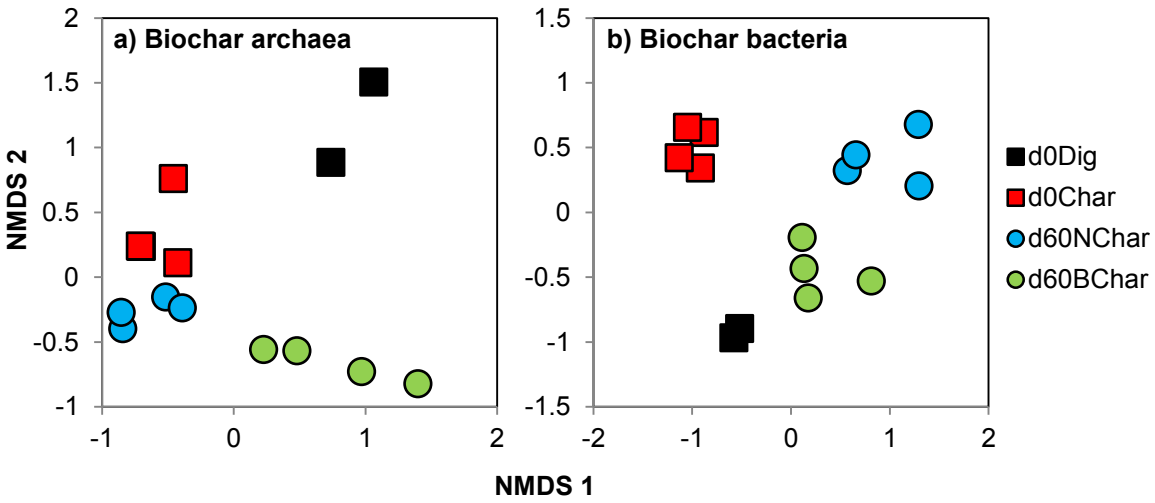

Figure 7.13. 2D NMDS plots generated from the Bray-Curtis similarity matrices for (a) archaeal and (b) bacterial abundances assigned to 16S rRNA gene sequences from biochar surfaces after AD in sewage sludge anaerobic digestates without (N) and with (B) 5 g/L COD bio-oil from softwood pellets (SWP/BO). The digestate was sampled at the start (d0 Dig), with the biochars recovered and sampled at day 0 and 60. Day 60 biochars were pooled between duplicate reactors. Two biochars were used: Standard biochar (St) and CreChar® (Cr) with pre-incubated versions of the two biochars (Si and Ci) also utilised however the lack of significant differences between biochar types excludes their annotation. Pre-incubation was achieved by incubating the biochars in digestate for 48 hours anaerobically. 2D stress (a) = 0.06 and (b) = 0.03.

Such a pattern is also seen in the bacterial plot (Figure 7.13b), however, both N and B biochars show an equal dissimilarity in their bacterial relative abundance profile from the day 0 incubated biochars. Both the presence of bio-oil and the time of sampling cause the significant differences observed in the bacterial plot (PERMANOVA bio-oil P = 0.001; Pseudo-F = 7.986 and date P = 0.002; Pseudo-F = 8.756) neither of which can be explained by dispersion differences (PERMDISP bio-oil P = 0.293; F = 2.29 and date P = 0.857; F = 4.95×10^{-2}). Of note is that the higher similarity of the B reactors' day 60 biochars to the initial digestate compared to biochars from the N reactors can be clearly seen in the plot.

7.3.3 Results – Chemical Characterisation

Similarly to AD1 and AD2, the high amounts of similarity between the compounds that contribute to the digestate render the van Krevelen diagrams of the chemical data difficult to distinguish from one another, and these are therefore available electronically. BES-supplemented reactors however, show dramatically different plots, as can be seen in Figure 7.14.

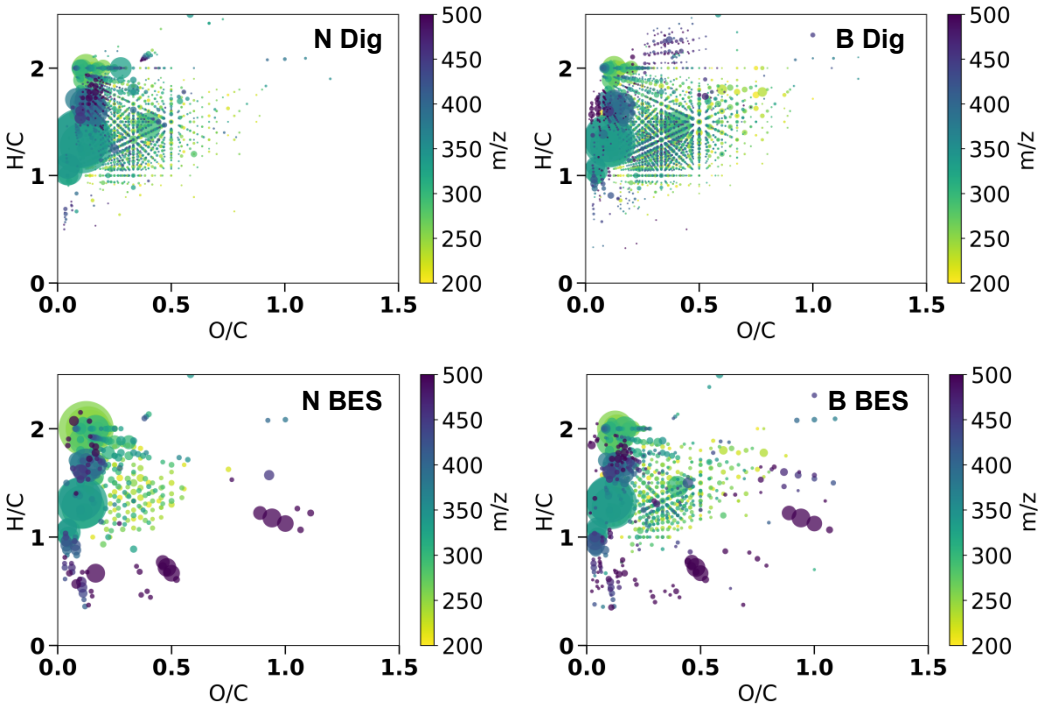

Figure 7.14. van Krevelen diagrams of AD4 day 20 digestates without (N) and with 5 g/L COD bio-oil (B) from softwood pellets (SWP/BO). The plots show the digestate only controls (Dig) at the top and the BES-supplemented reactors (BES) at the bottom to compare the dramatic difference in chemical composition. Formulae were assigned from ESI FT-ICR MS spectra. Plots are further colour-coordinated by the *m/z* of identified compounds with the relative abundance represented by the size of the point.

Although it is difficult to identify changes in chemical composition from the van Krevelen diagrams, the general trend for bio-oil-supplemented reactors to show a greater abundance of lignin and carbohydrate compounds in their van Krevelen diagrams can still be observed. The influx of BES into the supplemented reactors

seems to have drowned out the majority of peaks usually associated with digestate and as such it is difficult to identify the true changes that are occurring in these reactors. For this reason, the BES reactors are excluded from the following heteroatom and multivariate analysis.

The changes in the heteroatom classes for the AD4 digestates are show in Figure 7.15 and Figure 7.16 for the oxygen and nitrogen heteroatom-containing peaks identified by ESI FT-ICR MS. Reactors without the addition of bio-oil displayed similar levels of biogas production, irrespective of biochar addition or pre-incubation, and this is reflected in the heteroatom class data with little to discern the different treatments. There is a general trend for a decrease in abundance of the O_3 – O_4 heteroatom classes by day 60 and a slight increase in the number of higher O_x-containing classes; which is the opposite of what we see in the AD1 and AD2 experiments.

The bio-oil-supplemented reactors also do not show a great deal of difference between them in their oxygen heteroatom abundances. Bio-oil addition increases the number of higher O_x-containing classes and it is possible to see this reduction by day 60 in all the reactors. The digestate control reactor and, to a lesser extent, those reactors supplemented with standard biochar also see an increase in the number of O_1 – O_7-containing classes, whereas those reactors supplemented with CreChar® show a reduction in the number of O_4 – O_6-containing classes.

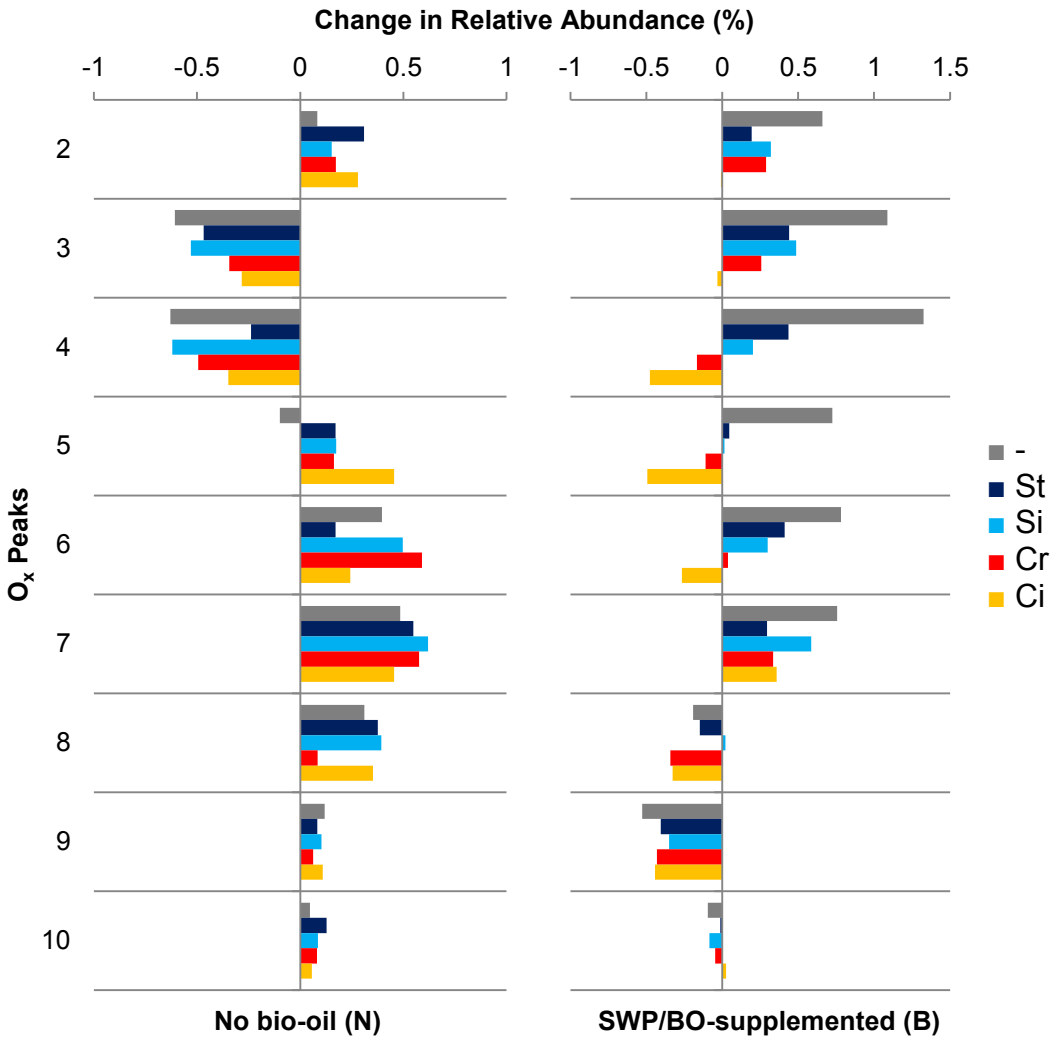

Figure 7.15. Change in oxygen heteroatom relative abundance plots of AD4 digestates without (N) and with (B) 5 g/L COD bio-oils from softwood pellets (SWP/BO). Plots show the difference between digestate sampled at the start and the end of the test. A digestate control (-) contained no supplements with the remaining reactors supplemented with two biochars: Standard char (St) and CreChar® (Cr), and pre-incubated versions of the two biochars (Si and Ci). Pre-incubation was achieved by incubating the biochars in digestate for 48 hours anaerobically. Formulae were assigned to peaks generated from ESI FT-ICR MS spectra.

The nitrogen plots (Figure 7.16) are similar to those seen in previous tests with a reduction in the higher N_x-containing classes across all reactors by the end of the test. Bio-oil addition, again, increases the number of N_4-containing classes, with these reactors seeing the largest decrease in this group of compounds. This is particularly the case for the BCi reactors which show a drop in the abundance of N_4-containing compounds beyond the other biochar treatments. Of note is that even for the NCi reactor, the decrease of N_3-containing compounds reaches its peak by day 20, faster than any other biochar treatment.

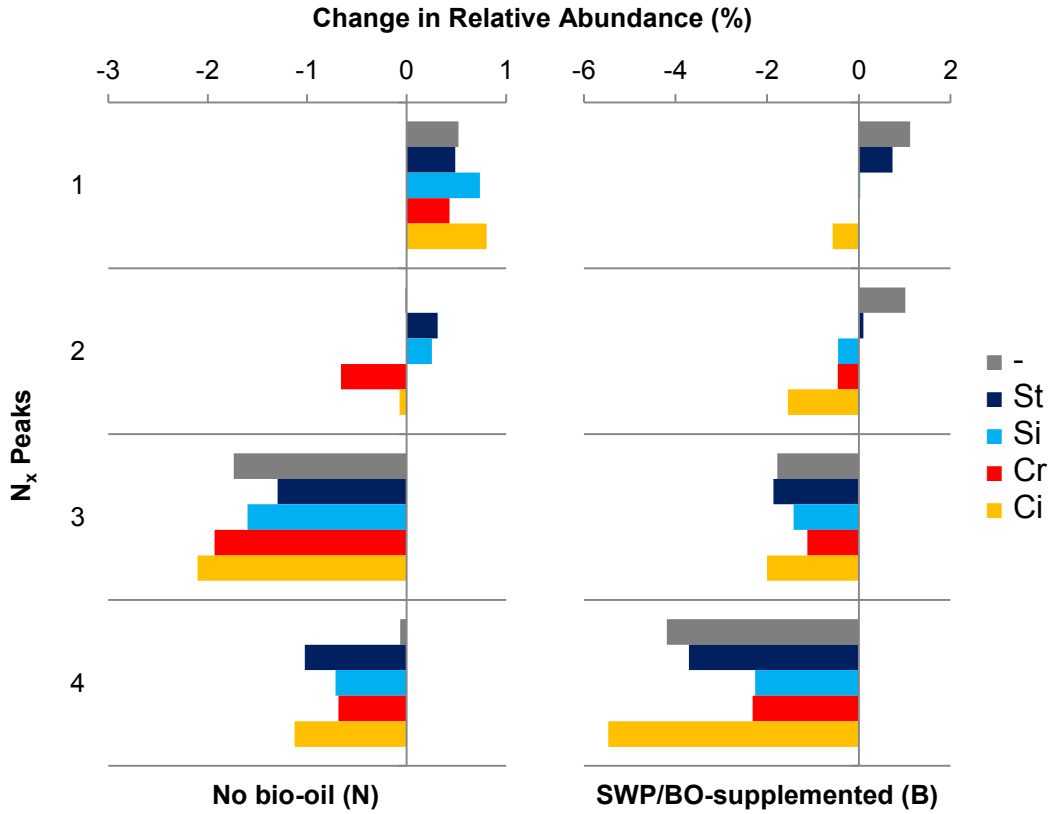

Figure 7.16. Change in nitrogen heteroatom relative abundance plots of AD4 digestates without (N) and with (B) 5 g/L COD bio-oils from softwood pellets (SWP/BO). Plots show the difference between digestate sampled at the start and the end of the test. A digestate control (-) contained no supplements with the remaining reactors supplemented with two biochars: Standard char (St) and CreChar® (Cr), and pre-incubated versions of the two biochars (Si and Ci). Pre-incubation was achieved by incubating the biochars in digestate for 48 hours anaerobically. Formulae were assigned to peaks generated from ESI FT-ICR MS spectra. N_x classes are the sum of all N_xO_y containing classes.

The Bray-Curtis similarity matrix for the total chemical abundance data is available electronically. Overall, the reactors display high similarity to one another despite bio-oil addition with an average Bray-Curtis similarity of 72.92 ± 8.65. However, bio-oil addition does create a similarity between the supplemented reactors that is significantly higher, to above a 99.9% confidence, than the non-bio-oil reactors, at 81.47 ± 5.19 compared to 72.87 ± 9.22 (two-sample t-test $P = 4.43 \times 10^{-16}$). In both the N and B reactors, those that were supplemented with Ci show the greatest dissimilarity from their day 0 digestates with an average similarity of 64.07 ± 9.68 compared to 77.66 ± 11.28 for N control reactors and 73.62 ± 2.4 compared to 75.07 ± 4.26 for B control reactors, these differences however are not significant.

NMDS plots of the similarity matrix for the identified peaks from the digestate chemical analysis are shown in Figure 7.17, with the dataset split by bio-oil addition, as the inclusion of both sets of data creates two clearly defined clusters that are difficult to analyse further. Neither N nor B reactors show clear clustering of the biochar supplements and no significant differences are observed between the type of biochar used (PERMANOVA N P = 0.448; Pseudo-F = 1.023 and B P = 0.872; Pseudo-F = 0.872).

It is possible to see the clusters for day 20 and day 60 samples in the non-bio-oil reactors, however, the day 40 samples are more dispersed. This is in contrast to the bio-oil supplemented reactors which also show two clear clusters for day 20 and day 40 with the day 60 reactors more dispersed. Significant differences are observed between the dates of the sampling (PERMANOVA N P = 0.004; Pseudo-F = 3.072 and B P = 0.001; Pseudo-F = 3.132), neither of which can be explained by differences in dispersion (PERMDISP N P = 0.051; F= 6.803 and B P = 0.16; F = 4.83).

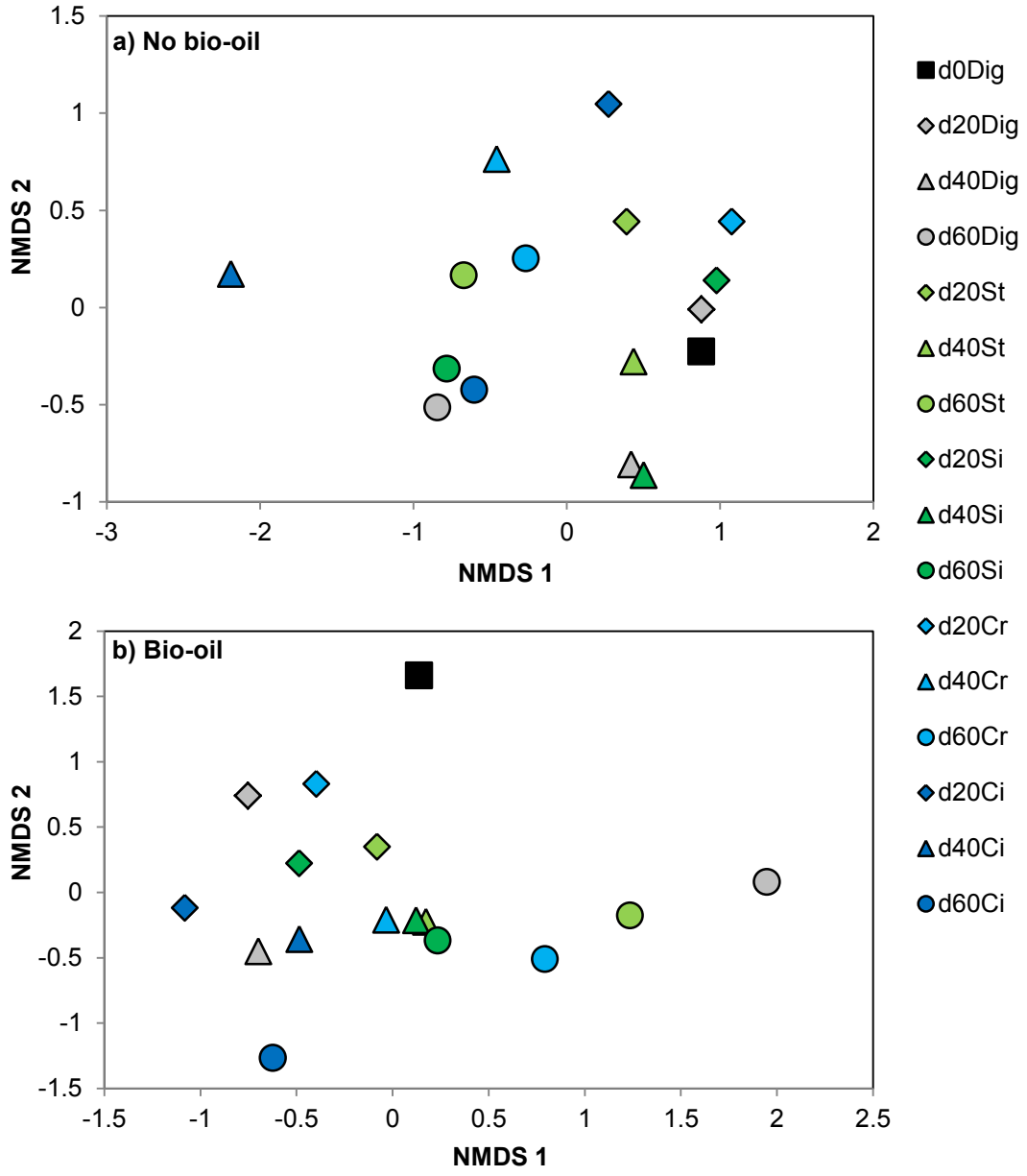

Figure 7.17. 2D NMDS plots generated from the Bray-Curtis similarity matrices for chemical formula assigned to ESI FT-ICR MS peaks from sewage sludge anaerobic digestates (a) with and (b) without the addition of 5 g/L COD bio-oil from softwood pellets (SWP). Samples were taken at the start (d0/black), day 20 (diamond), 40 (triangle) and 60 (circle). Reactors were as controls with no supplements (Dig/grey) or supplemented one of two biochars: Standard biochar (St/green) and CreChar® (Cr/blue) and pre-incubated versions of the two biochars (Si/dark green and Ci/dark blue). 2D stress 2D stress (a) = 0.05 and (b) = 0.07.

7.3.4 Relatedness

By matching the biological data to the chemical it is possible to see how well the patterns observed between them align. The similarity of the two data sets using a Spearman's rank correlation coefficient, without the addition of BES reactors, reveals a similarity of 0.391 between the two matrices to a 99% confidence. This shows that both data sets have a ~40% agreement in the patterns observed in the data. This figure is lower than that seen in AD1 and similar to that observed in AD2 despite a reduced concentration of bio-oil.

7.4 Discussion

AD3 demonstrated that autoclaving digestate was able to inhibit methanogenesis and retain the hydrolysis potential of AD reactors supplemented with bio-oil for the accumulation of VFAs as a more valuable product from AD, which although successfully demonstrated, still showed a reduced accumulation rate due to the inhibitory effect of bio-oil. Although the digestate chemistry was not analysed, the most abundant microbial genera were similar to those observed in AD1 and AD2. However, the addition of bio-oil to fresh digestate did not see the increase in *Cloacimonetes* seen in AD1 and AD2, which only increased in abundance with the addition of seed digestate from AD2. The differences observed between these tests suggested that the digestate or bio-oil had aged to a point where the degradation potential of SWP/BO by AD, was lowered. The appearance of *Pseudomonas,* which are generally aerobic, in the starting digestates could certainly be a response to the increased time of storage for the digestate.

Additionally, the inhibition of bio-oil-supplemented reactors with the seed digestate was not characterised by a specific difference in the highest contributing taxa of the microbial community when compared to control reactors without bio-oil, which showed no sign of inhibition. Thus, it is hypothesised that the most abundant microbial groups identified in the digestate are not the microorganisms responsible for the degradation of the inhibitory components of bio-oil. Instead, the task of overcoming bio-oil inhibition falls on the rarer taxa which can stall an AD reactor of

biogas production until they have completed the detoxification of the bio-oil. Alternatively, due to the majority of the AD tests requiring a reinoculation of digestate, it could be that the immediate toxicity of bio-oil is so great that it kills a significant proportion of the microbial community upon addition, which simply requires a boost in overall microbial cell number to overcome inhibition. This represents future work that can be performed on bio-oil addition to AD. Quantitative PCR (qPCR) of the 16S rRNA gene for digestates before and after the addition of bio-oil would help to estimate the number of gene copies as a proxy for microbial cell number so that bio-oil toxicity can be analysed.

The addition of seed digestate did rescue the methanogenic potential in autoclaved digestate fairly rapidly; however, it did not endow reactors with an increased ability to overcome bio-oil inhibition, despite having come from reactors that had successfully produced biogas from the same bio-oil. Additionally, although the seed digestate showed little variation in its microbial population over time, the mix of autoclaved and seed digestate saw two reactors become dominated by *Clostridiales* which negatively impacted biogas production. Indeed, the lack of variation in the reactors over time from the addition of seed digestate to autoclaved is unexpected. It could be hypothesised that the seed digestate community would diverge upon colonising the autoclaved digestate, which would have been severely disrupted from the treatment; however, the community remains similar throughout. As such it could indicate that the autoclaving procedure causes the release of some mild inhibitory compounds that limit the divergence of the seed community or that the familiarity of the environment causes the communities instead to converge.

Of interest is the microbial dynamics of the autoclaved digestates which were sterilised before use. No biogas was produced from reactors with autoclaved digestate that did not have the seed community; however, despite the heat and pressure treatment of autoclaving we see bacterial and archaeal DNA signatures in unseeded autoclaved digestates. Several genera of *Firmicutes* are present in the digestates, species of which are capable of forming endospores in life-threatening conditions and can survive a variety of stresses (Angert, Hutchison and Miller,

2014). This does not explain the presence of other bacterial phyla and the archaeal DNA that amplified during sequencing and it is important to note that the amplified sequences only give the abundances of specific sequences relative to the total amplified sample. Either the sterilisation procedure was incomplete or it is likely that extracted DNA was from either dead or inactive cells. Further work using qPCR would help to quantify the cell number between the autoclaved and fresh digestates and help estimate differences in abundance of microorganisms between treatments.

AD4 also demonstrated the ability to inhibit methanogenesis for VFA accumulation however did not see as much of an inhibitory effect on the accumulation of organic acids, presumably due to the targeted inhibition of methanogens as opposed to the broad spectrum inhibition by autoclaving in AD3. The test also investigated the addition of biochar to AD reactors and found that although the addition of two types of biochar had no significant effect on uninhibited or bio-oil-inhibited digestates, the addition of pre-incubated biochars significantly reduced the lag time before methanogenesis in bio-oil-inhibited reactors, particularly using CreChar®.

The biochars were found to be almost exclusively dominated by acetoclastic-capable methanogens and showed an increased diversity of bacterial species over that found in the digestate. Although an important substrate for acetoclastic methanogens, the biochar surfaces do not confer immunity to the toxic effect of bio-oil addition as they still see the now-distinctive reduction of *Methanosaeta* and increase in *Methanosarcina*. DIET-capable microorganisms were only identified on standard biochar after the initial pre-incubation and were reduced in abundance by the end of the test on biochar surfaces, indicating either a decreased necessity for DIET or a lack of understanding of other DIET-capable microorganisms. There were no significant changes observed in the microbial communities with pre-incubation of biochar surfaces and so it can be hypothesised that the addition of pre-incubated biochar supplies digestates with a stable initial community that is less affected by bio-oil inhibition and can therefore overcome the toxicity to begin methanogenesis faster than when it is added dry. This is encouraging for the prospect of bioaugmentation, where communities or single species that are chosen for their

ability to perform metabolic activities of interest, could be added to pre-existing microbial communities as biochar-bound biofilms.

There were similarities between all the tests that suggested some processes that were common to the degradation of bio-oil by AD; however, it is important to note that these conclusions are based solely on the use of a select group of bio-oils and a single digestate from a wastewater treatment plant. Different results would be expected from different inoculum and supplement sources. The most striking microbial pattern was the increased abundance of the acetoclastic methanogen, *Methanosaeta,* and an almost total loss of *Methanosarcina* in optimised reactors and the opposite in inhibited reactors where the methanogenic generalist, *Methanosarcina*, becomes dominant. Hydrogenotrophic methanogens did not show such an obvious pattern as each test saw different combinations of these microorganisms however in optimised reactors the ratio of acetoclastic and hydrogenotrophic methanogens was approximately equal.

The alpha diversity of the reactors also always showed a steady decrease in diversity with time, suggesting adaptation of the microbial population to a more efficient community. Which should be noted as potentially only being possible in such contained systems, where there is a lack of immigration of new microbial species. This decrease was also always stalled by the addition of bio-oil or by the inhibition of methanogenesis. Thus it can be hypothesised that either reactors with a high level of environmental stress require a greater diversity of microorganisms to continue AD processes or that the eventual decrease in diversity is inhibited by environmental stress. Coupled with this, the uninhibited reactors predominantly showed a greater degree of microbial variation with time compared to that seen in the inhibited reactors which again, seemed stalled in their ability to reach a similar level of adaptation.

Although the biochar microbial communities showed a greater alpha diversity than the starting digestate, there was still a reduction in diversity over time with pre-incubated CreChar® the only biochar surface to exhibit a diversity lower than the

starting digestate by the end of the test. This could indicate that, similarly to the digestate, a reduced diversity is a sign of optimisation of a community and that pre-incubation of biochar surfaces allows for a more rapid optimisation. Alternatively, we could be seeing a reduction in diversity due to a reduction in available substrates by day 60, as these reactors would have exhausted the available substrates more rapidly. If that is the case, then it is possible pre-incubation of CreChar® allows for a more rapid and efficient utilisation of available resources in AD. Although the biochar surfaces show a slight increase in alpha diversity compared to the digestates, this is a comparison between two different datasets with different sequencing depths, and as such, have incomparable Shannon indices.

The digestate chemistry was similar throughout the experiment as a general characterisation was performed as opposed to specific compounds being investigated. The large amount of compounds in the digestate made observations of the changes in the added bio-oil difficult to observe; however, multivariate analysis clearly identified common changes between reactor conditions that were relatable to changes in the biology. All the digestates showed the characteristic van Krevelen plots of increased amounts of lignin, lipids and proteins with the addition of bio-oil and a similar reduction of higher heteroatom states for both oxygen- and nitrogen-containing compounds, indicating successful reduction. There were however, definitive differences in the digestate chemistry between tests indicating ageing of the digestate, bio-oil or both. Particularly with the SWP/BO bio-oil, its inability to produce biogas volumes comparable with earlier tests certainly confirms the continued reactively of this bio-oil and suggests an increase in its recalcitrance. This has important implications for its use as a feedstock for AD.

CHAPTER 8: DISCUSSION

8.1 Overview

Bio-oil is a particularly difficult product to utilise due its highly complex chemistry, instability and pronounced toxicity to microorganisms. The presence of inhibitory phenols, furans, organic acids and its general extremes of pH, make microbial utilisation of the available carbon in the bio-oil extremely challenging. Indeed, many of the inhibitory compounds that are common to bio-oils have as-of-yet unknown methods of inhibition and are thought to act synergistically (Zaldivar, Martinez and Ingram, 1999). The difficulty of narrowing down the precise inhibitory pathways that makes bio-oil so potent, makes using microbial consortia more attractive, due to communities having a larger range of metabolic abilities that could potentially degrade the inhibitory compounds

However, as we have seen from this project, microbial communities still see inhibition from bio-oil and care must be taken to ensure that the bio-oil is diluted to an extent that it does not completely inhibit microbial degradation. It is possible to pre-treat bio-oil, for example by extracting fermentable sugars using solvent extraction techniques or adsorbing inhibitors to activated charcoal; however, every additional pre-treatment step incurs significant expense and as such, finding a direct utilisation of bio-oil would be of enormous benefit as interest in pyrolysis increases.

8.1.1 Bio-oil Chemistry

The bio-oils used in this study were from three different feedstocks: the lignocellulosic softwood pellets (SWP/BO) and the lignin-limited anaerobic digestate (AD/BO) and *M. pyrifera* (MP/BO). Analysis by Fourier transform ion cyclotron resonance mass spectrometry (FT-ICR MS) revealed a high degree of similarity between AD/BO and MP/BO bio-oils whose peaks were characterised as having a high proportion of lipids and proteins and high nitrogen content. These abundances were likely a result of the high amounts of these compounds in the feedstocks. Gas chromatography (GC) MS data revealed a high concentration of short chain fatty

acids in the AD/BO bio-oil but no such abundance in the MP/BO, thus it is likely the lipids observed in the van Krevelen diagrams for MP/BO, which also showed greater mass, belonged to long chain fatty acids. Conversely, SWP/BO bio-oil was characterised by a high proportion of lignin and carbohydrates and very low nitrogen content. It also contained the highest proportion of phenols and furans, known microbial inhibitors.

The characterisation of each of the bio-oils and their degradability as seen in Chapter 5 shows that despite the higher concentration of the known microbial inhibitors, phenols and furans, in SWP/BO, its inclusion into AD reactors saw the greatest promise. In both AD1 and AD2 the lag phase before significant biogas production was shorter than for the other bio-oils and the added COD was reduced to close to control levels by the end of the test. The major difference between these bio-oils was the higher proportion of nitrogen-containing compounds and as such it can be hypothesised that ammonia inhibition is the major barrier to successful bio-oil degradation. The fact that the pyrolysis of softwood pellets generated bio-oil of greater volume and greater COD than the other feedstocks further supports its preferential use as a potential AD supplement.

That said, AD/BO bio-oil did eventually produce more biogas than control reactors and SWP/BO bio-oil-supplemented reactors, in addition to an increased methane concentration. Thus, properly administered, potentially in reduced COD increments, anaerobic digestate could still prove a useful source of bio-oil for AD. Particularly on-site, if both technologies were available, as this would form a closed system of waste valorisation. The same cannot be said for the use of *M. pyrifera* as a feedstock for bio-oils for AD, which caused significant inhibition to AD reactors and little observed reduction in digestate COD. Although this is only a single macroalgae feedstock, macroalgae are characterised as containing a high proportion of nitrogenous compounds and it is therefore likely that similar problems will be encountered irrespective of algal species.

8.1.2 Bio-oil Degradation

For this project, both the aerobic and anaerobic utilisation of bio-oil was investigated for its conversion to value-added products. The main obstacle encountered in the aerobic degradation of bio-oil was its final conversion to a valuable product. Microbial communities isolated from natural environments were found to contain a diversity of microorganisms wide enough that they could utilise the bio-oil as the sole carbon source, in low COD concentrations. However, the question then remains of what to do with a depleted liquid medium and microbial biomass.

Further work would be required to ascertain which compounds were being utilised by the community and which were non-degradable. The communities seemed to reach a plateau of cellular growth, presumably due to the depletion of useable carbon; however, it is unknown how much of the bio-oil COD was utilised and whether there remains a persistent fraction that would cause complications in the future use of the medium. Indeed the medium used was not solely composed of bio-oil. M9 minimal medium requires several salt solutions which would have to be supplied if there were to be upscaling of aerobic cultures, and the same would be true for other potential growth media; which adds further cost to the process. Additionally, either disposal or reuse of the medium would be required and of the microbial biomass. Due to the nature of aerobic mixed microbial communities, there is no common end-product as there is in AD, and therefore guiding an aerobic community towards the production of a particular compound is extremely challenging. It is plausible that the initial microbial utilisation of the bio-oil medium has degraded the majority of inhibitors to the point it is no longer inhibitory, or that this could be reached with the right bioaugmentation strategy. Both the medium and biomass could potentially be pasteurised and then further used by monocultures for, as an example, ethanol production. But again, this represents additional steps in the conversion of bio-oil to a value-added product that AD does not require. As such the addition of bio-oil to aerobic mixed cultures is not recommended over the use of AD, due to the numerous benefits AD provides.

8.1.3 AD of Bio-oil

This project saw the successful use of AD for the conversion of bio-oil to biogas. In addition to bio-oil made from a lignocellulosic feedstock being more easily degraded by AD, AD1 and AD2 showed that increasing the concentration of bio-oil in AD reactors can cause significant changes in the digestate chemistry and biology even after the majority of the bio-oil has been degraded. This shows that the application of bio-oil in AD is limited, and that care must be taken when dosing a reactor, with bio-oil of a COD low enough that it does not cause permanent negative impacts on the digestate microbial community.

This leads to another finding of the project, in that the bio-oil became more difficult to degrade over time. AD3 was set up with bio-oil and digestate that were made or acquired ~150 days prior to the test and kept at 4 °C for the duration. This test saw a reduced methane yield from the addition of SWP/BO to digestate; however, a significantly larger volume of biogas was eventually produced from bio-oil supplemented reactors than controls with no bio-oil, as was seen in AD1 and AD2. This was not the case for AD4, where bio-oil supplemented reactors produced an equal amount of biogas to the non-bio-oil controls. AD4 was set up with a new sample of digestate that had not been in storage and showed a high level of activity by not requiring reinoculation of digestate to overcome bio-oil toxicity. The bio-oil was ~250 days old by this point and so it is likely that it had aged to a point where the majority of COD was locked into recalcitrant compounds that would either, not be degraded by AD, or would take a significantly longer period of time. This could also explain why, throughout the AD experiments, there was a general decrease in the methane yield of the reactors.

Bio-oil ageing proceeds faster at higher temperatures and has been found to be caused by the pyrolytic lignin, where some phenol compounds continue to react and polymerise to form higher molecular weight compounds. It can therefore be hypothesised that these larger phenolic compounds are resistant to the microbial species responsible for AD and were bio-oil to be used as an AD supplement for

increased biogas production, it would either need to be used immediately or frozen (Alsbou and Helleur, 2014).

Also of note regarding the bio-oil choice for AD, is the chosen temperature of pyrolysis, which can have a huge impact on the chemical properties of both the bio-oil and the biochar (Garcia-Perez *et al*., 2008). It has already been reported that bio-oils from higher temperature pyrolysis are more difficult to anaerobically digest (Hübner and Mumme, 2015) and thus a low pyrolysis temperature of 350 °C was chosen for this project to maximise the chances of successful degradation. However, a low pyrolysis temperature generally translates as less of the biomass being converted to condensable gases, due to the evaporation limits of different compounds. Thus, bio-oil produced using a higher temperature of pyrolysis contains a greater variety of compounds which presumably make it more difficult to degrade. Therefore bio-oil production for inclusion into AD would generate low pyrolysis-temperature biochars which still contain those compounds that were not vaporised, potentially impacting on its range of uses downstream.

The inhibition of methanogenesis was explored in AD3 and AD4; however, the autoclaving process in AD3 caused reactors with the addition of a seed community to fail, in two reactors, severely impacting on their ability to produces biogas. This was not observed in regular digestate and so indicates an unstable microbial community. AD4 had a more targeted approach to methanogenesis inhibition, and as such, digestates with bio-oil saw an increase in organic acid concentrations similar to bio-oil supplemented reactors. This was not observed in AD3, where the production of organic acids was also inhibited in bio-oil-supplemented reactors with autoclaved digestate. Thus, the targeted inhibition of methanogenesis would be preferable to autoclaving if there was continued interest in the accumulation of volatile fatty acids (VFAs) in AD reactors with bio-oil addition.

Biochar addition to AD has been reported to increase biogas yield and methane concentration (Cai *et al*., 2016; Meyer-Kohlstock *et al*., 2016); however, this was not observed in AD4 with the addition of either standard biochar from softwood pellets

or CreChar® to non-bio-oil-supplemented reactors. However, the addition of pre-incubated biochars significantly reduced the lag phase before biogas production in reactors supplemented with bio-oil. As previously mentioned, the digestate was recently acquired for the test and showed high microbial activity, and so it could be that the digestates without bio-oil addition were already producing biogas at a rate that biochar addition could not make a significant impact on. However, even when the reactors were inhibited with the addition of bio-oil, the inclusion of biochar also does not show any effect on biogas production on its own. Only when the biochars were pre-incubated do we see the reduction in the lag phase before biogas production. This is, however, a single test with a single digestate source and only two biochars tested, and therefore further work will be required to ascertain the effects of biochars added to AD digestate.

Pre-incubation of CreChar® not only reduced inhibition but also aided in the production of a greater volume of biogas. Therefore, CreChar® surfaces must have properties advantageous to AD, over the standard biochar; however, there are no noticeable patterns in the microbial and chemical data that suggests specific microbial activity in CreChar®-supplemented reactors or on their surfaces. As such the reasons behind their increased beneficial effects in AD are the subject of continuing research.

It was found from the *mcrA* gene abundance data that the number of methanogenic archaea rose and fell rapidly in the AD reactors and that the suspected rise in methanogen number for the uninhibited reactors was missed. A rise in *mcrA* gene abundance was observed at day 40 for the bio-oil-supplemented reactors which then fell back to control levels by day 60; highlighting the need for a higher frequency of sampling of reactors to gain a better resolution of methanogenic archaeal abundance over time. DNA on the biochar surfaces was shown to contain *mcrA* gene copies; however the abundance was not as great as that observed in the digestate after two days of pre-incubation which is likely due to the slower growth of these microorganisms.

Although the characterisation of the biology and chemistry of the digestates did not reveal patterns specific to pre-incubation, its impact on biogas production is still significant. It is hypothesised that the inclusion of a stable community of microorganisms on the biochar surfaces helps to immediately begin AD processes without the need for a sustained period of adaptation. However, depending on the digestate chemistry it may be more practical to alter the length of pre-incubation. If the slower growing methanogens are sought for an increased biogas production, or are required to clear an accumulation of VFAs, then a longer pre-incubation may be necessary to allow for the growth of these microorganisms; however, if the digestate contains inhibitory compounds whose degradation is predominantly by faster growing bacterial hydrolysers, then a shorter pre-incubation period may suffice.

8.1.4 Analysis Methods

This project utilised high-throughput biological and chemical assays to analyse the effects of supplementation of AD. There is a great deal of published work on the abilities of next-generation sequencing to characterise and compare microbial communities to an exceptionally high resolution; with this project proposing that the digestate chemistries can be treated compared similarly.

The taxonomy-based Unifrac index for computing the differences between microbial communities based on phylogenetic information requires the construction of a tree based on the tiered allocation of individuals into groups, separated by their phylogenetic distance (Lozupone and Knight, 2005). No such similarity index exists for chemicals, and as such it is currently not possible to analyse the chemical data in the same way. The use of multivariate analysis to create Bray-Curtis similarity matrices between samples goes some way towards assessing the similarity of samples based on chemical variables, when combined with the structural information obtained from van Krevelen diagrams and heteroatom plots. However, there is still a limitation on how much translatable information can be gained from chemical formula as supplied by FT-ICR MS. Further work is being done to continue the extraction of relevant data from the chemical formulas and its relatedness with

biological characterisation data which should allow for a greater understanding of the types of chemicals that are effecting and effected by AD.

8.2 Future Work

Although the characterisation techniques used in this project attempt to interpret as much of the total chemistry and biology of the AD systems as possible, there are still shortcomings of the techniques that can be addressed. Negative-mode electrospray ionisation (ESI) was the ionisation method used in this project for the FT-ICR MS; which has been used in several reports of bio-oil characterisation (Jarvis *et al*., 2012; Liu *et al*., 2012; Smith *et al*., 2012; Miettinen *et al*., 2015). However, negative-mode ESI is not able to ionise every compound and thus there is a fraction of the bio-oil that is not included in the characterisation. It has been shown that including compounds identified using a positive-mode ionisation source is able to increase the range of bio-oil compounds that are identified, and that using dopants can improve the ionisation efficiency by cationisation or anionisation (Hertzog *et al*., 2016). However, still, ESI exhibits poor ionisation of non-polar compounds, thus, to identify the greatest range of bio-oil compounds, requires the use of multiple ionisation sources, such as laser desorption ionisation (LDI) and atmospheric pressure photoionisation (APPI), in both positive and negative modes (Hertzog *et al*., 2017).

In addition to the ionisation mode, the mass/charge (*m/z*) cut-offs for identification and the range of heteroatoms can also be expanded in the assignment of peaks. This project focused on those compounds with an *m/z* between 200 and 500, which encapsulates the vast majority of peaks on the mass spectra. However, the expansion of this range may aid in the characterisation of bio-oils, especially for those compounds of low *m/z*, however expanding this range is dependent on the operational status of the FT-ICR MS. The inclusion of other heteroatoms may also increase the number of assigned peaks with chemical formula. On average, ~50% of the total peaks were assigned chemical formula thus there is a significant portion of the total peak list that is not included in the analysis. Additionally, this project only searched for compounds with the elemental composition of $C_{1\text{-}100}H_{2\text{-}200}O_{1\text{-}30}N_{0\text{-}4}$,

however with the identification of sulphur-reducing bacterial species in late-stage AD reactors; there could potentially be a significant sulphur contribution to the digestate. If certain feedstocks were pyrolysed to a sulphur rich bio-oil, their addition to AD could outcompete methanogens and cause significant inhibition of methanogenesis due to the sulphate-reducers higher affinity for hydrogen (Madden *et al*, 2014). Monitoring the hydrogen sulphide content of the biogas would act as an indicator of increased sulphate-reduction.

Similarly, the DNA extraction method can have a significant impact on the final identified microorganisms, as show in reports that have compared sequenced DNA extracted from the same samples using different techniques (Hart *et al*., 2015). The QIAGEN Powersoil kit used in this project is ideal for samples where it is unknown what the microbial community will be composed of; however, additional extraction techniques are likely to expand that range of microorganisms such that the identified community will be more inclusive of a greater diversity of microorganisms.

In addition to gaining greater coverage of the chemistry and biology of AD processes, there are some gaps in the analysis that can be resolved which could help explain some persisting queries. Most importantly, if the utilisation of bio-oils in AD was to become an established procedure, then it would have to be able to be continuously fed to a reactor without negative consequences. Thus far, the experiments on bio-oil addition to AD have been in batch reactors where the persistence of bio-oil has not been checked after the initial digestate has been utilised for biogas production. Experiments need to be designed that focus on the continuous feeding of a reactor to better mimic real-life scenarios. If it was found that a fraction of the bio-oil was unable to be degraded by AD and it accumulated over time to cause reactor failure, then the possibility of feeding bio-oils to AD would have to be re-evaluated. The same is true for the eventual use of the digestate from the supplemented reactor; if it still contained toxic compounds then its range of uses will be severely limited. This might translate to an increased retention time of bio-oil-supplemented digestates; which itself could instigate financial difficulties for an anaerobic digester.

In addition to this, the SWP/BO bio-oil displayed ageing to a point where it was becoming more difficult to degrade thus further tests should be performed investigating the long-term storage options of bio-oil and whether they can still be degraded after these periods. Due to the majority of ageing being attributed to the continued reactivity of phenolic compounds, it may be found that bio-oils from biomass with a limited amount of lignin, such as anaerobic digestate, is a more feasible option if freshly produced bio-oil cannot be utilised immediately.

The monitoring of the microbial communities in any further work should also include additional sampling periods for the qPCR of *mcrA* gene copy number. The transient nature of methanogenic archaeal abundance makes the periods of intense methanogenic growth difficult to capture with only a limited number of sampling points. It would also be beneficial to include sampling periods when significant biogas production is observed to begin as these periods were often missed and could reveal which members of the microbial community are active at this crucial step.

Apart from the direct introduction of bio-oil compounds and resultant pH change, it is still unknown what effects the addition of bio-oil has to digestate chemistry. The aqueous phase of bio-oil (used in this project) is soluble in water and thus immediately becomes a part of the aqueous phase of the digestate. Although there are reports of certain inhibitory compounds in bio-oil becoming adsorbed onto solid supplements with porous surfaces, such as activated carbon and biochars, the association of bio-oil with the solid fraction of digestate has not been analysed. Indeed, this could aid in the identification of the missing COD in some of the AD tests where, despite a significant decrease in aqueous phase digestate COD, the biogas production was not enhanced, thus leading to the hypothesis that it was associated with the solid fraction of the digestate. COD analysis of only the aqueous fraction of the digestates also led to methane yields per gCOD above the theoretical limit, as the calculation could not include the solid fraction contribution. Analysis of the solid fraction COD was attempted; however, the non-heterogeneous nature of digestate causes a great deal of variation among replicate measurements of COD.

This could potentially be circumvented by sonicating the digestate to break apart the solid matter.

The significant changes to the pH of the digestates after bio-oil addition was also an uncontrolled variable in the AD tests, as the differences between the reactors concentration of hydrogen ions were drastically different. The pH of an anaerobic digester should be closely monitored as hydrolysis generates acids that, when accumulated, can become inhibitory to methanogens. As such, to gain a better understanding of the inhibitory potential of the compounds in bio-oil it is recommended that the pH of the resultant mix with digestate is standardised across reactors.

Quantification of total ammonia nitrogen (TAN) and VFA analysis should also be performed for the chemical characterisation of the digestates. It was hypothesised that the inhibition observed from the bio-oils with a high proportion of lipids and proteins was due to their degradation to ammonia, the most common inhibitory compound in AD reactors. To confirm this, and to better understand the inhibitory action of specific bio-oils, the levels of ammonia must be analysed. This is also true for the VFAs in the digestate, which can cause inhibition when they accumulate. However, if more work is to be performed on the potential use of methanogenic inhibition for acetic acid accumulation as a product of greater value than biogas, it will need to be confirmed that acetic acid is being accumulated in these reactors.

In addition to this confirmation, a method of isolation and purification of acetic acid is required. A small amount of research was performed on the potential utilisation of conventional electrodialysis (CED) for this purpose using a CED stack, detailed in Figure 8.1, consisting of two electrodes housed in individual anode and cathode chambers, across which an electrical potential is established via an external power source, at either end of anion and cation exchange membranes separated by spacers through which diluate and concentrate solutions flow through. This technique has been successfully applied to VFAs accumulated in dark fermentation broths for

hydrogen production (Jones *et al*., 2015) which are similar to methanogenic inhibited anaerobic digestates.

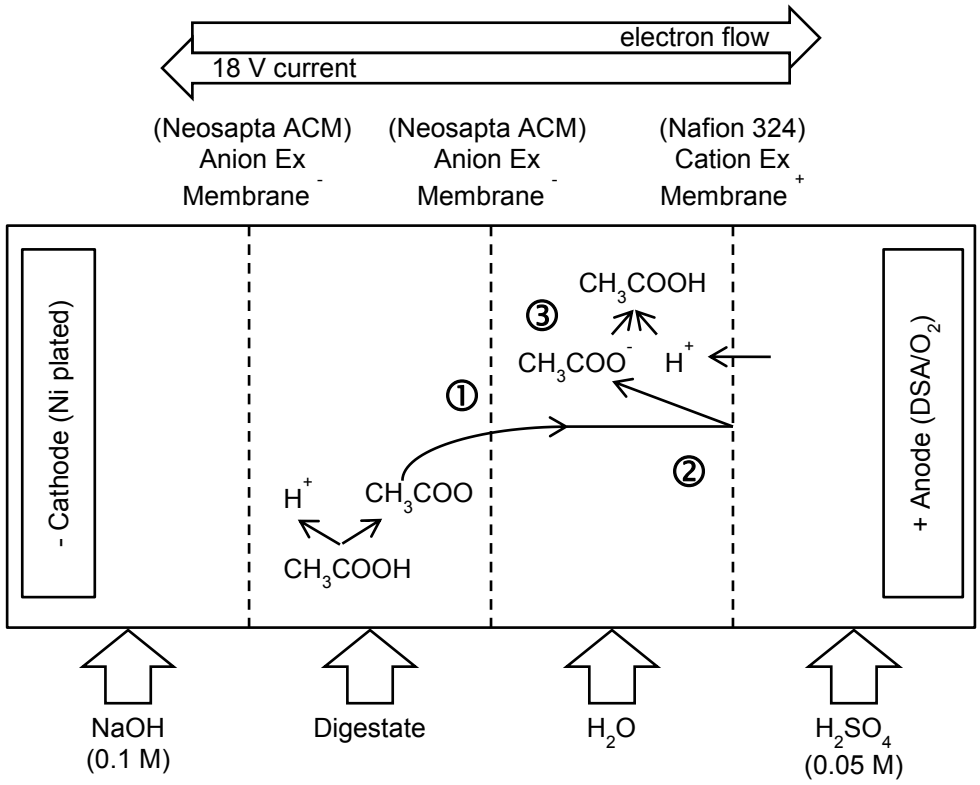

Figure 8.1. Conventional electrodialysis (CED) stack for the isolation of acetic acid from centrifuged digestate. The technique relies on the acetate ion being drawn from a digestate solution, through an anion specific exchange membrane① into a neighbouring flow of deionised water. Here the acetate ion cannot proceed into the anode chamber due to the cation exchange membrane②. The protons flowing from the anode chamber across the cation exchange membrane react with acetate to form acetic acid③ which is concentrated in the deionised water.

Further work can also be undertaken on combining the analyses of each AD experiment in this project and comparing their biological and chemical similarities. Due to the identical methods in the assays for each test, the data sets should be comparable and could help identify the changes that are occurring due to ageing of the bio-oil and the digestate.

One of the largest areas of research that can be further investigated is the use of biochars in AD, which is becoming an area of growing interest due to the advantages it can confer. Although the microbial communities were analysed at the start and end of AD4, again, they would benefit from additional sampling periods so better resolution of microbial adherence to the surfaces of biochar over time can be obtained. This would require upscaling of the experiment as the removal of enough biochar for DNA extraction could potentially have an impact on its effects on AD. It is also unknown if the biochars themselves contribute to changes in the digestate chemistry by the release of nutrients into the digestate, similarly to how nutrient-enriched biochars in soils behave (Gwenzi *et al*., 2017). This could be achieved by simultaneously incubating biochars in a solution of water for the duration of their addition to digestates, and then analysing the water upon completion of the experiment.

Pre-incubation of the biochar surfaces with the microorganisms already present in digestate caused a reduction in the inhibitory phase caused by bio-oil in the supplemented reactors of AD4. However, the exact inhibitory pathways responsible for the lag phase are still unknown and presumably due to the myriad compounds present in bio-oil. It is hypothesised that the biochar communities provide a stable microbial "backbone" that can immediately begin AD, whereas those reactors without this support require a period of adaptation. Further work can therefore investigate the pre-incubation of different communities, or single species, on the biochar surfaces in an attempt to bioaugment the AD community.

Several of the single species identified during attempts at aerobic degradation of bio-oil are facultative anaerobes, and so could provide the AD community with an enhanced ability to degrade bio-oil if added as biochar-associated cultures. This would potentially circumvent the general intolerance to bioaugmented microorganisms observed in mixed microbial communities, as the input of cells would be associated with a stable matrix. Alternatively cultures of methanogens could be pre-incubated on the biochar surfaces or pre-incubation in digestate for a

greater period of time, to facilitate growth of these slower-growing archaeal species. However the pre-incubation is performed, it will require additional analysis techniques to confirm their adherence and persistence on the biochar surfaces. As such, electron microscopy of the biochar surfaces and staining techniques could be employed to visualise these cells.

8.2.1 Lessons Learnt

Although the use of techniques such as next-generation sequencing and ultra-high resolution mass spectrometry are powerful tools for the characterisation of the biological and chemical components of AD systems, they are not without their limitations, and it is within these limitations that additional lessons have been learnt. Microbial community composition from sequencing of microbial DNA in a sample does not translate to the function of the community. Although it is possible to see patterns in the relative abundance of the top contributing genera, even with knowledge of their metabolic capacities, conclusions based on their activity *in vivo* are still speculative without specific analysis. It is also within the rarer species that a great deal of metabolic potential lies and is still not accounted for by sequencing techniques (Jousset *et al*., 2017).

The same is true for the chemical composition of the microbial environment, especially where there are known inhibitors of key metabolic processes. The overall understanding of the types of compounds in the digestates was useful to see the changes occurring between reactors and to better characterise the complexity of the bio-oils. However, quantification of specific compounds such as ammonia, sulphates and VFAs are required for an understanding of how the AD process is affected by supplementation. It is also important to understand that the relationships between these two data sets only give correlations and not cause. Thus, the characterisation of such broad experimental parameters must be complemented with specific analyses of important processes within the system that can give direct evidence for conclusions to be based upon.

8.3 Conclusion

The addition of fresh bio-oil to AD for its conversion to a value-added product as biogas is possible without immediate negative effects on the digestate. However, further work needs to be performed to investigate whether there are any persistent remnants of bio-oil that could cause process failures if left to accumulate and at what point bio-oil ages to become too recalcitrant to use as an additive. Additionally, bio-oil from lignocellulosic biomass pyrolysed at 350 °C is more easily utilised by the microorganisms in wastewater treatment digestate than bio-oils from lignin-limited feedstocks, such as anaerobic digestate and *M. pyrifera*. The addition of pre-incubated biochar to AD alleviates some of the inhibition observed from bio-oil supplementation and requires further investigation into its use as a delivery mechanism for other communities or species for bioaugmentation of AD. It is also important to take into consideration the limitations of characterisation techniques and ensure that they are complemented with quantified analysis of known markers of process constitution.

REFERENCES

Aboulkas, A., Hammani, H., El Achaby, M., Bilal, E., Barakat, A. & El harfi, K. (2017) Valorization of algal waste via pyrolysis in a fixed-bed reactor: Production and characterization of bio-oil and bio-char. *Bioresource Technology*, 243, 400–408.

Akhiar, A., Battimelli, A., Torrijos, M. & Carrere, H. (2017) Comprehensive characterization of the liquid fraction of digestates from full-scale anaerobic co-digestion. *Waste Management*, 59, 118–128.

Ali Shah, F., Mahmood, Q., Maroof Shah, M., Pervez, A. & Ahmad Asad, S. (2014) Microbial Ecology of Anaerobic Digesters: The Key Players of Anaerobiosis. *The Scientific World Journal*, 2014, 1–21.

Almeida, T.M., Bispo, M.D., Cardoso, A.R.T., Migliorini, M. V, Schena, T., de Campos, M.C. V, Machado, M.E., López, J.A., Krause, L.C. & Caramão, E.B. (2013) Preliminary studies of bio-oil from fast pyrolysis of coconut fibers. *Journal of Agricultural and Food Chemistry*, 61(28), 6812–21.

Alsbou, E. & Helleur, B. (2014) Accelerated Aging of Bio-oil from Fast Pyrolysis of Hardwood. *Energy & Fuels*, 28(5), 3224–3235.

Alsouleman, K., Linke, B., Klang, J., Klocke, M., Krakat, N. & Theuerl, S. (2016) Reorganisation of a mesophilic biogas microbiome as response to a stepwise increase of ammonium nitrogen induced by poultry manure supply. *Bioresource Technology*, 208, 200–204.

Amaya, O.M., Barragán, M.T.C. & Tapia, F.J.A (2013) Microbial Biomass in Batch and Continuous System, Biomass Now - Sustainable Growth and Use, Dr. Miodrag Darko Matovic (Ed.), *InTech*.

Anderson M.J., Gorley R.N. & Clarke K. R. (2008) PERMANOVA+ for PRIMER: guide to software and statistical methods. Plymouth, UK

Anderson, M, Gorley, R.N. & Clarke, K. (2008) PERMANOVA+ for primer: Guide to software and statistical methods.

Andreoni, V., Bonfanti, P., Daffonchio, D., Sorlini, C. & Villa, M. (1990) Anaerobic digestion of wastes containing pyrolignitic acids. *Biological Wastes*, 34(3), 203–214.

Angert, E.R., Hutchison, E.A. & Miller, D.A. (2014) Sporulation in Bacteria: Beyond the Standard Model, in: The Bacterial Spore: From Molecules to Systems. *American Society of Microbiology* (pp. 87–102).

Ariesyady, H.D., Ito, T. & Okabe, S. (2007) Functional bacterial and Archaeal community structures of major trophic groups in a full-scale anaerobic sludge digester. *Water Research*, 41(7), 1554–68.

Bartsch, S., Gensch, A., Stephan, S., Doetsch, A. & Gescher, J. (2017) *Metallibacterium scheffleri*: Genomic data reveal a versatile metabolism. *FEMS Microbiology Ecology*, (January), fix011.

Beaudet, R., Lévesque, M.J., Villemur, R., Lanthier, M., Chénier, M., Lépine, F. & Bisaillon, J.G. (1998) Anaerobic biodegradation of pentachlorophenol in a contaminated soil inoculated with a methanogenic consortium or with *Desulfitobacterium frappieri* strain PCP-1. *Applied Microbiology and Biotechnology*, 50(1), 135–41.

Bennett, N.M., Helle, S.S. & Duff, S.J.B. (2009) Extraction and hydrolysis of levoglucosan from pyrolysis oil. *Bioresource Technology*, 100(23), 6059–6063.

Berdugo-Clavijo, C. & Gieg, L.M. (2014) Conversion of crude oil to methane by a microbial consortium enriched from oil reservoir production waters. *Frontiers in Microbiology*, 5(May), 197.

Bergmann, G.T., Bates, S.T., Eilers, K.G., Lauber, C.L., Caporaso, J.G., Walters, W.A., Knight, R. & Fierer, N. (2011) The under-recognized dominance of *Verrucomicrobia* in soil bacterial communities. *Soil Biology and Biochemistry*, 43(7), 1450–1455.

Boon, N. & Verstraete, W. (2010) Bioaugmentation of Hydrocarbons. In K.N. Timmis (Ed.), *Handbook of Hydrocarbon and Lipid Microbiology* (pp. 2531–2543) Berlin, Heidelberg: Springer Berlin Heidelberg.

Bratina, B., Šorgo, A., Kramberger, J., Ajdnik, U., Zemljič, L.F., Ekart, J. & Šafarič, R. (2016) From municipal/industrial wastewater sludge and FOG to fertilizer: A proposal for economic sustainable sludge management. *Journal of Environmental Management*, 183, 1009–1025.

Cai, J., He, P., Wang, Y., Shao, L. & Lü, F. (2016) Effects and optimization of the use of biochar in anaerobic digestion of food wastes. *Waste Management & Research: The Journal of the International Solid Wastes and Public Cleansing Association,* ISWA, 34(5), 409–16.

Camarero, S., Galletti, G.C. & Martinez, A.T. (1994) Preferential degradation of phenolic lignin units by two white rot fungi. *Applied and Environmental Microbiology*, 60(12), 4509–4516.

Caporaso, J.G., Kuczynski, J., Stombaugh, J., Bittinger, K., Bushman, F.D., Costello, E.K., Fierer, N., Peña, A.G., Goodrich, J.K., Gordon, J.I., Huttley, G.A., Kelley, S.T., Knights, D., Koenig, J.E., Ley, R.E., Lozupone, C.A., McDonald, D., Muegge, B.D., Pirrung, M., Reeder, J., Sevinsky, J.R., Turnbaugh, P.J., Walters, W.A., Widmann, J., Yatsunenko, T., Zaneveld, J. & Knight, R. (2010) QIIME allows

analysis of high-throughput community sequencing data. *Nature Methods*, 7(5), 335–6.

Caporaso, J.G., Lauber, C.L., Walters, W.A, Berg-Lyons, D., Huntley, J., Fierer, N., Owens, S.M., Betley, J., Fraser, L., Bauer, M., Gormley, N., Gilbert, J.A, Smith, G. & Knight, R. (2012) Ultra-high-throughput microbial community analysis on the Illumina HiSeq and MiSeq platforms. *The ISME Journal*, 6(8), 1621–1624.

Caporaso, J.G., Lauber, C.L., Walters, W.A., Berg-Lyons, D., Lozupone, C.A., Turnbaugh, P.J., Fierer, N. & Knight, R. (2011) Global patterns of 16S rRNA diversity at a depth of millions of sequences per sample. *Proceedings of the National Academy of Sciences*, 108(Supplement_1), 4516–4522.

Cassa-Barbosa, L. A., Procópio, R. E. L., Matos, I. T. S. R. & Filho, S. A. (2015) Isolation and characterization of yeasts capable of efficient utilization of hemicellulosic hydrolyzate as the carbon source. *Genetics and Molecular Research*, 14(3), 11605–11612.

Chen, J. L., Ortiz, R., Steele, T. W. J. & Stuckey, D. C. (2014) Toxicants inhibiting anaerobic digestion: A review. *Biotechnology Advances*, 32(8), 1523–1534.

Chen, L., Hu, M., Huang, L., Hua, Z., Kuang, J., Li, S. & Shu, W. (2015) Comparative metagenomic and metatranscriptomic analyses of microbial communities in acid mine drainage. *The ISME Journal*, 9(7), 1579–1592.

Chen, S. & Dong, X. (2005) *Proteiniphilum acetatigenes* gen. nov., sp. nov., from a UASB reactor treating brewery wastewater. *International Journal of Systematic and Evolutionary Microbiology*, 55(Pt 6), 2257–61.

Chen, S., Rotaru, A.-E., Liu, F., Philips, J., Woodard, T.L., Nevin, K.P. & Lovley, D.R. (2014) Carbon cloth stimulates direct interspecies electron transfer in syntrophic co-cultures. *Bioresource Technology*, 173, 82–86.

Chen, S., Rotaru, A.-E., Shrestha, P.M., Malvankar, N.S., Liu, F., Fan, W., Nevin, K.P. & Lovley, D.R. (2015) Promoting Interspecies Electron Transfer with Biochar. *Scientific Reports*, 4(1), 5019.

Chen, X., Li, Z., Zhang, X., Hu, F., Ryu, D. D. Y. & Bao, J. (2009) Screening of oleaginous yeast strains tolerant to lignocellulose degradation compounds. *Applied Biochemistry and Biotechnology*, 159(3), 591–604.

Chen, Y., Cheng, J.J. & Creamer, K.S. (2008) Inhibition of anaerobic digestion process: A review. *Bioresource Technology*, 99(10), 4044–4064.

Cherubini, F. (2010) The biorefinery concept: Using biomass instead of oil for producing energy and chemicals. *Energy Conversion and Management*, 51(7), 1412–1421.

Chouari, R., Le Paslier, D., Daegelen, P., Ginestet, P., Weissenbach, J. & Sghir, A. (2005) Novel predominant Archaeal and bacterial groups revealed by molecular analysis of an anaerobic sludge digester. *Environmental Microbiology*, 7(8), 1104–1115.

Clarke, K.R. & Warwick, R.M. (2001) Change in Marine Communities: An Approach to Statistical Analysis, 2nd edn Primer-E: Plymouth, UK.

Cooney, M.J., Lewis, K., Harris, K., Zhang, Q. & Yan, T. (2016) Start up performance of biochar packed bed anaerobic digesters. *Journal of Water Process Engineering*, 9, e7–e13.

Coram, N.J. & Rawlings, D.E. (2002) Molecular Relationship between Two Groups of the Genus *Leptospirillum* and the Finding that *Leptospirillum ferriphilum* sp. nov. Dominates South African Commercial Biooxidation Tanks That Operate at 40 C. *Applied and Environmental Microbiology*, 68(2), 838–845.

Da Cunha, V., Gaia, M., Gadelle, D., Nasir, A. & Forterre, P. (2017) *Lokiarchaea* are close relatives of *Euryarchaeota*, not bridging the gap between prokaryotes and eukaryotes. *PLOS Genetics*, 13(6)

Das, O. & Sarmah, A.K. (2015) Value added liquid products from waste biomass pyrolysis using pretreatments. *Science of the Total Environment*, 538, 145–151.

Dedysh, S.N., Pankratov, T.A, Belova, S.E., Kulichevskaya, I.S. & Liesack, W. (2006) Phylogenetic Analysis and In Situ Identification of Bacteria Community Composition in an Acidic Sphagnum Peat Bog. *Applied and Environmental Microbiology*, 72(3), 2110–2117.

Deng, Y., Xu, J., Liu, Y. & Mancl, K. (2014) Biogas as a sustainable energy source in China: Regional development strategy application and decision making. *Renewable and Sustainable Energy Reviews*, 35, 294–303.

Desai, M. & Madamwar, D. (1994) Anaerobic digestion of a mixture of cheese whey, poultry waste and cattle dung: a study of the use of adsorbents to improve digester performance. *Environmental Pollution*. 86(3,) 337–340.

Díez, B., Pedrós-Alió, C., Marsh, T.L. & Massana, R. (2001) Application of denaturing gradient gel electrophoresis (DGGE) to study the diversity of marine picoeukaryotic assemblages and comparison of DGGE with other molecular techniques. *Applied Environmental Microbiology*. 67, 2942–51.

Dorigo, U., Bérard, A. & Humbert, J.F. (2002) Comparison of eukaryotic phytobenthic community composition in a polluted river by partial 18S rRNA gene cloning and sequencing. *Microbial Ecology*, 44, 372–380.

Dubber, D. & Gray, N. F. (2010) Replacement of chemical oxygen demand (COD) with total organic carbon (TOC) for monitoring wastewater treatment performance to

minimize disposal of toxic analytical waste. *Journal of Environmental Science and Health*, Part A, 45(12), 1595–1600.

Duran, M., Tepe, N., Yurtsever, D., Punzi, V. L., Bruno, C. & Mehta, R.J. (2006) Bioaugmenting anaerobic digestion of biosolids with selected strains of *Bacillus, Pseudomonas*, and *Actinomycetes* species for increased methanogenesis and odor control. *Applied Microbiology and Biotechnology*, 73(4), 960–966.

EBA Biomethane & Biogas Report 2015

Edgar, R. C. (2010) Search and clustering orders of magnitude faster than BLAST, *Bioinformatics,* 26(19), 2460-2461.

Eloe-Fadrosh, E.A., Ivanova, N.N., Woyke, T. & Kyrpides, N.C. (2016) Metagenomics uncovers gaps in amplicon-based detection of microbial diversity. *Nature Microbiology*, (February), 15032.

Fabbri, D. & Torri, C. (2016) Linking pyrolysis and anaerobic digestion (Py-AD) for the conversion of lignocellulosic biomass. *Current Opinion in Biotechnology*, 38, 167–173.

Fagbohungbe, M.O., Herbert, B.M.J., Hurst, L., Ibeto, C.N., Li, H., Usmani, S.Q. & Semple, K.T. (2017) The challenges of anaerobic digestion and the role of biochar in optimizing anaerobic digestion. *Waste Management*, 61, 236–249.

Feng, G., Cheng, Y., Wang, S.-Y., Borca-Tasciuc, D.A., Worobo, R.W. & Moraru, C.I. (2015) Bacterial attachment and biofilm formation on surfaces are reduced by small-diameter nanoscale pores: how small is small enough? *Npj Biofilms and Microbiomes*, 1(1), 15022.

Fisher, R. A. (1925) Statistical methods for research workers. 18th Redition, Edinburgh, Oliver and Boyd.

Fitamo, T., Treu, L., Boldrin, A., Sartori, C., Angelidaki, I. & Scheutz, C. (2017) Microbial population dynamics in urban organic waste anaerobic co-digestion with mixed sludge during a change in feedstock composition and different hydraulic retention times. *Water Research*, 118, e14–e15.

FitzGerald, J.A., Allen, E., Wall, D.M., Jackson, S.A., Murphy, J.D. & Dobson, A.D.W. (2015) *Methanosarcina* Play an Important Role in Anaerobic Co-Digestion of the Seaweed *Ulva lactuca*: Taxonomy and Predicted Metabolism of Functional Microbial Communities. *PloS ONE*, 10(11), e0142603.

Fotidis, I.A., Karakashev, D., Kotsopoulos, T.A., Martzopoulos, G.G. & Angelidaki, I. (2013) Effect of ammonium and acetate on methanogenic pathway and methanogenic community composition. *FEMS Microbiology Ecology*, 83(1), 38–48.

Fuentes, S., Barra, B., Caporaso, J.G. & Seeger, M. (2016) From Rare to Dominant: a Fine-Tuned Soil Bacterial Bloom during Petroleum Hydrocarbon Bioremediation. *Applied and Environmental Microbiology*, 82(3), 888–896.

Future Market Insights (2017) Biogas Market: Asia Pacific Anticipated to Witness Significant Growth Till 2020: Global Industry Analysis and Opportunity Assessment 2016-2026 [online]. Report Code: REP-GB-1397

Gallert, C., Bauer, S. & Winter, J. (1998) Effect of ammonia on the anaerobic degradation of protein by a mesophilic and thermophilic biowaste population. *Applied Microbial Biotechnology*, 50, 495–501.

Gao, S., Zhao, M., Chen, Y., Yu, M. & Ruan, W. (2015) Tolerance response to in situ ammonia stress in a pilot-scale anaerobic digestion reactor for alleviating ammonia inhibition. *Bioresource Technology*, 198, 372–379.

Garcia-Perez, M., Chaala, A., Pakdel, H., Kretschmer, D. & Roy, C. (2007) Characterization of bio-oils in chemical families. *Biomass and Bioenergy*, 31(4), 222–242.

Garcia-Perez, M., Wang, S., Shen, J., Rhodes, M., Lee, W. J. & Li, C.-Z. (2008) Effects of Temperature on the Formation of Lignin-Derived Oligomers during the Fast Pyrolysis of Mallee Woody Biomass. *Energy & Fuels*, 22(3), 2022–2032.

Grossman, J.M., O'Neill, B.E., Tsai, S.M., Liang, B., Neves, E., Lehmann, J., Thies, J.E. (2010) Amazonian anthrosols support similar microbial communities that differ distinctly from those extant in adjacent, unmodified soils of the same mineralogy. *Microbial Ecology*, 60(1), 192– 205

Guo, J., Peng, Y., Ni, B.-J., Han, X., Fan, L. & Yuan, Z. (2015) Dissecting microbial community structure and methane-producing pathways of a full-scale anaerobic reactor digesting activated sludge from wastewater treatment by metagenomic sequencing. *Microbial Cell Factories*, 14(1), 33.

Gutierrez, T., Berry, D., Yang, T., Mishamandani, S., McKay, L., Teske, A. & Aitken, M.D. (2013) Role of Bacterial Exopolysaccharides (EPS) in the Fate of the Oil Released during the Deepwater Horizon Oil Spill. *PloS One*, 8(6), e67717.

Gutierrez, T., Singleton, D. R., Berry, D., Yang, T., Aitken, M. D. & Teske, A. (2013) Hydrocarbon-degrading bacteria enriched by the Deepwater Horizon oil spill identified by cultivation and DNA-SIP. *The ISME Journal*, 7(11), 2091–104.

Gwenzi, W., Nyambishi, T.J., Chaukura, N. & Mapope, N. (2018) Synthesis and nutrient release patterns of a biochar-based N–P–K slow-release fertilizer. *International Journal of Environmental Science and Technology*. 15, 405–414.

Haegeman, B., Hamelin, J., Moriarty, J., Neal, P., Dushoff, J. & Weitz, J.S. (2013) Robust estimation of microbial diversity in theory and in practice. *The ISME Journal*, 7(6), 1092–1101.

Hao, L., Bize, A., Conteau, D., Chapleur, O., Courtois, S., Kroff, P., Desmond-Le Quéméner, E., Bouchez, T. & Mazéas, L. (2016) New insights into the key microbial phylotypes of anaerobic sludge digesters under different operational conditions. *Water Research*, 102, 158–169.

Hart, M.L., Meyer, A., Johnson, P.J. & Ericsson, A.C. (2015) Comparative Evaluation of DNA Extraction Methods from Feces of Multiple Host Species for Downstream Next-Generation Sequencing. *PloS ONE*, 10(11), e0143334.

Hassanshahian, M., Emtiazi, G., Caruso, G. & Cappello, S. (2014) Bioremediation (bioaugmentation/biostimulation) trials of oil polluted seawater: a mesocosm simulation study. *Marine Environmental Research*, 95, 28–38.

Heal, K & Salt, C.A. (1999) Treatment of acidic metal-rich drainage from reclaimed ironstone mine spoil. *Water Science & Technology*, 39(12), 141-148.

Heidrich, E.S., Curtis, T.P. & Dolfing, J. (2011) Determination of the Internal Chemical Energy of Wastewater. *Environmental Science and Technology,* 45, 827–832.

Helffrich, D. & Oechsner, H. (2003) The Hohenheim biogas yield test: comparison of different laboratory techniques for the digestion of biomass. *Agrartechnische Forschung*, 9(1/3), 27–30.

Hendriks, A.T. W.M. & Zeeman, G. (2009) Pretreatments to enhance the digestibility of lignocellulosic biomass. *Bioresource Technology*, 100(1), 10–18.

Hertkorn, N., Frommberger, M., Witt, M., Koch, B.P., Schmitt-Kopplin, P. & Perdue, E.M. (2008) Natural Organic Matter and the Event Horizon of Mass Spectrometry. *German Research*, 80(October), 8908–8919.

Hertzog, J., Carré, V., Le Brech, Y., Dufour, A. & Aubriet, F. (2016) Toward Controlled Ionization Conditions for ESI-FT-ICR-MS Analysis of Bio-Oils from Lignocellulosic Material. *Energy & Fuels*, 30(7), 5729–5739.

Hertzog, J., Carré, V., Le Brech, Y., Mackay, C.L., Dufour, A., Mašek, O. & Aubriet, F. (2017) Combination of electrospray ionization, atmospheric pressure photoionization and laser desorption ionization Fourier transform ion cyclotronic resonance mass spectrometry for the investigation of complex mixtures – Application to the petroleomic analysis. *Analytica Chimica Acta*, 969, 26–34.

Hockaday, W.C., Grannas, A.M., Kim, S. & Hatcher, P.G. (2007) The transformation and mobility of charcoal in a fire-impacted watershed. *Geochimica et Cosmochimica Acta*, 71(14), 3432–3445.

Hsu, L.C., Fang, J., Borca-Tasciuc, D.A., Worobo, R.W. & Moraru, C.I. (2013) Effect of Micro- and Nanoscale Topography on the Adhesion of Bacterial Cells to Solid Surfaces. *Applied and Environmental Microbiology*, 79(8), 2703–2712.

Huang, C., Chen, X., Xiong, L., Yang, X., Chen, X., Ma, L. & Chen, Y. (2013) Microbial oil production from corncob acid hydrolysate by oleaginous yeast *Trichosporon coremiiforme*. *Biomass and Bioenergy*, 49(2), 273–278.

Hübner, T. & Mumme, J. (2015) Integration of pyrolysis and anaerobic digestion – Use of aqueous liquor from digestate pyrolysis for biogas production. *Bioresource Technology*, 183, 86–92.

Hwang, H., Oh, S., Cho, T.-S., Choi, I.-G. & Choi, J.W. (2013) Fast pyrolysis of potassium impregnated poplar wood and characterization of its influence on the

formation as well as properties of pyrolytic products. *Bioresource Technology*, 150, 359–66.

Ijmker, H.M., Gramblička, M., Kersten, S.R.A., van der Ham, A.G.J. & Schuur, B. (2014) Acetic acid extraction from aqueous solutions using fatty acids. *Separation and Purification Technology*, 125(0), 256–263.

Ionov, R., El-Abed, A., Goldmann, M. & Peretti, P. (2004) Structural Organization of α-Helical Peptide Antibiotic Alamethicin at the Air/Water Interface. *The Journal of Physical Chemistry B*, 108(24), 8485–8488.

Iwaki, A., Kawai, T., Yamamoto, Y. & Izawa, S. (2013) Biomass Conversion Inhibitors Furfural and 5-Hydroxymethylfurfural Induce Formation of Messenger RNP Granules and Attenuate Translation Activity in *Saccharomyces cerevisiae*. *Applied and Environmental Microbiology*, 79(5), 1661–1667.

Jarboe, L.R., Wen, Z., Choi, D. & Brown, R.C. (2011) Hybrid thermochemical processing: fermentation of pyrolysis-derived bio-oil. *Applied Microbiology and Biotechnology*, 91(6), 1519–23.

Jarvis, J.M., McKenna, A.M., Hilten, R.N., Das, K.C., Rodgers, R.P. & Marshall, A.G. (2012) Characterization of Pine Pellet and Peanut Hull Pyrolysis Bio-oils by Negative-Ion Electrospray Ionization Fourier Transform Ion Cyclotron Resonance Mass Spectrometry. *Energy & Fuels*, 26(6), 3810–3815.

Jiang, Y., Banks, C., Zhang, Y., Heaven, S. & Longhurst, P. (2018) Quantifying the percentage of methane formation via acetoclastic and syntrophic acetate oxidation pathways in anaerobic digesters. *Waste Management*. 71, 749–756.

Jiménez, D.J., Korenblum, E. & van Elsas, J.D. (2014) Novel multispecies microbial consortia involved in lignocellulose and 5-hydroxymethylfurfural bioconversion. *Applied Microbiology and Biotechnology*. 98, 2789–2803.

Jolis, D. (2008) High-solids anaerobic digestion of municipal sludge pretreated by thermal hydrolysis. *Water Environment Research*, 80 (7), 654-66.

Jones, R.J., Massanet-Nicolau, J., Guwy, A., Premier, G.C., Dinsdale, R.M. & Reilly, M. (2015) Removal and recovery of inhibitory volatile fatty acids from mixed acid fermentations by conventional electrodialysis. *Bioresource Technology*, 189, 279–284.

Jönsson, L.J., Alriksson, B. & Nilvebrant, N.-O. (2013) Bioconversion of lignocellulose: inhibitors and detoxification. *Biotechnology for Biofuels*, 6(1), 16.

Jousset, A., Bienhold, C., Chatzinotas, A., Gallien, L., Gobet, A., Kurm, V., Küsel, K., Rillig, M.C., Rivett, D.W., Salles, J.F., van der Heijden, M.G.A., Youssef, N.H., Zhang, X., Wei, Z. & Hol, W.H.G. (2017) Where less may be more: how the rare biosphere pulls ecosystems strings. *ISME Journal*. 11, 853–862.

Kekäläinen, T., Venäläinen, T. & Jänis, J. (2014) Characterization of Birch Wood Pyrolysis Oils by Ultrahigh-Resolution Fourier Transform Ion Cyclotron Resonance Mass Spectrometry: Insights into Thermochemical Conversion. *Energy & Fuels*, 28(7), 4596–4602.

Keller, M. & Zengler, K. (2004) Tapping into microbial diversity. *Nature Reviews Microbiology*, 2(2), 141–150.

Kew, W., Blackburn, J.W.T., Clarke, D.J. & Uhrín, D. (2017) Interactive van Krevelen diagrams - Advanced visualisation of mass spectrometry data of complex mixtures. *Rapid Communications in Mass Spectrometry*, 31(7), 658–662.

Keweloh, H., Weyrauch, G. & Rehm, H.-J. (1990) Phenol-induced membrane changes in free and immobilized *Escherichia coli*. *Applied Microbiology and Biotechnology*, 33(1), 66–71.

Kim, S., Kramer, R.W. & Hatcher, P.G. (2003) Graphical Method for Analysis of Ultrahigh-Resolution Broadband Mass Spectra of Natural Organic Matter, the Van Krevelen Diagram. *Analytical Chemistry*, 75(20), 5336–5344.

Koch, B.P. & Dittmar, T. (2006) From mass to structure: An aromaticity index for high-resolution mass data of natural organic matter. *Rapid Communications in Mass Spectrometry*, 20(5), 926–932.

Kozich, J.J., Westcott, S.L., Baxter, N.T., Highlander, S.K. & Schloss, P.D. (2013) Development of a dual-index sequencing strategy and curation pipeline for analyzing amplicon sequence data on the MiSeq Illumina sequencing platform. *Applied and Environmental Microbiology*, 79(17), 5112–20.

Kraiem, T., Hassen, A. Ben, Belayouni, H. & Jeguirim, M. (2017) Production and characterization of bio-oil from the pyrolysis of waste frying oil. *Environmental Science and Pollution Research*, 24(11), 9951–9961.

Krastanov, A., Alexieva, Z. & Yemendzhiev, H. (2013) Microbial degradation of phenol and phenolic derivatives. *Engineering in Life Sciences*, 13(1), 76–87.

Kristjansson, J.K., Schönheit, P. & Thauer, R.K. (1982) Different Ks values for hydrogen of methanogenic bacteria and sulfate reducing bacteria: An explanation for the apparent inhibition of methanogenesis by sulfate. *Archives of Microbiology*, 131, 278–282.

Kruskal. J.B. (1964) Multidimensional-scaling by optimizing goodness of fit to a nonmetric hypothesis. *Psychometrika* 29: 1–27.

Laird, D.A., Fleming P., Davis, D.D., Horton, R., Wang B., Karlen, D.L. (2010) Impact of biochar amendments on the quality of a typical Midwestern agricultural soil. *Geoderma*, 158(3-4), 443–449.

Legendre, P. & Anderson, M.J. (1999) Distance-Based Redundancy Analysis: Testing Multispecies Responses in Multifactorial Ecological Experiments. *Ecological Monographs*, 69(1), 1.

Lerm, S., Kleyböcker, A., Miethling-Graff, R., Alawi, M., Kasina, M., Liebrich, M. & Würdemann, H. (2012) Archaeal community composition affects the function of anaerobic co-digesters in response to organic overload. *Waste Management*, 32(3), 389–399.

Li, J., Liang, Z., Jia, P., Liu, J., Xu, Y., Chen, Y., Shu, H., Kuang, J., Liao, B. & Shu, W. (2017) Effects of a bacterial consortium from acid mine drainage on cadmium phytoextraction and indigenous soil microbial community. *Plant and Soil*, 415(1–2), 347–358.

Li, Y., Jin, Y., Borrion, A., Li, H. & Li, J. (2017) Effects of organic composition on the anaerobic biodegradability of food waste. *Bioresource Technology*, 243, 836–845.

Li, Y., Zhang, Y., Sun, Y., Wu, S., Kong, X., Yuan, Z. & Dong, R. (2017) The performance efficiency of bioaugmentation to prevent anaerobic digestion failure from ammonia and propionate inhibition. *Bioresource Technology*, 231, 94–100.

Lian, J., Chen, S., Zhou, S., Wang, Z., O'Fallon, J., Li, C.-Z. & Garcia-Perez, M. (2010) Separation, hydrolysis and fermentation of pyrolytic sugars to produce ethanol and lipids. *Bioresource Technology*, 101(24), 9688–99.

Liebetrau, J., Sträuber, H., Kretzschmar, J., Denysenko, V. & Nelles, M. (2017) Anaerobic Digestion. *In Advances in biochemical engineering/biotechnology*, 1-19.

Liu, H., Wang, J., Wang, A. & Chen, J. (2011) Chemical inhibitors of methanogenesis and putative applications. *Applied Microbiology and Biotechnology*, 89(5), 1333–1340.

Liu, Y., Shi, Q., Zhang, Y., He, Y., Chung, K. H., Zhao, S. & Xu, C. (2012) Characterization of Red Pine Pyrolysis Bio-oil by Gas Chromatography–Mass Spectrometry and Negative-Ion Electrospray Ionization Fourier Transform Ion Cyclotron Resonance Mass Spectrometry. *Energy & Fuels*, 26, 4532–4539.

Lovley, D.R. (2017) Syntrophy Goes Electric: Direct Interspecies Electron Transfer. *Annual Review of Microbiology*, 71(1), 643–664.

Lozupone, C. & Knight, R. (2005) UniFrac: a new phylogenetic method for comparing microbial communities. *Applied and Environmental Microbiology*. 71(12), 8228–8235.

Lü, F., Luo, C., Shao, L. & He, P. (2016) Biochar alleviates combined stress of ammonium and acids by firstly enriching *Methanosaeta* and then *Methanosarcina*. *Water Research*, 90, 34–43.

Lua, A. C., Yang, T. & Guo, J. (2004) Effects of pyrolysis conditions on the properties of activated carbons prepared from pistachio-nut shells. *Journal of Analytical and Applied Pyrolysis*, 72(2), 279–287.

Luton, P.E., Wayne, J.M., Sharp, R.J. & Riley, P.W. (2002) The *mcrA* gene as an alternative to 16S rRNA in the phylogenetic analysis of methanogen populations in landfill. *Microbiology* 148, 3521–3530.

Machu, L., Misurcova, L., Ambrozova, J., Orsavova, J., Mlcek, J., Sochor, J. & Jurikova, T. (2015) Phenolic Content and Antioxidant Capacity in Algal Food Products. *Molecules*, 20(1), 1118–1133.

Madden, P., Al-Raei, A.M., Enright, A.M., Chinalia, F.A., de Beer, D., O'Flaherty, V. & Collins, G. (2014) Effect of sulfate on low-temperature anaerobic digestion. *Frontiers in Microbiology*, 5, 1–15.

Mao, C., Feng, Y., Wang, X. & Ren, G. (2015) Review on research achievements of biogas from anaerobic digestion. *Renewable and Sustainable Energy Reviews*, 45, 540–555.

Marshall, A.G. & Rodgers, R.P. (2004) Petroleomics: The Next Grand Challenge for Chemical Analysis. *Accounts of Chemical Research*, 37(1), 53–59.

Marshall, A.G., Hendrickson, C.L. & Jackson, G.S. (1998) Fourier transform ion cyclotron resonance mass spectrometry: A primer. *Mass Spectrometry Reviews*, 17(1), 1–35.

Matos, Í.T.S.R., Cassa-Barbosa, L.A., Costa Neto, P.Q. & Astolfi Filho, S. (2012) Cultivation of *Trichosporon mycotoxinivorans* in sugarcane bagasse hemicellulosic hydrolyzate. *Electronic Journal of Biotechnology*, 15(1), 1–7.

Maus, I., Cibis, K.G., Bremges, A., Stolze, Y., Wibberg, D., Tomazetto, G., Blom, J., Sczyrba, A., König, H., Pühler, A. & Schlüter, A. (2016) Genomic characterization of *Defluviitoga tunisiensis* L3, a key hydrolytic bacterium in a thermophilic biogas plant and its abundance as determined by metagenome fragment recruitment. *Journal of Biotechnology*, 232, 50–60.

Maus, I., Koeck, D.E., Cibis, K.G., Hahnke, S., Kim, Y.S., Langer, T., Kreubel, J., Erhard, M., Bremges, A., Off, S., Stolze, Y., Jaenicke, S., Goesmann, A., Sczyrba, A., Scherer, P., König, H., Schwarz, W.H., Zverlov, V. V., Liebl, W., Pühler, A., Schlüter, A. & Klocke, M. (2016) Unraveling the microbiome of a thermophilic biogas plant by metagenome and metatranscriptome analysis complemented by characterization of bacterial and archaeal isolates. *Biotechnology for Biofuels*, 9(1), 171.

McArdle, B.H. & Anderson, M.J. (2001) Fitting Multivariate Models to Community Data: A Comment on Distance-Based Redundancy Analysis. *Ecology*, 82(1), 290.

Méndez-García, C., Mesa, V., Sprenger, R.R., Richter, M., Diez, M.S., Solano, J., Bargiela, R., Golyshina, O. V, Manteca, Á., Ramos, J.L., Gallego, J.R., Llorente, I., Martins dos Santos, V.A., Jensen, O.N., Peláez, A.I., Sánchez, J. & Ferrer, M. (2014) Microbial stratification in low pH oxic and suboxic macroscopic growths along an acid mine drainage. *The ISME Journal*, 8(6), 1259–1274.

Messing, J. (1983) New M13 vectors for cloning. *Methods in Enzymology*, 101, 20-78.

Meyer-Kohlstock, D., Haupt, T., Heldt, E., Heldt, N. & Kraft, E. (2016) Biochar as additive in biogas-production from bio-waste. *Energies*, 9(4)

Miettinen, I., Mäkinen, M., Vilppo, T. & Jänis, J. (2015) Compositional Characterization of Phase-Separated Pine Wood Slow Pyrolysis Oil by Negative-Ion Electrospray Ionization Fourier Transform Ion Cyclotron Resonance Mass Spectrometry. *Energy & Fuels*, 29(3), 1758–1765.

Mitik-Dineva, N., Wang, J., Stoddart, P.R., Crawford, R.J. & Ivanova, E.P. (2008) Nano-structured surfaces control bacterial attachment. *Proceedings of the 2008 International Conference on Nanoscience and Nanotechnology*, ICONN 2008, 113–116.

Moestedt, J., Malmborg, J. & Nordell, E. (2015) Determination of Methane and Carbon Dioxide Formation Rate Constants for Semi-Continuously Fed Anaerobic Digesters. *Energies*, 8(1), 645–655.

Mohan, D., Pittman, C.U. & Steele, P.H. (2006) Pyrolysis of Wood/Biomass for Bio-oil: A Critical Review. *Energy & Fuels*, 20(3), 848–889.

Moita Fidalgo, R., Ortigueira, J., Freches, A., Pelica, J., Gonçalves, M., Mendes, B. & Lemos, P.C. (2014) Bio-oil upgrading strategies to improve PHA production from selected aerobic mixed cultures. *New Biotechnology*, 31(4), 297–307.

Monlau, F., Sambusiti, C., Barakat, A., Guo, X.M., Latrille, E., Trably, E., Steyer, J.-P. & Carrere, H. (2012) Predictive Models of Biohydrogen and Biomethane Production Based on the Compositional and Structural Features of Lignocellulosic Materials. *Environmental Science & Technology*, 46, 12217–12225.

Monlau, F., Sambusiti, C., Barakat, A., Quéméneur, M., Trably, E., Steyer, J.P. & Carrère, H. (2014) Do furanic and phenolic compounds of lignocellulosic and algae biomass hydrolyzate inhibit anaerobic mixed cultures? A comprehensive review. *Biotechnology Advances*, 32(5), 934–951.

Moralı, U., Yavuzel, N. & Şensöz, S. (2016) Pyrolysis of hornbeam (*Carpinus betulus L.*) sawdust: Characterization of bio-oil and bio-char. *Bioresource Technology*, 221, 682–685.

Morris, R., Schauer-Gimenez, A., Bhattad, U., Kearney, C., Struble, C. A., Zitomer, D. & Maki, J.S. (2014) Methyl coenzyme M reductase (mcrA) gene abundance correlates with activity measurements of methanogenic H2/CO2-enriched anaerobic biomass. *Microbial Biotechnology*, 7(1), 77–84.

Mourant, D., Lievens, C., Gunawan, R., Wang, Y., Hu, X., Wu, L., Syed-Hassan, S.S.A. & Li, C.-Z. (2013) Effects of temperature on the yields and properties of bio-oil from the fast pyrolysis of mallee bark. *Fuel*, 108, 400–408.

Müller, B., Sun, L., Westerholm, M. & Schnürer, A. (2016) Biotechnology for Biofuels Bacterial community composition and *fhs* profiles of low ‐ and high ‐ ammonia biogas digesters reveal novel syntrophic acetate ‐ oxidising bacteria. *Biotechnology for Biofuels*, 1–18.

Mumme, J., Srocke, F., Heeg, K. & Werner, M. (2014) Use of biochars in anaerobic digestion. *Bioresource Technology*, 164, 189–197.

Munk, B., Guebitz, G.M. & Lebuhn, M. (2017) Influence of nitrogen-rich substrates on biogas production and on the methanogenic community under mesophilic and thermophilic conditions. *Anaerobe*, 1–9.

Muyzer, G., de Waal, E.C. & Uitterlinden, A.G. (1993) Profiling of complex microbial populations by denaturing gradient gel electrophoresis analysis of polymerase chain reaction-amplified genes coding for 16S rRNA. *Applied and Environmental Microbiology*, 59(3), 695–700.

Narihiro, T. & Sekiguchi, Y. (2007) Microbial communities in anaerobic digestion processes for waste and wastewater treatment: a microbiological update. *Current Opinion in Biotechnology*, 18(3), 273–278.

Narihiro, T. & Sekiguchi, Y. (2011) Oligonucleotide primers, probes and molecular methods for the environmental monitoring of methanogenic archaea. *Microbial Biotechnology*, 4(5), 585–602.

Naushad, S., Adeolu, M., Wong, S., Sohail, M., Schellhorn, H.E. & Gupta, R.S. (2015) A phylogenomic and molecular marker based taxonomic framework for the order *Xanthomonadales*: proposal to transfer the families *Algiphilaceae* and *Solimonadaceae* to the order *Nevskiales* ord. nov. and to create a new family within the order *Xanthomonadales*. *Antonie van Leeuwenhoek*, 107(2), 467–485.

Negahdar, L., Gonzalez-Quiroga, A., Otyuskaya, D., Toraman, H.E., Liu, L., Jastrzebski, J.T.B.H., Van Geem, K.M., Marin, G.B., Thybaut, J.W. & Weckhuysen, B.M. (2016) Characterization and Comparison of Fast Pyrolysis Bio-oils from Pinewood, Rapeseed Cake, and Wheat Straw Using 13 C NMR and Comprehensive GC × GC. *ACS Sustainable Chemistry & Engineering*, 4(9), 4974–4985.

Nielfa, A., Cano, R., Pérez, A. & Fdez-Polanco, M. (2015) Co-digestion of municipal sewage sludge and solid waste: Modelling of carbohydrate, lipid and protein content influence. *Waste Management & Research*, 33(3), 241–249.

Oasmaa, A., van de Beld, B., Saari, P., Elliott, D. C. & Solantausta, Y. (2015) Norms, Standards, and Legislation for Fast Pyrolysis Bio-oils from Lignocellulosic Biomass. *Energy & Fuels*, 29(4), 2471–2484.

Oguntunde, P., Fosu, M., Ajayi, A., Giesen, N. (2004) Effects of charcoal production on maize yield, chemical properties and texture of soil. *Biology and Fertility of Soils*, 39(4), 295–299.

Pagaling, E., Strathdee, F., Spears, B.M., Cates, M.E., Allen, R.J. & Free, A. (2014) Community history affects the predictability of microbial ecosystem development. *The ISME Journal*, 8(1), 19–30.

Pagaling, E., Vassileva, K., Mills, C.G., Bush, T., Blythe, R.A., Schwarz-Linek, J., Strathdee, F., Allen, R.J. & Free, A. (2017) Assembly of microbial communities in replicate nutrient-cycling model ecosystems follows divergent trajectories, leading to alternate stable states. *Environmental Microbiology*, 19, 3374–3386.

Pelletier, E., Kreimeyer, A., Bocs, S., Rouy, Z., Gyapay, G., Chouari, R., Riviere, D., Ganesan, A., Daegelen, P., Sghir, A., Cohen, G.N., Medigue, C., Weissenbach, J. & Le Paslier, D. (2008) "*Candidatus Cloacamonas Acidaminovorans*": Genome Sequence Reconstruction Provides a First Glimpse of a New Bacterial Division. *Journal of Bacteriology*, 190(7), 2572–2579.

Plugge, C.M., Balk, M., Zoetendal, E.G. & Stams, A.J.M. (2002) *Gelria glutamica* gen . nov ., sp . nov ., a thermophilic , obligately syntrophic , glutamate-degrading anaerobe. *International Journal of Systematic and Evolutionary Microbiology*, 52, 401–407.

Podosokorskaya, O.A., Bonch-Osmolovskaya, E.A., Novikov, A.A., Kolganova, T.V. & Kublanov, I.V. (2013) *Ornatilinea apprima* gen. nov., sp. nov., a cellulolytic representative of the class *Anaerolineae*. *International Journal of Systematic and Evolutionary Microbiology*, 63(Pt 1), 86–92.

Poirier, S., Desmond-Le Quéméner, E., Madigou, C., Bouchez, T. & Chapleur, O. (2016) Anaerobic digestion of biowaste under extreme ammonia concentration: Identification of key microbial phylotypes. *Bioresource Technology*, 207, 92–101.

Prosen, E.M., Radlein, D., Piskorz, J., Scott, D.S. & Legge, R.L. (1993) Microbial utilization of levoglucosan in wood pyrolysate as a carbon and energy source. *Biotechnology and Bioengineering*, 42(4), 538–41.

Prosser, J.I. (2012) Ecosystem processes and interactions in a morass of diversity. *FEMS Microbiology Ecology*, 81(3), 507–519.

Quast, C., Pruesse, E., Yilmaz, P., Gerken, J., Schweer, T., Yarza, P., Peplies, J. & Glöckner, F.O. (2013) The SILVA ribosomal RNA gene database project: improved data processing and web-based tools. *Nucleic Acids Research*, 41(D1), D590–D596.

Raunkjær, K., Hvitved-Jacobsen, T. & Nielsen, P.H. (1994) Measurement of pools of protein, carbohydrate and lipid in domestic wastewater. *Water Research*, 28(2), 251–262.

Regueiro, L., Carballa, M. & Lema, J.M. (2016) Microbiome response to controlled shifts in ammonium and LCFA levels in co-digestion systems. *Journal of Biotechnology*, 220, 35–44.

Reilly, M., Dinsdale, R. & Guwy, A. (2014) Mesophilic biohydrogen production from calcium hydroxide treated wheat straw. *International Journal of Hydrogen Energy*, 39(30), 16891–16901.

Righi, S., Bandini, V., Marazza, D., Baioli, F., Torri, C. & Contin, A. (2016) Life Cycle Assessment of high ligno-cellulosic biomass pyrolysis coupled with anaerobic digestion. *Bioresource Technology*, 212, 245–253.

Rinzema, A., Boone, M., van Knippenberg, K. & Lettinga, G. (1994) Bactericidal effect of long chain fatty acids in anaerobic digestion. *Water Environment Research*, 66(1), 40–49.

Rivière, D., Desvignes, V., Pelletier, E., Chaussonnerie, S., Guermazi, S., Weissenbach, J., Li, T., Camacho, P. & Sghir, A. (2009) Towards the definition of a core of microorganisms involved in anaerobic digestion of sludge. *The ISME Journal*, 3(6), 700–714.

Sanger, F., Nicklen, S. & Coulson, A.R. (1977) DNA sequencing with chain-terminating inhibitors. *Proceedings of the National Academy of Sciences*, 74(12), 5463–5467.

Sauer, M., Porro, D., Mattanovich, D. & Branduardi, P. (2008) Microbial production of organic acids: expanding the markets. *Trends in Biotechnology*, 26(2), 100–108.

Shankar, S., Kansrajh, C., Dinesh, M.G., Satyan, R.S., Kiruthika, S. & Tharanipriya, A. (2013) Application of indigenous microbial consortia in bioremediation of oil-contaminated soils. *International Journal of Environmental Science and Technology*, 11(2), 367–376.

Shanmugam, S.R., Adhikari, S., Wang, Z. & Shakya, R. (2017) Treatment of aqueous phase of bio-oil by granular activated carbon and evaluation of biogas production. *Bioresource Technology*, 223, 115–120.

Shen, Y., Jarboe, L., Brown, R. & Wen, Z. (2015) A thermochemical–biochemical hybrid processing of lignocellulosic biomass for producing fuels and chemicals. Biotechnology Advances. 33, 1799–1813

Siegert, I. & Banks, C. (2005) The effect of volatile fatty acid additions on the anaerobic digestion of cellulose and glucose in batch reactors. *Process Biochemistry*, 40, 3412–3418.

Sierra-Alvarez, R. & Lettinga, G. (1991) The effect of aromatic structure on the inhibition of acetoclastic methanogenesis in granular sludge. *Applied Microbiology and Biotechnology*, 34(4), 544–550.

Smith, E.A, Park, S., Klein, A.T. & Lee, Y.J. (2012) Bio-oil Analysis Using Negative Electrospray Ionization: Comparative Study of High-Resolution Mass Spectrometers and Phenolic versus Sugaric Components. *Energy & Fuels*, 26(6), 3796–3802.

Snedecor, G.W. and Cochran, W.G. (1989) *Statistical Methods*, Eighth Edition, Iowa State University Press.

Sorokin, D.Y., Tourova, T.P., Mußmann, M. & Muyzer, G. (2008) *Dethiobacter alkaliphilus* gen. nov. sp. nov., and *Desulfurivibrio alkaliphilus* gen. nov. sp. nov.: two novel representatives of reductive sulfur cycle from soda lakes. *Extremophiles*, 12(3), 431–439.

Stephens, M.A. (1974) EDF Statistics for Goodness of Fit and Some Comparisons. *Journal of the American Statistical Association*, 69(347), 730-737

Sudasinghe, N., Dungan, B., Lammers, P., Albrecht, K., Elliott, D., Hallen, R. & Schaub, T. (2014) High resolution FT-ICR mass spectral analysis of bio-oil and residual water soluble organics produced by hydrothermal liquefaction of the marine microalga *Nannochloropsis salina*. *Fuel*, 119, 47–56.

Sugita, T., Nishikawa, A. & Shinoda, T. (1998) Rapid detection of species of the opportunistic yeast *Trichosporon* by PCR. *Journal of Clinical Microbiology*, 36(5), 1458–1460.

Sukhbaatar, B., Li, Q., Wan, C., Yu, F., Hassan, E.-B. & Steele, P. (2014) Inhibitors removal from bio-oil aqueous fraction for increased ethanol production. *Bioresource Technology*, 161C, 379–384.

Sun, L., Cruz, R., Meng, X.-Y., Tourlousse, D.M., Yamaguchi, T., Tamaki, H., Matsuura, N., Toyonaga, M., Hanada, S., Sekiguchi, Y. & Ohashi, A. (2016) *Lentimicrobium saccharophilum* gen. nov., sp. nov., a strictly anaerobic bacterium representing a new family in the phylum *Bacteroidetes*, and proposal of *Lentimicrobiaceae* fam. nov. *International Journal of Systematic and Evolutionary Microbiology*, 66(7), 2635–2642.

Sundqvist, T., Solantausta, Y., Oasmaa, A., Kokko, L. & Paasikallio, V. (2016) Heat Generation during the Aging of Wood-Derived Fast-Pyrolysis Bio-oils. *Energy & Fuels*, 30(1), 465–472.

Sung, S. & Liu, T. (2003) Ammonia inhibition on thermophilic anaerobic digestion. *Chemosphere,* 53, 43–52.

Sunyoto, N.M.S., Zhu, M., Zhang, Z. & Zhang, D. (2016) Effect of biochar addition on hydrogen and methane production in two-phase anaerobic digestion of aqueous carbohydrates food waste. *Bioresource Technology*, 219, 29–36.

Tessini, C., Vega, M., Müller, N., Bustamante, L., von Baer, D., Berg, A. & Mardones, C. (2011) High performance thin layer chromatography determination of cellobiosan and levoglucosan in bio-oil obtained by fast pyrolysis of sawdust. *Journal of Chromatography A*, 1218(24), 3811–3815.

Thauer, R.K., Kaster, A.-K., Seedorf, H., Buckel, W. & Hedderich, R. (2008) Methanogenic archaea: ecologically relevant differences in energy conservation. *Nature Reviews Microbiology*, 6(8), 579–591.

Torri, C. & Fabbri, D. (2014) Biochar enables anaerobic digestion of aqueous phase from intermediate pyrolysis of biomass. *Bioresource Technology*, 172, 335–341.

van Krevelen, D.W. (1950) Graphical-statistical method for the study of structure and reaction processes of coal, *Fuel*, 29, 269-84.

van Teeseling, M.C.F., Pol, A., Harhangi, H.R., van der Zwart, S., Jetten, M.S.M., Op den Camp, H.J.M. & van Niftrik, L. (2014) Expanding the Verrucomicrobial Methanotrophic World: Description of Three Novel Species of *Methylacidimicrobium* gen. nov. *Applied and Environmental Microbiology*, 80(21), 6782–6791.

Vanwonterghem, I., Jensen, P.D., Ho, D.P., Batstone, D.J. & Tyson, G.W. (2014) Linking microbial community structure, interactions and function in anaerobic digesters using new molecular techniques. *Current Opinion in Biotechnology*, 27, 55–64.

Vartoukian, S.R., Palmer, R.M. & Wade, W.G. (2007) The division "*Synergistes*." *Anaerobe*, 13(3–4), 99–106.

Wang, D., Ai, J., Shen, F., Yang, G., Zhang, Y., Deng, S., Zhang, J., Zeng, Y. & Song, C. (2017) Improving anaerobic digestion of easy-acidification substrates by promoting buffering capacity using biochar derived from vermicompost. *Bioresource Technology*, 227, 286–296.

Wang, H., Livingston, D., Srinivasan, R., Li, Q., Steele, P. & Yu, F. (2012) Detoxification and fermentation of pyrolytic sugar for ethanol production. *Applied Biochemistry and Biotechnology*, 168(6), 1568–83.

Wang, L.-Y., Nevin, K.P., Woodard, T.L., Mu, B.-Z. & Lovley, D.R. (2016) Expanding the Diet for DIET: Electron Donors Supporting Direct Interspecies Electron Transfer (DIET) in Defined Co-Cultures. *Frontiers in Microbiology*, 7(MAR), 1–7.

Wang, Y., Sheng, H.-F., He, Y., Wu, J.-Y., Jiang, Y.-X., Tam, N. F.-Y. & Zhou, H.-W. (2012) Comparison of the Levels of Bacterial Diversity in Freshwater, Intertidal Wetland, and Marine Sediments by Using Millions of Illumina Tags. *Applied and Environmental Microbiology*, 78(23), 8264–8271.

Wang, Y., Zhang, Y., Wang, J. & Meng, L. (2009) Effects of volatile fatty acid concentrations on methane yield and methanogenic bacteria. *Biomass Bioenergy*, 33, 848-853.

Watnick, P. & Kolter, R. (2000) Biofilm, City of Microbes. *Journal of Bacteriology*,. 182, 2675–2679.

Westerholm, M., Leven, L. & Schnurer, A. (2012) Bioaugmentation of Syntrophic Acetate-Oxidizing Culture in Biogas Reactors Exposed to Increasing Levels of Ammonia. *Applied and Environmental Microbiology*, 78(21), 7619–7625.

Westerholm, M., Müller, B., Arthurson, V. & Schnürer, A. (2011) Changes in the Acetogenic Population in a Mesophilic Anaerobic Digester in Response to Increasing Ammonia Concentration. *Microbes and Environments*, 26(4), 347–353.

Wittmann, C., Zeng, A.-P. & Deckwer, W.-D. (1995) Growth inhibition by ammonia and use of a pH-controlled feeding strategy for the effective cultivation of *Mycobacterium chlorophenolicum*. *Applied Microbial Biotechnology*. 44, 519–525.

Wu, Z., Rodgers, R.P. & Marshall, A.G. (2004) Two- and Three-Dimensional van Krevelen Diagrams: A Graphical Analysis Complementary to the Kendrick Mass

Plot for Sorting Elemental Compositions of Complex Organic Mixtures Based on Ultrahigh-Resolution Broadband Fourier Transform Ion Cyclotron Resonance. *Analytical Chemistry*, 76(9), 2511–2516.

Xiong, L., Huang, C., Li, X.-M., Chen, X.-F., Wang, B., Wang, C., Zeng, X.-A. & Chen, X.-D. (2015) Acetone-Butanol-Ethanol (ABE) Fermentation Wastewater Treatment by Oleaginous Yeast *Trichosporon cutaneum*. *Applied Biochemistry and Biotechnology*, (2)

Yang, Z., Bai, Z., Sun, H., Yu, Z., Li, X., Guo, Y. & Zhang, H. (2014) Biomass pyrolysis liquid to citric acid via 2-step bioconversion. *Microbial Cell Factories*, 13(1), 182.

Yenigün, O. & Demirel, B. (2013) Ammonia inhibition in anaerobic digestion: A review. *Process Biochemistry*, 48(5–6), 901–911.

Yun, Y.M., Kim, D.H., Cho, S.K., Shin, H.S., Jung, K.W. & Kim, H.W. (2016) Mitigation of ammonia inhibition by internal dilution in high-rate anaerobic digestion of food waste leachate and evidences of microbial community response. *Biotechnology and Bioengineering*, 113(9), 1892–1901.

Zaldivar, J., Martinez, A. and Ingram, L.O. (1999) Effect of selected aldehydes on the growth and fermentation of ethanologenic *Escherichia coli*. *Biotechnology and Bioengineering*, 65(1), 24–33

Zhang, C., Yuan, Q. & Lu, Y. (2014) Inhibitory effects of ammonia on methanogen *mcrA* transcripts in anaerobic digester sludge. *FEMS Microbiology Ecology*, 87(2), 368–377.

Zhang, S., Winestrand, S., Guo, X., Chen, L., Hong, F. & Jönsson, L.J. (2014) Effects of aromatic compounds on the production of bacterial nanocellulose by *Gluconacetobacter xylinus*. *Microbial Cell Factories*, 13(1), 62.

Zhao, Z., Zhang, Y., Holmes, D.E., Dang, Y., Woodard, T.L., Nevin, K.P. & Lovley, D.R. (2016) Potential enhancement of direct interspecies electron transfer for syntrophic metabolism of propionate and butyrate with biochar in up-flow anaerobic sludge blanket reactors. *Bioresource Technology*, 209, 148–156.

Zhao, Z., Zhang, Y., Woodard, T.L., Nevin, K.P. & Lovley, D.R. (2015) Enhancing syntrophic metabolism in up-flow anaerobic sludge blanket reactors with conductive carbon materials. *Bioresource Technology*, 191, 140–145.

Zhu, X., Siegert, M., Yates, M.D. & Logan, B.E. (2015) Alamethicin suppresses methanogenesis and promotes acetogenesis in bioelectrochemical systems. *Applied and Environmental Microbiology*, 81(11), 3863–3868.

Ziegler, S., Waidner, B., Itoh, T., Schumann, P., Spring, S. & Gescher, J. (2013) *Metallibacterium scheffleri* gen. nov., sp. nov., an alkalinizing *gammaproteobacterium* isolated from an acidic biofilm. *International Journal of Systematic and Evolutionary Microbiology*, 63(Pt 4), 1499–1504.

Zion Research (2016) Acetic Acid Market for VAM, Acetate Esters, Acetic Anhydride, PTA and Other Application: Global Industry Perspective, Comprehensive Analysis, Size, Share, Growth, Segment, Trends and Forecast, 2015 – 2021 [online] Report Code: ZMR-31

Zitomer, D., Maki, J., Venkiteshwaran, K. & Bocher, B. (2016) Relating Anaerobic Digestion Microbial Community and Process Function. *Microbiology Insights*, 8(Suppl. 2), 37.